UNIVERSITY OF Southampton

Strength Assessment of Damaged Steel Ship Structures

A Thesis Submitted for the Degree of

Engineering Doctorate

by

James Mathieson Underwood

Fluid Structure Interactions Research Group

Faculty of Engineering and the Environment

University of Southampton

April 2013

UNIVERSITY OF SOUTHAMPTON

ABSTRACT

FACULTY OF ENGINEERING AND THE ENVIRONMENT
Fluid Structure Interactions Research Group
Engineering Doctorate

Strength Assessment of Damaged Steel Ship Structures

by
James Mathieson Underwood

In 2012 106 vessels over 100 gross tonnes were lost. During the damage incidents many of these vessels required assistance from shore based emergency response services with regards to their damaged strength to stabilise the situation, preserve life, prevent environmental disaster and limit financial costs to owners and insurers. The research work presented in this Engineering Doctorate Thesis surrounds the strength assessment of damaged steel ship structures, the influence of damage on the strength of steel-plated structures and methods for assessing the residual strength of a vessel in an emergency. The focus of the work is to improve the modelling of damaged steel ship structures within an emergency situation, in order to improve guidance provided to a stricken vessel during a damage incident or salvage process.

Literature study has shown that structural idealisation through the use of interframe progressive collapse analysis, to be the current state of the art method for the rapid assessment of intact and damaged ship structures. However, a number of weaknesses have been identified in the method when applied to damage assessment. The literature study has also shown a lack of understanding of the effect of damage on steel-plated structures as specific analysis has not been performed previously.

Significant research has been undertaken into the influence of damage, in the form of a hole, on the ultimate collapse strength of steel-plated structures. Three levels of structural modelling have been used, stiffened-plate, stiffened panel and grillage.

Comparison of the predicted ultimate collapse strength by finite element analysis (FEA) with predictions using the interframe progressive collapse idealisation, has shown the calculated results to be conservative for the assessment of damaged structure when the failure mode remains in the interframe collapse form. However, changes in the failure mode lead to the interframe progressive collapse method over predicting the ultimate collapse strength. The analysis shows that even small damage events can lead to significant changes to the failure mode and resulting ultimate collapse strength of the structure. Such influences must be accounted for in any simplified method.

A new method for the assessment of damaged ship structures is proposed that is capable of modelling a damage scenario more accurately. Demonstration of the method has shown the results to be less conservative than the current state of the art, when compared to FEA, for local analysis of damaged steel-plated structure. The ability of the method to account for the influence of damage, and the resulting failure modes, that may significantly influence the ultimate bending strength of the structure has also been demonstrated. The method implements a compartment level progressive collapse analysis with structural data captured through the use of the response surface method 'kriging', using data points provided from FEA. This method allows the critical damage variables to be captured and strength data accessible quickly for use in the analysis.

The time to provide a solution to the damage scenario is equivalent to the existing interframe progressive collapse method. Therefore, the method is suitable for application within an emergency response or salvage service.

[Blank Page]

CONTENTS

TABLES

FIGURES

[Blank Page]

AUTHOR'S DECLARATION

I, James Mathieson Underwood declare that this thesis entitled:

Strength Assessment of Damaged Steel Ship Structures

and the work presented within are both my own and have been generated by me as the result of my own original research. I confirm that:

- This work was done wholly or mainly whilst in candidature for a research degree at the University of Southampton;
- Where any part of this thesis has previously been submitted for a degree or any other qualification at this University or any other institution, this has been clearly stated;
- Where I have consulted the published work of others, this is always clearly attributed;
- Where I have quoted from the work of others, the source is always given. With the exception of such quotations, this thesis is entirely my own work;
- I have acknowledged all main sources of help;
- Where the thesis is based on work done by myself jointly with others, I have made clear exactly what was done by others and what I have contributed myself;
- Parts of this work have been published as:
  - Underwood J M, Sobey, A J, Blake J I R, Shenoi R A (2010). Local Stress Sensitivity Analysis of Damaged Steel Ship Hulls. *Practical Design of Ships and Other Floating Structures (PRADS 2010); pp1006-1014.*
  - Sobey A J, Underwood J M, A J, Blake J I R, Shenoi R A (2010). Reliability Analysis of Damaged Steel Structures Using Finite Element Analysis. *5th International ASRANet Conference (ASRANet 2010). Digital Proceedings.*

- Underwood J M, Sobey A J, Blake J I R, Shenoi R A, Cuckson B R (2011). Determination of critical factors for the strength assessment of damaged steel ship structures. *30th International Conference on Ocean, Offshore and Arctic Engineering (OMAE 2011). Digital Proceedings.*

- Underwood J M, Sobey A J, Blake J I R, Shenoi R A (2012). Ultimate collapse strength assessment of damaged steel-plated structures. *Engineering Structures 38; pp1-10.*

- Underwood J M, Sobey A J, Blake J I R, Shenoi R A (2012). Determination of Critical Factors for the Damaged Strength Assessment of Steel Grillages. *22nd International Ocean and Polar Engineering Conference (ISOPE 2012). Digital Proceedings.*

- Underwood J M, Sobey A J, Blake J I R, Shenoi R A (2012). Reliability Analysis of the Damage Strength of Steel Grillages for use in Ship Emergency Response. *6th International ASRANet Conference (ASRANet 2012). Digital Proceedings.*

- Underwood J M, Sobey A J, Blake J I R, Shenoi R A (2013). Strength Assessment Of Damaged Steel Ships During Emergency Response. *RINA Damaged Ship II; pp84-91.*

Signed: . . . . . .

Date: . . . . . .

ACKNOWLEDGEMENTS

The author would like to thank the UK Ministry of Defence and Lloyd's Register EMEA for their sponsorship and continued support and without whom this research would not have been possible. In particular the author would like to thank Dr Chris Cole for allowing the opportunity to undertake this work, Mr Colin Snell, Mr Paul James, Mr Mike Mogford and Mr Ben Cuckson for their time, input and support of the work throughout.

The author would also like to thank Prof. Ajit Shenoi, Dr James Blake and Dr Adam Sobey at the University of Southampton for their advice, support and time during this work; as well as Dr Sobey's insistence of "Friday beers" and for all those who joined, where many issues have been resolved. The author would also like to acknowledge the use of the IRIDIS 3 High Performance Computing Facility, and associated support services at the University of Southampton in the completion of this work.

The author would also like to thank his wife Rebecca for her continued support throughout the course of the work and ability to drag him back in to the real world after another dark day of FEA; and finally to thank his beautiful daughter Isabelle, for her giggles and smiles of joy that spurred on completion of the work, never stop exploring and learning.

[Blank Page]

NOMENCLATURE

A	Cross-sectional area
A_m	Maximum deflection amplitude
Ao	Deflection shape coefficient
D	Flexural rigidity
E	Young's modulus
F	Force
G	Shear modulus
I	Second moment of area
L	Length
M	Bending moment
R	Radius of curvature
Rx Ry Rz	Rotational constraints about respective axes
P	Load
P_{u0}	Calculated ultimate collapse load
P_{sq}	"Squash Load" or material ultimate collapse load ($A\sigma_y$)
Q	Lateral pressure load
Ux Uy Uz	Displacement constraints in respective x,y,z directions
a	Length of Section
b	Breadth of section
p_j	Response surface smoothness correlation function
r	Radius of gyration (or correlation vector for response surface definition)
t	Section thickness
w	Load
w_{oplm}	Maximum plate initial imperfection size
w_{ocm}	Maximum stiffener column type initial imperfection size
w_{osm}	Maximum stiffener sideways initial imperfection size
x	Displacement, orientation defined locally for specific equations
y	Displacement, orientation defined locally for specific equations
z	Displacement, orientation defined locally for specific equations
β	Plate slenderness ratio
$\hat{\beta}$	kriging model global position
Δ	Change in parameter
ε	Strain (or error for response surface definition)
θ	Angle
λ	Column slenderness ratio
ν	Poisson's Ratio
σ	Direct Stress (or standard deviation for response surface definition)
σ_{cr}	Critical buckling stress
σ_y	Yield stress
τ	Shear stress
τ_u	Shear strength
τ_y	Shear yield stress

[Blank Page]

1 INTRODUCTION

1.1 Background

In an unpredictable world where human intervention fails or unexpected environmental conditions can prevail, damage can occur to manmade structures. Despite the advances in modern navigational techniques, ship to ship or ship to land collisions continue to occur. Such events do not regularly result in total loss of the vessel, but result in the stricken vessel requiring assistance and guidance on how to control the situation and salvage the vessel. Whilst structural design will allow for redundancy or a structural capability beyond the general working load of the structure, it is imperative to be able to analyse and understand the residual capability of a damaged structure. This must be done to ensure the safety of personnel in the vicinity of the structure, limit any potential environmental impact resulting from the damage and potentially limit the financial cost to owners or insurers by stabilising the scenario and assessing the potential for salvage and to facilitate repair. Additionally, without being able to demonstrate sufficient structural capability of a damaged vessel, access to safe haven within a port is unlikely to be granted.

Demonstrating the diversity of damage events, a number of more recent events are detailed. In January 2013 the minesweeper vessel USS GUARDIAN ran aground on a reef off the Philippine coast in a similar fate to that of the container vessel MV RENA, who ran aground and eventually broke in half on a reef of the New Zealand coast. In January 2012 the cruise ferry COSTA CONCORDIA grounded on a rock off the Italian coast causing significant structural damage along her portside, resulting in her capsizing in shallow water and leading to the tragic loss of 32 lives [1]. In November 2010 the Northlink ferry MV RHOSSEY was struck by the supply vessel MAERSK FINDER leaving two deep gouge marks in the side of the vessel, partially penetrating the steel plate above the waterline [2]. In October 2009, 18000 gallons of fuel oil were leaked off Galveston, US, following the collision between the Aframax crude tanker KRYMSK and the offshore supply vessel AET ENDEAVOUR [3]. In October 2009, the Japanese Destroyer KURAMA collided with a South Korean container vessel, CARINA STAR, off southern Japan causing significant damage to the bow of the Destroyer and resulted in a large fire in the vessel's paint store [3]; in both cases the vessels were damaged but secured and able to head for port for structural assessment. From this short but varied list it can be seen that collisions and grounding events continue to occur and are not limited to the commercial freight, military or passenger vessel sectors of the marine industry.

It is reported that in 2012 alone there were a total of 106 vessels lost in excess of 100 gross tons; an increase of 91 from the previous year, though 27% less than the ten-year average [4,5]. Of these losses 49% were due to foundering or sinking, 22% due to wrecking or grounding whilst only 5% were due to collisions, Figure 1.1, with the vessels involved spread across the commercial fleet, Figure 1.2.

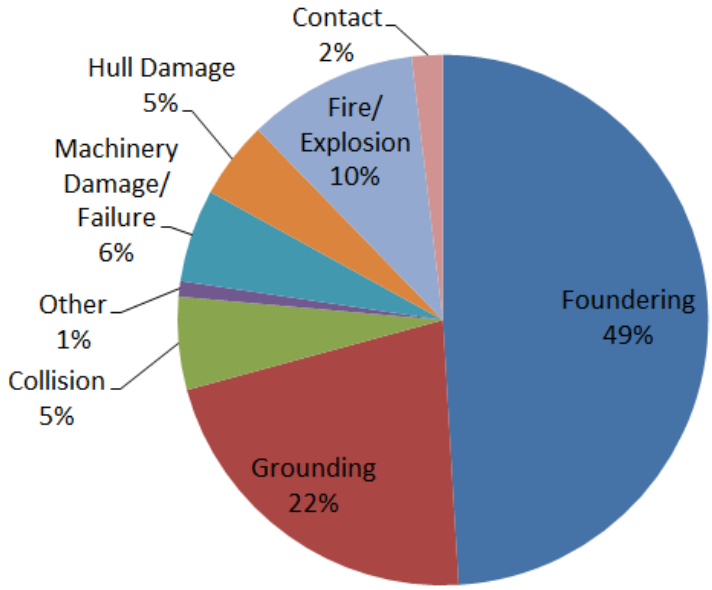

Figure 1.1 – Cause of Loss of Vessels for 12 months to 25th November 2012 [4,5]

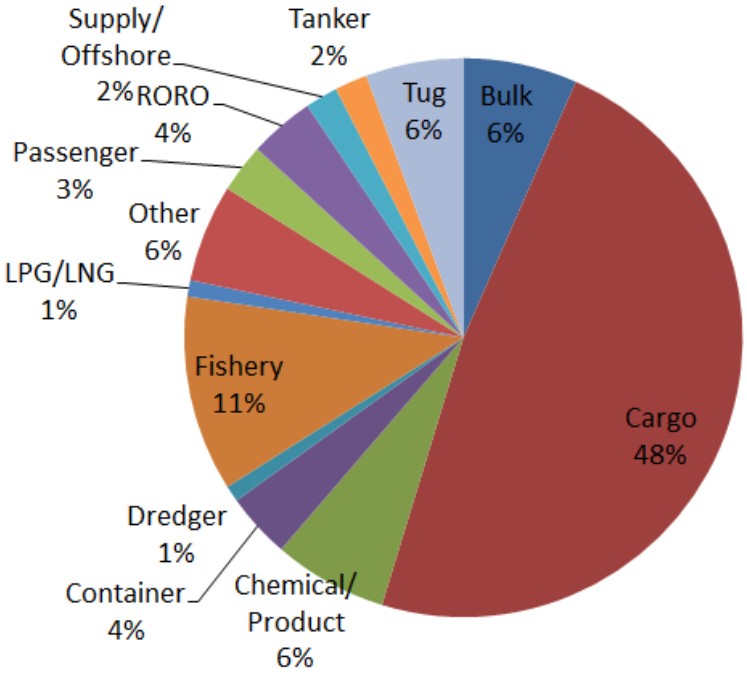

Figure 1.2 – Losses of Vessel by Type for 12 months to 25th November 2012 [4,5]

The sponsorship drive for this work stemmed from one particular incident. In July 2002, the UK Royal Navy vessel HMS NOTTINGHAM, a Type 42 Destroyer, hit Wolf Rock off the coast of Australia whilst on passage to Wellington, New Zealand. In the grounding, the vessel suffered from severe raking[1] damage to the forward section, stretching aft over a significant portion of the vessel's length [6]. Following the crew's initial damage control and shoring[2] efforts, the vessel was stabilised and no longer in immediate danger of sinking. At this stage guidance was sought from UK Ministry of Defence (MoD) headquarters regarding the residual strength of the vessel and her ability to withstand the forecast sea conditions. Such a scenario is common in the commercial sector of the marine industry, with the crew and owner seeking advice from emergency response services predominantly run by classification societies; however, it should be noted that the ability of the crew to take remedial measures is significantly lower on a commercial vessel.

Discussions with the UK MoD Salvage and Marine Operations (SALMO) Project Team have indicated that having access to better damaged structural assessment tools could have reduced the salvage duration by weeks or even months. This could have potentially reduced the costs incurred in shoring the vessel by focusing efforts on critical areas and potentially removed the need for the use of a heavy lift vessel to transport the Destroyer to a suitable repair facility, if the vessel had proved to be towable.

Following the HMS NOTTINGHAM incident, the UK MoD took steps to implement a scheme of research to better understand the residual capabilities of damaged vessels, in order to be able to provide better guidance to those in distress. The work documented within this thesis forms the third part of the implemented research initiative and is intended to investigate the effects of damage on the structural strength of a vessel.

Concurrent work [7,8,9,10,11] being undertaken for the UK MoD and Lloyd's Register has investigated the local and global loads on a damaged ship in a seaway, both stationary and with forward speed, focussing on the hydrodynamic pressures generated by the seaway and floodwater and research into the associated structural loads from the hydrodynamic pressure field. Whilst it is appreciated that such factors will influence the structural response of a damaged vessel, they have not been included in the work presented in this thesis.

[1] Raking is a shipping term relating to damage caused to the underside of a vessel by grounding on an object.
[2] The efforts of reinforcing structure using additional material, for example wooden beams.

1.2 Industry Emergency Response Techniques

Regulation 37.4 of the revised MARPOL 73/78 Annex I states that "All oil tankers of 5000 tons deadweight or more shall have prompt access to computerised, shore-based damage stability and residual structural strength calculation programs." [12] Whilst this regulation only relates to tankers, the benefit of access to such a facility is well recognised by ship owners and has been implemented in relation to a wide variety of vessels around the world.

In order to provide such a facility to their clients, many classification societies operate an emergency response service. In the case of Lloyd's Register (LR), their Ship Emergency Response Service (LR SERS) is available 24 hours a day on emergency call out, to provide assistance to a stricken vessel when making decisions to bring the situation under control. These encompass a range of concerns from stability issues, such as the effects of closing or opening tanks, moving ballast water or cargo between tanks as well as how these decisions may impact on the residual strength of the vessel. Advice can also be provided on local structural issues, such as the requirement for additional shoring of bulkheads and decks as well as the decision whether to abandon, though ultimate responsibility still lies with the master of the vessel.

At LR SERS, the residual structural strength of a damaged vessel is calculated using a simplistic software tool that implements progressive collapse analysis, originally proposed by Smith and Dow [13,14]. The tool allows the user to manually input or read in a pre-defined ship model, in the form of 2D interframe cross-sections, for which it is able to calculate the global ultimate bending strength of each section. In a damage scenario, the user is able to deselect the "damaged" structure, identified from crew reports at the scene, in order to remove them from the strength calculation. Doing so will allow the user to calculate the ultimate residual strength of the section. The survivability of the vessel can be indicated by comparing the ultimate bending strength in the damaged condition to the expected bending loads, which are determined by undertaking a separate global ship bending moment assessment for the damaged condition. Further details and discussion of the progressive collapse method are discussed later in Chapter 2.2.3.

Such structural calculations performed in a live damage situation need to provide enough confidence from which decisions can be made, whilst being quick enough to be relevant. Due to the simplified approach to whole ship structural analysis, the calculation process is more basic and potentially less accurate than, for example, a finite element model of the damaged vessel; however, the timescales to be able to model and provide answers from the analysis are much faster. The LR SERS approach can potentially start to provide answers within an hour and can be easily manipulated whilst, for example, a full finite element analysis (FEA) could take weeks or months to provide any structural information, too slow for an emergency situation even if a pre-existing intact FE model was available from which to work from.

1.3 The Case of the Damaged Ship

Damage has been described as any accidental modification or intentional harm to the "as-built" condition [7]. Paik et al. [15] described the contributing factors to the potential loss of a vessel, in their case a bulk carrier, through the use of the diagram in Figure 1.3. An additional 'Local Dent or Damage' box has been added to the original Paik diagram [15], to complete the picture in relation to this work. The factors contributing to the decrease of hull girder strength are considered to be within the scope of this research; however, fatigue and crack propagation have not been included due to time limitations and by request of the project sponsor, though it is appreciated that both may affect the time to failure of a vessel in a seaway.

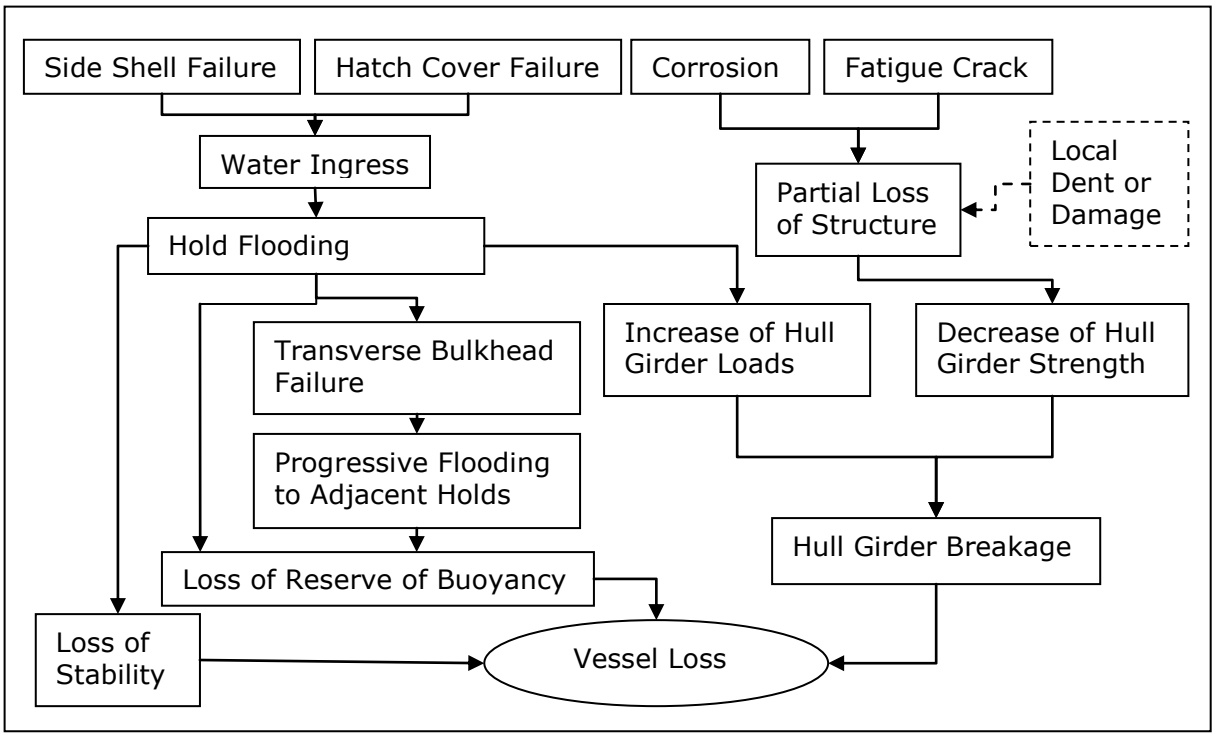

Figure 1.3 - Vessel Loss Scenarios [15], With Additional Damage Box

Other research work sponsored by the UK MoD and Lloyd's Register, noted in Section 1.1, is concerned with the factors influencing the increase of hull girder loads shown in Figure 1.3. The link between hold flooding to increased hull girder loads represents how the flooding of a hold can lead to an increased loading in its vicinity as well as changes to the bending moment the vessel is experiencing. This, coupled with the reduction in hull girder strength, illustrates how the streams of research work will be used to assess whether a vessel may be lost or not.

In an event where damage occurs to a vessel's hull below the waterline, the scenario can be seen as having three distinct phases, as detailed by Smith [7]:

1. An initial transient response, characterised by large motions and violent floodwater motion;

2. A period of progressive flooding when water ingress, slowed by internal obstructions, finds an approximate equilibrium;

3. Steady state floodwater behaviour; the oscillation of floodwater about an approximate equilibrium water level.

During the first two damage phases, it is expected that the vessel crew of the vessel are working to assess the damage, secure watertight boundaries, shore-up or plug minor damage and stabilise the event. It is not expected that the crew will be able to relay information from which structural analysis can be made until the steady state phase has been reached. Therefore, it is not intended that that this research will focus on the dynamic replication of the damage event, nor assessment of the structural responses prior to the steady state phase, though it is appreciated that these phases can affect the steady state condition of the vessel.

From this understanding of the damaged ship and current emergency response procedures, the following research aim and objectives have been developed.

1.4 Research Aim

The research aim is to develop understanding of the influence of damage on steel ship structures for the assessment of, or to aid in the assessment of, the residual structural strength of a damaged vessel.

1.5 Research Objectives and Purpose

In order to achieve the research aim, the following objectives have been developed on which the research is based.

1. To undertake a comprehensive literature review into methods for assessing a damaged steel structure and their application in an emergency response scenario.

2. To identify state of the art methods for assessment of damaged structures and their application in emergency response scenarios.

3. Develop a model for the assessment of the mechanics of failure of local models of damaged ship structures.

4. Investigation of potentially influential factors on the strength of a damaged steel structure through application of the model as well as undertaking reliability and sensitivity studies of the results. Factors to assess include:

    (i) Plate thickness variations due to corrosion or plate rolling tolerances;

    (ii) Damage aperture shape;

    (iii) Damage aperture size;

    (iv) Loading condition.

5. Development of a methodology for global structural analysis of ship structures in a damage situation.

1.6 Scope of Work

Steel has been the predominant material of choice for the construction of large transoceanic vessels since the 1800's. However, since the 1940's, the prominent production method of using rivets to join large steel plates together to create the hull form has been replaced by welding, which continues to be the predominant method of ship construction. As such, the focus of this research into the strength of damaged ship structures has been focused around steel plated structures connected by welded joints.

Section 1.3 has explored some of the factors that contribute to the strength of a damaged steel ship. Due to various constraints on the research project, the following have been excluded from the scope of work:

1. Experimental tests;
2. Fluid structure interactions;
3. Assessment of crack propagation;
4. Assessment of fatigue effects on damaged steel structure;
5. Dynamic modelling of damage events.

1.7 Research Novelty

The novel and original contribution of this work surrounds the increased understanding of the influence of damage, in the form of a hole, on the ultimate collapse strength of steel-plated structures under compressive axial loading. This has been demonstrated through research studies on the damaged strength of local structural arrangements at stiffened-plate, stiffened-panel and grillage level, including factors that may influence the mechanics of the failure of the structure. No previous work has been undertaken to investigate these influences, as can be seen from the reviewed literature in Chapter 2 and the summary in Table 2.7. The findings demonstrate how even small damage events can lead to significant changes in the ultimate collapse strength.

These findings have led to the development of a novel method to assess the residual strength of a damaged steel ship that accounts for the demonstrated influences. The method uses the response surface method (RSM) 'kriging' coupled with the fundamentals of progressive collapse analysis to undertake a more holistic compartment level damage assessment of the vessel, whilst maintaining the timescales required for use in emergency response. This approach has not been presented previously and allows the incorporation of a large number of variables, for example damage size, location, material condition, etc., which can be present in a damaged scenario to be included in the analysis.

To date, assessment of damaged vessels in emergency response has been limited to interframe assessment, neglecting the influence of the damage on the mode of failure of the vessel, assuming failure will occur in the same mode as per the intact condition; research presented later in this thesis demonstrates that this is not always correct. The method developed and presented in this thesis will allow a significant step forward in the assessment of the damaged strength of a vessel in an emergency scenario.

1.8 Thesis Structure

This thesis has been structured so as to provide a natural flow to the development of the understanding of the influence of damage on steel plated structure and the development of the proposed new method for whole ship damaged strength assessment. Chapter 2 presents a literature review of the state of the art methods for modelling steel structures and comments on their applicability to damage assessment. Chapter 3 details the research methodology and proposed new method for the compartment level ultimate bending strength assessment of damaged ship structures using response surfaces with progressive collapse analysis. Chapter 4 presents verification of the models used within the subsequent research studies, along with the investigation into potential use of RSM for the capture of damaged strength information. Chapter 5 presents the investigation of the application of structural idealisation at stiffened-plate level for damaged strength analysis. Chapter 5 also provides discussion on influential factors in the assessment of damaged steel structures, with the intention of being able to limit the variables required to be captured by the response surface to aid efficiency of implementation of the developed new methodology. Chapter 6 presents an investigation into the effects of the damage aperture on the collapse strength of damaged steel structure, highlighting further benefits of the proposed new method. Chapter 7 presents an investigation into the influence of damage aperture size on the collapse strength of grillages. Chapter 8 demonstrates the proposed new compartment level progressive collapse method. Overall conclusions are presented in Chapter 9, with recommendations for future work including understanding of the influence of damage on steel-plated structures and development of the proposed method presented in Chapter 10.

Appendices to the document present the prior publication of aspects of this thesis during the course of this work and additional data as appropriately referenced throughout the thesis.

[Blank Page]

2 LITERATURE REVIEW

2.1 Introduction

Steel ship structures are predominantly comprised of plate and stiffener combinations, welded together with the stiffening members running in a longitudinal direction. These stiffened sections are supported at each end by deep transverse stiffening members which, when connected to support adjoining stiffened panels, form a grillage arrangement along the length of the vessel. Grillages wrap around the vessel to form the hull and decks and are supported at each end by a bulkhead to close the defined compartment. These compartments when connected together form the vessel.

Hughes [16] defines a grillage as 'a plane structure of intersecting beams, with or without plating, which carries a lateral load through the action of beam bending'. Likewise, analysis of a stiffened panel is often undertaken under the assumption that the panel is a piece of plate, continuously stiffened from edge to edge either transversely or longitudinally, and supported along at least two edges. This is echoed by Faulkner et al. [17], who state that 'secondary structure is referred to as a grillage when it contains stiffening in two orthogonal directions, whereas the word 'panel' is reserved for elements stiffened in one direction only'.

Example compartment, grillage and stiffened-plate arrangements are illustrated in Figure 2.1 and Figure 2.2. Compartment level or whole ship analysis can be undertaken to directly assess the global structural strength by utilising comprehensive analysis methods such as FEA; though these methods tend to have long lead times to provide results. However, due to the structural configuration, structural analysis of a vessel can be made at different levels of detail. By understanding the global forces acting on a vessel as well as the local response of plates, stiffened panels or grillage arrangements, the structural capability of the whole ship can be understood and assessed. Analysis methods such as progressive collapse and Idealised Structural Unit Method (ISUM), both discussed in more detail later in this chapter, utilise the understanding of the strength of local structural elements summed together to calculate the overall global strength. Such methods can allow rapid whole ship structural assessment to be performed.

Many of the analysis methods, developed over time to be able to assess structural strength at the different levels of detail, have been done in relation to intact structural strength. As such, this literature review has been divided into the different detail levels (global, stiffened plates, stiffened panels and grillages) in order to review the current state of the art methods available for structural strength assessment and to review their use or potential use in assessing the structural strength of a damaged vessel.

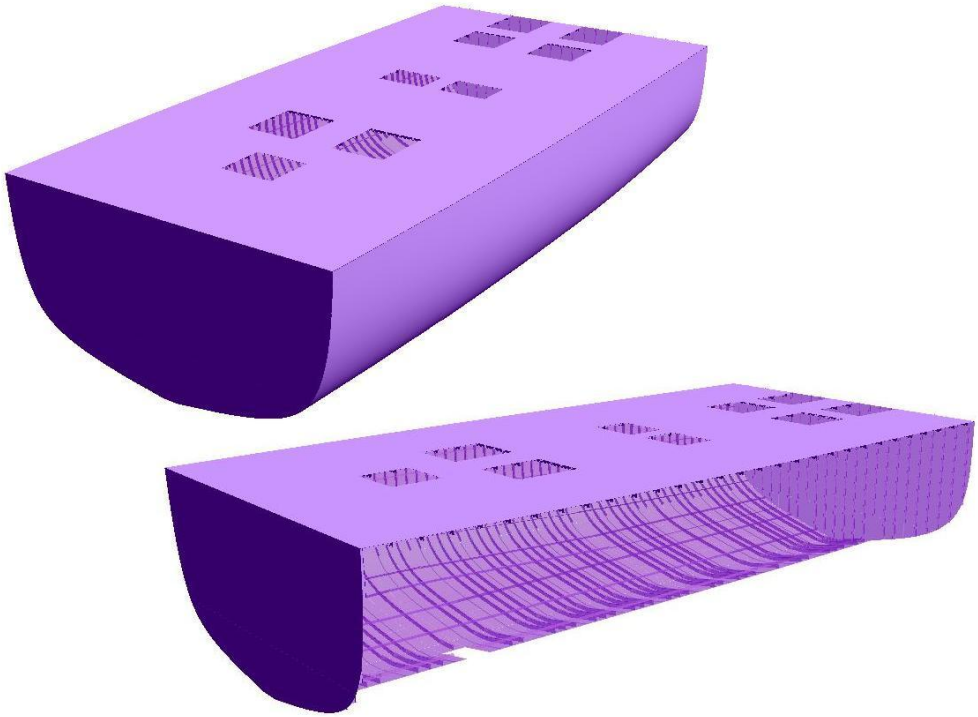

Figure 2.1 - Example Compartment Level Ship Structural Model

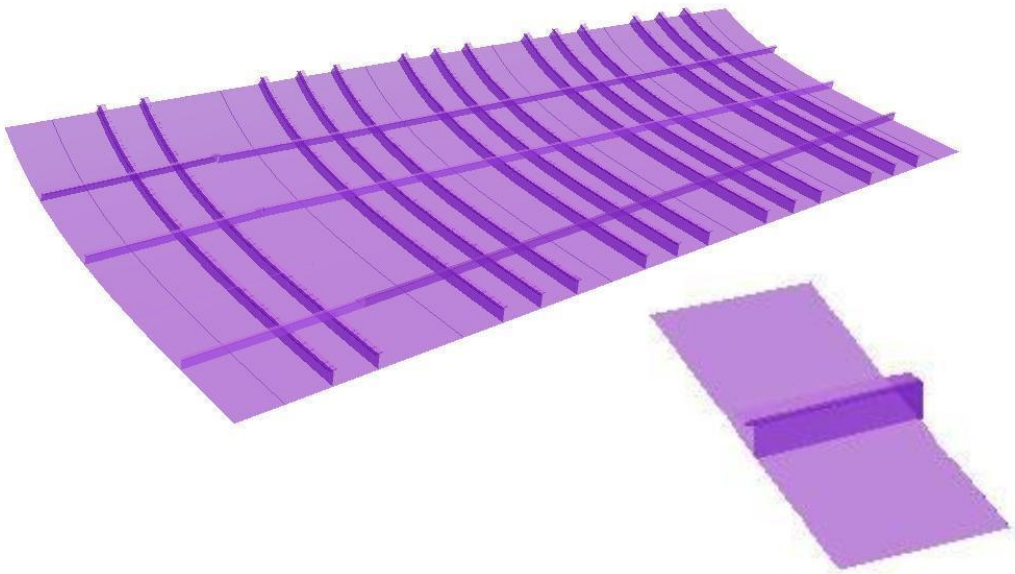

Figure 2.2 - Example Grillage and Stiffened-Plate Structural Models

2.2 Whole Ship Global Strength Assessment

2.2.1 Elastic Beam Theory

Understanding the structural characteristics of a ship as an entity, not just on a localised level, is important to be able to understand the structural capability of the whole vessel and not just its component parts. This allows assessment of the capability against the expected loading from hydrostatic and hydrodynamic forces. The most simplified whole ship models reduce the vessel problem to that of an unconstrained or free-free beam to calculate the longitudinal bending strength of the vessel. Through the use of elastic beam theory it is possible to integrate the load curve for a vessel to obtain the shear force, bending moment and deflection characteristics along its length. The load curve is calculated as the difference between the vessel's weight and buoyancy forces along its length for a static analysis or balanced on a wave of length equal to the length of the vessel for quasi-static analysis. Equations (1) to (5) show this relationship for a uniform beam, with the orientation of the applied axis shown in Figure 2.3.

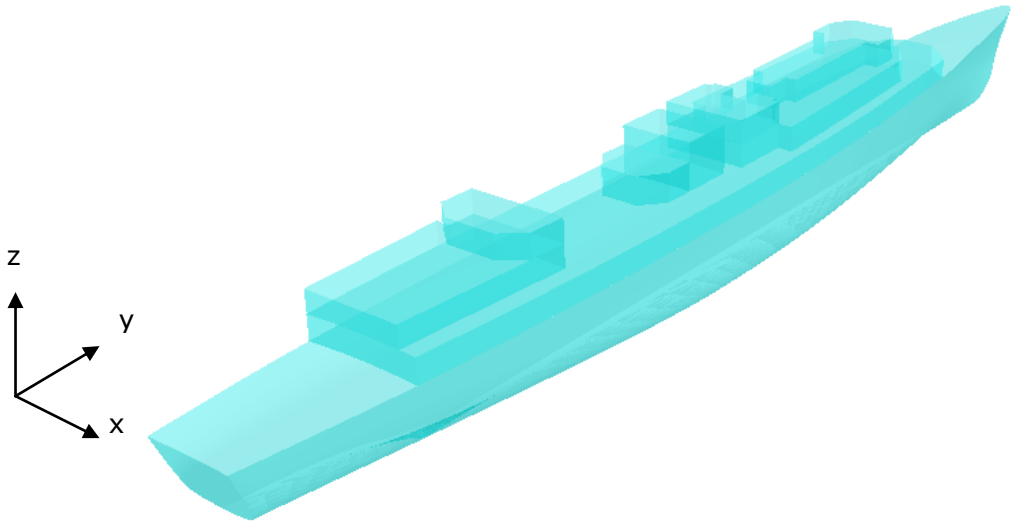

Figure 2.3 – Axis direction definition

Load Distribution: $$EI_x \frac{d^4z}{dy^4} = -w \quad (1)$$

Shear Force: $$EI_x \frac{d^3z}{dy^3} = -wy + A \quad (2)$$

Bending Moment: $$EI_x \frac{d^2z}{dy^2} = -\frac{wy^2}{2} + Ay + B \quad (3)$$

Rate of Change of Deflection: $$EI_x \frac{dz}{dy} = -\frac{wy^3}{6} + \frac{Ay^2}{2} + By + C \quad (4)$$

Deflection: $$z = \frac{-\frac{wy^4}{24} + \frac{Ay^3}{6} + \frac{By^2}{2} + Cy + D}{EI_x} \quad (5)$$

where w is the uniformly distributed load along the length of the beam, y is the distance along the length of the beam, z is the vertical displacement, E is the Young's modulus of the material, I_x is the second moment of area of the beam's cross-section about x (where x is the horizontal direction across the ship) and A, B, C and D are functions of the boundary conditions. It should be noted that the load distribution for a vessel is a function of the weight and the buoyancy of the section at each point along its length.

For a simple beam where the load distribution can be defined as a function varying with y, the shear force, bending moment and deflection characteristics can be found by mathematical integration. However, the loading of a vessel cannot usually be described in this manner; hence numerical integration techniques are required. Once the beam characteristics are known, the stresses in the vessel can be assessed using the relationships in Equations (6) and (7).

$$\frac{M}{I_x} = \frac{\sigma}{y} = \frac{E}{R} \quad (6)$$

and

$$\tau = \frac{F\, A\bar{y}}{I_x b} \quad (7)$$

where M is the bending moment, σ is the direct stress, y is the distance from the neutral axis of the section, R is the radius of curvature, τ is the shear stress at the location being assessed, F is the shear force, $A\bar{y}$ is the first moment of area of part of the total section from where τ is evaluated and b is the breadth of the section.

From the above relationships and knowing the material properties of the structure, the stress distribution in the vessel's structure can be calculated. The maximum stress is then compared to the yield strength of the material to assess whether the design is within safe working limits as determined by the utilised factor of safety.

In relation to a damaged vessel, through the use of beam theory, it is possible to assess the direct stress or shear stress in the damaged area due to global bending. By adjusting the first and second moment of area values as applicable in Equations (6) and (7) to reflect the damaged state, damaged bending and shear stresses can be calculated. However, this method has limitations in modelling the true behaviour of the damaged vessel's structure. The method only assesses the strength based on elastic material properties; hence the failure is based on the yield strength or an allowable elastic strength of the material and not the ultimate strength. Similarly the method does not allow the calculation of failure of the structure due to any local collapse mechanism. Equation (7) does not allow assessment of the true shear flow through a complex arrangement as may be found in a ship, particularly when damaged. As such, the method is not suitable in this form for calculating the residual strength of a damaged ship.

2.2.2 Caldwell Method

A more detailed analysis method for assessing the ultimate strength of a vessel is that described by Caldwell [18]. This method describes the ultimate longitudinal strength of a ship as "the bending moment which will 'break the back'[3] of the hull girder" and the margin of safety being "the difference between this ultimate bending moment and the maximum bending moment experienced by the ship during its lifetime". It should be noted that the margin of safety "maximum bending moment" is based on the largest theoretical wave a vessel is expected to see in its intact state and does not consider the influence of the damage on the bending.

When applying the Caldwell method [18] it is possible to assess the failure of structures under tensile and compressive loads. The method assumes that for a transversely stiffened deck, collapse between these transverse frames, termed inter-frame collapse, will be the prominent mode of failure and may occur at a critical value less than the yield strength. By knowing the strength characteristics of the deck structural arrangement, the ultimate strength of the section can be calculated.

[3] The expression "to break the back" of a ship refers to the ultimate failure of the main longitudinal structural members of the vessel's hull. This can either be a tensile or compressive failure.

The method employed by Caldwell [18] to determine the ultimate strength, assumes that the material within the structure that is in tension has fully yielded and all of the material under compression has reached its ultimate buckling strength (calculated by simply factoring down the material yield strength). Therefore, an abrupt change is assumed at the neutral axis between material that has fully yielded under tension to the material buckling under compression, as can be seen in Figure 2.4, where σ_y is the yield strength of the material in tension and $f\sigma_y$ is the collapse strength of material under compression. As more material is allowed to reach its limit state than will occur in an actual vessel, the resulting calculated ultimate bending moment for the section will be greater than the actual value [19], leading to an unconservative assessment of the ultimate longitudinal bending strength capability.

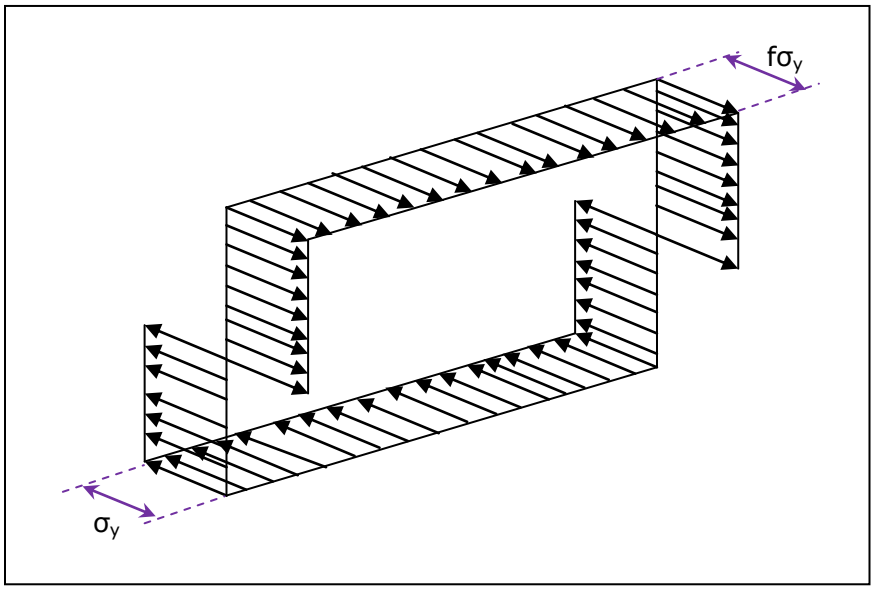

Figure 2.4 - Caldwell method material limit state assumption [18]

To take into account the more realistic scenario where the structural material between the deck and keel is unlikely to reach its limit state, the Caldwell method [18] is further developed by Qi et al. [20] adopting a method developed by Paik et al. [21]. Both methods assume the material in-between the deck and keel initially remains in its elastic state, assuming a linear relationship in the side structure of the section as the forces change from tension to compression, and becoming non-linear as structure progressively yields. This can be seen in Figure 2.5 for a section under sagging moment where σ_{yS}, and σ_{yB} are the yield stresses of the parts of the side and keel in tension, whilst σ_{uS} and σ_{uD} are the yield stresses of the parts of the side and upper deck in compression respectively. N.A. is the location of the neutral axis of the section. The developments made by Qi et al. [20] and Paik et al. [21] lead to the method being more realistic than in the form presented by Caldwell [18].

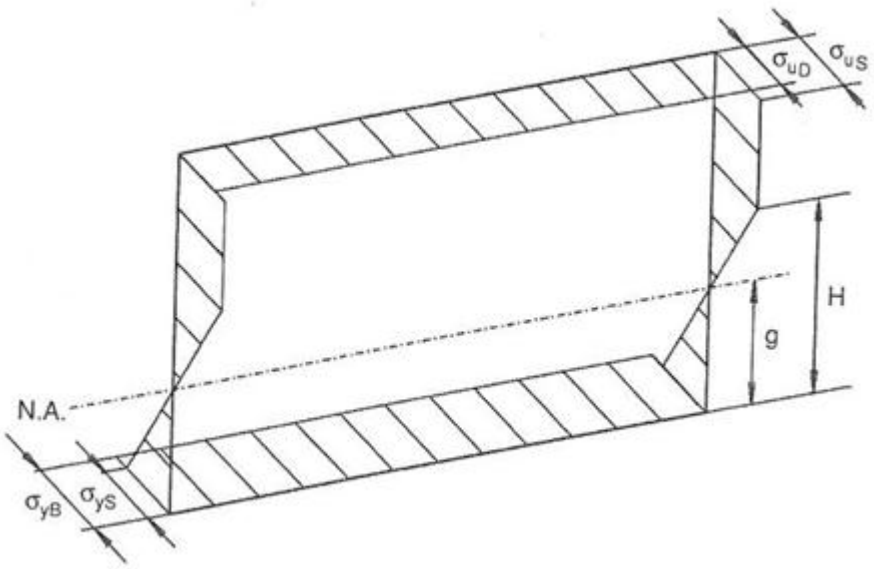

Figure 2.5 - Paik and Qi method material limit state assumption [21,20]

The Caldwell [18] method applies an orthotropic plate assessment to the component parts of the structure to determine the strength characteristics. This is another weakness to the method for application to damaged structural analysis, as the influence of the damage on the structure won't be accounted for in the analysis. Application of the method modified by Qi et al. [20] and Paik et al. [21] is undertaken by implementing structural idealisation in the form originally described by Smith et al. [13,14]. This method is described in detail in Section 2.2.4 and allows more realistic modelling of the structure.

2.2.3 Idealised Structural Unit Method (ISUM)

Reference to the Idealised Structural Unit Method (ISUM) is specifically in relation to the method developed by Ueda et al. [22,23]. In their proposal of the method, Ueda et al. [22] described the concept of structural idealisation as an efficient method of analysing the non-linear behaviour until collapse of structures [24]. In contrast to FEA (described in more detail later in this chapter), whereby the structural response is assessed by discretising the known structural arrangement into small elements with multiple degrees of freedom, ISUM reduces the number of degrees of freedom so that the number of unknowns in the finite stiffness matrix decreases, reducing computational cost. This is achieved by modelling the object structure with large structural units whose structural response behaviour is known under a given load application [25,26]. Ueda et al describe this division into "a relatively small number of the largest possible structural units" [24].

Steel-plated structures are fundamentally constructed of large steel plates, stiffened through the welded attachment of appropriately sized and spaced stiffeners, specific types of which are detailed in Section 2.3. The idealisation of a steel plated structure could be individual plate elements, plate stiffener combinations, columns, etc. Having selected the level of division, the units are constructed containing the least number of nodal connections with the least number of degrees of freedom. The structural responses of the elements are pre-calculated by FEA to allow assessment of all possible modes of failure [24]. The formulation of the solution is then constructed in a similar manner to FEA, though having significantly reduced the number of degrees of freedom in the structure compared to a full FEA model, which reduces the number of unknowns in the finite element stiffness matrix [27]. This ultimately results in a much faster solution time. A flow diagram for the development of an ISUM unit element can be seen in Figure 2.6.

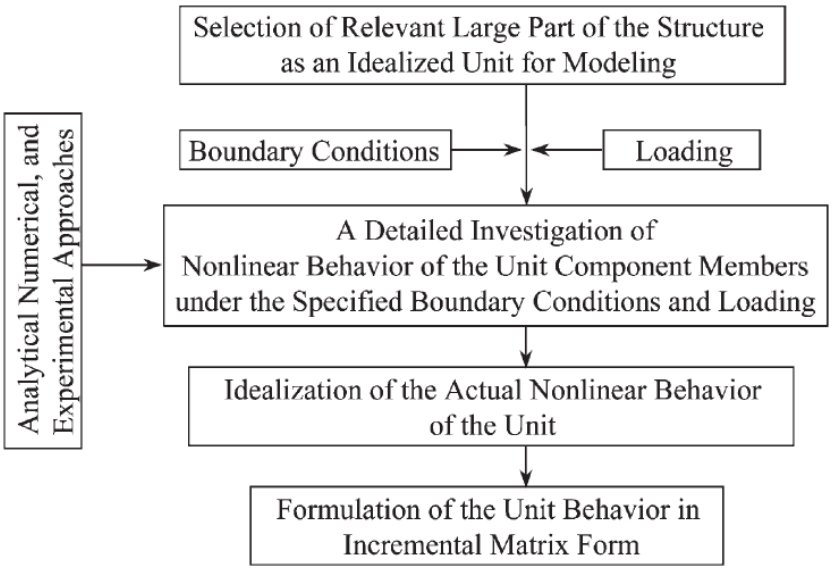

Figure 2.6 – Procedure for the development of an ISUM Unit [27]

Formulation of a ship hull for ISUM assessment is frequently performed by dividing the cross-section into elements of plates between stiffeners and beam-columns to represent longitudinal stiffening members. For the application of ISUM to the assessment of damaged vessels, the assessment is performed by removing the damaged elements from the analysis and calculating the residual strength based on the remaining elements whose structural response remains the same as for the intact condition. Therefore, whilst there are nodal connections between adjacent ISUM elements, the method is not able to account for the influence, or presence, of damage adjacent to them.

In order to increase the fidelity of the global modelling of a vessel, ISUM elements have been coupled with a more detailed finite element model of a particular area of interest. Figure 2.7 shows the model developed by Pei et al. [28] to combine ISUM with FEA, where the central region is modelled using FEA, with the less computationally intensive ISUM elements used to model the forward and aft regions of the vessel. Whilst this type of modelling could lead to improved modelling of a damage scenario, the added complexity of creating the model and the time and computational cost of the detailed FEA modelling of the damaged area does not improve the potential application of ISUM within an emergency response scenario.

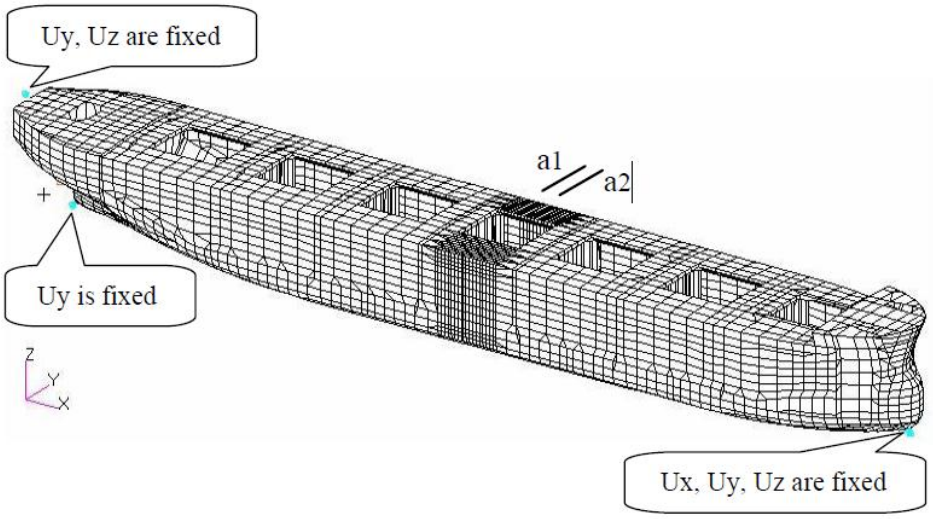

Figure 2.7 – ISUM/FEA Model and Boundary Conditions [28]

Despite developments to ISUM over the years since its conception, Paik et al. [27] state that the number of users of the method in commercial application remains limited. It is not believed that the method is currently used by any emergency response services. However, the concept of structural idealisation is used in other methods, specifically progressive collapse method described below.

2.2.4 Progressive Collapse Method

The term progressive collapse is not limited to the assessment of the failure of marine structures. The term is used when collapse of a structure commences with the failure of one or a few structural components which then progresses over successive components [29].

Focussing on ship structural arrangements and maintaining the assumption, presented by Caldwell [18], that inter-frame collapse is the prominent mode of failure of a longitudinally stiffened and transversely framed vessel, Smith et al. [13,14] first presented a method referred to as progressive collapse method or commonly as the Smith method. This method, to perform the ultimate strength analysis of a ship structure, is implemented by discretising the structure into component parts of stiffened-plate for which the individual structural response is known. Therefore, by understanding the individual responses of the components of the section, the response of the whole section can be calculated. Whilst referred to as progressive collapse analysis, the method is a form of structural idealisation similar to the ISUM [22,23] previously discussed in this chapter, though differs in its formulation. It should be noted that progressive collapse method is the method that is currently implemented by LR SERS, Naval Architectural Design and Classification Society Rules software.

For progressive collapse analysis of ship hull structure, discretisation is commonly made into an assembly of plate-stiffener combination units [25] rather than the separate plate and beam-column elements commonly used in ISUM [27]. The structural response of the idealised units is stored in the form of stress-strain curves, plotting normalised stress against strain, for both tensile and compressive loading from zero, through plastic yielding to failure or collapse, which are calculated experimentally, analytically or by FEA in advance of any progressive collapse assessment. The stress-strain curves in the compressive region are often referred to as load shortening curves, derived from plots of applied load against compressive displacement for specific elements, converted to normalised stress vs strain curves to be more generally applicable.

The method of assessment by progressive collapse analysis is shown by Figure 2.8, which has been devolved from Smith et al. [13], and is undertaken by incrementally increasing the assumed structural deformation due to the applied loads, from which the strains in each of the structural units can be calculated and assessed against the pre calculated stress-strain curves. Upon failure of an element, the element is removed from the analysis and the iteration continued until the overall ultimate collapse strength of the structure is calculated.

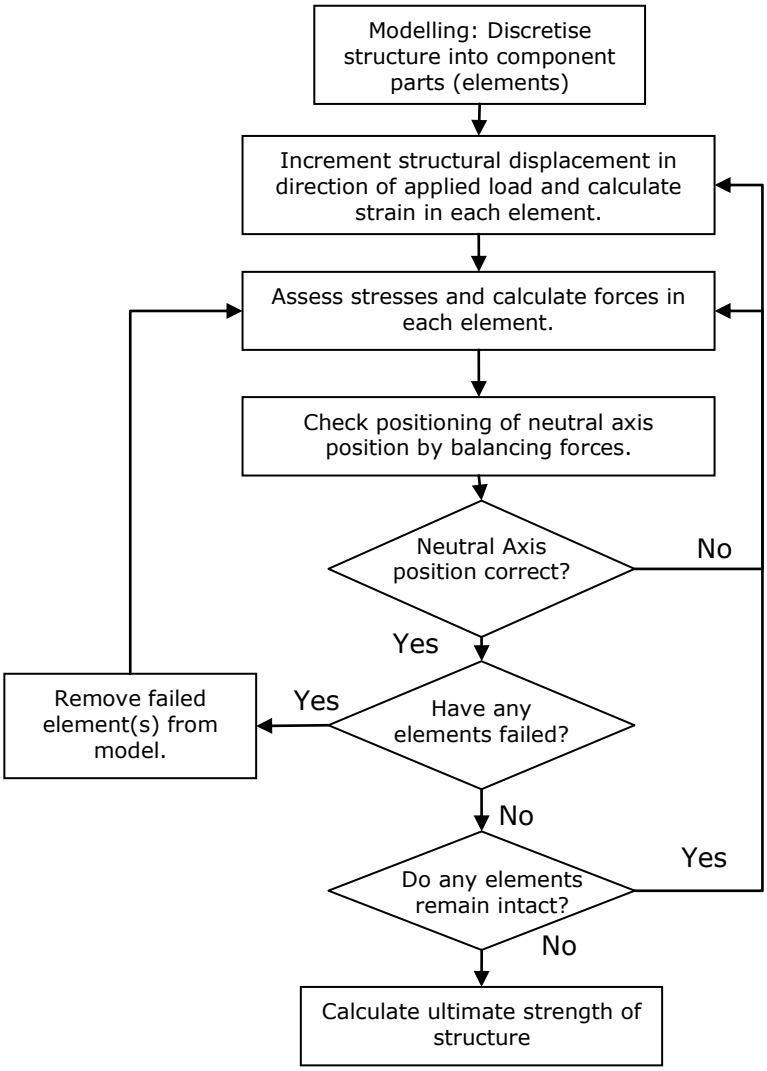

Figure 2.8 – Progressive Collapse application flow diagram

Figure 2.9, shows a typical discretisation of a ship's cross-sectional structure into stiffened-plate elements. In order to use the progressive collapse method to assess the ultimate strength of a ship, the assessment is carried out assuming no deformation in the supporting transverse stiffeners; hence, only the longitudinally stiffened inter-frame structure between transverse frames need be modelled, Figure 2.10, assuming no influence from connecting longitudinal structure.

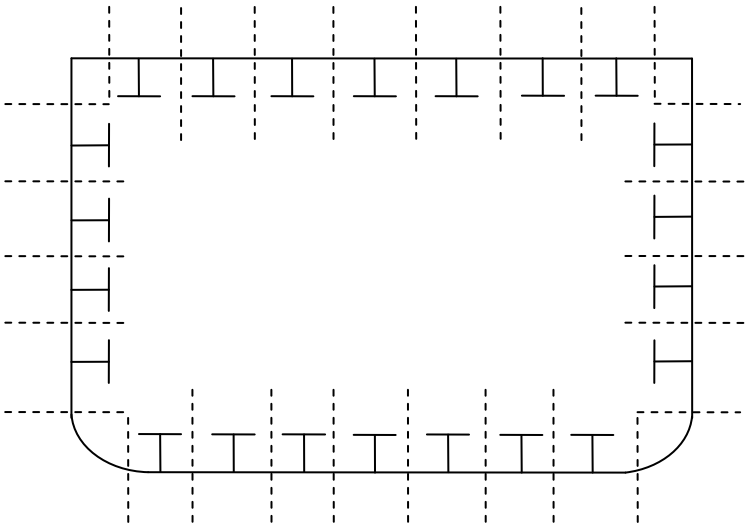

Figure 2.9 - Progressive Collapse Analysis Section Division

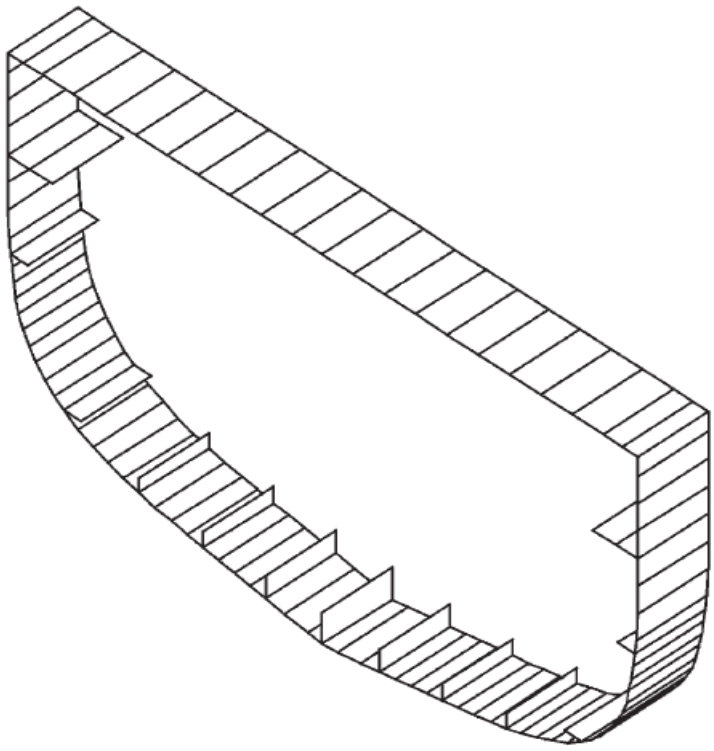

Figure 2.10 – Progressive Collapse Analysis Inter-frame Section Longitudinal Definition [27]

Curvature is induced into the vessel by applying a rotation to the inter-frame section. The relationship between bending curvature (defined as R^{-1}) and rotation angle θ_x is shown in Equation 8 and Figure 2.11, where L is the length of the interframe section [30].

$$\frac{1}{R} = \frac{\theta_x}{L} \tag{8}$$

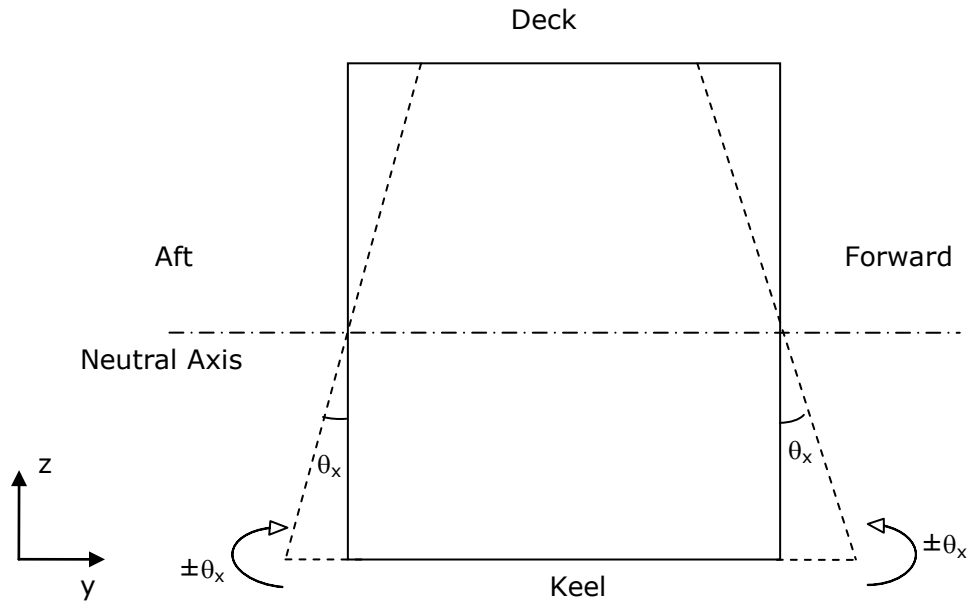

Figure 2.11 – Applied rotation to inter-frame section [30]

Through the use of trigonometry, the displacement and hence strain in each element is calculated. Assessment of the plate stiffener elements is done through the use of pre-calculated load-shortening curves to assess the compressive strength of the structural elements and tensile stress-strain curves to assess the strength of elements under tensile loads. Together, the curves present the strength characteristics of discretised sections of plate-stiffener combinations through the full spectrum of tensile to compressive failure.

An intermediate step is undertaken to check that the assumed neutral axis is correctly positioned, ensuring the sum of element forces above (F_a) and below (F_b) the neutral axis are equal (Equation 9), with the neutral axis repositioned until this condition is achieved.

$$F = \left(\sum_{i=1}^{i} F_{ai}\right) - \left(\sum_{j=1}^{j} F_{bi}\right) = 0 \tag{9}$$

As elements are deemed to have failed by reaching their pre-calculated strain limit, they are removed from the analysis and the section reassessed. The curvature is then further increased until the section cannot support the bending induced stresses and the ultimate strength is calculated.

The modifications to the Caldwell method [18] made by Qi et al. [20] and Paik et al. [21], implement the progressive collapse method by using elasto-plastic analytical methods to directly calculate the strength of the individual idealised structural elements as opposed to the pre-calculated stress-strain curves used by the Smith & Dow et al. method [13, 14].

Applied to the assessment of damaged ship and offshore structures, progressive collapse has been shown to provide reasonable results when compared to FEA [31,14]. Beyond the more detailed modelling of the structure than that afforded by the Caldwell method [18], progressive collapse method will also allow the ability to adjust and tilt the neutral axis of the section to reflect the actual neutral axis of a damaged section.

Developing the progressive collapse method presented by Dow et al. [13], Smith et al. [14] presented a paper using the method to assess the residual ultimate strength of a damaged vessel. As stated by Smith et al. [14], damage to ships caused by collisions, hydrodynamic impact, explosions, etc. usually takes the form of lateral elasto-plastic deformation of stiffened panels (ie out of plane loading causing bending of the plating and/or stiffener), and can lead to a reduction of stiffness and strength in the panel under lateral or in-plane loads, leading to a reduction in ultimate hull-girder strength. In their paper, it is stated that the stiffness and strength of a damaged structure will be influenced by geometric distortion and residual stresses caused by plastic deformation followed by predominantly elastic unloading [14]. The paper presents a number of load-shortening curves for plates under compression with either symmetrical or unsymmetrical damage and suggests changes to the characteristics of the load-shortening curves from those for an intact panel. The authors state that through their work to develop the paper, they have confirmed previous findings that the ultimate strength of a ship's hull is likely to be substantially less than the fully plastic strength due to local compressive failure of stiffened bottom shell or deck panels, and that the ultimate strength is strongly influenced by buckling strength and the post-collapse behaviour of stiffened panels forming the cross section [14].

In their own work to investigate the residual strength of a damaged warship, Ren et al. [19] cite the Smith progressive collapse method as suitable for calculation of residual capability of a damaged ship. This is because, as they state, 'the method reflects the actual collapse increment iteration, and the effect of post buckling of structural components is included. In addition, the assumption of stress distribution in the cross section is not needed in this method, and the asymmetry of the effective residual section can be reflected by adjusting the position of the section neutral axis.' This means that the redistribution of stresses due to the asymmetry caused by the damage is taken into account by adjustment of the location of the neutral axis of the section prior to inducing bending curvature.

Smith et al. [14] finally conclude that in order to fully account for the residual stresses within a damaged structure caused by the damage incident itself, it may be necessary to include a simulation of the damage process in any analysis of residual stiffness and strength, for example using dynamic FEA. This is because in a real damage event, inter-frame collapse may not be the prominent mode of failure due to damage to the transverse frames, though this is not accounted for in the method in the discussed form. Although the pre-calculated load shortening stress-strain curves can be calculated to include damage or distortion, it is not feasible to have curves available for all possible combinations of damage or material state variations that could be present in a damage event.

Reviewing work done by other authors to investigate the residual strength of damaged ships, Das et al.[32] concluded that the work done mainly focuses on either estimating the influence of damaged ship members on the hull girder ultimate strength or is based on empirical and semi-analytical methods. Such analytical methods are used to assess the residual longitudinal strength of a ship after collision and grounding to provide tools to make decisions in event of an emergency, even at the cost of some accuracy [32]. The Das et al. [32] paper presents a procedure based on the Smith progressive collapse method to evaluate the residual ultimate hull girder strength of a damaged ship after collision or grounding, and considers the asymmetrical cross section and shift in neutral axis assessing both vertical and horizontal bending of the vessel.

Das et al. [32] conclude that the use of incremental-iterative approach based on the Smith method is adequate to estimate the ultimate strength of a damaged ship. They also conclude, as would be expected, that the structural arrangement of the vessel significantly influences the damaged hull ultimate strength and that the presence of damage will reduce the ultimate strength of the hull to an extent influenced by the prominent failure mode of the structure. In relation to the location of damage and ultimate strength, Gordo et al. [33] conclude that the hogging[4] moment is much more affected by bottom damage than the sagging[5] moment and in a grounding scenario it is preferable to keep the ship in a sagging condition, as its ability to resist bending remains almost intact.

From the review of whole ship strength, it can be seen that there have been many studies to investigate the intact bending and ultimate strength of a vessel as well as several investigations into the strength of a damaged vessel. Most of these investigations are based around variations of the Smith progressive collapse method and it is this method that is most widely implemented in ship structural analysis software such as Lloyd's Register Ship Rules and Naval Ship Rules software, and commercial naval architectural software such as Paramarine. It is the same method that is also implemented in the LR SERS software as mentioned in Section 1.2.

Guedes Soares et al. [31] undertook an investigation into the accuracy of the Smith method, comparing the results of the ultimate strength of a number of vessels, calculated using the Smith method, to results through the use of finite element modelling of the vessels. It was concluded that the results compared well against each other for both intact and damaged conditions. It was noted that the results from the Smith method were conservative in comparison to the finite element results for hogging by 29.3%. However, it was shown for the test case that the Smith method was not conservative for the sagging condition, calculating an ultimate strength 10% greater than that calculated by FEA, although no experimental work was done to assess the accuracy of either the FEA or analytical methods within the Guedes Soares et al. study [31].

[4] Hogging refers to the two node bending shape of a vessel with amidships section above the bow and stern sections and is the opposite of sagging.
[5] Sagging refers to the two node bending of a vessel with the amidships section below the bow and stern sections producing a bending displacement similar to a simply supported beam with central point load.

The most significant recent development to the progressive collapse method is that made by Benson et al. [34,35] to develop a method to undertake a compartment level assessment. The work recognises the need to potentially assess alternative failure modes to inter-frame collapse in relation to the strength assessment of lightweight aluminium structures. The method implemented uses orthotropic plate approach (as originally used by Caldwell [18] for interframe assessment) to model larger grillage sections of structure across multiple frame bays. This allows assessment of the structure for potential overall collapse modes whilst simultaneously performing the traditional inter-frame assessment; therefore, ensuring the correct failure mode is used in the ultimate strength assessment. Orthotropic plate approach represents a structure, for example a grillage, as a continuous thick plate having different stiffness characteristics in each orthogonal direction. Whilst this approach has been shown to be suitable for the assessment of a intact vessels [34,35] it is not believed to be a suitable method to capture the strength characteristics of large damaged structures. The use of orthotropic plate method is discussed in more detail later in this chapter.

Whilst progressive collapse method is well understood and improvements have been made since its original conception, the following assumptions are made in its application, which limit its ability to fully assess the strength of a damaged ship:

1. Plane sections remain plane and inter-frame collapse is the prominent mode of failure. In the case of a damaged ship, it is unlikely that supporting frames are not deformed or damaged, though this cannot be modelled by the method in its current form.

2. Damaged or partially damaged elements are removed from the analysed section in their entirety. The residual strength of partially damaged structure is not accounted for.

3. The physical separation of the progressive collapse elements at stiffened-plate level does not allow for the influence of the damage on the surrounding structure to be captured in the assessment.

4. Stress-strain curves are limiting for the capture of damage to elements as it is not practical to develop a library of curves for all possible damage permutations in order to be able to capture the residual strength of damaged elements.

5. Pre-stressing of the structure as a result of the damage event is neglected, though local deformation of stiffened-plates can be incorporated.

6. Only bending induced failure is assessed, neglecting any torsional or shear effects.

2.2.5 Shear and Torsion Loads

The methods described above all relate to the ultimate strength of a vessel under bending. Little work has been presented to investigate the effects of shear and torsion loads on vessels. Paik et al. [36] presented a study on the ultimate strength of ships under combined bending and shear forces using FEA. Paik et al. [37] also investigated the strength of ship hulls under torsion to assess the warping effects in the structure. Hu et al. [38] investigated ship hulls under torsion loads to determine the limit state based on the distribution of shear stress and compared to classification rules. The paper concludes that for the large container ships with large hatch openings assessed in the case study, it is necessary to pay attention to torsion loadings [38]. No work has been identified regarding the effects of shear or torsion loads on damaged ships or methods for assessment.

2.2.6 Finite Element Analysis of Global Structural Arrangements

Probably the most versatile and potentially accurate method of assessing the strength of either an intact or damaged structure is Finite Element Method (FEM) through the use of FEA computational software. The level of modelling performed can either be at whole ship, compartment or local sections of structure as required and either static or dynamic in their nature. The previously detailed progressive collapse method and ISUM predominantly use FEA to perform the structural assessment of the plate stiffener combinations, the results of which are then captured and used in the analysis. ISUM then uses the same formulation process as FEA in its implementation.

Advances in the capabilities of commercial finite element software packages and also the processing power of modern computers have led to FEA becoming the preferred means of performing detailed and complex structural analysis in the detailed design phase or investigations following damage events.

FEA divides the geometrical arrangement of a structure into a large number of smaller elements defined by their bounding nodes and containing multiple degrees of freedom at each node. By applying loads and boundary conditions to the structure as well as defining material properties, analysis of the structure can be performed at a detailed level, calculating how the strains, and hence the associated stresses, propagate throughout the structure.

FEA has a lot of advantages over analytical methods in relation to its ability to perform numerous types of analysis at once; whereas multiple calculations may be required to use analytical methods to understand the characteristics of a complex system and ultimately their potential interaction may not be fully understood. The main disadvantages of the finite element method are the time it takes to set up and run an analysis and verification of the accuracy of the results. For a small local piece of structure this could be quite quick, in the region of several hours, though for a large whole ship model it could be weeks or months before reliable results are produced. In a design situation it may well be possible to perform such an analysis; however, in an emergency response situation it is unlikely that finite element analysis will be employed to help give structural information to the crew at the scene.

Although it is not expected that whole ship or compartment FEA models will be built or assessed in an emergency situation, the use of such analysis is relevant to the verification of simpler methods that can be used. As mentioned above, FEA is well proven in its ability to be able to model the complex loading and failure of structures, of which the ultimate bending strength assessment of ship hulls is one not just due to the complexities of the connection between deck and keel with the side shell. Under vertical bending of the form expected to be encountered by a ship at sea, the structure will naturally bend around its neutral axis position leaving a portion of the structure under tensile loading on one side of the neutral axis and the remaining structure on the other side under compressive loading, as detailed in Section 2.2. The failure of a ship's hull section is often progressive in its nature. Prior to the structure reaching its ultimate bending strength, sections of the structure furthest from the neutral axis under compressive loading will usually collapse first, though without leading to immediate total structural failure. This is because, as structure begins to fail the neutral axis of the section will move away from the collapsed structure, rebalancing some of the forces within the section and allowing the structure to resist further bending [30]. Therefore, it is important that the FE model is capable of capturing this complex failure mechanism.

Verification of the developed ship FE model is also challenging, as experimental data is rarely available that is suitable for comparison, leading to the common reliance on simplified analytical or semi-analytical approaches. The Smith interframe progressive collapse method detailed in Section 2.2.4 is commonly used as a verification tool for whole ship FE models. However, benchmark studies undertaken by ISSC 2006 and ISSC 2012 Ultimate Strength committees [39,40] have shown that variations in the calculated ultimate bending strength can occur between users of the Smith interframe progressive collapse method, users of different FE software applications and users of the same FE software applications.

ISSC 2006 [39] presents a comparison of the ultimate strength of a cruise ship calculated by FEA using the commercial LS-DYNA 3D FEA software, with results of the Smith interframe progressive collapse method performed by six different users using the commercial software PROCOL or in house applications that implement the method. Table 2.1 shows a comparison of the results which can be seen to be up to 35.74% greater than the calculated FEA results for the same hullform, showing the interframe progressive collapse method to over predict the ultimate bending strength when compared to FEA.

Method (Analyst)	Ultimate Bending Strength – Hogging (kNm)	Difference of Method to FEA (%)	Ultimate Bending Strength – Sagging (kNm)	Difference of Method to FEA (%)
FEA (Naar)	2.44E+06	-	1.78E+06	-
Smith (PROCOL-Paik)	2.90E+06	15.86	1.93E+06	7.77
Smith (PROCOL-I.C.)	3.07E+06	20.52	2.62E+06	32.06
Smith (PROCOL-Hughes)	3.37E+06	27.60	2.77E+06	35.74
Smith (Principia Marine)	2.97E+06	17.85	2.08E+06	14.42
Smith (Yao)	3.18E+06	23.27	2.37E+06	24.89
Smith (Gordo)	2.66E+06	8.27	2.27E+06	21.59

Table 2.1 – ISSC 2006 Committee III.1 Benchmark Study Results Comparison [39]

More recently, ISSC 2012 Ultimate Strength Committee presented a benchmark study comparing the ultimate bending strength assessment of six hullforms for which the structural arrangement was available for distribution amongst the contributing parties [40]. Similar variation can be seen in the results between users of the Smith interframe progressive collapse method as per the 2006 ISSC benchmark study [39] as well variation in the results between users of the same and different FEA software. The results of the FEA analysis undertaken and the differences between users can be seen in Table 2.2 (a) & (b), with the comparison against the experimental results for the Dow test hull shown in Table 2.3.

The differences presented in the results do not provide a clear indication with regards to the best FEA software to undertake the ultimate bending strength assessment of a hull or box girder structure. However, discussion of the results suggests that some of the discrepancies encountered between FE users may be due to the different modelling approaches and the handling of further complexities such as initial imperfections and residual stresses [40]. A similar account is presented for the discrepancies between results from the Smith interframe collapse method [39], where the strength data for the stiffened-plate and hard-corner elements may be extrapolated from generic curves stored within the software or bespoke data calculated and input by the user before analysis.

	Dow's Test Hull (MNm)		Container (GNm)		Bulk Carrier (GNm)	
Method (Analyst)	Hogging	Sagging	Hogging	Sagging	Hogging	Sagging
ANSYS (PNU)	11.235	10.618	6.969	6.951	17.5	15.8
ANSYS (ISR)	-	-	7.409	7.176	18.326	17.726
ABAQUS (CR)	12.357	10.708	7.664	7.631	18.396	16.855
Difference PNU – ISR (%)	-	-	6.3%	3.2%	4.7%	12.2%
Difference PNU – CR (%)	10.0%	0.8%	10.0%	9.8%	5.1%	6.7%
Difference ISR – CR (%)	-	-	3.4%	6.3%	0.4%	-4.9%

	D/H Suezmax (GNm)		S/H VLCC (GNm)		D/H VLCC (GNm)	
Method (Analyst)	Hogging	Sagging	Hogging	Sagging	Hogging	Sagging
ANSYS (PNU)	14.066	11.151	17.355	16.179	27.335	22.495
ANSYS (ISR)	-	-	21.2	20.21	30.106	28.175
ABAQUS (CR)	16.16	14.258	21.86	20.625	31.006	24.995
Difference PNU – ISR (%)	-	-	22.2%	24.9%	10.1%	25.3%
Difference PNU – CR (%)	14.9%	27.9%	26.0%	27.5%	13.4%	11.1%
Difference ISR – CR (%)	-	-	3.1%	2.1%	3.0%	-11.3%

Table 2.2 – (a) & (b) ISSC 2012 Committee III.1 Benchmark Study Results Comparison [40]

Method	Dow's Test Hull – Sagging
Experimental Test (MNm)	9.64
Smith interframe progressive collapse method (MNm)	9.825
Difference Test – Smith (%)	1.92
Difference Test – ANSYS (PNU) (%)	10.15
Difference Test – ABAQUS (CR) (%)	11.08

Table 2.3 - ISSC 2012 Committee III.1 Benchmark Study Experimental Test Results Comparison [40]

A number of studies to investigate the dynamic collision of ships have been presented demonstrating the capability of FEA to perform dynamic collision simulations of detailed ship models [41, 42, 43, 44, 45]. However, these investigations focus their interest on the crashworthiness of the vessels and the extents of damage caused by a collision, with no assessment made of the residual strength of the vessels post collision. Dynamic damage analysis is a complex scenario to model. It is regularly acknowledged that once the FE models have been created, the simulation time for even a relatively short time sequence can take many weeks to complete. For this reason dynamic simulation of events for use in emergency response has not been considered as currently viable.

2.2.7 Finite Element Analysis with Response Surface Method

Response Surface Methods (RSMs) are becoming an increasingly popular method to allow the use of computationally intensive modelling techniques within computationally intensive analysis techniques to reduce overall computational time. RSM are described by Toal et al. [46] as a surface fitting method, capable of capturing multi-dimensional variations. Conceptually, RSM is a means of fitting a surface through a set of data. Whilst this may be easy to visualise for a set containing three variables, or where animation may be utilised to visualise the surface change with respect to a fourth dimension, it is difficult to visualise a surface containing more variables, though mathematically it is possible.

Response surface models utilise the form utilised by Simpson et al. [47]:

$$y(x) = f(x) + \varepsilon \qquad (10)$$

where y(x) is the unknown function of interest, f(x) is the polynomial approximation of (x) and ε is the random error that is assumed to be normally distributed with mean zero and variance σ^2. The error at each observation is assumed to be independent and identically distributed, whilst the polynomial function f(x) used to approximate y(x) is assumed to be either linear or quadratic [47].

A number of methods for formulating a response surface are available. The simplest forms are first and second order RSMs. These methods use first or second order functions to map between known data points within the defined 'design space'. Whilst the methods can provide good mapping of the design space, as the number of variables being used increases and/or the relationship between variables is non-linear, the development of appropriate formulations becomes increasingly difficult. This can lead to inaccuracies increasing, particularly towards the edges of the design space. An alternative RSM that can reliably develop non-linear response surfaces containing large numbers of variables is 'kriging'.

The kriging method was first developed by Krige [48] for use by geologists to estimate mineral concentrations based on core samples, but is now used in a wide variety of different applications including aerodynamics, structures and multi-objective problems [46]. Kriging is particularly suited to the development of the response surface from "experimental" data, or from FEA. The method uses the known data points as hard points within the surface, rather than the approximation that may result from first or second order RSM. The method then maps between data points to provide a local formulation that provides a smooth surface through the hard data points and their nearest neighbours.

Kriging has been well presented, for example Jones [49] and Forrester et al. [50], and a brief summary is given here. The basis function used within kriging is given in Equation (11),

$$\mathrm{cov}[Y(x^{(i)}),Y(x^{(j)})] = \sigma^2 R\left[\exp\left(-\sum_{k=1}^{n}\theta_k\left|x_k^{(i)}-x_k^{(j)}\right|^{p_j}\right)\right] \tag{11}$$

where predicted estimates, $\hat{y}(x)$, of the response $y(x)$ at untried values of x are given by Equation (12),

$$\hat{y} = \hat{\beta} + r^T(x)R^{-1}(y - f\,\hat{\beta}) \tag{12}$$

where y is the predicted response value at untried x, the sample points, θ are the unknown correlation parameters used to fit the model, $\hat{\beta}$ is the constant underlying global portion of the kriging model, r is the correlation vector of length n, R is an n×n symmetric matrix with a value of unity along the diagonal, f is a column vector of length n and p_j denotes the smoothness of the correlation function.

Equation (11) is used to define the surface, adjusting the values of θ and P_j to optimise the surface and ensure a smooth fit between data points. Equation (12) is used to extract data from the response surface for a desired combination of variables. Accuracy of the defined surface between data points can be influenced by the number of points used and the data's shape. Sufficient points utilising a suitable combination of variables spread across the design space must be used to ensure accuracy of the surface in all dimensions. Tuning of the variable parameters used to define the surface can also improve the accuracy and smoothness of the surface. Sampling methods such as Latin Hypercube are frequently used to define the variables for each data point, for which the experimental or computational data, such as from FEA, is obtained to build the surface.

Assessment of intact or damaged ship structures through the use of RSM has not previously been undertaken. It has been included in this literature review as a method that could be utilised to capture structural data, for example provided by FEA, to be used by a progressive collapse method. This would allow the method to benefit from the advantages of structural modelling by FEA, removing the previously discussed limitations of the current use of stress-strain curves whilst retaining the time benefits of progressive collapse analysis. It is this approach and its potential benefits to emergency response that is researched within this thesis.

The author believes that the method could also allow the structural strength data of larger structural units to be captured and allow a progressive collapse method to be implemented across frame boundaries removing limitations of other methods detailed earlier in this section.

2.2.8 Whole Ship Strength Assessment Conclusions

Whilst methods are available for the assessment of the strength of a vessel in either an intact or damaged condition, when choosing which method to apply in an emergency response situation a compromise must currently be made between speed of obtaining results and their potential accuracy.

Table 2.4 shows how the author perceives some of the key differences that affect the choice of method in both ship design and emergency response scenarios. It is highly unlikely that either full scale or even model scale experiments will be undertaken during an emergency response situation due to the speed and cost involved, though a number of experimental studies have been presented of intact vessels [51, 52, 53].

METHOD	ACCURACY	SPEED	COST
Full Scale Experiment	Very High	Very Slow	Very High
Model Scale Experiment	Medium/High	Very Slow	High
Finite Element Method	Medium/High	Slow	Medium
FEA by Response Surface Method *(Potential)*	Medium/High	Fast	Medium/ Low
Analytical Methods	Medium/High	Fast	Low

Table 2.4 - Structural Assessment Method Advantages and Disadvantages

Due to the speed of performing FEA, it is currently not possible to perform this type of analysis in an emergency response situation in the required timescales, despite the achievable levels of accuracy that have been demonstrated in studies such as by Storhaug [54] to investigate the failure of the containership MSC NAPOLI. Therefore, it is more probable that analytical methods or hybrid analytical methods that utilise pre-calculated strength characteristics by experiment or FEA, will continue to be used.

2.3 Local Structural Idealisation and Strength Assessment

As detailed in Section 2.2, the most commonly implemented method of whole ship structural analysis for both intact and damaged vessels (Smith progressive collapse method [14]), divides the structure of the vessel into smaller discrete elements. By summing the strength of the component parts, it is then possible to predict the overall structural response. Therefore, it is important to understand the structural behaviour of local structural elements.

Within this section, the structural assessment of fundamental components of a ship's structure have been reviewed along with their potential application to damaged structural assessment and use in a progressive collapse analysis.

2.3.1 Strength of Plates and Stiffened-Plates

The most fundamental part of a ship's structure for which the strength characteristics need to be understood is that of a flat plate. The tensile strength of plates is well understood, whilst the compressive strength is a more complex problem. Bryan [55] first investigated the buckling of a simply supported plate under edge compression, presenting methods for assessing the stability of both rectangular and circular plates through the application of energy methods.

Energy methods have been extensively applied for the structural assessment of plates. For a flat plate of length a, breadth b and thickness t, simply supported along all edges and free to move inwards as a result of the in-plane load applied along the length of the plate, it is mathematically possible to determine the critical buckling stress, σ_{cr}, using the Equation (13).

$$\sigma_{cr} = \frac{\pi^2 D}{b^2 t}\left[\frac{mb}{a} + \frac{a}{mb}\right]^2 \quad (13)$$

where:

$$D = \frac{Et^3}{12(1-\nu^2)} \quad (14)$$

and D is the flexural rigidity of the plate, m is the number of half sine waves the plate buckles into along its length, E is the Young's modulus of the material and ν is the Poisson's ratio of the material. It should be noted that in order to buckle, m must be an integer and satisfy the condition a/b≤√(m(m+1)).

Equation (13) is formed by using the assumed displacement field as shown in Equation (15).

$$z = A_m sin\frac{m\pi x}{a} sin\frac{\pi y}{b} \quad (15)$$

Modifying the assumed displacement field, the method can be utilised to assess the critical buckling stress of dented or deformed plates, as presented by Paik et al. [56]. However, manipulations to apply the method to damaged plated structure have not been presented.

The above methods assume that at all times, the material remains in its elastic state. In order to fully understand the ultimate limit state of a plate under in plane tensile or compressive loading in terms of ultimate strength or ultimate collapse strength, more detailed analysis techniques are required. Such results can be plotted on stress-strain curves to demonstrate the strength characteristics in either tensile or compressive loading. Such curves plotted for the in-plane compressive relationship only have historically been referred to as load-shortening curves [57].

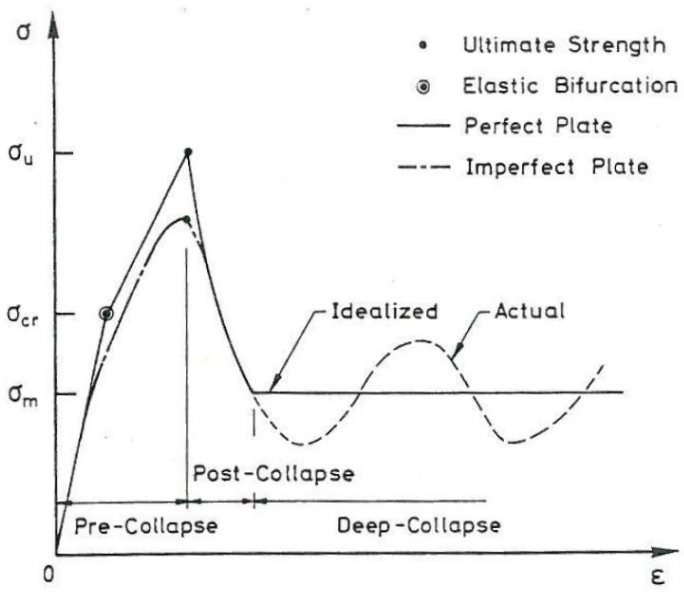

Figure 2.12 – Stages of collapse of thin-walled structures [56]

The analytical method developed by Paik et al. [56] to calculate the pre-, post- and deep-collapse[6] behaviour (Figure 2.12) of plated steel structures under static or dynamic loads, is more applicable when assessing the structure by an elastic and a plastic model for the different collapse phases. In the method, the structure is idealised as a number of plate units to reduce the number of degrees of freedom in the structure and computing time, and assumes no fracture of the material. Modelling of the pre-collapse phase for initial buckling of the plate is undertaken using Equation (13) to calculate the bifurcation point. Post this phase the mathematical model is derived whereby the plate is replaced by an "imaginary" flat plate with reduced equivalent in-plane stiffness to calculate the ultimate strength, which will occur when the most stressed boundaries yield. In the post-collapse phase, the load carrying capacity decreases in the axial direction and is calculated through the average stress increment, $\Delta\sigma_{xav}$, and average strain increment, $\Delta\epsilon_{xav}$, shown in Equation (16).

$$\Delta\sigma_{xav} = (\sigma_{xu} + \frac{a_3}{a_1})\frac{a_3}{a_1}\frac{1}{\epsilon_{xav}^2}\Delta\epsilon_{xav} \qquad (16)$$

where a_1 and a_3 are functions of the mode of failure, length and breadth of plate; σ_{xu} is the ultimate compressive strength and ϵ_{xav} is the average membrane strain [56].

[6] Deep-collapse refers to the collapse stage when compressive displacements are very large and where contact between compressed sections of structure may occur.

When undertaking analysis of the post collapse regime of damaged plating under compressive load, such as following a collision, Paik et al. [56] suggest that an approach based on energy absorption capacity should be used, rather than an approach based on load-carrying capacity, where deformations are considerably larger than the wall thickness [56]. The strength results of the method described by Paik et al. [56] are validated against experimental work undertaken by Ueda et al. [58]. In the studies on the post collapse regime, fracture of the material is not considered, which could be significant, particularly in the deep collapse phase where extensive plastic deformation would be expected.

Significant work to investigate and develop load-shortening curves for plates under in-plane compression was undertaken by Smith et al. [57]. Through the use of nonlinear FEA and regression analysis of test results, load-shortening, stress/strain curves were developed through the full tensile ultimate strength to compressive failure range. The regression analysis drew on results from both European and Japanese large scale tests for plates under in plane tension and compression, simply supported or clamped boundary conditions and unconstrained longitudinal in-plane boundary conditions [57]. A large number of curves are presented for rectangular and square plates under longitudinal and transverse loading with different levels of initial imperfection. Such curves developed in this manner allow more detailed assessment of the strength of the plates and the strength of a vessel's section if incorporated into an idealised structural assessment by including post yield non-linear material properties.

Smith et al. [57], suggest the data could "be used in a simple, lower-bound design procedure without application of supplementary partial safety margins" or "in a more rigorous limit state design process, with the application of supplementary partial safety factors" [57].

The above described research and methods of assessment of the collapse strength of plates relates to intact structure. No work has been identified to investigate the strength of damaged plates. However, Paik [59] investigated the strength of plates with a circular central hole. Through the use of FEA and regression analysis closed form empirical formula were derived for use in "first-cut strength estimations" or reliability analyses [59]. El-Sawy et al [60] present similar design curves for plates under biaxial load with single central hole. Assessment of the structure is again by FEA with the presented curves expected to be used by designers for initial assessment purposes.

Although studies have been undertaken and analytical methods been developed for the elastic and plastic, pre- and post-buckling analysis of plates, it is believed that the idealisation of a ship structure to this level of detail is too fine and implementation of this level of idealisation in a progressive collapse method is limiting due to the high level of discretisation of the structure that is required.

In modern shipbuilding, steel plates are welded together and stiffened through the use of "stiffeners" of short flat bar, 'T', 'L' or offset bulb plate (OBP) sections welded perpendicular to the plate to form stiffened panels as shown in Figure 2.13, or in a lattice formation to form a grillage. Modelling techniques have been developed to assess the strength of grillage arrangements and are believed to be more applicable to the damaged ship structural analysis and are discussed in more detail later in this chapter. Within a structure, plates are bounded by frames and stiffeners which are both generally designed to have sufficient strength to support the plating. Therefore the plate will deform and could fail before the failure of the supporting structure [61]. Therefore, assessment of the plate strength in its own right is still applicable.

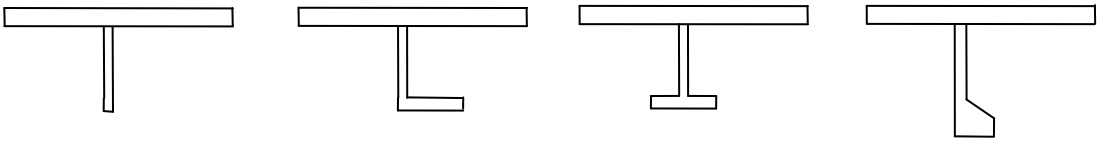

Bar Stiffener | L-Shaped Stiffener | T-bar Stiffened Plate | Offset Bulb Stiffened Plate

Figure 2.13 – Stiffened-Plate Sections

It is possible to idealise the stiffened-plate under in-plane axial compression as a column and undertake an elastic buckling analysis through the use of the Euler formula.

$$\frac{P}{A} = \frac{C\pi^2 E}{\left(L/r\right)^2} \tag{17}$$

where P is the total load, A is the cross-sectional area, E is the Young's Modulus, L/r is the slenderness ratio where L is the original column length and r is the radius of gyration; where $r=\sqrt{I/A}$ and I is the second moment of area of the section. C is a function of the end conditions, where C=1 for simply supported case and C=4 for fully fixed end conditions.

However, implementation assumes the load is in plane axial compression only, hence is not believed to be suitable for use within a progressive collapse method, even if applied using the Secant method to account for eccentricity in the column loading.

Presenting an overview of the methods of ultimate limit state assessment, Paik et al.[62] argue that limit state assessment is now mature enough to enter day-to-day design and strength assessment practice. The ultimate limit state is defined by Zhang et al. [63] as "the point beyond which an additional increment of applied loading cannot be supported". It is argued that the method should be used instead of allowable stress methods as without knowing the ultimate limit state, the true margin of safety cannot be determined [62]. In the assessment of stiffened and unstiffened plates using FEA techniques, it should be noted that ultimate strength behaviour is significantly affected by various parameters such as plate initial deflection shape, boundary conditions and loading conditions among others [62]. Fracture of material is generally neglected when assessing the ultimate limit state, though may be significant when assessing the post collapse region.

Applying energy methods, as detailed earlier in this section, to the assessment of stiffened-plates is more suitable, and analytical formulations have been proposed for the pre- and post- buckling of stiffened-plates [25]. However, as per the assessment of plates, these formulations have not been developed for the strength assessment of damaged stiffened-plates.

Previously described methods allow assessment of direct stresses, however shear stresses in a vessel's structures also need to be considered. Shear stress is particularly prevalent in the side shell and bulkheads of ship structures and needs consideration in the design or assessment of structure. Elastically, the shear stress in a plate can be calculated by the sum of the orthogonal plane strain gradients multiplied by the modulus of rigidity or shear modulus shown in Equation (18).

$$\tau_{xy} = G\left(\frac{\partial \mathrm{v}}{\partial x} + \frac{\partial u}{\partial y}\right) \tag{18}$$

where:

$$G = \frac{E}{2(1+\nu)} \tag{19}$$

where E is the Young's Modulus and ν is the Poisson's Ratio.

Zhang et al. [63] have further investigated the shear in plates to better understand the ultimate shear strength. The case of ultimate strength under pure edge shear of a simply supported plate is considered. The paper proposes Equation (20), which is validated against FEA and other published results,

$$\frac{\tau_u}{\tau_y} = 1 \qquad \text{for } \beta_\tau < 1$$

$$\frac{\tau_u}{\tau_y} = \frac{2}{\beta_\tau} - \frac{1}{\beta_\tau} \qquad \text{for } \beta_\tau \geq 1 \tag{20}$$

where:

$$\beta_\tau = \frac{\beta}{1+\left(\frac{b}{a}\right)^{3/2}} \quad \text{and} \quad \beta = \frac{b}{t\sqrt{\frac{\sigma_y}{E}}} \quad \text{and} \quad \tau_y = \frac{\sigma_y}{\sqrt{3}}$$

where τ_u is the shear strength, β is the plate slenderness, τ_y is the shear yield stress by von Mises relationship for pure shear, E is the Young's Modulus, a is the plate length, b is the plate breadth and t is the plate thickness. Investigation of the ultimate shear strength of plates under edge loads has been further developed by Paik [64] to take into account the effects of dents and initial distortions. Paik [65] also looked at the effects of edge shear on perforated plates in order to provide strength curves for "first-cut strength estimates" [65].

Whilst some of the detailed methods within this section are able to account for distortions and initial deflections in the structural arrangement, none have been applied or assessed in relation to the assessment of damaged structure.

2.3.2 Strength of Stiffened Panels and Grillages

As detailed in Section 2.2, the Smith progressive collapse method [14], assumes that inter-frame collapse is the prominent mode of failure of the vessel being analysed and the supporting frames remain plane. Maintaining this assumption, it has been noted in Section 2.2 that due to the separation of elements at stiffened-plate level the effects of the damage on surrounding structure may not be captured. Increasing the size of the progressive collapse elements may allow such effects to be captured. However, in a damage event, it is unlikely that the supporting frames will remain plane. As a result, inter-frame collapse may no longer be the prominent mode of failure of the hull, longer modes of failure spanning across multiple transverse frame boundaries may be the limiting factor causing failure of the structure. Therefore it is important to understand how longer modes of failure can be calculated through the assessment of larger structural elements such as larger stiffened panels and grillage arrangements.

Idealisation of a stiffened panel can be made in a number of different ways, for example, discretising the structure into a series of beams, into a series of plates and beams, or as an orthotropic plate with increased thickness to account for the increased stiffness due to the presence of the stiffeners, as shown in Figure 2.14 (a), (b) and (c) respectively by Paik et al. [25].

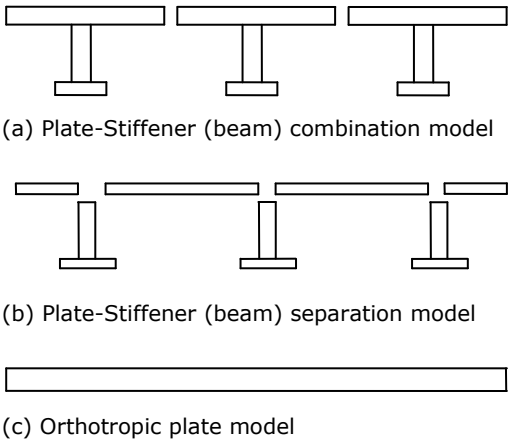

Figure 2.14 - Three types of structural idealization possible for steel-plated structure [25]

Assessment of a damaged stiffened panel by progressive collapse method, as per the technique shown in Figure 2.14(a), would require the removal of the damaged plate-stiffener elements or inclusion of the damage in the modelling of the damaged elements. The former option of removing the damaged elements in their entirety is the approach currently adopted when using this level of discretisation for the strength assessment of a damaged vessel by progressive collapse method. This is because it is unfeasible to incorporate all possible damage combinations in a stress-strain curve library, as per the current method, due to the large number of curves that would be required.

Utilising the discretisation of the panel as shown in Figure 2.14(b), accurate modelling of a damaged panel could be more closely attained. However, due to the detachment of the stiffeners' beam elements from the plate elements, the complexities of the interaction between the plate and stiffeners are not modelled, which may lead to a less accurate assessment. This is the level of discretisation that is implemented within the ISUM method described earlier in this chapter. For the assessment of damaged panel, accurate assessment of the damaged strength would be difficult due to the requirement to either remove damaged or partially damaged structural elements from the idealisation, or to assess the residual strength of multiple component parts for reassembly in to the damaged arrangement. It may be expected that the first option would lead to a conservative estimate of the residual strength, whilst the second option may not lead to an accurate representation of how the damaged structure would actually fail and may lead to an unsafe residual strength assessment by potentially over predicting the damaged strength.

It is not believed that the third method shown in Figure 2.14(c), orthotropic plate approach, is useful when assessing the strength of a damaged stiffened panel, as it is not possible to model any of the detail of the damage event by this method.

Analytical methods for the assessment of intact grillages are well established, be they simplistic approximations by orthotropic plate approach or more intricate techniques. A number of different analytical modelling methods of grillages and stiffened panels are described below.

Intersection reaction method of grillage analysis considers each member of the structure as an individual beam in simple bending. The reaction at each end of the beam under the applied loads is then applied to the supporting member as a point load at the connection. This is then expanded to each member within the section; hence the solution can be obtained for the entire section. Shear deflection in the members and their torsional stiffness are usually neglected. The method can be applied to grillages with irregularities in member stiffness and spacing as well as varying section boundary conditions, as presented by Chalmers [66].

Whilst the aforementioned method is simple to apply, as the section to be analysed increases in its number of members, the assessment process can become quite laborious. Despite this, the method can be applied to the assessment of a damaged grillage by removing the damaged members of the panel from the analysis. However, use of the method is limited to loading that induces bending curvature into the grillage and is not considered suitable for assessment of a grillage that is axially loaded. Therefore, the method is unlikely to be implemented into the assessment of a damaged ship structure where both lateral and axial loadings would be expected to occur within the local structure.

The plate analogy method assumes the grillage to be equivalent to a plate of equal stiffness of the girders in the direction of the girders and the stiffness of the beams in the direction of the beams and is the method applied within the Caldwell method [18] discussed in Section 2.2. This reduces the problem to a plate loading problem, but with different stiffness in each direction, and can be solved by plate theory for an orthotropic plate [66]. This method is the same as that described for assessment of a stiffened panel by orthotropic plate method with equivalent limitations for the assessment of damaged grillage arrangements.

Employing the principles of minimum potential energy of an elastic body under load, energy methods can be used to assess the strain energy in a grillage [66]. Energy methods can also be used to assess the strain energy in a stiffened panel, calculating the deflection of a panel in relation to the modes into which the panel deflects. However, the use of the energy method is limited to assessing the elastic buckling mode of a plate under axial compression and cannot assess the plastic collapse of a panel.

Energy methods have been coupled with plastic methods by Paik et al. [25] to allow buckling and post buckling behaviour of grillages to be assessed, though the methods have not been developed for the assessment of damaged grillage arrangements.

FEA, discussed in Section 2.2, is suited to the assessment of complex structural arrangements such as the analysis of stiffened panels and grillages. However, the time taken to utilise FEA in an emergency response scenario limits direct application. It can be a suitable method to generate structural data for use by other analytical methods, for example the creation of load shortening curves or the use of response surface method as detailed in Section 2.2.

Over the years, a number of individual grillage and stiffened panel studies have been undertaken and presented by different authors.

In their work to investigate welded grillages, Faulkner et al. [17] state that in the failure of a grillage it is the longitudinal stiffeners that provide the support at the unloaded edges of the plate elements. Therefore, failure occurs when the compressive stress at the plate edges and in the stiffeners reaches some limiting value. This leads to two possible modes of failure, strut or 'column' failure of the stiffener-plate, or sideways tripping of the stiffener about its line of attachment to the plate [17].

In terms of grillage failure, it is through general instability where plate and stiffeners act together, yielding due to bending when under axial and lateral loads, or shear yielding of webs under lateral loads that Faulkner et al. [17] consider to be the possible modes.

Smith [67], presented the results of experimental full scale tests on steel grillages under compressive load and developed load shortening curves to describe the failure of the sections.

More recently, Daley et al. [68], undertook a series of experiments to investigate the plastic behaviour and ultimate strength of frames and grillages under lateral loads as part of work undertaken for the Ship Structures Committee. Comparisons were then made to FEA through the use of the ANSYS software package, showing relationships between the different failure mechanisms and overall plastic collapse. Figure 2.15 shows the direction of the loading on an indicative stiffened panel arrangement.

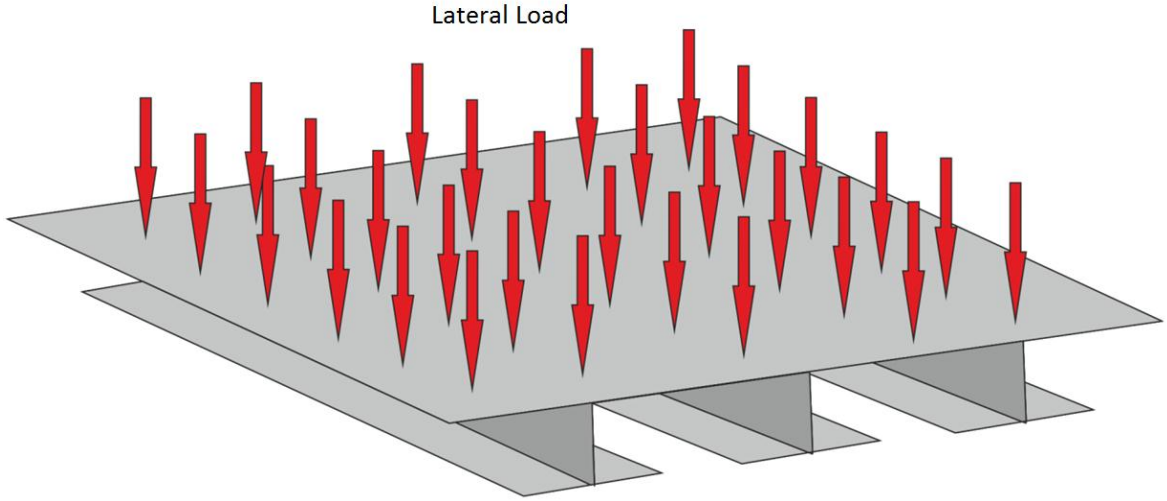

Figure 2.15 - Lateral Loading of a Stiffened Panel

Adopting the generalised Merchant-Rankine formula as a base, Cho et al. [69] developed a method to assess the ultimate strength of a grillage under combined axial compression, end bending moment and lateral pressure. The Merchant-Rankine formula is a numerical method to approximate the collapse load based on the Rankine amplification factor and allows the development of strength formulations whilst reducing influential parameters such as imperfections, load eccentricity, etc. to simple factors within the equations [70]. The applied factors have been developed from a large set of experimental tests which shows to provide improved accuracy to previous methods [69].

In relation to stiffened panels, experimental research was undertaken by Hu et al. [71] investigating the load-carrying characteristics, for the development of load shortening curves, of stiffened steel panels under combined axial and lateral loads though full scale testing. Twelve panels were tested and included deformed and damaged panels as well as "as-built" sections [71]. The results of the testing showed that the panels failed by combined plate and flexural buckling, stiffener tripping or local collapse, depending on the magnitude of lateral loads and local damage. The developed load shortening curves showed that small lateral load could change the failure mode from flexural buckling to tripping [71]. In a damage situation, knowledge of the extent of damage in terms of deformation of panels beyond any obviously holed section could be significant in determining the overall residual structural strength of the section.

Similar analysis to that undertaken by Hu et al. [71] on stiffened panels was studied by Nikolov [72] using FEA and considering the effect of residual stresses and deflections. Within the FEA, the damage was simulated by application and removal of lateral pressure causing elasto-plastic symmetric deformation and residual stresses. Nikolov's results showed that the compressive strength may be overestimated by more than 15% when damage related to residual stresses is not considered. Nikolov also concluded that for 'stocky', low aspect ratio, panels with uniform 'dishing', or indentations, the compressive strength may increase and that a larger magnitude of initial dishing does not necessarily result in a lower ultimate strength. This is due to the potential for the dishing to stabilise the panel and preventing buckling mode development [72].

Investigating different computational methods to analyse the ultimate limit state of stiffened panels subjected to combined biaxial compression and lateral pressure actions, Paik et al. [73] presented comparison of results obtained through the use of ANSYS non-linear FEA software with results from DNV PULS (Panel Ultimate Limit State) method and the authors' own ALPS (Analysis of Large Plated Structures)/ULSAP (Ultimate Limit State Assessment Program) methods. The results show both methods provide close results to those obtained from the ANSYS FEA software.

Whilst there has been significant work undertaken to investigate the strength of a grillage or stiffened panel, little work has been undertaken to investigate the strength of these structures under damaged conditions.

Witkowska et al. [74] investigated the collapse strength of stiffened panel with local dent damage as would be caused by the fall or strike of an object. In their research they found that the panels retained a good amount of performance when dented; however, depending on geometrical characteristics, stiffener deformation could occur which may significantly lower the ultimate strength of the panel [74].

Due to the presence of access or lightening holes in tanks and voids of ship and offshore structures, some work has been undertaken to investigate the effects on the strength of stiffened panels with central cut-outs.

In 1993, work was presented by Gendy et al. [75] on their investigation of the strength of stiffened panels with regular cut-outs under bending and shear. In their work they presented design curves for the buckling stresses of simply supported stiffened panels with central cut-outs and lateral stiffeners under in-plane loading calculated by energy method. In the development of the curves, a formulation based on the Hellinger/Reissner mixed variational principle with independently assumed displacement and strain fields was formulated. The developed design curves presented are for stiffened panels of varying aspect ratio between 0.75 and 1.25, with central cut-out varying between 20% and 50% of the panel's surface area.

By physical experimentation, the problem investigated by Gendy et al. [75] was investigated by Alagusundaramoorthy et al. [76] in 1999. Collapse tests were carried out on eighteen longitudinally stiffened steel panels with cut-out and initial imperfections under axial compression, with simply supported boundary conditions along both loaded and unloaded edges. The panels were stiffened with open section rectangular flats. Six panels without cut-out, six with square cut-out extending full width between stiffeners (d/b=1.0), four panels with rectangular cut-out (d/b=1.5) and two panels with reinforced rectangular cut-out were tested [76].

Failure of the specimens was shown to occur rapidly [76], synonymous with the load exceeding the critical buckling stress where stability of the panel rapidly diminishes. Load deflection curves of the different panel arrangements were presented in the paper. The results show that the presence of a cut-out reduces the strength of the panel for both plate and stiffener initiated failure. It was also shown that the presence of a rectangular cut-out reduces the strength of the panel to a greater extent than a square cut-out [76].

The work done by both Gendy et al. [75] and Alagusundaramoorthy et al. [76] provides a basis to the more recent work undertaken by Suneel Kumar et al. [77], presented in 2009. The paper itself presents a numerical study on the ultimate strength of a stiffened panel with central circular opening subjected to axial load, lateral load and a combination of axial and lateral loads. Evaluation was undertaken considering geometric and material non-linearities using ANSYS FEA software. Arrangements of different stiffener spacing and open section unequal angle stiffener dimensions were assessed, covering plate and column slenderness ratios of 1.0 - 4.5 and 0.32 - 1.0 respectively, keeping the opening ratio (the ratio of hole diameter to stiffener spacing) equal to 1.0 were considered [77].

The developed interaction curves for stiffened panels with angle stiffeners and circular opening were found to be non-linear for lower plate slenderness ratio up to 2.0 and for the range of column slenderness ratio covered by the study. Interaction equations were also proposed based on non-linear regression analysis for determining the ultimate strength of stiffened panel under axial, lateral and combined axial and lateral load [77].

Whilst the work undertaken by Gendy et al. [75], Alagusundaramoorthy et al. [76] and Suneel Kumar et al. [77] applies methods to assess a holed stiffened panel, in each case the assigned hole is centrally placed and of a regular shape and there is no discontinuity in the stiffeners, i.e. all of the stiffeners run continuously from edge to edge of the panel. In the case of a damaged ship section, it is unlikely that the damaged area will be a regular shape with rounded edges and it is also likely that one or more stiffening members will be breached.

2.4 Modelling of Geometric Imperfections in Welded Steel Panels

Discussion in Section 2.3.2 concerned the effects of initial imperfections and residual stresses in steel stiffened-plates, panels and grillages on the ultimate collapse strength of the structure. This is echoed in the proceedings of the International Ship and Offshore Structures Ultimate Strength committee report in 2009 [78] where it is noted that initial imperfections are a significant parameter in the design and modelling of stiffened panels and are believed to be a similarly influential parameter for the modelling of orthogonally stiffened panels. Initial imperfections and residual stresses occur predominantly due to imperfections in the base material from its own manufacturing process or the welding process during fabrication, where weld induced residual stresses are introduced due to the heat generated from the process leading to deformation of the panel which does not reduce once cooled [79,80].

When modelling initial imperfections, great effort can be applied to accurately model the exact imperfections that have been measured within existing structures. However, the intention of the modelling is to include the imperfection size in a form that will ultimately allow the structure to assume the correct failure mode as the collapse develops. If initial imperfections are not included, the structure may fail under pure compression of the material due to its geometrical perfection, which is not achieved in reality. In the modelling of plates, stiffened-plates and stiffened panels with simply supported boundary conditions and under axial compressive load, the expected mode of failure may be considered to be a single half sine wave along the length of the panel, being equivalent to the buckling mode that may give the lowest resistance against the load [73]. Eurocode EN1993-1-1 refers to this form as a bow imperfection [81].

However, in the modelling of grillages where the boundary conditions are more rigid, the definition of the mode of failure is more complex and a more detailed definition is required.

In total, three forms of initial imperfections are seeded into a model to account for the potential failure modes in the plate and stiffeners. These are plate vertical imperfection (w_{opl}), stiffener column-type vertical imperfection (w_{oc}) and stiffener sideways imperfection (w_{os}). Application of the imperfection modes of failure is commonly achieved through the use of a Fourier series as shown in Equations 21-23.

$$w_{opl} = \left[\sum_{i=1}^{m} A_{om} \sin\left(\frac{m\pi x}{a}\right) sin\left(\frac{\pi y}{b}\right)\right] w_{oplm} \quad (21)$$

$$w_{oc} = \left[\sum_{i=1}^{n} A_{oi} \sin\left(\frac{i\pi U}{a}\right)\right] w_{ocm} \quad (22)$$

$$w_{os} = \left[\frac{W}{h_w}\sum_{i=1}^{n} A_{oi} \sin\left(\frac{i\pi U}{a}\right)\right] w_{osm} \quad (23)$$

where A_o is the coefficient of the initial deflection shape, m and i are the mode shape number, a and b are the plate or stiffener length and plate breadth respectively, x and y are the location along the length and across the breadth of the plate respectively, U is the position along the length of the stiffener and w_{oplm}, w_{ocm}, w_{osm} are the maximum imperfection values for each imperfection type.

The equations are based on a specified maximum initial imperfection for each type for which values can be calculated based on the relationships defined in Table 2.5 presented in work from Smith [82] and ISSC 2009 [78].

	Smith [82]			ISSC [78]
	Slight	Average	Severe	
w_{oplm}	$0.025\beta^2 t$	$0.1\beta^2 t$	$0.3\beta^2 t$	b/200
w_{ocm} (λ>0.2) (λ>0.4) (λ>0.6)	0.00025a	0.0008a 0.0012a 0.0015a	0.002a 0.0038a 0.0046a	0.0015a
w_{osm}	-	-	-	0.0015a

Table 2.5 – Maximum initial welding imperfection definitions for stiffened steel panels

When considering the initial imperfection shape of the plating of a stiffened steel plated structure (Equation 21), it is often considered more realistic to model the imperfection shape as a single displacement direction in a "hungry" or "thin-horse" mode [40,82,83,]. In this form the deflection direction between stiffeners is the same across the panel and not alternating as would be the case for a standard sine wave form. Along the length of the plate, the dominant form of weld induced imperfections is of a "barrelled" shape (Figure 2.16) [79,84]. Ueda et al. [80] state that for plates under compressive loading, "all components of the initial deflection increase until the load approaches the buckling load." "When the plate is thin, the deflection increases further before plasticity occurs. Above the buckling load, only one mode component of initial deflection is amplified and becomes stable. This mode is not necessarily the buckling mode, but is usually one or two modes higher. Only the component of the stable deflection mode influences ultimate strength." Configuration of this desired initial imperfection form can be achieved through the summation of the single half sine wave mode with the two mode shapes above the elastic buckling mode, calculated as,

Elastic Buckling Mode = ((a/b)+1) (24)

where a is the plate length and b is plate breadth. Within Equation 21, the influence coefficients A_o for the single half sine wave form and lowest elastic buckling mode plus one having coefficient are set to 0.8 and 0.2 respectively [79,34]. To prevent the developed shape being perfectly symmetrical, which can lead to solution instability problems, the second mode above the lowest elastic buckling mode is also included, with coefficient A_o of 0.01 [79,34]. A single half sine wave form is utilised across the breadth between longitudinal stiffeners (Figure 2.17).

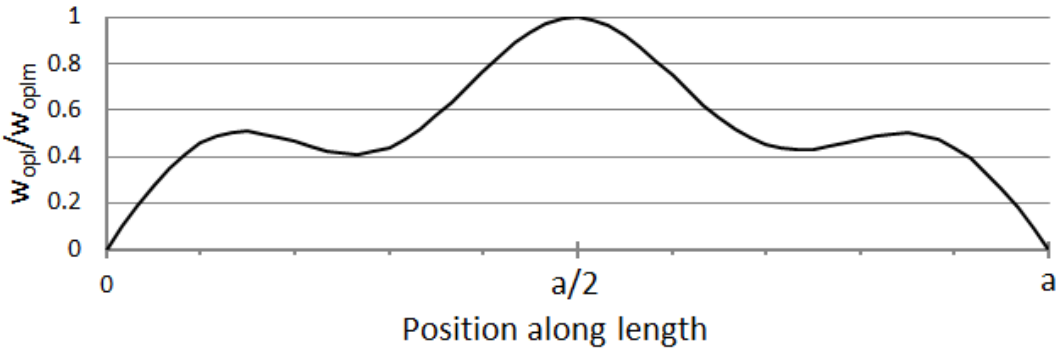

Figure 2.16 – Example plate imperfection shape along length between transverse stiffeners at b/2

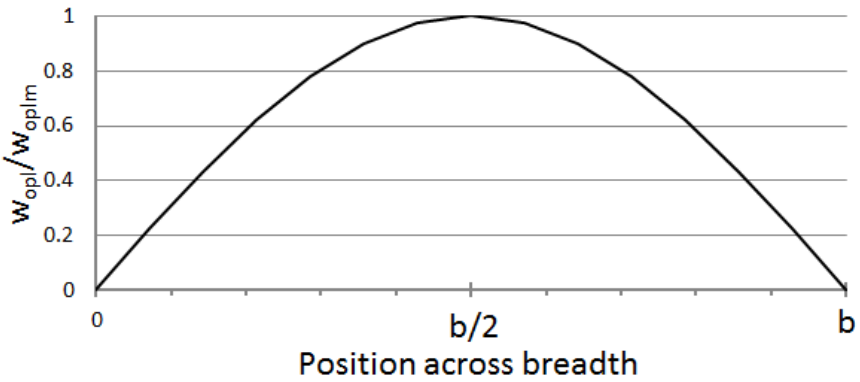

Figure 2.17 - Example plate imperfection shape across breadth between longitudinal stiffeners at a/2

Complementing the "hungry-horse" form, a single direction column imperfection is utilised, whilst an alternating direction stiffener sideways imperfection is used. Figure 2.18 shows an example displacement plot of the applied imperfections prior to application of the axial compressive loading.

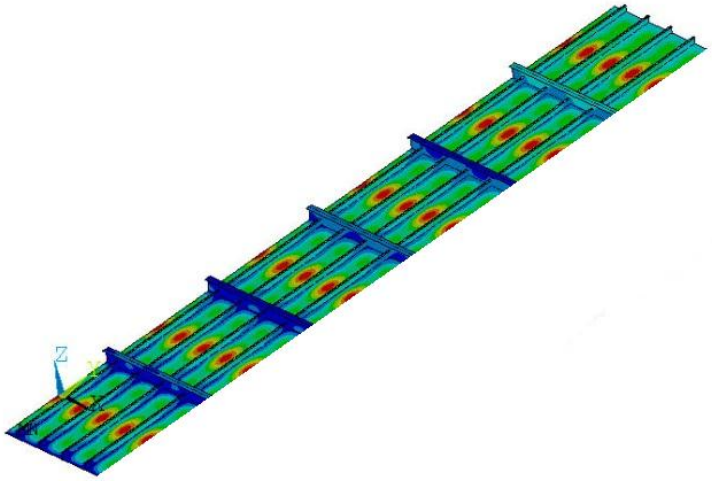

Figure 2.18 - Example displacement plot of applied imperfections

Residual stresses are the internal stresses which remain within the material of a plate or shape after the thermal cycle of welding [85]. These residual stresses develop as tensile stresses in the heat affected zone and complimentary compressive stresses away from the heat affected zone [25]. Figure 2.19 shows a typical idealisation of residual stresses within a plate welded along all four edges, where σ_{rtx} and σ_{rty} are the residual tensile stresses in x and y direction respectively and σ_{rcx} σ_{rcy} are the compressive residual stresses in the x and y direction respectively.

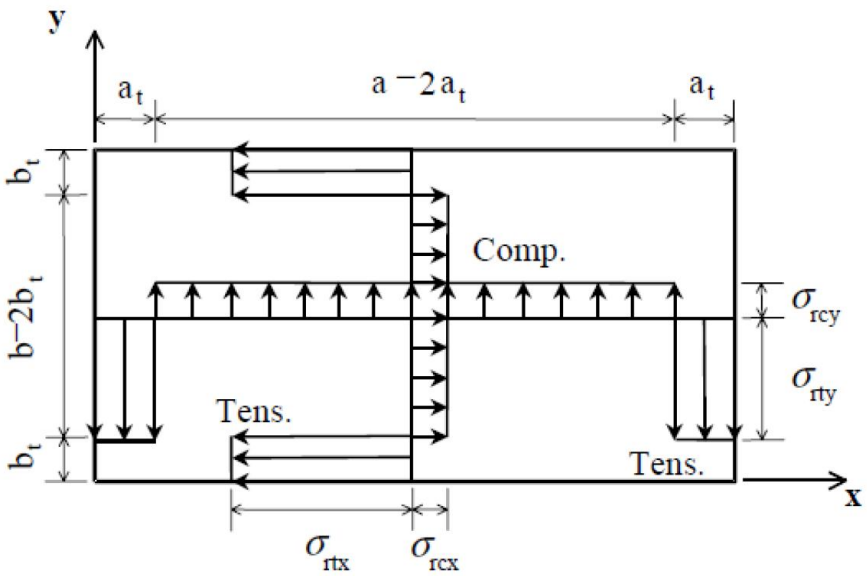

Figure 2.19 – Typical idealisation of weld induced residual stresses in steel plates [25]

Whilst formulations have been presented to quantify the tensile and compressive stresses [25], it is accepted that the residual stresses in welds may be partly or fully redistributed or relaxed during the elastic shakedown caused by overload during the operation of the ship's hull structure [40]. Therefore, quantifying the residual stresses in an aged vessel is difficult and quantifying the existence of residual stresses in a damaged vessel could be almost impossible.

2.5 Structural Design Codes

A number of design codes are available for the strength assessment of steel structures. UK MoD design codes for the design of ship or submarine structures are SSCP 23 [86] (now extant and incorporated into Lloyd's Register's Naval Ship Rules [87]) and SSP 74 [88] respectively. These codes provide structural guidance for the design of steel-plated structures in respect to their specific applications, presenting formulations for design purposes. These guides do not provide any information regarding the strength of damaged structure, utilising sufficient safety margins to allow for residual strength in a damage scenario.

Lloyd's Register's Naval Ship Rules [87] provides details for the residual strength assessment of a damaged vessel to be undertaken in the design phase to ensure adequate survivability of the vessel. The assessment can be performed using the Lloyd's Register Naval Ship Rules software, which implements the progressive collapse method as previously detailed in Section 2.2 of this thesis.

British Standard Eurocode BS EN 1990:2002 entitled "Basis of structural design" [89], proposes a limit state approach to the design of structures. Eurocode EN1993-1-1 [81] regarding steel structures and buildings and Eurocode EN1993-2 regarding steel bridges [90] both look to implement the basis of limit state design to their relevant structures. Whilst all three codes refer to the need for accidental limit state consideration, none specify how damaged structural assessment should be handled in the design phase, or what effects damage may have on the local or global structural response. However, within the code it is specified that all efforts should be made to reduce the risk of damage to a structure and sufficient redundancy should be present in the structure for it to survive the removal of an individual member or part of the structure or the occurrence of acceptable localised damage [89].

2.6 Literature Review Overview

2.6.1 Global Strength

From the reviewed literature it can be seen that a number of analytical or semi-analytical methods have been developed for the global strength assessment of intact structures. Some of these methods, in particular the Smith interframe progressive collapse method, have been well developed and applied widely in numerous studies and software applications for the ultimate strength assessment of a vessel under bending. The method has also been applied to the strength assessment of damaged ship structures, though a number of weaknesses have been identified which are presented in Section 2.2.4. Despite these weaknesses, the progressive collapse method is considered to be the current state of the art method for the strength assessment of intact and damaged ship structures.

Table 2.6 shows how the referenced literature can be categorised to demonstrate the limited extent of work that has been presented in relation to the global strength assessment of damaged ship structures. No methods have been developed for the incorporation of torsion or shear loads into assessments of the global strength of a damaged vessel.

In advancing the global strength assessment of damaged ship structures, this research looks to address the weaknesses identified in the current state of the art method by developing a new methodology for the ultimate bending strength assessment that may in future be able to incorporate the assessment of shear and torsion loading assessment on a damaged vessel.

2.6.2 Local Strength

From the reviewed literature it can be seen that a large number of numerical models exist for the assessment of local steel-plated structural arrangements. However, as demonstrated by Table 2.7, a limited quantity of published literature exists for the assessment of structure with cut-out holes or damaged structural arrangements. This lack of information indicates a need for the advancement in the understanding of the structural capability of damage stiffened steel structures and efforts will be made within this research to advance the knowledge in this area. The expected areas of novel contribution of this research, with respect to local strength assessment, are shaded grey in Table 2.7.

2.6.3 Structural Methods Overview

To summarise the methods reviewed within this literature, Table 2.8 is presented to collate the methods and their capabilities. The table shows that whilst a number of methods of varying speed are available for potential use for the global strength assessment of a damaged vessel, compromises have to be made between speed and potential accuracy when selecting the appropriate method to implement for the required scenario. As quick methods are required for implementation in an emergency response scenario, currently the modified Caldwell and interframe progressive collapse method are the only available options. The key difference between the two methods is that the modified Caldwell method utilises analytical methods for the assessment of structural elements, whilst the interframe progressive collapse method utilises FEA to pre calculate stress-strain curves for use by its solution algorithm. Implementing interframe progressive collapse analysis in its current form on a pre-defined ship model using pre-calculated stress-strain curves, the model can be amended to reflect the damage condition and provide bending strength information within an hour.

In relation to local strength assessment of damaged structure, Table 2.8 shows the lack of methods available.

All of the identified potential methods for damaged strength assessment, except for interframe progressive collapse method and ISUM, are slow to implement and hence not suitable for application in an emergency response scenario. Whilst interframe progressive collapse method and ISUM are potentially quick to implement in a damage scenario, time consuming setup is required to fully implement the methods.

	Intact	Damaged Vessel - Raking	Damaged Vessel - Collision	Damaged Vessel - Aged/ Corroded
Static Bending	[13] [14] [18] [19] [20] [21] [22] [23] [24] [25] [26] [31] [32] [33] [34] [35] [36]	[13] [14] [19] [20] [21] [31] [32] [33] [91]	[13] [14] [19] [20] [21] [31] [91] [92]	[15] [93]
Shear Loading	[22] [23] [24] [25] [36]	*None Found*	*None Found*	[15]
Torsion Loading	[37] [38]	*None Found*	*None Found*	*None Found*
Numerical Models Developed	[13] [14] [19] [20] [21] [22] [23] [24] [25]	[13] [14] [19] [20] [21] [91]	[13] [14] [19] [20] [21] [91]	*None Found*
Experimental Tests	[51] [52]	*None Found*	*None Found*	*None Found*

Table 2.6 - Global Structural Strength Reference Matrix

	Plates with Cut-outs	Stiffened-Plates and Panels with Cut-outs	Grillages with Cut-outs	Damaged Plates	Damaged Stiffened Plates/Panels	Damaged Grillages
Static Axial Loading- Tensile	*None Found*	*None Found*	*None Found*	*None Found*	*None Found*	*None Found*
Static Axial or Biaxial Loading- Compressive	[59] [60] [65]	[75] [76] [77]	*None Found*	*None Found*	*None Found*	*None Found*
Static Bending	*None Found*	[75]	*None Found*	*None Found*	*None Found*	*None Found*
Shear Loading	[65]	*None Found*	*None Found*	*None Found*	*None Found*	*None Found*
Numerical Models Developed	[59] [65]	[75] [75]	*None Found*	*None Found*	*None Found*	*None Found*
Experimental Tests	*None Found*	[76]	*None Found*	*None Found*	*None Found*	*None Found*

Table 2.7 - Local Structural Strength Reference Matrix for Holed and Damaged Structure

Arrangement	Method	Loading Tensile (T), Compressive (C), Bending (B)	Can Include Damage in Arrangement?	Elastic/ Non-Linear	Comparative Accuracy		Comparative Speed of Assessment
					Intact	Damaged	
Plate	Energy Method	T,C,B	No	E	Good	N/A	Quick
	Finite Element	T,C,B	Yes	E/NL	Very Good	Very Good	Slow
Plate and Single Stiffener	Beam Theory	B	No	E	Average/Good	N/A	Quick
	Column Buckling	C	No	E	Average	N/A	Quick
	Finite Element	T,C,B	Yes	E/NL	Very Good	Very Good	Slow
Stiffened Panel	Beam Theory	B	No	E	Good	N/A	Quick
	Orthotropic Plate	T,B,C	No	E	T,B = Average C = Poor	N/A	Quick
	Energy Method	T,B	No	E	Good	N/A	Medium
	Finite Element	T,C,B	Yes	E/NL	Very Good	Very Good	Slow
Grillage	Intersection Reaction Method (Beam Theory)	B	Yes	E	Good	Average/ Good	Slow
	Plate Analogy/ Orthotropic Plate	T,B,C	No	E	T,B = Average C = Poor	N/A	Quick
	Energy Method	T,B	No	E	Average/Good	N/A	Medium
	Idealised Structural Unit Method (ISUM)	T,C,(B)	Yes	E/NL	Good	Good	Quick
	Finite Element	T,C,B	Yes	E/NL	Very Good	Very Good	Slow
Inter-Frame Analysis	Caldwell Method	T,C,B	No	E	Poor	N/A	Quick
	Modified Caldwell Method	T,C,B	Yes	E/NL	Good	Average/Good	Quick
	ISUM	T,C,B	Yes	E/NL	Good	Average/Good	Quick
	Progressive Collapse	T,C (B)	Yes	E/NL	Good	Average/ Good	Quick
	Finite Element	T,C,B	Yes	E/NL	Very Good	Very Good	Very Slow
Compartment or Whole Ship	Finite Element	T,C,B	Yes	E/NL	Very Good	Very Good	Very Slow

Table 2.8 - Structural Arrangement Analysis Methods Overview

3 METHODOLOGY

3.1 Research Methodology

As discussed in Section 2.2, the most commonly implemented method of assessing the ultimate strength of an intact or damaged ship is through the use of interframe progressive collapse method, utilising the concept of structural idealisation by discretising the vessel's interframe structure into elements of plate-stiffener combinations [14]. Whilst the method has been proven to have good accuracy when assessing an intact vessel's ultimate strength, the scenario of a damaged vessel is understandably more complex. A review of the method has identified a number of potential weaknesses for application to damaged ship analysis, which are listed in Section 2.2.4. However, due to the lack of research into the effects of damage on the strength of stiffened steel plated structures, as identified in Table 2.7, it is currently unclear if all of these identified weaknesses are correct, or whether the current methodology is suitable for the assessment of damaged vessels.

The research into the strength assessment of damaged steel plated structures has been approached in relation to the identified interframe progressive collapse weaknesses; primarily though development of the understanding of the influence of damage on the ultimate strength. Further to this research, work has been undertaken into an alternative method for damage strength data capture and finally the test of a proposed new method to undertake the bending strength assessment of a damaged vessel.

3.1.1 Damage Influence

Under vertical bending, a vessel would be expected to fail by interframe collapse, initiated by the compressive failure of the longitudinally stiffened structure. The current interframe progressive collapse method fundamentally works due to the understanding of the collapse strength of the component parts, or elements, that the vessel is divided into. The level of discretisation is at stiffened-plate level, which is believed to be the lowest level of discretisation that allows the true collapse mechanism of the structure to be understood. Therefore, it is critical to understand the ultimate compressive strength of damaged structure to be able to judge the effectiveness of the interframe progressive collapse method for use in a damage scenario.

To understand the influence of damage, in the form of a hole, on the collapse strength of stiffened steel structure, and to evaluate the validity of weakness 1, 2 and 3 (surrounding the inability to allow distortion in supporting frames or account for the influence of the damage on the surrounding transverse or longitudinal structure and its influence on the developing failure mode) identified in Section 2.2.4, research studies were undertaken at three distinct levels through the use of non-linear FEA, and are presented later in this thesis. The first is at stiffened-plate level, maintaining the level of discretisation consistent with the current interframe progressive collapse method. The second is a stiffened panel, which again maintains the assessment of interframe collapse. The final level is that of damaged grillage arrangements, allowing assessment of both interframe and potential overall collapse modes of failure and the influence of damage on such failure modes.

The research undertaken has demonstrated the weaknesses 1,2 and 3 to be correct, demonstrating the need for alternative analysis methods to interframe progressive collapse for the assessment of damaged vessels.

3.1.2 Damage Strength Data Capture

The use of stress-strain curves for the capture of structural data for use in progressive collapse analysis has been identified as weakness number 4 in Section 2.2.4. To resolve this weakness, the use of response surface method using FEA of damaged structural arrangements has been researched for the capture of the required structural data. This was done at both stiffened-plate and grillage level structural idealisation with the expectation that using larger progressive collapse elements would allow the capture of the influence of the damage on the collapse strength of the structure.

The research has demonstrated the use of the RSM kriging as suitable for the capture of damaged strength data.

3.1.3 Compartment Level Progressive Collapse Analysis

The research concludes with demonstration of a compartment level progressive collapse assessment, demonstrating the benefits of utilising this approach and the potential hazards of using the interframe method for damaged strength assessment. Further details of the proposed new method for compartment level progressive collapse can be seen below.

3.2 Damaged Ship Structural Analysis Tool Methodology

As detailed in Section 1.3, the initial transient and progressive flooding phases of a damage incident progress rapidly, with crew working to stabilise the vessel and control the damage event. In these earlier phases little structural data can be transferred to a shore based emergency response service, save for potential interpolation based on how the damage occurred, for example by collision or grounding, and extents of flooding within the vessel. For these reasons, the application of the proposed method is focussed on providing benefit within the steady state damage condition from the moment that structural information can be provided by the crew, through to eventual completion of a salvage operation. Although developed with the focus on damaged structural assessment, the tool is equally applicable to intact structural assessment and the ship design environment.

It is envisioned that the method could be suitably developed into a new or existing computational analysis software package, though the actual coding of the method is considered outside of the scope of this research.

In order to address the weaknesses to the current progressive collapse method (Section 2.2.4) with respect to the structural analysis of a damaged vessel, and accounting for the large number of potential variables in a damage scenario, a new progressive collapse method using the response surface method (RSM) kriging is proposed. The new method allows the use of larger progressive collapse elements and the efficient capture of the required structural data for use by the method, allowing assessment of the damaged structure at a more holistic compartment level.

The RSM is developed from FEA to capture the progressive collapse element strength data and allow prediction of either the stress in the structure for a given loading scenario or its ultimate failure load limit state. Figure 3.1 shows a flow diagram of how the method is implemented. The method utilises two response surfaces, the first to assess the failure of the elements by capturing the displacement or strain at which the ultimate strength point occurs and beyond which the element is considered to have failed, and the second to assess the stress and forces in the remaining elements that have not failed by capturing the stress strain curve data from which the element forces can be calculated or capturing the force displacement data from which the required data can be obtained directly. There are two main reasons for the use of two response surfaces. Firstly, the progressive collapse method requires knowledge of the stress-strain data, or load deflection data, from which to perform the analysis and ensure correct positioning of the neutral axis, for which the second response surface is used. Secondly, the analysis of the post collapse region is complex for intact structures and potentially more subjective for damaged structures; therefore, whilst the post collapse region may be assessed and calculated it is not recommended to be used without significant understanding of this region being developed, leading to the use of the first response surface to define the strain at which the ultimate strength is reached, with the element being declared as failed if this is exceeded. However, it is advisable in the development of a response surface to avoid an effective "cliff edge" as data runs out in one variable's direction, particularly if this is a region of interest for data extraction. Therefore, some of the post collapse data will be included in the second response surface, to ensure accuracy of data up to the desired ultimate strength point.

Whilst it is required to develop two response surfaces for use by the method, both are created from the same FEA cases utilising the resulting data in different manners. Therefore, there is no FEA analysis penalty from adopting this approach.

Through the implementation of the proposed progressive collapse analysis by RSM method in an industrial emergency response service, a potentially less conservative approach to the residual strength assessment of a damaged vessel can be achieved within the required timescales. The development of the method and quantification of the need for the method has been demonstrated through the damaged stiffened structure studied presented in this thesis in Chapters 5 to 7. These studies have also assisted in identifying the variables that should be included within the response surface in order to allow the amount of FEA required to create the surfaces to be reduced as far as possible.

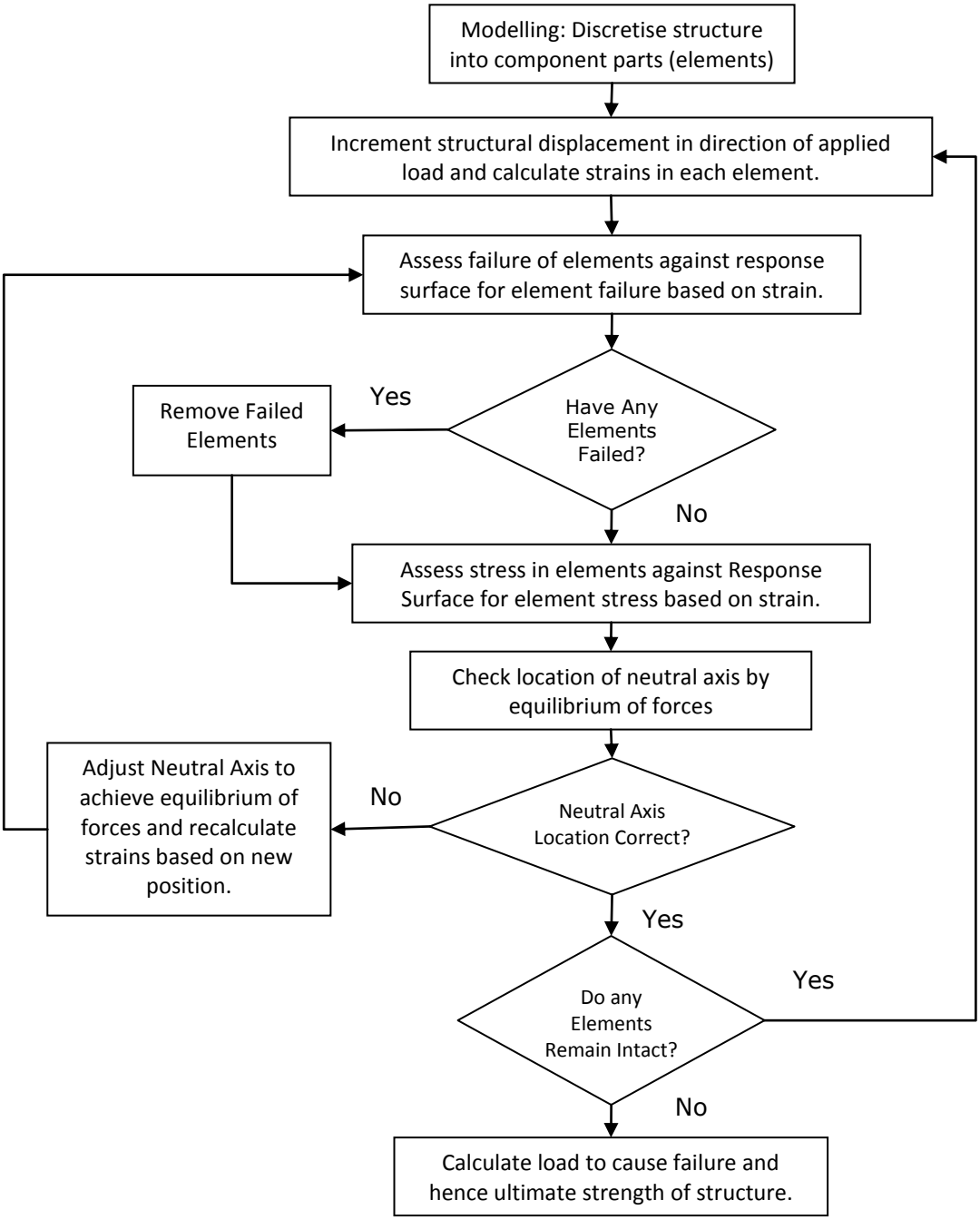

Figure 3.1 - Progressive Collapse Analysis by Response Surface Method

[Blank Page]

4 VERIFICATION OF MODELS

4.1 Introduction

As discussed in Chapter 3, in order to understand the influence of damage in the form of a hole on the ultimate collapse strength of stiffened steel plated structure, research studies have been undertaken using FEA at three levels. To be able to undertake these research studies, FE models have been created and verified as suitable for use within the studies presented later in this thesis. This chapter initially details the verification of the FE models before progressing on to the validity of using response surface method for the capture of damaged structural data for use within the new progressive collapse method detailed in Chapter 3.

The final section of this chapter details the verification of a box girder FE model. This model has been used in Chapter 8 for verification of the new progressive collapse method.

4.2 FEA Verification – Stiffened-Plate Model

4.2.1 FE Model Definition

A stiffened panel is generally constructed by welding a bar, T-shaped or L-shaped stiffener or OBP to a flat plate, as detailed in Section 2.3. The stiffeners themselves are made of flat plate welded together or extruded form in the case of OBP, which can be approximated as an L-shaped stiffener for modelling purposes.

Within the FEA software, there are three main element types that can be implemented to model the stiffened-plate scenario; these are beam, shell or solid elements.

Beam elements are suitable for modelling individual plate stiffener combinations, because the cross-sectional properties can be accurately modelled. However, the analysis of the beam elements is through the use of elastic beam theory. As such, beam elements are not versatile enough to accurately model the desired scenario, introducing damage or initial distortion to the model.

Three dimensional shell elements allow more detailed modelling of the desired structure than would be possible with beam elements. Through the use of multiple quadrilateral or triangular elements of defined thickness, the user can mesh the structure to a high level of detail. Shell elements are capable of performing both linear and non-linear analysis in relation to both geometrical and material properties. Shell elements are particularly suited to modelling plate structures, though selection of the appropriate element must be made in relation to the plate thickness being modelled, structural loading and potential failure mechanisms that might be expected.

Solid elements can allow greater fidelity of a model than is achievable with shell elements. For example, greater detail of connections between adjoining sections can be modelled and assessed through the use of solid elements. However, the processing time to solve a solid element model in comparison to an equivalent shell element plate model can be much greater, due to the additional degrees of freedom included in the model by the additional nodes to define each element. Solid elements are particularly prevalent when modelling thick plates due to their ability to model through thickness deformations that shell elements are unable to do.

Both shell and solid elements are isoparametric in their nature and are able to distort away from their regular equilateral triangular, prismatic, rectangular or cuboidal form. Therefore, they are able to model irregular shapes and complex geometries.

For the modelling of stiffened plate and stiffened panel arrangements constructed from steel, shell element have been selected as suitable, being able to perform the desired analysis, whilst allowing easier automation of the geometrical definition by limiting the number of nodes, which also reduces the number of degrees of freedom in the model, reducing computational time to converge on the solution.

The structural modelling of the stiffened-plates has been undertaken through the use of the commercial FEA software, ANSYS. The analysis takes into account both material and geometric non-linearities of a stiffened panel under both out-of-plane lateral and in-plane compressive axial loading. Discrete stiffened-plate approach is adopted for modelling in order to represent the panel as part of a larger structural arrangement. Lateral loading is assumed to arise from either cargo load or uniform hydrostatic pressure and is applied in full, prior to incremental application of the axial load.

Performing non-linear collapse analysis of a stiffened panel is a complex problem. Whilst such an assessment of a damaged panel does not appear to have been previously undertaken, an assessment of the collapse loads of stiffened panels with central circular cut-out, with radius equal to half the breadth, was undertaken by Suneel Kumar et al. [77], and has been used for the verification of the damaged models. In their paper, interaction curves are developed for a panel of 1500mm in length (L) and thickness (t) of 6mm of varying breadths (b) of 170mm, 340mm, 510mm and 765mm, with the plate longitudinally stiffened with one of four Unequal Indian Standard Angle ordinary stiffeners (ISA5030 6, ISA7045 6, ISA10065 6 or ISA12595 6). The dimensions of the stiffeners are shown in Table 4.1.

Indian Standard Angle Type	Overall Stiffener Height (mm)	Flange Breadth (mm)	Web and Flange Thickness (mm)
ISA5030 6	50	30	6
ISA7045 6	70	45	6
ISA10065 6	100	65	6
ISA12595 6	125	95	6

Table 4.1 - Indian Standard Angle Definition

4.2.2 FE Model Verification

In order to validate the FEA model, the Suneel Kumar et al. [77] model was recreated, whose work has been verified against both analytical and experimental work. On this basis the ANSYS model was created using a four noded quadrilateral isoparametric linear shell element (SHELL181), to model both the plate and stiffener. This element is suitable for undertaking the analysis of linear, large-rotation and large strain non-linear plates and thus suitable for this study. The element itself has six degrees of freedom at each node (UX, UY, UZ, ROTX, ROTY, ROTZ).

Regular quadrilateral elements with element edge length of 25mm, having aspect ratio of 1, were used for meshing areas within the plate and stiffener, whilst triangular elements were used to mesh the area around the circular cut-out; these were confirmed suitable by the convergence study undertaken by Suneel Kumar et al. [77]. Material non-linearities were accounted for using a bilinear isotropic rate independent hardening with von Mises yield criteria assuming an elasto-perfectly plastic stress strain relationship.

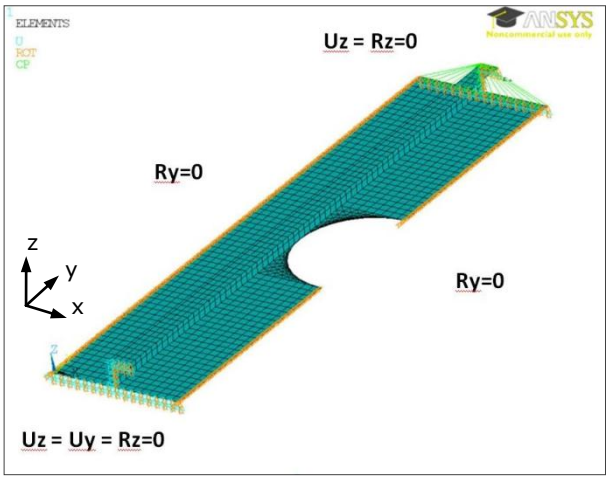

Figure 4.1 - Meshed Stiffened-Plate and Applied Boundary Conditions

The model was constrained by simply supported boundary conditions along the loaded and reactive edges. Rotation about the longitudinal direction was constrained at all nodes along the longitudinal edges with the displacement along the same edges allowed to freely move in the x direction. This arrangement allows for continuity between adjacent stiffened-plates. To ensure uniform compressive displacement of the loaded edge, a coupled constraint equation was applied to the loaded edge before the load was applied incrementally. Figure 4.1 shows the meshed model and applied boundary conditions of a panel with central circular cut-out, as used for verification purposes.

Suneel Kumar et al. [6] validated their model through the use of numerical methods for stiffened panels under either lateral or axial load. The validated results of panels of varying plate slenderness ratio, β (25) and column slenderness ratio λ (26), were plotted against either normalised axial load (P_{u0}/P_{sq}) for panels under axial load only or normalised lateral load (Qn) for panels under lateral load only.

$$\beta = \frac{b}{t}\sqrt{\frac{\sigma_y}{E}} \tag{25}$$

$$\lambda = \frac{L}{r\pi}\sqrt{\frac{\sigma_y}{E}} \tag{26}$$

In the above relationships, σ_y is the Yield Stress of the material, E is the Young's Modulus and r is the radius of gyration. P_{u0} is the calculated ultimate axial load for the panel, whilst P_{sq} is the compressive "squash" load, defined in (27) as

$$P_{sq} = \left(\sigma_{yp} A_p\right) + \left(\sigma_{ys} A_s\right) \tag{27}$$

where A_p cross-sectional area of the plate, σ_{yp} is the yield stress of the plate, A_s is the cross-sectional area of the stiffener and σ_{ys} the yield stress of the stiffener. Q_n is defined in Equation (28) where Q is the applied lateral pressure load.

$$Q_n = \frac{QE}{\sigma_y^2} \tag{28}$$

The results of the recreated model are shown with the results of the Suneel Kumar et al. [77] cases in Figure 4.2 and Figure 4.3. Comparing the plots, it can be seen that the model is working correctly as expected.

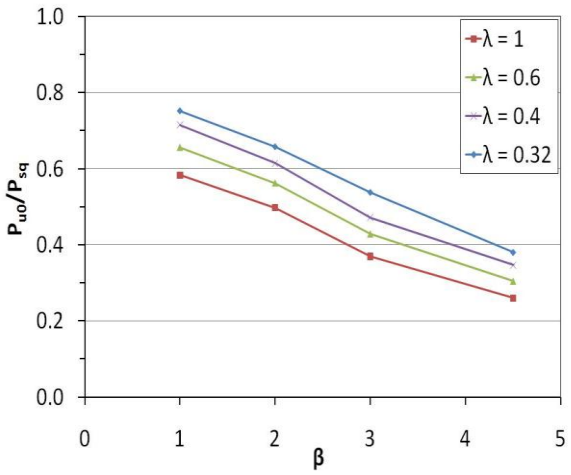

Figure 4.2**(a)**

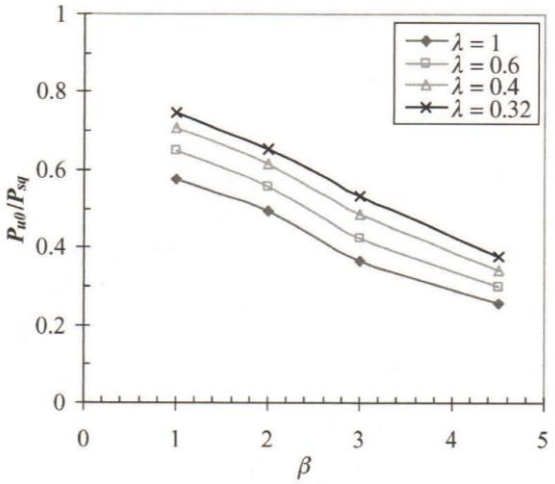

Figure 4.2**(b)**

Figure 4.2 - Effect of Normalised Column Slenderness Ratio on Normalised Axial Load (a) Model and (b) Suneel Kumar Model [77]

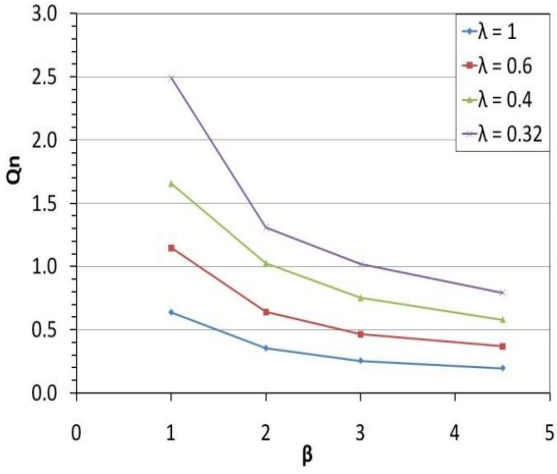

Figure 4.3**(a)**

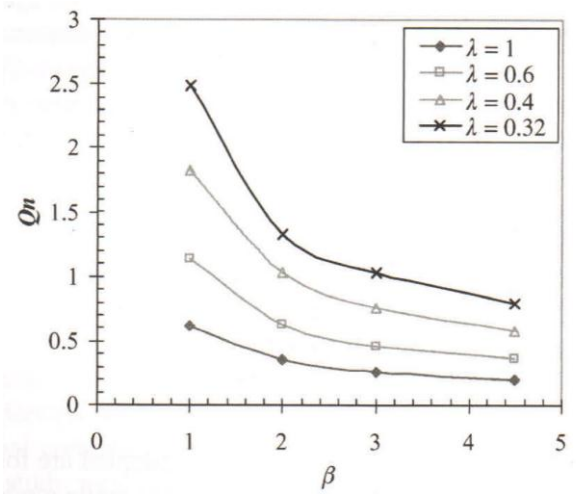

Figure 4.3**(b)**

Figure 4.3 - Effect of Normalised Column Slenderness Ratio on Normalised Lateral Load (a) Model and (b) Suneel Kumar Model [77]

The results of the verification study show that the model is working as expected, showing good correlation with the verification cases used. This provides sufficient confidence in the model for use within the desired research studies detailed later in this thesis. From here the model geometry can be amended to run the cases required for the damaged stiffened-plate studies. These have been generated through the use of a MS Excel and VBA tool developed by the author, to write the required APDL (ANSYS Parametric Design Language) code to create and run the damaged stiffened-plate FEA models.

4.3 FEA Verification – Grillage Model

4.3.1 FE Model Definition

Analysis of the collapse strength of grillage structures is a complex problem. Whilst previous analysis has been undertaken on intact structures both analytically and experimentally [17, 67, 68, 94], as identified in Table 2.7, no previous work has been undertaken to investigate the strength of damaged or holed grillage structures nor how such damage would affect the mode of failure encountered.

Assuming failure of the structure is by interframe collapse, which is the failure of the structure due to collapse between adjacent transverse frames, Hughes [16] states that three failure modes exist that must be considered: failure of stiffener, failure of plate and failure of both stiffener and plate combination. However, as noted by Paik et al. [25], when considering the failure of a grillage arrangement a total of six possible failure modes may exist, whereby the "real ultimate strength is the minimum value of ultimate strengths obtained from the six solutions." [73].

1. Mode I: overall collapse mode;
2. Mode II: collapse of plating between stiffeners without failure of stiffeners;
3. Mode III: beam-column type collapse of stiffeners with attached plating;
4. Mode IV: local buckling of stiffener web after collapse of plating;
5. Mode V: lateral-torsional buckling of stiffeners after collapse of plating;
6. Mode VI: gross yielding of entire panel.

Therefore, the proposed FE model must be able to assess all of these modes of failure to be considered suitable for the assessment of the collapse strength of a grillage. The approach to the modelling of the grillage is similar to that of the stiffened-plate model detailed in Section 4.2, due to the similarity in the fundamentals of the structural arrangement though on a larger scale; hence, the grillage model has been created using the same ANSYS shell element (SHELL181) for the same reasons as detailed in Section 4.2. The MS Excel and VBA APDL tool has been developed to be able to generate and run the required intact and damaged grillage FE models

The overall size of grillage to be used within the subsequent research studies consists of four regularly spaced identical longitudinal stiffeners and five equally spaced, deeper orthogonally connected transverse stiffeners. The grillage is assumed to be bounded at its transverse ends by deep frames or bulkheads, which are assumed to remain plane, and bounded along its longitudinal edges by further grillage structure. The overall dimensions selected are within the extents of grillage structure regularly found within ship sections, whilst being large enough to assess the required damage sizes and locations within the subsequent damaged grillage study.

Table 4.2 shows the stiffener profile definitions used in the verification, where the ISA70456 profile is used in the longitudinal direction and Admiralty T section is used in the transverse direction. The plating thickness is maintained at 6mm and transverse stiffener spacing of 1500mm used, giving a fixed grillage length of 9000mm. The longitudinal stiffener spacing is then varied to provide plate slenderness ratios, β, (Equation 25) of 1, 2, 3 & 4, therefore varying the overall breadth of the grillage as plate slenderness is increased; this subsequently provides λ values of 0.61, 0.66, 0.67 & 0.68 respectively. No lateral pressure load is applied to the grillage in this assessment.

Stiffener Profile	ISA70456	Admiralty T, Type 2, 4.5”
Overall Height (mm)	70	114.3
Flange Breadth (mm)	45	44.5
Flange Thickness (mm)	6	9.5
Web Thickness (mm)	6	5.1
Second Moment of Area (mm^4)	$0.326x10^6$	$1.263x10^6$

Table 4.2 – Grillage model stiffener profile definitions

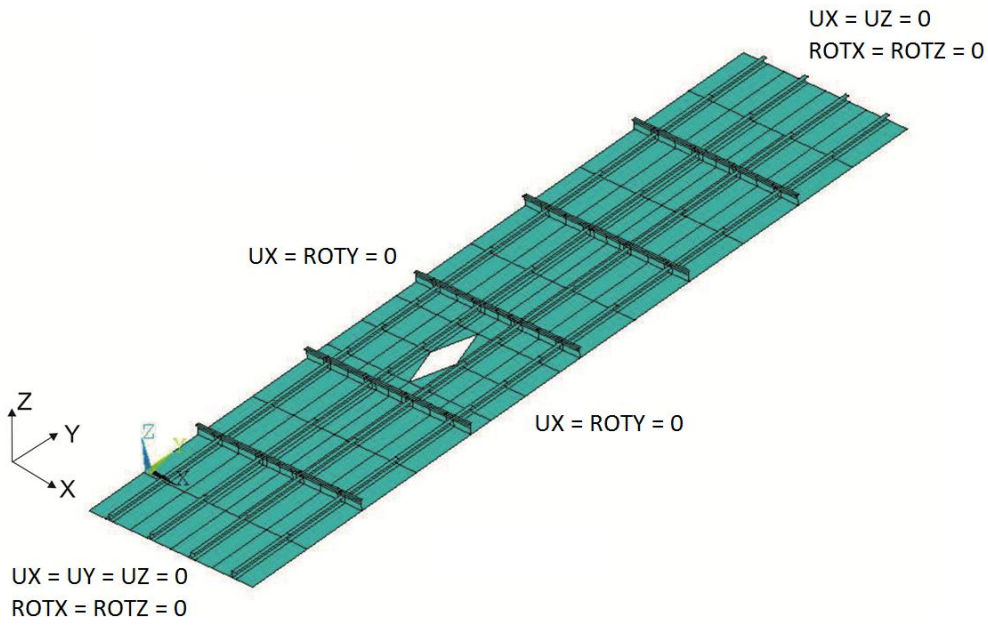

Figure 4.4 – FE Grillage Model Boundary Conditions

Figure 4.4 shows an example grillage arrangement with damage aperture and applied boundary conditions. Symmetry boundary conditions described by Paik et al. [73] have been applied to the unsupported longitudinal edges of the grillage, with clamped boundary conditions applied to the loaded and reactive transverse edges to simulate the connection to stiffer structure. On the loaded edge, an additional coupled constraint equation was applied to ensure the edge remains plane as the load was applied.

In the assessment of stiffened panels under axial compression published within the ISSC 2009 Ultimate Strength committee report [78], it was shown that the material model used can influence the predicted ultimate collapse strength of the panel by allowing or not allowing strain-hardening of the model. Whilst it was shown that the inclusion of strain hardening leads to an increased ultimate collapse strength of the panel due to increased stiffness, the modes of failure did not change. Therefore, no strain hardening was included in the applied material model through utilisation of an elasto-perfectly-plastic stress-strain relationship, so as to provide a conservative prediction of the ultimate collapse strength. A Young's Modulus of 200GPa, Poisson's Ratio of 0.3 and Yield Stress of the material of 250MPa was used in the convergence study.

Section 2.4 discussed the modelling of imperfections in grillage arrangements. As the connection between the longitudinally stiffened-plates and the transverse stiffeners within the structure is no longer considered to be simply supported, a single half sine wave imperfection is no longer suitable. For the reasons discussed in Section 2.4, a Fourier series summation using Equations 21 – 23 has been applied to induce suitable imperfection shapes in to the plating between stiffeners and longitudinal stiffeners themselves. A "hungry-horse" mode shape whereby the deflection direction between stiffeners is the same across the panel for both the plate and stiffener vertical imperfections and alternating stiffener sideways imperfection has been applied. The Smith et al. [82] average imperfection definitions for maximum plate and stiffener vertical imperfection and ISSC 2009 definition for stiffener sideways imperfection [78] have been applied. These definitions can be seen in Table 2.5. As discussed in Section 2.4, values of A_o have been set to 0.8 for the single half sine wave mode, 0.2 for the first mode above the elastic buckling mode and 0.01 for the second mode above the elastic buckling mode [80, 34].

Having applied the initial imperfection shapes to the model, the geometry was updated to provide a "clean" unstressed model for assessment. The loading condition was applied through a stepped displacement to the "loaded end", hence applying an in-plane axial compressive load along the length of the longitudinal stiffeners. The reaction forces of the reactive end can then be obtained and the ultimate strength calculated as the peak load that can be sustained by the structure.

4.3.2 FE Model Mesh Convergence

Convergence of the FE model mesh has been undertaken by comparing ultimate strength results against element edge length and the number of elements between transverse stiffeners. Figure 4.5, Figure 4.6 and Table 4.3 (where normalised axial failure load is calculated as Pu0/Psq as detailed in Section 4.2) show the mesh convergence results, demonstrating good convergence for element edge length 20mm and below.

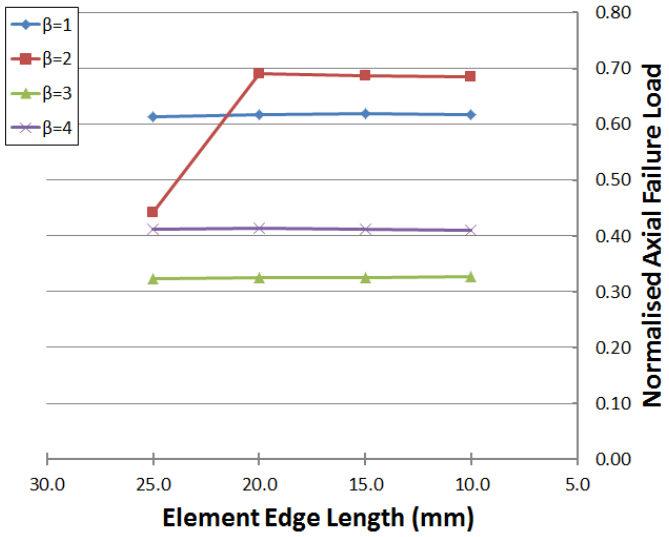

Figure 4.5 – FE mesh convergence against element edge length

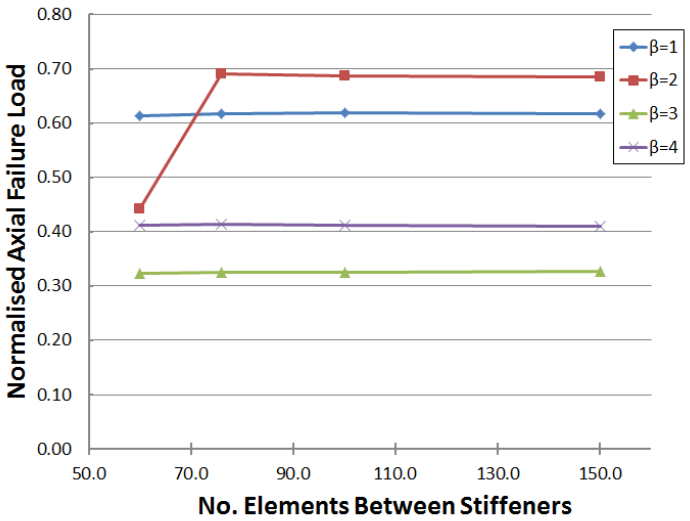

Figure 4.6 – FE mesh convergence for number of elements between transverse stiffeners

β	Difference (%) 25mm to 20mm	Difference (%) 20mm to 15mm	Difference (%) 20mm to 10mm	Difference (%) 15mm to 10mm
1	0.78%	0.29%	0.00%	-0.29%
2	56.33%	-0.70%	-0.84%	-0.15%
3	0.43%	0.23%	0.48%	0.25%
4	0.33%	-0.62%	-0.89%	-0.27%

Table 4.3 – FEA mesh convergence results for normalised axial failure load

4.3.3 FE Model Verification

Verification of the grillage FE model has been undertaken by modelling a number of experimental intact grillage collapse cases performed by Smith [67], using the same modelling approach as detailed above. Smith et al. [67] test cases 3a, 3b, 5 and 6 were modelled and assessed, as these cases had most comparable plate slenderness (β) and column slenderness (λ) values to the grillage arrangements detailed above. Table 4.4 shows the definition of the test grillage dimensions, material properties and initial imperfection sizes.

		Smith 1975 Grillage 3a	Smith 1975 Grillage 3b	Smith 1975 Grillage 5	Smith 1975 Grillage 6
	Overall Length	6096	6096	6096	6096
	Overall Breadth	3048	3048	3048	3048
	No. Longitudinal Stiffeners	11	11	6	6
	No. Transverse Stiffeners	5	5	5	6
Plate	Thickness (mm)	6.38	6.38	6.43	6.33
	Yield Stress (MPa)	254.76	256.30	251.67	260.94
Longitudinal Stiffeners	Spacing (mm)	304.80	304.80	609.60	609.60
	Overall Depth (mm)	77.72	77.72	116.08	76.20
	Flange Breadth (mm)	25.91	25.91	46.23	27.43
	Flange Thickness (mm)	6.35	6.35	9.53	6.35
	Web Thickness (mm)	4.52	4.52	5.33	4.55
	Yield Stress (MPa)	231.6	226.96	234.69	245.50
Transverse Stiffeners	Spacing (mm)	1524.00	1524.00	1524	1219.20
	Overall Depth (mm)	156.21	156.21	154.18	114.55
	Flange Breadth (mm)	78.99	78.99	77.22	46.23
	Flange Thickness (mm)	14.22	14.22	14.22	9.53
	Web Thickness (mm)	6.81	6.81	6.76	5.36
	Yield Stress (MPa)	270.2	277.92	274.83	270.20
	Lateral Pressure Load (MPa)	0.02068	-	-	-
	Young's Modulus (MPa)	205000	205000	205000	205000
	Poisson's Ratio	0.3	0.3	0.3	0.3
	w_{oplm} (mm)	2.83	4.57	6.10	7.62
	w_{ocm} (mm)	4.42	2.90	1.22	2.44
	w_{osm} (mm)	2.29	2.29	2.29	1.83
	β	1.68	1.68	3.31	3.42
	λ	0.70	0.70	0.45	0.75

Table 4.4 – Smith et al. [67] grillage definitions

	Smith 1975 Grillage 3a	Smith 1975 Grillage 3b	Smith 1975 Grillage 5	Smith 1975 Grillage 6
Collapse Load by Experimentation (MN)	4.585	4.048	5.206	3.264
Collapse Load by FEA (MN)	4.166	4.200	4.877	2.731
% Difference	9.12%	3.76%	6.31%	16.34%

Table 4.5 – Grillage FE model verification results

As can be seen from Table 4.5, good correlation has been achieved between the experimental results and the FE model using the discussed method and applied boundary conditions. Some error would be expected between the results as it is not possible to model the exact condition of the experimental cases, as insufficient data is available to model the true imperfections seen in the experimental models. Additionally no information on residual stresses in the test models is available, and these stresses have been neglected in the FE model. However, in addition to the believed acceptable level of error between the FE and experimental results, the modes of failure seen in the FE models are also consistent in their overall form with the observations recorded of the experimental tests [67]. Images of the experimental failure results and equivalent FEA displacement plot results for the assessed cases can be seen in Figure 4.7 to Figure 4.14 to demonstrate the failure mode consistencies. Case 3a, 3b and 5 (Figure 4.7 - Figure 4.12) fail by an interframe mode, whilst case 6 (Figure 4.13 - Figure 4.14) demonstrates a longer mode of failure spanning multiple frame spacing.

Despite these similarities of form, some discrepancies can also be seen in the comparisons. It is not clear how far past the ultimate strength point the grillage tests were taken, or at what point the photos were taken, however the creasing of longitudinal stiffeners as seen in Figure 4.7, Figure 4.9 and Figure 4.13 is not demonstrated in the FE modelling. From these figures it can also be seen that the longitudinal edges of the test grillages are restrained in the vertical direction, which has not been applied in the FE model. Therefore, whilst the overall failure mode shape is considered consistent in the longitudinal direction, the transverse form does differ. Whilst these discrepancies exist, the correlation of the results and consistency in overall form provides sufficient confidence in the operation of the model.

Figure 4.7 – Smith [67] Grillage Experiment Case 3a Failure Condition

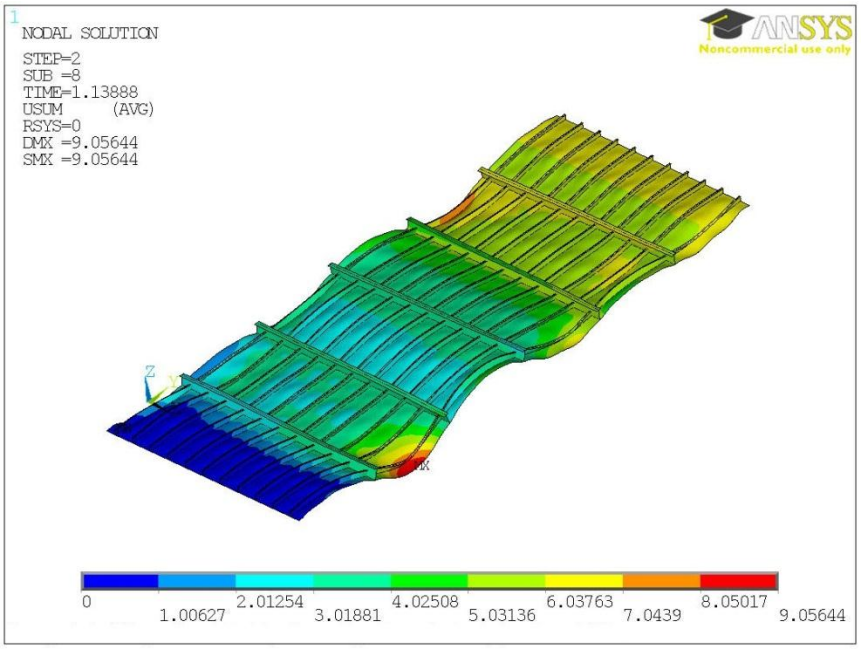

Figure 4.8 - Smith [67] Case 3a FEA Failure Condition – Magnified Displacement Plot

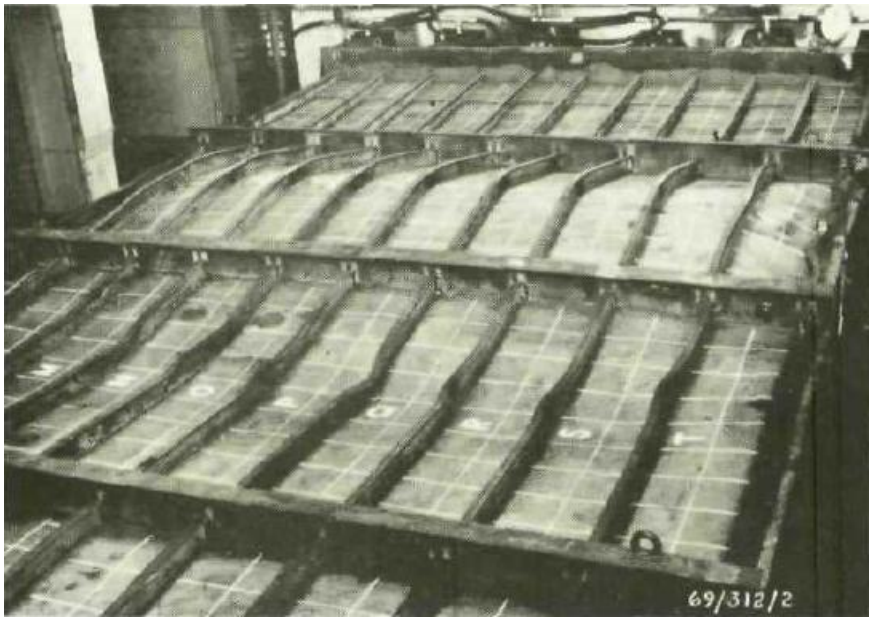

Figure 4.9 - Smith [67] Grillage Experiment Case 3b Failure Condition

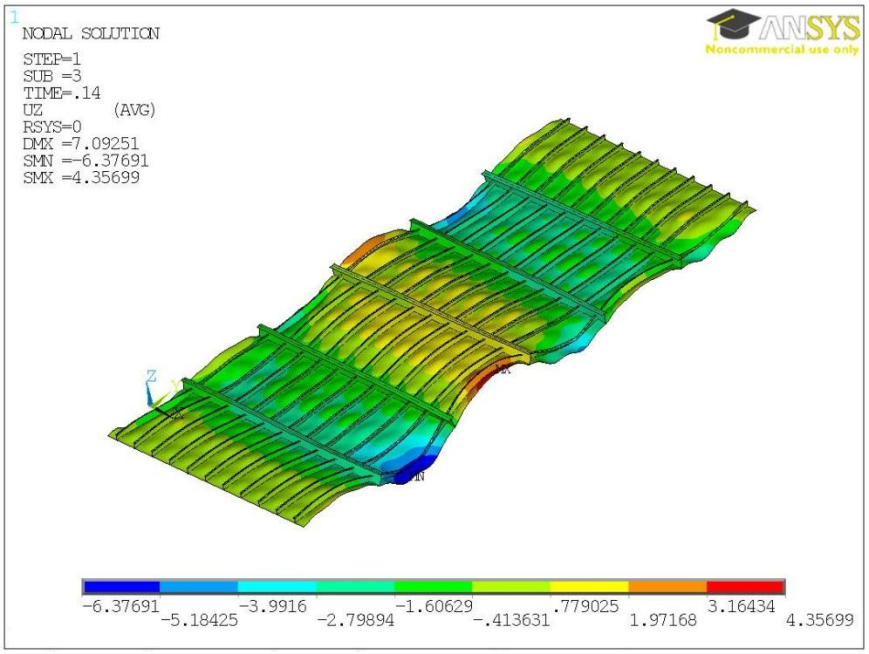

Figure 4.10 - Smith [67] Case 3b FEA Failure Condition – Magnified Displacement Plot

Figure 4.11 - Smith [67] Grillage Experiment Case 5 Failure Condition

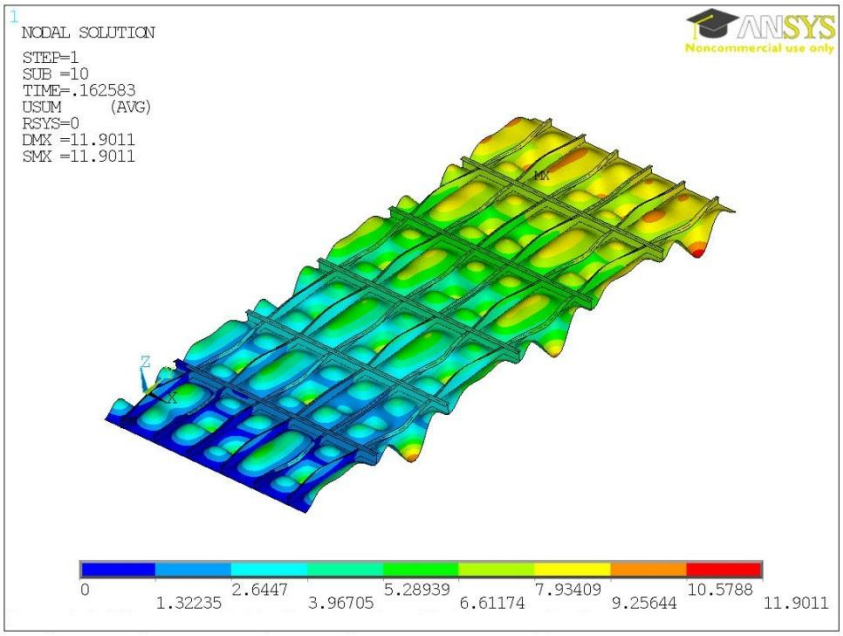

Figure 4.12 - Smith [67] Case 5 FEA Failure Condition – Magnified Displacement Plot

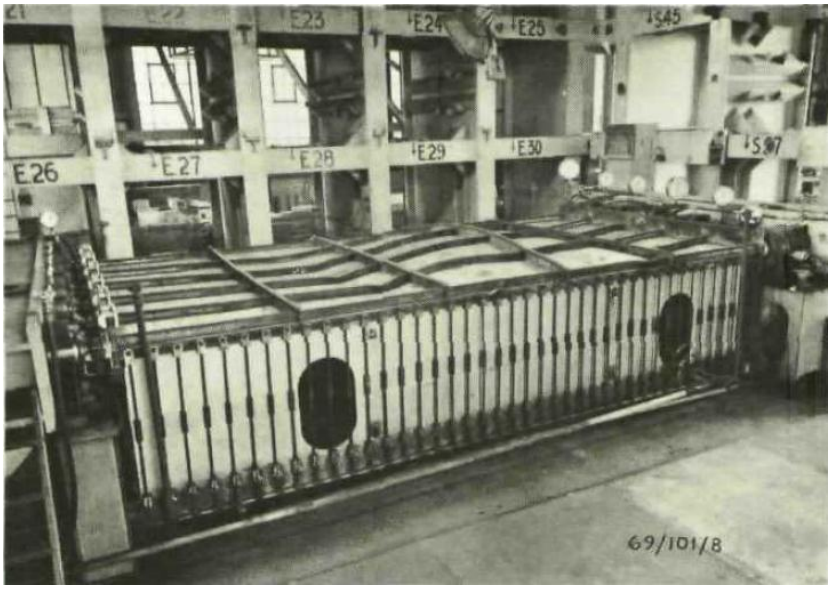

Figure 4.13 - Smith [67] Grillage Experiment Case 6 Failure Condition

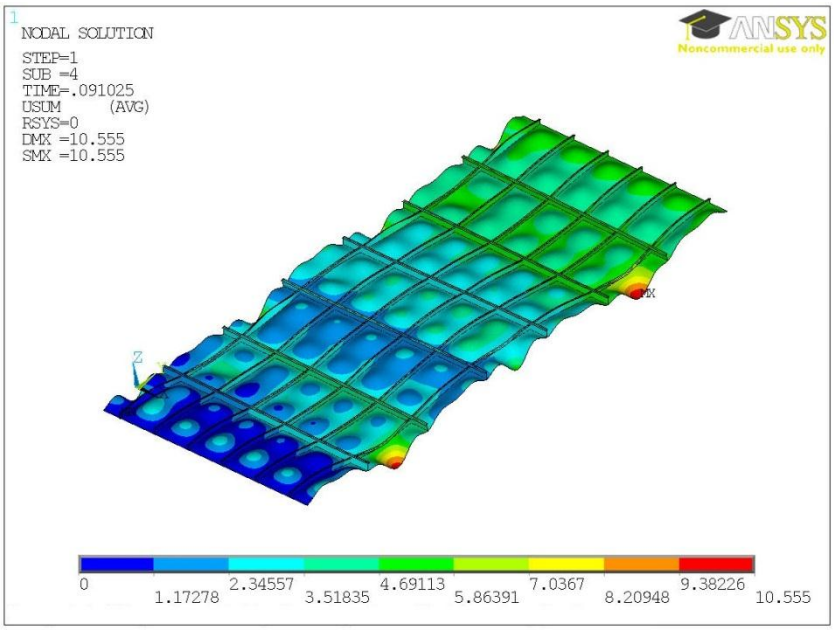

Figure 4.14 - Smith [67] Case 6 FEA Failure Condition – Magnified Displacement Plot

Figure 4.15 shows the results for the convergence cases with element edge length of 20mm plotted against the experimental results with the most similar λ values. Smith [67] Case 5 has been excluded from the figure as the column slenderness value is too different from the convergence cases for direct comparison. From the plot it can be seen that the trend seen in the convergence cases match with the experimental results.

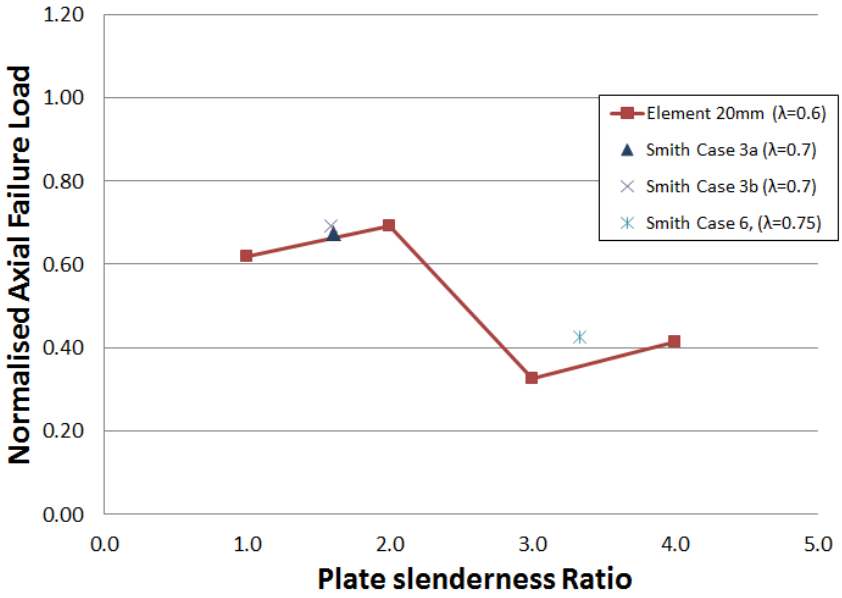

Figure 4.15 – Verification case, element 20mm, plotted against experimental test cases

From this verification study, sufficient confidence has been gained that the grillage FE model is working as expected and can be used for the desired research studies presented later in this thesis.

4.4 Response Surface Generation and Verification

4.4.1 Response Surface Data Generation

Section 2.2.7 discusses the method for the use of the response surface method (RSM) kriging to map the strength data containing a number of variables, by using FEA to provide the required base data points. This section details the verification of the use of this method for the capture of strength data of damaged stiffened steel structure for use within the proposed new progressive collapse method.

To be able to create the response surface, a "design space" is defined, within which the surface will map. It is then necessary to define the required FEA cases that will provide the hard data points within this design space which the response surface will pass through and use to assess the gradients of the surface between points in the directions of the included variables.

The method for selecting the FEA cases or data points was that of a Latin Hypercube. This method allows a non-uniform spread of points across the entire sample space, selecting FE cases with different parameters within the design space. The number of points required to generate the surface was gradually increased to determine the difference in time and accuracy to give an understanding of the minimum number of points required to achieve a suitable accuracy of results. Accuracy of the surface prediction between hard data points was undertaken through the use of an additional set of FE cases that were different to those used to create the surface, though still lie within the design space. Figure 4.16 shows a flow diagram of how the response surface data has been generated

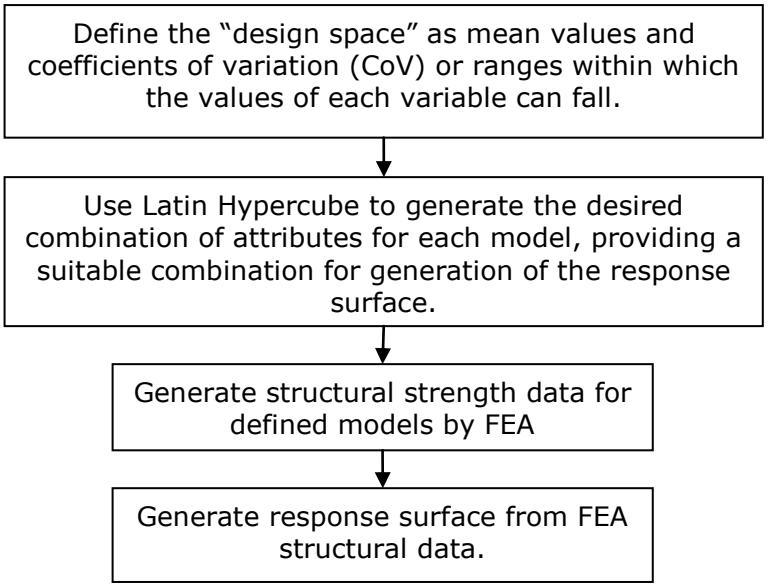

Figure 4.16 - Response Surface Generation Flow Diagram

The response surface has been generated using an in house MATLAB based response surface tool. To find the optimum values of the correlation parameters θ and P_j in Equation (11), the tool uses a genetic algorithm. This genetic algorithm used is the standard algorithm within the programming language MATLAB.

4.4.2 Response Surface Verification – Single Stiffened Plates

Using the verified stiffened panel FE model detailed in Section 4.2, a single arrangement was selected to verify the use of RSM for storing the damaged strength data at this level of structural idealisation.

The chosen panel dimensions were length 1500mm and breadth 340mm. The panel is fitted with a Unequal Indian Stiffened Angle ISA7045 6 which has an overall stiffener height of 70mm, flange breadth of 45mm with both flange and web thickness of 6mm. Mean values for the properties to vary were selected about which the chosen values would be distributed. These can be seen in Table 4.6 to be a mean plate thickness of 6mm, material properties for Young's modulus of 200 GPa and Yield Stress of 250 MPa. Poisson's ratio was maintained at 0.3.

Using appropriate distributions and mean values about which the individual characteristics are varied, the required case dimensions and material properties to successfully create the response surface were selected using the Latin Hypercube. Table 4.6 shows the different panel dimensions and material properties varied, the mean value and distribution used to create the appropriate spread of points. The selection of the mean values, ranges and distributions had two goals, firstly to provide a realistic design space to test the suitability of RSM to capture the required data, and secondly to allow the response surface to be used for a reliability analysis, as presented in the Sobey et al ASRANet 2010 conference paper detailed in Appendix A.

Property	Mean Value	CoV	Distribution	Range
Damage Diameter (mm)	226.667	0.5	Normal	3 - 744
Damage Position (mm)	170	0.5	Normal	23 - 665
Plate Thickness (mm) [95]	6	0.011	Normal	5.93 - 6.07
Lateral Load (N/mm^2) [95]	0.035	0.25	Weibull	0.021 - 0.0384
In-Plane Axial Load (N) [95]	340152	0.1	Largest Extreme Value Type I	331 - 707680
Young's Modulus (N/mm^2) [96]	2×10^5	0.02	Normal	196040 - 203960
Yield Stress (N/mm^2) [96]	250	0.07	Normal	232.68 - 267.33

Table 4.6 – Stiffened-Plate Property Variation Values and Distribution

Damage location was defined as a y-axis coordinate (Figure 4.1) that positions the centre of the damage at a point along the longitudinal edge such that the model remains representative of the verification cases, with mean value in the middle of the panel. In all cases the "damage" aperture was a circular hole with diameter restricted such that the stiffener was not damaged.

Initially 13 ANSYS FE analysed panel cases were used to provide data points to create the response surface, plotting the maximum stress calculated in the panel against the varied properties. The accuracy of the surface between the data points, was assessed using results from additional test panel arrangements. This showed an error in the surface of 15%. By increasing the number of points used to create the surface, the error was able to be reduced.

Number of Points	Maximum Stress RMSE (%)	Collapse Load RMSE (%)
13	15	-
25	8	-
50	1	4

Table 4.7 - Surface Accuracy in Relation to Points Used

Table 4.7 shows how the error in the surface reduced as the number of points to create the response surface increased. This assessment of the use of response surface for the capture of strength data of damaged stiffened panels has shown that for the defined "design space" 50 hard data points provides an RMSE error of 1% for the prediction of maximum stress and 4% for ultimate collapse load. This level of accuracy was believed to be suitable for implementation within the proposed new progressive collapse method by RSM and verifies the use of RSM for damaged strength data capture at this level of structural idealisation.

4.4.3 Response Surface Verification – Grillages

For verification of RSM for the capture of damaged strength data for grillages, the FE model detailed and verified in Section 4.3 has been used. A single arrangement was chosen, whose fixed geometrical properties are defined in Table 4.8. The stiffener profile definitions used can be seen in Table 4.2. The defined variables and their property ranges can be seen in Table 4.9.

Property	Value
Overall Grillage Length	9000 mm
Overall Grillage Breadth	1360 mm
Transverse Stiffener Spacing	1500 mm
Longitudinal Stiffener Spacing	340 mm
Plate Thickness	6 mm
Transverse Stiffener Profile	Admiralty T, Type 2, 4.5"
Longitudinal Stiffener Profile	ISA70456
Young's Modulus	$2x10^5$ MPa
Poisson's Ratio	0.3
Yield Stress	250 MPa

Table 4.8 – Grillage fixed property definitions

Property	Mean Value	CoV	Distribution	Range
Damage Length (mm)	750	0.5	Normal	377.5 – 1122.5
Damage Breadth (mm)	340	0.5	Normal	171 – 509
Damage Position Longitudinally (mm)	750	0.5	Normal	2627.5 – 3372.5
Damage Position Transversely (mm)	680	0.5	Normal	342 – 1017
Lateral Load (MPa) [95]	0.0036	0.25	Weibull	0.000035 - 0.0075

Table 4.9 – Grillage property variation values and distributions

The Latin hypercube was used to define 150 FE case configurations within the defined "design space". For generation of the response surface, the variables for damage length and breadth were combined to provide a damage area variable. Therefore the response surface for this arrangement was produced using 4 variables.

No. of Points	RMSE (%)	Average Deviation
10	14.03	0.1296
20	10.91	0.0524
30	10.85	0.0470
40	10.66	0.0419
50	10.74	0.0496
60	10.91	0.0563
70	10.50	0.0331
80	10.33	0.0216
90	10.83	0.0448
100	10.48	0.0271
110	10.83	0.0514
120	11.06	0.0614
130	11.40	0.0726
140	11.60	0.0765
150	11.00	0.0562

Table 4.10 – Grillage response surface convergence results for ultimate collapse load

Table 4.10 shows the convergence results for the generation of the response surface, comparing the number of points used to create the surface with the error seen between the surface and additional test FEA models created that are within the design space envelope, but have different parameters to those used to generate the surface. Initially it can be seen that as the number of points used to define the surface is increased, the average deviation in predicted ultimate collapse strength reduces. However, beyond 100 points it can be seen that the average deviation diverges as the increased number of points appears to influence the ability of the tool to accurately model the surface. Therefore, from the convergence results it can be seen that 100 cases provides the most accurate surface, showing a RMSE of 10.48% for ultimate collapse load. Whilst this is a larger error than the 4% RMSE shown by the stiffened panel response surface, it is believed that this has demonstrated the ability of the response surface to capture the damaged strength data of grillage arrangements for use by the new progressive collapse method by RSM. It is possible that the divergence of the results as the number of data points passes 100 could be due to the influence of or relationship between certain parameters or errors, or noise, within the FEA data, leading to the RSM attempting to map a smooth surface between data points that don't represent a smooth correlation. Further understanding of the influential parameters on the collapse strength of damaged grillage arrangements and the resulting changes to the design space definition should allow increased accuracy on the surface to be achieved through tuning of the parameters used to define the surface.

4.5 FEA and Progressive Collapse Tool Verification – Box Girder Model

4.5.1 Hull and Box Girder FE Modelling Overview

The structural models developed and verified above in Sections 4.2 and 4.3 have been defined in relation to the type of structure that is commonly found locally within a ship's hull girder and the level of structural idealisation currently used, or proposed for use, within the progressive collapse method (details of the Smith interframe progressive collapse method can be seen in Section 2.2.4). However, it is also important to understand the overall influence of these component parts and their interactions through the analysis of whole ship or ship compartment models. In cross-section, a typical hull can be seen to be a continuous envelope of stiffened steel structure, save for any deck openings to allow access of personnel or cargo; for this reason, parallels are often drawn between ship hulls and box girders.

Assessment of the ultimate bending strength of whole ship hulls or box girder arrangements is a complex problem, as discussed in Section 2.2.6. From the ISSC 2006 and 2012 benchmark studies [39,40] presented in Section 2.2.6, it can be seen that large variations in results obtained between different FE users of the same or different software can occur as well as variations in results between FEA and those obtained from simpler methods such as the Smith interframe progressive collapse method. Discussions of these benchmark studies state that some of the variation in the results may arise from the different modelling approaches and the handling of initial imperfections and residual stresses, though are not due to the limitations of any one piece of software or method over another.

Due to the familiarity with ANSYS FEA software and the knowledge of the handling of initial imperfections within the software, developed during the work presented earlier in this chapter, and the similar performance demonstrated to other FEA software, ANSYS has been used for the modelling presented below. It is believed that by understanding the construction of the models and using the same definitions, method of application and sizes of imperfections, suitable comparison can be made between damaged girder models and models assessed by progressive collapse method; as is desired for use within the subsequent work presented in Chapter 8.

In order to allow demonstration of the ability of the proposed new progressive collapse method described in Section 3, a progressive collapse tool was developed by the author.

4.5.2 Box Girder Model Definition

It is discussed in Section 2.2.6 that the verification of ship hull models is often challenging due to the lack of experimental data available, leading to the reliance on methods such as the Smith interframe progressive collapse method for verification purposes. However, experimental data is available for the ultimate bending strength assessment of box girder structures, which have many similarities to ship hull structures.

Recently a number of box girder ultimate bending strength experimental tests have been performed by Gordo et al. [97,98] and Saad-Eldeen et al. [99,100]. Due to the extents of the model, which span multiple frame bays, and the lack of corrosion within the model, the Gordo et al. high tensile steel box girder model [98] was selected for development and verification of a box girder FE model. Development of the model also benefited from work presented by Benson [34] who modelled this same box girder arrangement using the commercial FE software ABAQUS, and investigated the boundary conditions being applied to the box girder by the test rig. The work by Benson [34] also included the assessment of one of the box girder arrangements by interframe progressive collapse, which has been used for the verification of the tool developed by the author.

In their work, Gordo et al. [98] performed ultimate bending strength experimental tests on three box girder structures manufactured out of high tensile steel with Young's Modulus 211GPa, yield stress of 745MPa and Poisson's Ratio 0.3. The geometrical arrangement and dimensions of the box girders and the experimental test rig arrangement can be seen in Table 4.11, Figure 4.17 and Figure 4.18.

Box ID	Length (mm)	Frame Spacing (mm)	Breadth (mm)	Depth (mm)	Plate Thickness (mm)	Longitudinal Stiffener Profile		Transverse Stiffener Profile			
						Height (mm)	Web Thickness (mm)	Height (mm)	Web Thickness (mm)	Flange Breadth (mm)	Flange Thickness (mm)
H200	100+4*200+100 =1000	200	800	600	4	20	4	50	6	20	6
H300	100+3*300+100 =1100	300	800	600	4	20	4	50	6	20	6
H400	100+3*400+100 =1400	400	800	600	4	20	4	50	6	20	6

Table 4.11 – Box Girder Dimensions [98]

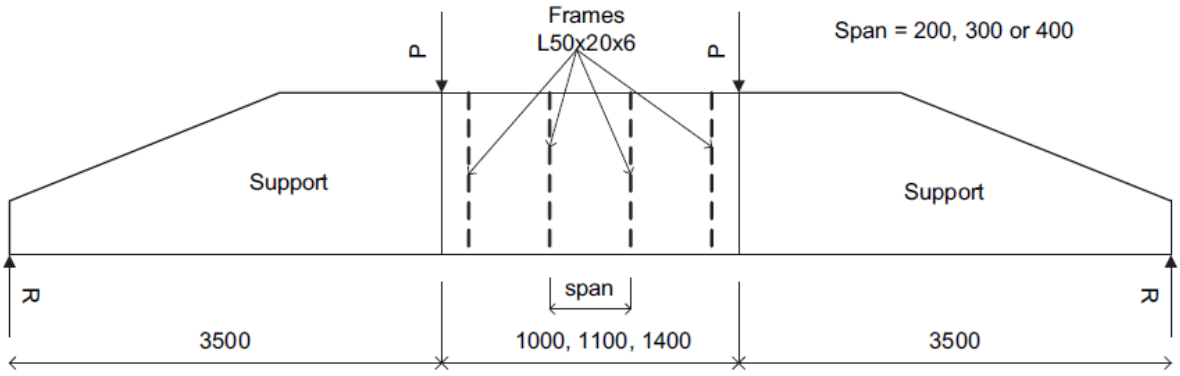

Figure 4.17 – Box Girder Experimental Test Rig Arrangement [98]

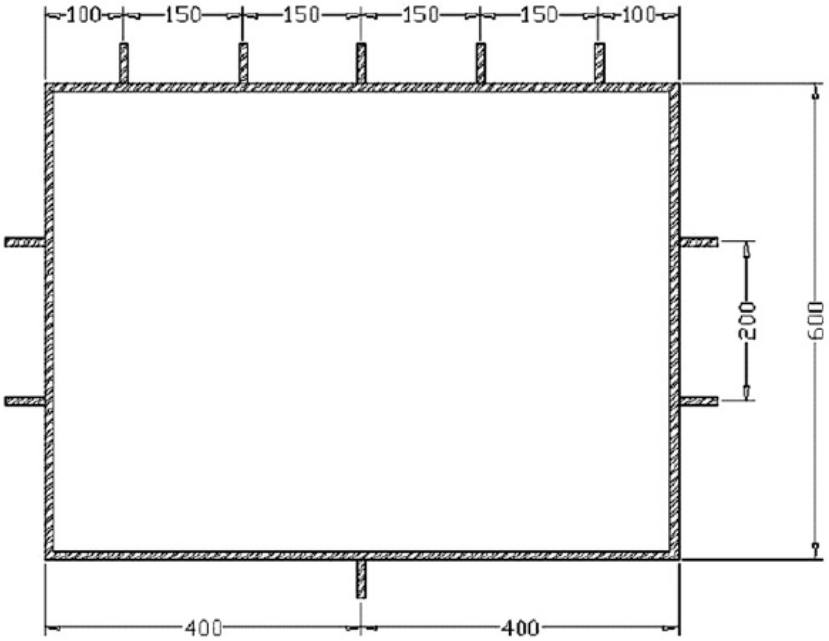

Figure 4.18 – Box Girder Cross Section Geometry [98]

4.5.3 Progressive Collapse Tool Verification

Within the work presented by Benson [34], results are presented comparing the FE replication of the Gordo et al. [98] H200 box girder with those calculated using the Smith interframe progressive collapse method. This method has been well documented in Section 2.2.4, and has been implemented in a tool developed by the author using a combination of MS Excel and VBA. This tool was developed, instead of the use of commercially available software that implements the same method, to allow greater control over the configuration of the models being assessed. Some of the discrepancies between different solutions obtained for the benchmark study performed by ISSC 2006 Ultimate Strength committee [39] discussed in Section 2.2.6, have been accounted for due to the progressive collapse element strength data used in the assessments. Many of the commercial ship design or emergency response software codes utilise generic strength data curves from which new curves are extrapolated. Implementation of the method in this manner limits the ability of the user to control the exact strength data used including the handling of parameters such as initial imperfections. By developing a bespoke tool to implement the method using specific strength data generated through the use of the FE models detailed earlier in this chapter, the resulting bending strength assessment should correlate more closely with box girder or ship compartment FE models created using the same structural definitions.

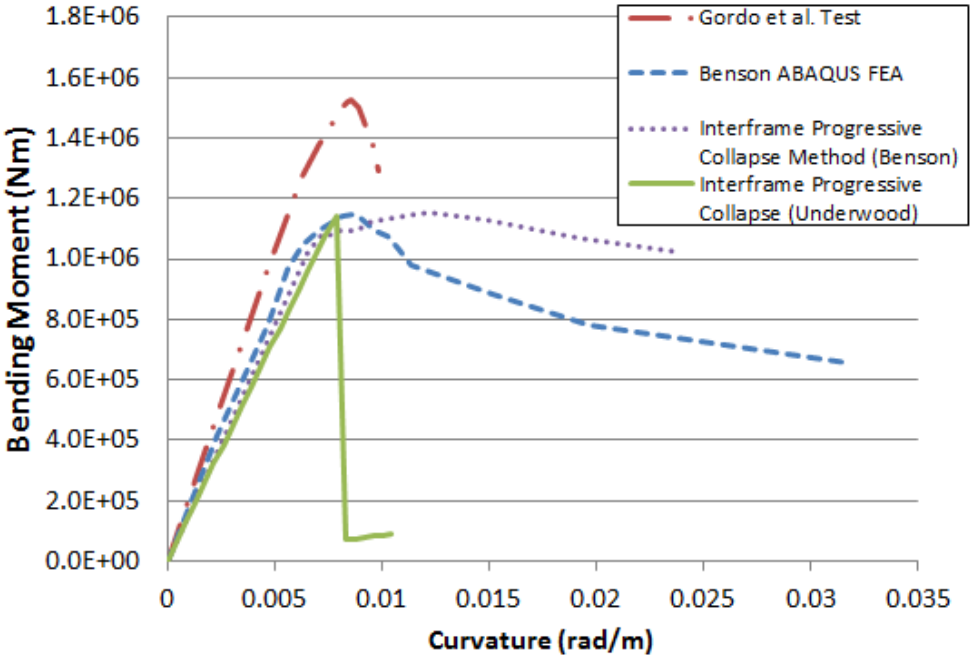

Figure 4.19 – H200 Box Girder Results Comparison

The specific progressive collapse method implemented by the developed tool is that detailed in Figure 3.1, though using specific strength data curves instead of the detailed response surfaces. The results of the assessment of the Gordo et al. [98] H200 box girder can be seen in Figure 4.19. The discrepancy between the calculated and experimental results is discussed below in Section 4.5.4, with the comparison of results being made between those calculated by the different computational methods. As can be seen in Figure 4.19 and Table 4.12, good correlation has been achieved between the ABAQUS FEA, and interframe collapse assessments for prediction of the ultimate bending strength of the box girder arrangement, though there are some differences in the initial stiffness of the different models. The reasons for these differences are unclear, but could be due to the different algorithms used in the assessment, the way different users have defined parameters such as initial imperfections, or the inclusion of residual stresses in the Benson [34] assessment that has been neglected in the work presented in this thesis. Such variations can affect the calculated strength data of the elements used within the methods.

	Maximum Bending moment (Nm)
Gordo et al. Test	1528096.68
Benson ABAQUS FEA	1147432.02
Interframe Progresive Collaspe (Benson)	1153432.84
Interframe Progresive Collaspe (Underwood)	1138632.06
Difference Benson ABAQUS FEA -Underwood Interframe Progressive Collapse (%)	-0.77
Difference Underwood - Benson Interframe Progressive Collapse (%)	1.30

Table 4.12 – H200 Box Girder Ultimate Bending Strength Results

In Figure 4.19 it can be seen that post the ultimate bending strength point calculated by the developed interframe progressive collapse tool, there is a dramatic reduction in the bending strength of the section. This is in contrast to the more gradual collapse shown by the Benson ABAQUS FEA and interframe progressive collapse results. This is due to the use of defined failure strains for the progressive collapse elements which coincide with their ultimate strength, as is required when implementing the method using response surfaces to capture the strength data, Figure 3.1. Therefore, the post collapse region of the individual element strength data is not being used in the bending strength assessment as discussed in Chapter 3. The Benson FEA and interframe progressive collapse method account for the post collapse strength, leading to a smoother curve beyond the point at which the ultimate bending strength is reached. This results in a rapid failure of the structure for this assessed case, though demonstrates the ability of the method to calculate a reliable ultimate bending strength. Assessment of the Gordo et al. [98] H300 and H400 box girders and comparison against the Benson [34] ABAQUS FEA shows similar results.

Figure 4.20, Figure 4.21, Table 4.13 and Table 4.14 show the results of H300 and H400 box girder assessments. The calculated ultimate bending strength of the box girders can be seen to be within 5.5% of the ABAQUS FEA models for both arrangements. The initial stiffness of the different assessment methods can again be seen to vary and similar sharp reductions in the interframe collapse method can be seen post the ultimate bending strength. However, in both the H300 and H400 cases, the progressive collapse nature of the structure can be seen as the bending strength begins to increase again before failure of the section.

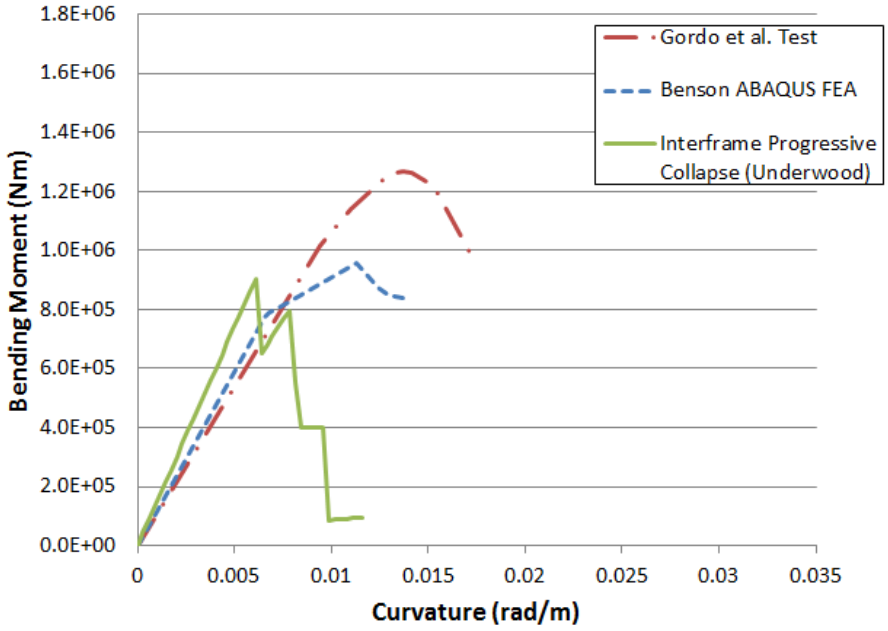

Figure 4.20 – H300 Box Girder Results Comparison

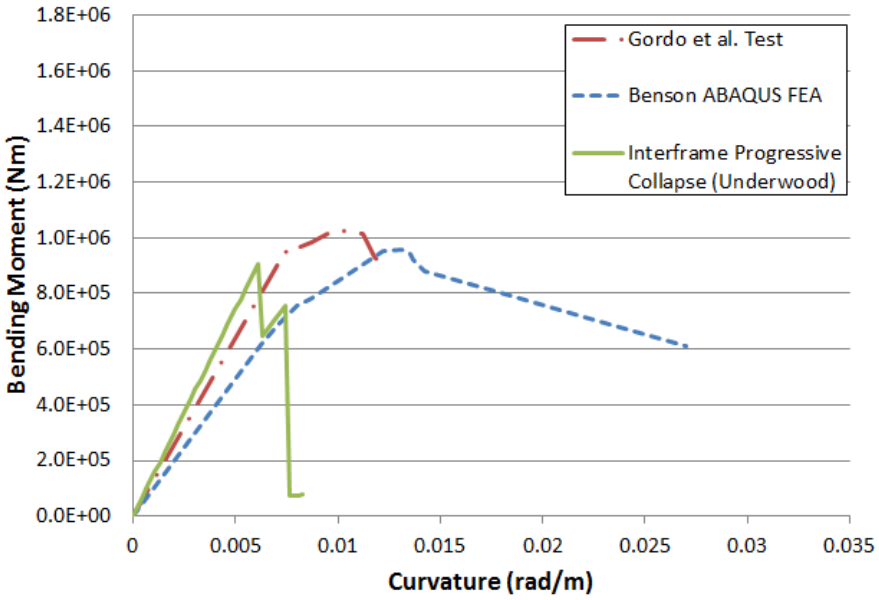

Figure 4.21 – H400 Box Girder Results Comparison

	Maximum Bending Moment (Nm)
Gordo et al. Test	1268181.82
Benson ABAQUS FEA	956250.00
Interframe Progressive Collapse (Underwood)	904628.23
Difference Benson ABAQUS FEA - Interframe Progressive Collapse (%)	-5.40

Table 4.13 – H300 Box Girder Ultimate Bending Strength Results

	Maximum Bending Moment (Nm)
Gordo et al. Test	1024137.93
Benson ABAQUS FEA	956896.55
Interframe Progressive Collapse (Underwood)	906547.53
Difference Benson ABAQUS FEA - Interframe Progressive Collapse (%)	-5.26

Table 4.14 – H400 Box Girder Ultimate Bending Strength Results

The assessments detailed above provide sufficient confidence that the developed tool is operating correctly, though further assessment of the tool will be made during the verification of the ANSYS FEA box girder model detailed below.

4.5.4 FE Model Definition

Verification of the FEA box girder model using ANSYS has been undertaken by modelling the Gordo et al. [98] H300 and H400 test cases, as described in Section 4.5.2.

The FE modelling of the box girders utilised an elasto-perfectly-plastic stress-strain relationship. This aligns with the modelling detailed previously in this chapter, and is suitable for obtaining ultimate bending strength data, though may lead to a conservative calculation of the post collapse region. The box girder has been modelled using the ANSYS shell element SHELL181. This is the same element that has been used in the previous stiffened steel structural models discussed earlier in this chapter and is suitable for this type of application where large structural distortion and non-linear effects are expected.

Provided the experimental test rig has applied a pure bending moment to the box girder structures, it should not be necessary to model the entire test rig to replicate the results using FEA. Therefore the FE modelling has only replicated the box girder structure with suitable boundary conditions. It is desirable to assess the structure under pure free bending, as the loading form applied to ship structures when at sea.

Application of the boundary conditions and load to the FE box girder model must ensure overall stability of the model whilst applying a load that allows application of the required pure bending moment. The modelling must also account for the shift in neutral axis that will occur as the structure progressively fails. The boundary conditions discussed by Hughes et al [30] have been applied to ensure these conditions are met. Therefore, one end of the box girder has been fixed using a clamped boundary condition, whilst the nodes on the other end have been tied to a single reference node using the ANSYS rigid beam element MPC184. The rotational displacement to induce the desired bending moment is then applied to this reference node. The rotational point is located on the transverse centre line of the box girder, at a vertical position equal to 1/5 of the total height of the box. The vertical height of the point is arbitrary and does not affect the solution obtained provided the point is allowed to freely translate as the rotational displacement is applied. However, the reference node was positioned such that the neutral axis would be expected to remain above it during the complete solution. The applied boundary conditions can be seen in Figure 4.22.

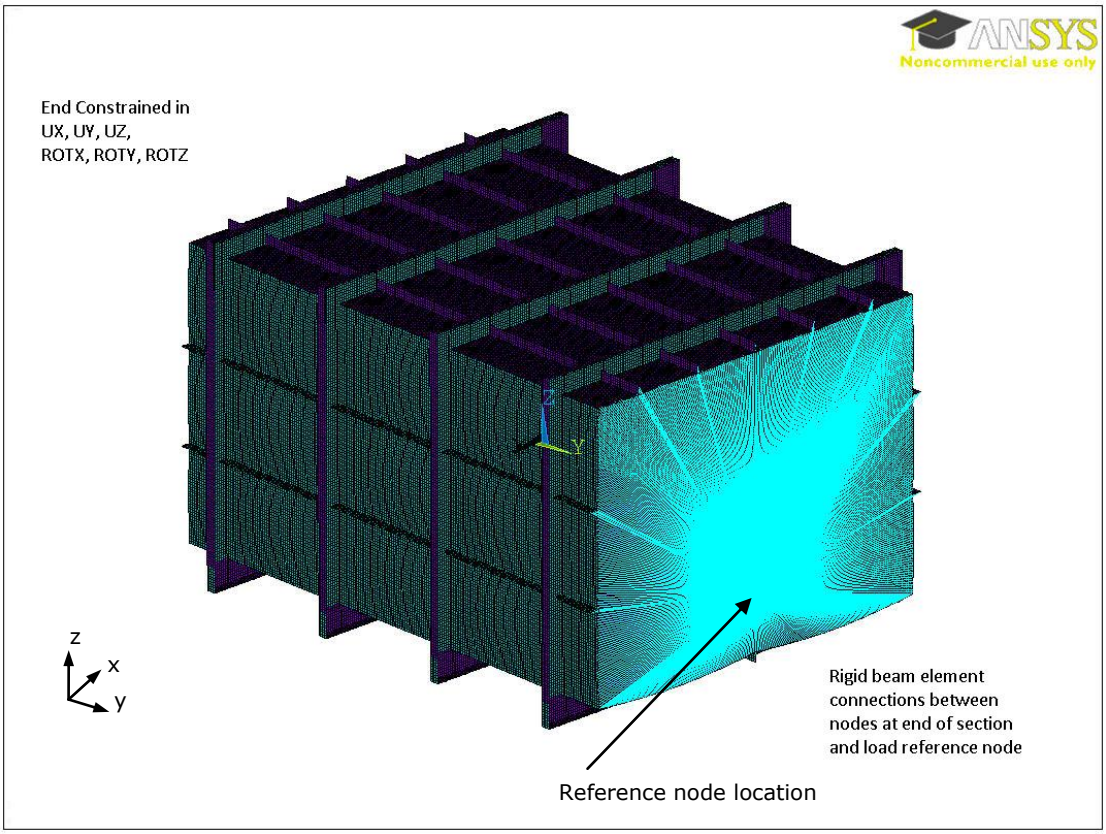

Figure 4.22 – Box Girder FE Model Applied Boundary Conditions

Inclusion of initial imperfections within the model was undertaken using the same approach as described in Section 2.4 and implemented within the grillage FE model described in Section 4.3 using average imperfection levels as detailed in Table 2.5.

To aid convergence of the solution where required, a stabilisation energy coefficient was included within the ANSYS solution phase. This stabilisation coefficient is described within the ANSYS structural analysis guide [101] and referred to as the energy dissipation ratio, and defined as the ratio of work done by stabilising forces to element potential energy, and having a value between 0 and 1. However, application of this factor can influence the results by artificially stiffening the structure. To ensure the results obtained are not being influenced by the level of stabilisation energy being applied, the total stabilisation energy was kept below 1% of the total potential energy in the structure, in accordance with the ANSYS structural analysis guide [101].

4.5.5 FE Model Verification

In his work to recreate the Gordo et al. [98] box girder experimental tests using FEA, Benson [34] performed the analysis, using ABAQUS FEA software, under pure bending as an isolated box girder in the same manner described above, as well as modelling the box girder within the test rig. The results showed significant discrepancies between the isolated box girder and the experimental test results. Benson hypothesised that an additional constraint was being applied to the box girder by the test rig due to the application of the bending load. By replicating this additional constraint, through the use of a nonlinear spring, good correlation between the FE and experimental results can be seen for the H200 and H300 cases as shown in Figure 4.23 and Figure 4.24. For the H400 case, shown in Figure 4.25, whilst the ultimate bending strength correlates well between the FEA and experimental results, with and without the application of the nonlinear spring boundary condition, the initial stiffness appears quite different. The study by Benson [34] demonstrates the complexities of verifying against experimental results. As the development of the box girder for use within the research presented in this thesis surrounds replication of the free bending of a ship hull, no attempt has been made to recreate the Gordo et al. [98] experimental test results by application of additional boundary conditions. Instead, verification has been attained through comparison with the free bending FE results presented by Benson [34] in conjunction with analysis by interframe progressive collapse method using the progressive collapse tool developed by the author, detailed in Section 4.5.

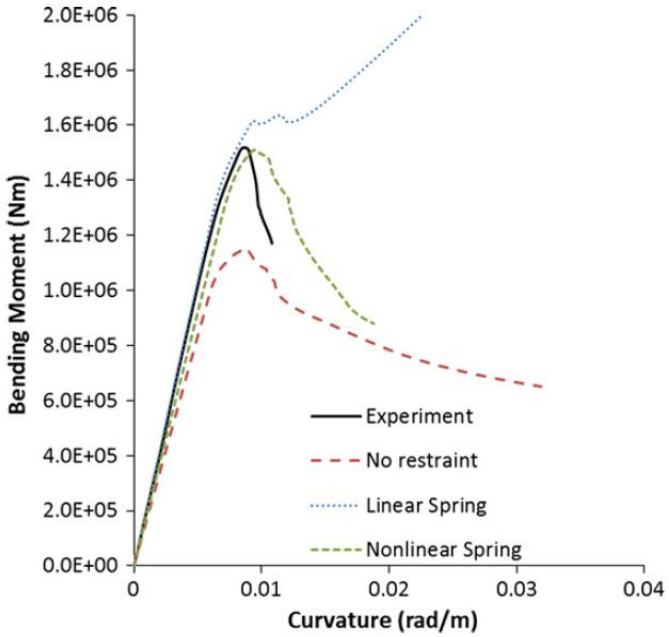

Figure 4.23 – Benson [34] ABAQUS FE Results Comparison with Experimental Test – H200

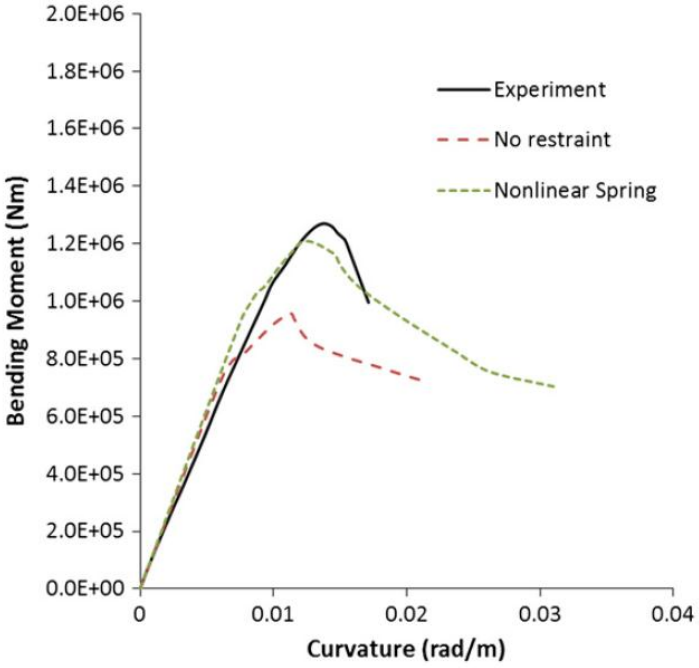

Figure 4.24 – Benson [34] ABAQUS FE Results Comparison with Experimental Test – H300

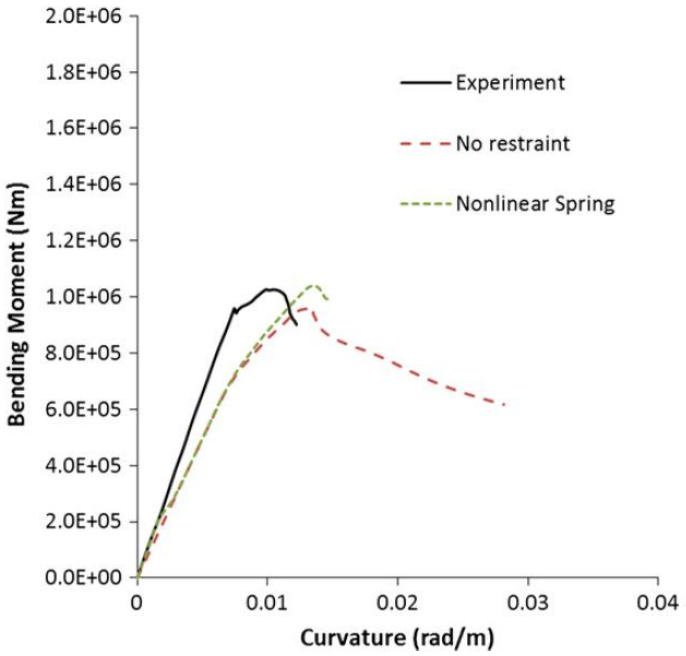

Figure 4.25 – Benson [34] ABAQUS FE Results Comparison with Experimental Test – H400

A convergence study of the mesh size within the box girder FE models was undertaken by solving a number of cases using different element sizes of average element edge length of either 20mm, 10mm or 5mm, the results for which can be seen in Figure 4.26 and Table 4.15 to Table 4.18. From the box girder definition in Table 4.11 it can be seen that the longitudinal stiffener height is relatively small at only 20mm. However, the expected element edge length expected to provide sufficient accuracy of the overall model could lead to the stiffener being defined by only one or two elements. In the regions of the box girder under compression, a significant amount of distortion of the longitudinal stiffeners is expected, and such a coarse mesh in these areas could lead to solution issues. Therefore, regardless of element edge length, the longitudinal stiffeners were defined with 6 elements within the height. This level of division is believed sufficient to allow accurate modelling of the stiffener deformation.

The mesh convergence results can be seen in Figure 4.26 and Table 4.15 to Table 4.18 for the H300 and H400 cases. The results show good convergence for both models using an element edge length of 10mm. This also provides a suitable solution time for completing the analysis. It can be seen that an energy dissipation ratio of 0.015 was applied to the H300 box girder, leading to a maximum stabilisation energy level of 0.9% of the total potential energy of the system. The ratio used is believed to be acceptable in accordance with the ANSYS user documentation [101], and was required to ensure the solution progressed past the first failure point of the section whilst minimising the amount of artificial stabilisation energy within the model. However, no stabilisation energy was required to aid the solution phase of the H400 box girder cases.

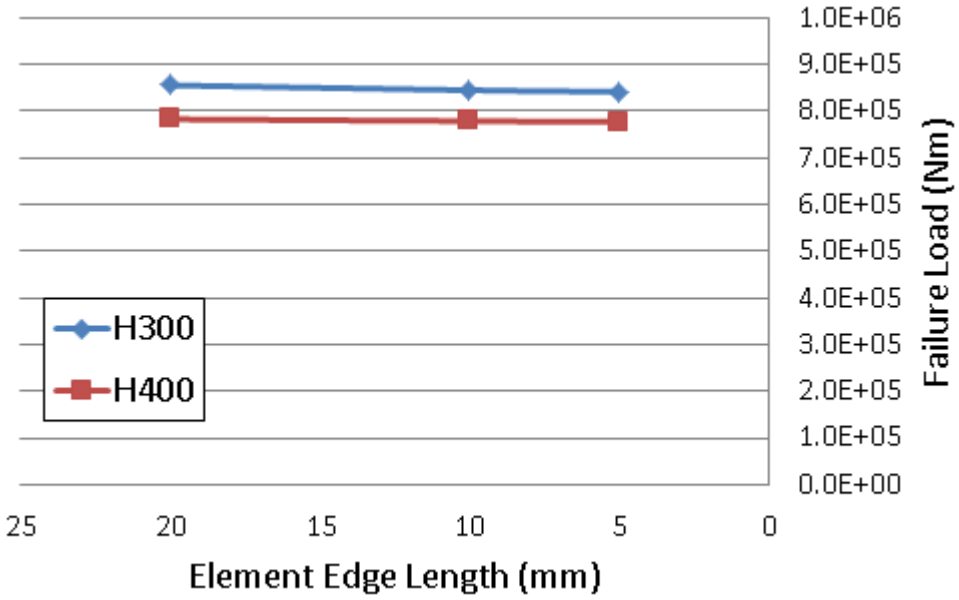

Figure 4.26 – ANSYS Box Girder FEA Ultimate Bending Strength Convergence for Element Edge Length

Element Size	Energy Dissipation Ratio	Maximum Stabilisation Energy: Potential Energy	Maximum Bending Moment (Nm)	Time to Solve
20mm	0.015	0.96%	855903.02	1 hour
10mm	0.015	0.90%	845556.58	3.5 hours
5mm	0.015	0.88%	842264.26	5 hours

Table 4.15 – H300 Box Girder ANSYS FEA Results

Element Size Change	Difference in Max BM
20mm - 10mm	-1.21%
10mm-5mm	-0.39%

Table 4.16 - H300 Box Girder ANSYS FEA Results Comparison

Element Size	Energy Dissipation Ratio	Maximum Stabilisation Energy: Potential Energy	Maximum Bending Moment (Nm)	Time to Solve
20mm	0.00	0.00%	783303.28	1 hour
10mm	0.00	0.00%	779240.70	8 hours
5mm	0.00	0.00%	777693.1	>3 days

Table 4.17 – H400 Box Girder ANSYS FEA Results

Element Size Change	Difference in Max BM
20mm - 10mm	-0.52%
10mm-5mm	-0.20%

Table 4.18 - H400 Box Girder ANSYS FEA Results Comparison

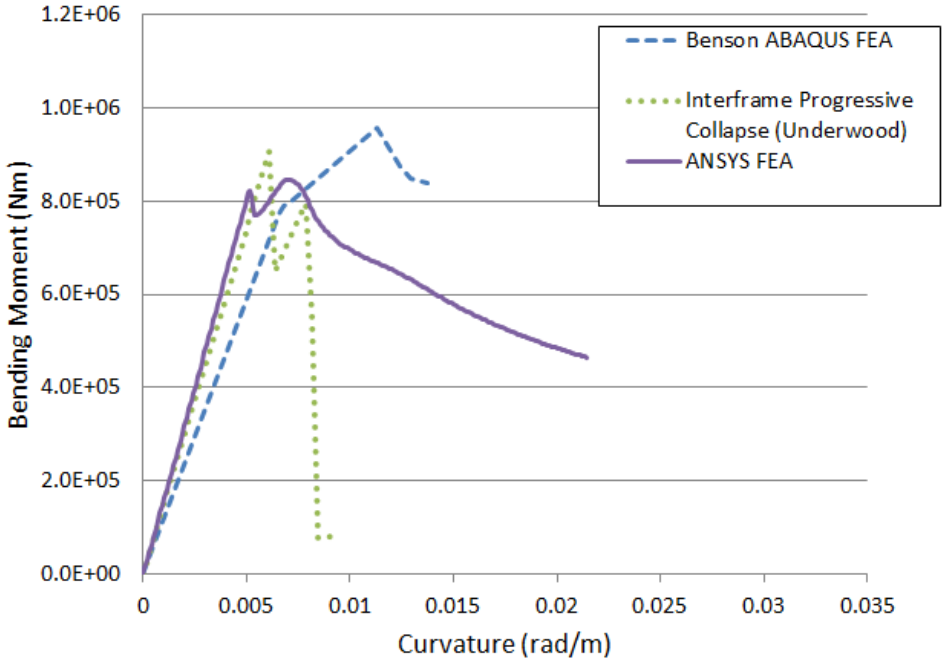

Figure 4.27 – H300 Intact Box Girder Results

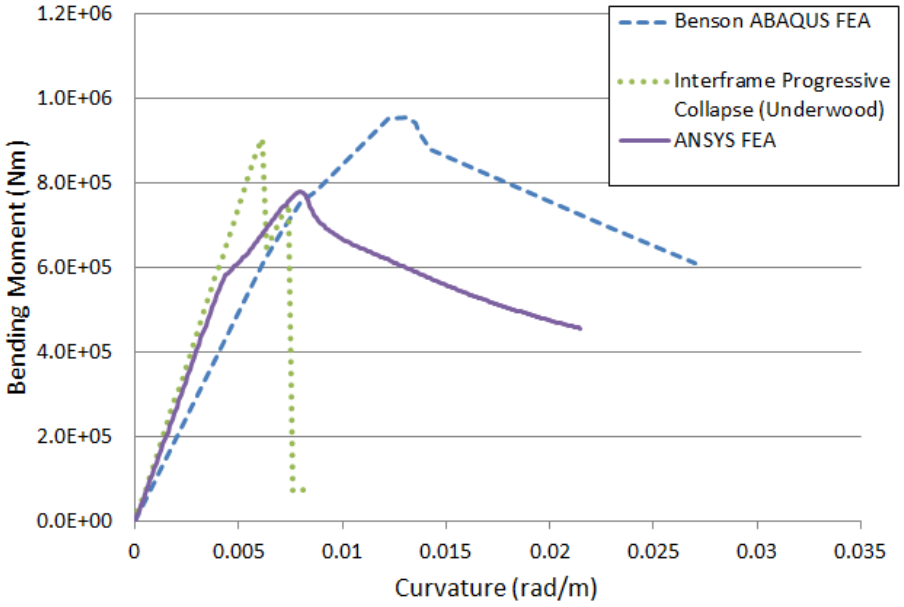

Figure 4.28 – H400 Intact Box Girder Results

	Maximum Bending Moment (Nm)
Benson ABAQUS FEA	956250.00
ANSYS FEA	842264.26
Interframe Progressive Collapse (Underwood)	904628.23
Difference Benson ABAQUS FEA – ANSYS FEA	-11.92 %
Difference Interframe Progressive Collapse – ANSYS FEA	-6.89 %

Table 4.19 - H300 Intact Box Girder Results

	Maximum Bending Moment (Nm)
Benson ABAQUS FEA	956896.55
ANSYS FEA	779240.70
Interframe Progressive Collapse (Underwood)	906547.53
Difference Benson ABAQUS FEA – ANSYS FEA	-18.57
Difference Interframe Progressive Collapse – ANSYS FEA	-14.04

Table 4.20 – H400 Intact Box Girder Results

The results of the ANSYS FEA of the H300 and H400 box girders are presented in Figure 4.27, Figure 4.28, Table 4.19 and Table 4.20. Both sets of results show the ANSYS FEA to be stiffer in the initial elastic region than the ABAQUS FEA, though matches well with the interframe progressive collapse analysis of the box girders. The H300 box girder results show suitable correlation with the ABAQUS results, and comparable to the variation demonstrated by the ISSC 2012 Ultimate Strength committee [40] bench mark study discussed in Section 2.2.6. Good correlation with the interframe progressive collapse analysis is also demonstrated with the H300 ANSYS FEA.

The H400 box girder results show a larger variation between the ABAQUS and ANSYS FEA; however, this is still within the possible levels of variation demonstrated in the ISSC 2012 Ultimate Strength committee [40] bench mark study. Whilst the initial stiffness matches well with the interframe progressive collapse assessment, the ANSYS FEA reaches a much earlier first failure point, which leads to a lower prediction of the ultimate bending strength by FEA. Whilst it is unclear why these discrepancies arise, it is believed that the ANSYS FEA solution is operating correctly and is suitable for use within the research study presented later in this thesis.

Potential sources for differences in the results could be the FEA solvers or solver algorithms being used by the different software, it is possible that differences such as initial imperfection definition approach and the exclusion of residual stresses within the ANSYS FEA could account for this. ABAQUS uses the RIKS solver applying ARC Length method, which is generally assumed suitable for collapse analysis. Whilst ANSYS has this solver available, it is not possible to use it in conjunction with the MPC184 rigid beam element type used to apply the bending rotation. Therefore, the ANSYS Sparse solver has been used, applying a rotation to the reference node and using stabilisation energy within the solution phase. This approach is also considered suitable for this type of analysis. [101]

4.6 Conclusions

This chapter has detailed the verification of the key models used within the research presented in this thesis. The holed stiffened-plate, intact grillage and intact box girder models have been sufficiently verified against existing literature and experimental test cases to provide sufficient confidence in their assessment of the ultimate collapse strength. The verified cases have been created through the use of a tool developed by the author to create the APDL code to generate and solve the FE models. Therefore, the developed tool is considered to be creating the models in the desired manner and is suitable for use within the damaged structural studies presented within this thesis.

Despite the variations demonstrated between the reference models, the box girder FEA model results provide sufficient confidence in the operation of the model, which is believed suitable for use within later research studies. A tool for implementing the interframe progressive collapse method using MS Excel and VBA has also been developed and verified as operating correctly.

The RSM kriging has been demonstrated to be capable of capturing the damaged strength data of stiffened steel structures at both stiffened-plate and grillage level. These are believed to be the smallest and largest levels of structural idealisation to be able to capture the influence of damage on the ultimate collapse strength and for use within a new progressive collapse method. The data generated for development of the response surfaces is through the use of FE models verified within this chapter.

5 APPLICATION OF STRUCTURAL IDEALISATION TO DAMAGED PANEL ANALYSIS

5.1 Introduction

As discussed in Section 2.2, structural idealisation, originally proposed by Ueda et al. [22], is now a well-established method of simplifying the analysis of complex structural arrangements. In Section 2.2 structural idealisation has been discussed in relation to its application for assessment of ship ultimate strength in the form of progressive collapse analysis. In Section 2.2.4 a number of potential weaknesses are raised regarding its application to damaged structure in its current form. In this assessment, the application of the progressive collapse approach has been applied to the assessment of damaged stiffened panels under combined lateral and axial loading. To assess the sensitivity of the collapse strength of a stiffened panel within the model, variations in material properties and plate thickness, to account for corrosion or rolling tolerances, are incorporated, as detailed in Table 4.6.

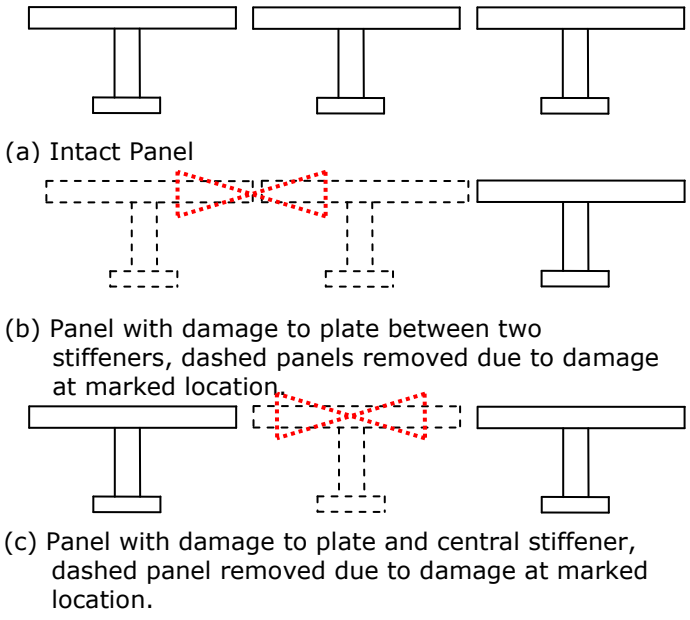

Figure 5.1 – Intact and damaged structural idealisation of a stiffened panel - cross-section view

Simplifying the problem to that of an intact stiffened panel containing three attached stiffeners, the idealised plate-stiffener combination, is that of the sum of three individual plate-stiffener elements as shown in Figure 5.1(a). Introducing damage to the same panel at a location between two stiffeners, though not damaging any stiffeners, the approximated idealisation is that of a single intact element, as shown in Figure 5.1(b). Currently, this assumption has to be made as the method does not account for the residual strength of partially damaged elements as only stress-strain data for intact elements is captured. Introducing damage to the panel with location such that it damages a stiffener, the approximated idealisation is reduced to that of two intact elements as shown in Figure 5.1(c). As can be seen from this example, the current modelling of damaged structures is simplified, and can therefore be represented by the formulation in Equation (29),

$$P_{u0} = \sum_{i=1}^{n} P_{ui} \qquad (29)$$

where P_{u0} is the ultimate collapse load of the structure, P_{ui} is the collapse load of the intact elements (obtained from the pre-calculated stress-strain data) and n is the number of intact elements. It is likely that formulation in this form will result in an overly pessimistic assessment of the residual strength of the structure by not accounting for the residual strength of the damaged elements.

5.2 New Idealisation for Damaged Structural Assessment

In order to be able to benefit from the rapid modelling capability of the progressive collapse method, but be able to capture the damage to a stiffened panel and hence more accurately model the total structure, it is proposed that additional data is captured in relation to the collapse strength of the damaged panels and included in the formulation. This is achieved by modifying Equation (29) to include the residual strength of the damaged element(s), as shown in Equation (30),

$$P_{u0} = \sum_{i=1}^{n} P_{ui} + \sum_{d=1}^{m} P_{ud} \qquad (30)$$

where P_{ud} is the collapse load of the damaged element (obtained from pre-calculated data) and m is the number of damaged elements.

5.3 Progressive Collapse Element Assessment by Finite Element Method

In order to investigate the applicability of progressive collapse method for the collapse analysis of damaged steel-plated structures, FEA has been performed utilising the stiffened-plate FE model detailed in Section 4.2. This model has been used to pre-assess the collapse strength of the elements (P_{ui} and P_{ud} in Equation 29 and 30) used in the progressive collapse assessment.

Utilising the same assumptions as for the stiffened-plate model, including boundary conditions and mesh definition, the model was extended to allow modelling of stiffened panels with multiple stiffeners. This allows direct comparison between collapse strength calculated by the progressive collapse idealised method, Equation 29, the improved progressive collapse idealisation, Equation 30, and full panel FEA results. An example full panel damaged case can be seen in Figure 5.2 with applied boundary conditions detailed. Variations in material properties, plate thickness, plate slenderness β (Equation 25), damage length and damage breadth, as detailed in Table 4.6, have been included in the assessments to determine the influence of these parameters on the panel's collapse strength. The damage aperture shape was also varied between ellipse, rectangle and diamond form.

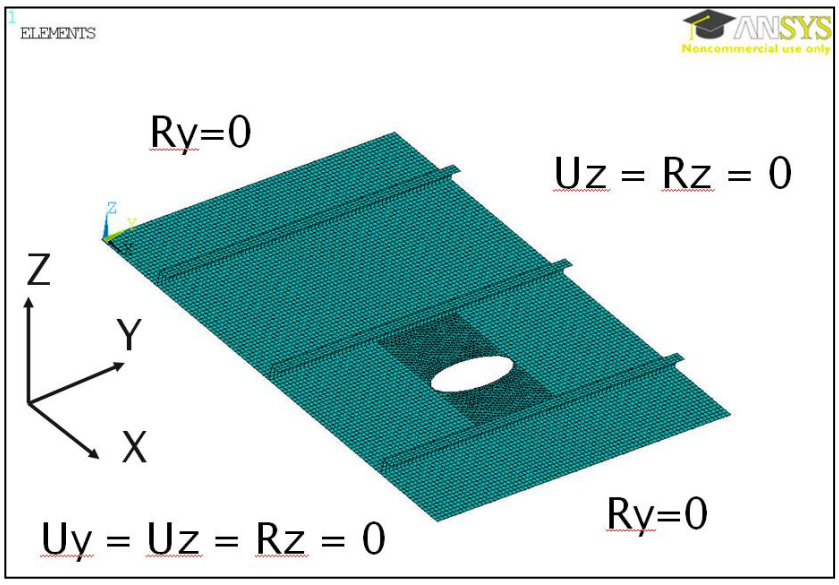

Figure 5.2 - Meshed Stiffened Panel and Applied Boundary Conditions

The assessment of the influence of the included variables has been undertaken through the assessment of three different arrangements. The first is an intact stiffened panel, the second is a damaged stiffened panel where damage was located only in the plate itself, and the third is a damaged panel where the damage location results in loss of a single stiffener. These cases are shown in Figure 5.1.

Damage to the panels was simulated by removing areas of structure consistent with the damage event being modelled. An example of a damaged singularly stiffened panel and its equivalent multiple stiffened panel are shown in Figure 5.3(a) and Figure 5.3(b) respectively. In all cases, the attached stiffener profile was that of an Indian Standard Angle, ISA7045 6 with overall height of 70mm, flange breadth of 45mm and 6mm thickness for both flange and web. A number of simulations for each model arrangement were run to determine the effects of different variables. The combinations of variables for 100 cases were chosen using a Latin hypercube, based on a mean value and range of allowable values, as shown in Table 4.6. The ranges were selected based on referenced literature and the likelihood of those values occurring in a real life situation.

For the configuration used, the overall collapse mode is through the development of a plastic hinge within the panel, influenced by the damage.

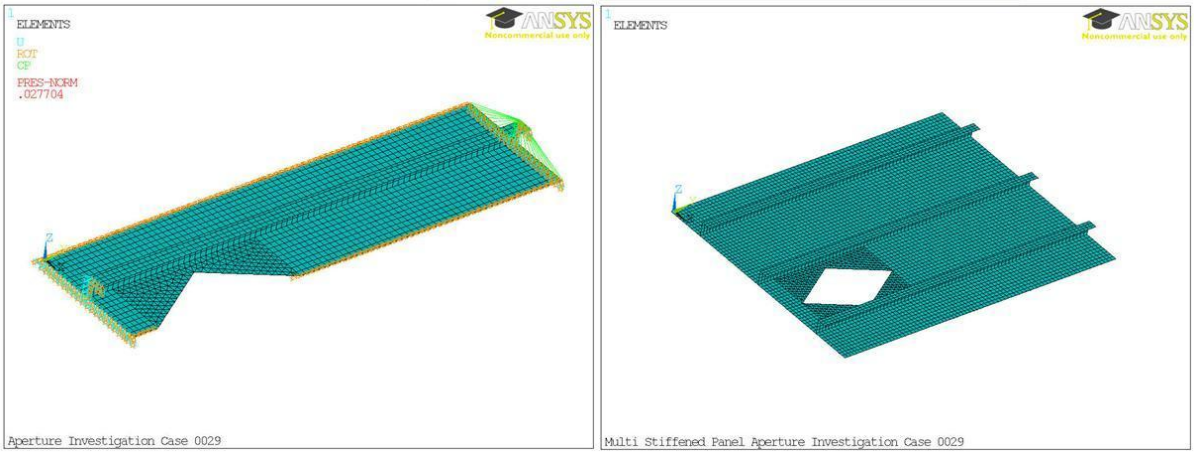

Figure 5.3**(a)** **Figure** 5.3**(b)**

Figure 5.3 - Example case of damaged singular stiffened and equivalent multi-stiffened panels

The results for the different simulations are shown in Section 5.4 - Section 5.6, followed by an analysis of how the variation affected the failure. This allowed comparison to be made between the predictions that would be given by implementing progressive collapse method for damage assessment to those performed using FEA for a whole multiple-stiffened panel.

The results of assessments have been presented by plotting plate slenderness ratio, β (Equation 25) against normalised axial load (P_{u0}/P_{sq}).

5.4 Intact Plate Analysis Results

This section presents the results of the assessment of the defined 100 stiffened panels in their intact condition. Figure 5.4 shows the results for the single stiffener idealised arrangement, Equation 29, and Figure 5.5 shows the results for the multiple stiffened panel arrangement, plotting normalised axial failure load against plate slenderness ratio. The results from this analysis show that there is a low variability in the resulting failure load for the different input variables. This variability is smaller at a low slenderness ratio and grows larger as the slenderness ratio increases. There is a high similarity between the results in this analysis, with a mean difference of 4.7% for the normalised failure load with a range of 0-10%. The results show that the stiffened panel idealised into stiffened-plate elements is a good approximation to the multiple stiffened complete panel for the intact case, and that this idealisation was always conservative in its prediction of collapse strength of an intact panel.

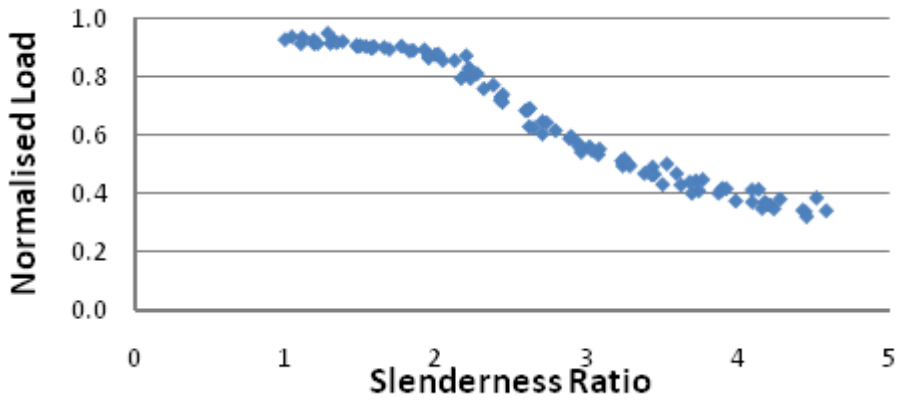

Figure 5.4 - Normalised Axial Failure Load for Intact panel against Slenderness Ratio (Single Stiffener Idealisation)

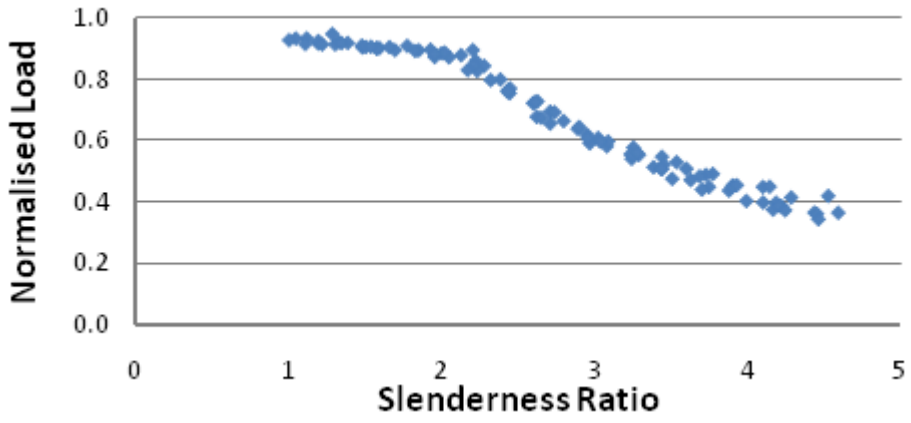

Figure 5.5 - Normalised Axial Failure Load for Intact Panel against Slenderness Ratio (Multiple Stiffened Panel)

5.5 Damaged Plate Analysis - Plate Damage Only

Investigating the effects of damage to the plate between stiffeners, the same set of 100 cases were run, though incorporating damage such that the centre of the damage is located at the midpoint between stiffeners ensuring neither adjacent stiffener is damaged, as per the example in Figure 5.3(b).

Implementing the progressive collapse method idealisation for assessing damage in this configuration, Equation 29, the multiple stiffened panel consisting of three stiffeners is reduced to a single intact stiffened-plate, as shown in Figure 5.1(b). As would be expected for this arrangement, due to the damaged idealisation being a single intact stiffened-plate, the resulting plot followed a similar trend for normalised failure load in comparison with the slenderness ratio, as seen in the intact condition; this can be seen comparing Figure 5.6 to Figure 5.4. However, it can be seen for these results that the failure load is much lower than for the other cases. This is because it is assumed that two of the stiffeners are removed as damage has been caused to these elements for which the residual strength is not accounted for.

Implementing the modified progressive collapse idealisation, Equation 30, the results are shown in Figure 5.7. Here the strength of the damaged panel is calculated as the sum of a single intact stiffened-plate element and two appropriately damaged stiffened-plate elements, which is far more representative of the case being modelled. It can be seen in Figure 5.7 that the failure load is much higher than for the original idealisation, Figure 5.6. The variability on this plate was also larger than for the intact situation.

Assessing the damaged cases by full panel FEA, the results are shown in Figure 5.8. The results again followed a similar trend to those produced for the intact panel but with a larger variation for arrangements with higher plate slenderness ratios.

Finally it was possible to compare the difference between the multiple stiffener model and the progressive collapse model, the results of which are shown in Figure 5.9. Due to the nature of the current idealisation treating any failure in the plate with removal of the adjacent stiffener, it can be seen that this results in a large difference between the two methods. The range of the difference between the two methods was 55%-70% with a mean value of 65%. This result is expected, as the assumed arrangement removes 2/3rds of the structure; however, it demonstrates the conservative nature of the method when applied to a damaged structure.

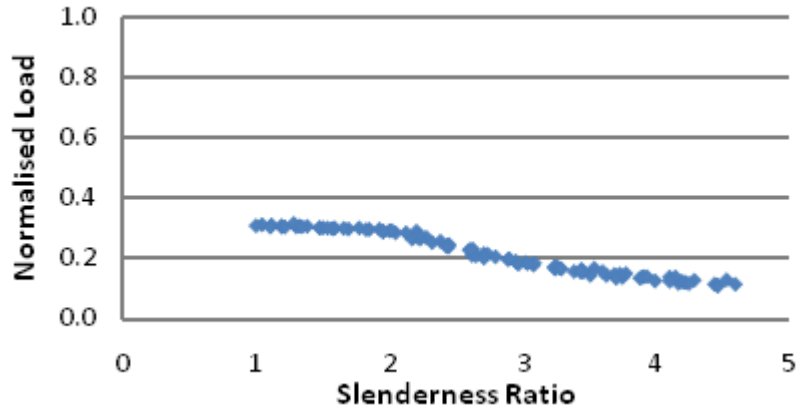

Figure 5.6 - Normalised Axial Failure Load against Slenderness Ratio for Panel with Plate Damage Only (Single Stiffener Idealisation)

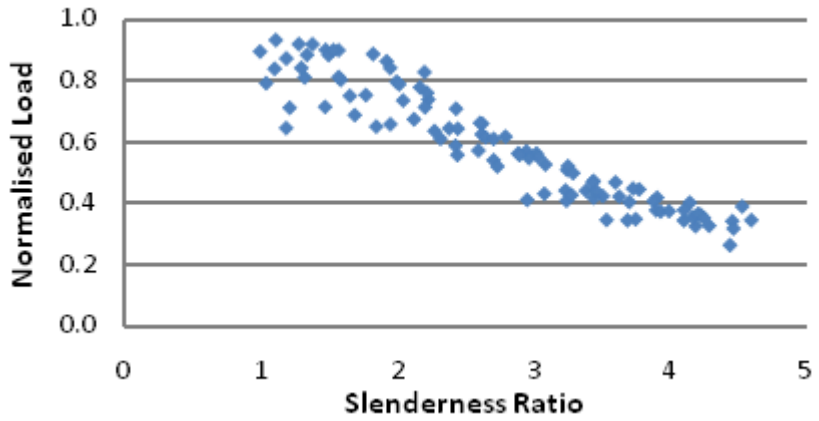

Figure 5.7 - Normalised Axial Failure Load against Slenderness Ratio for Panel with Plate Damage Only (New Single Stiffener Idealisation)

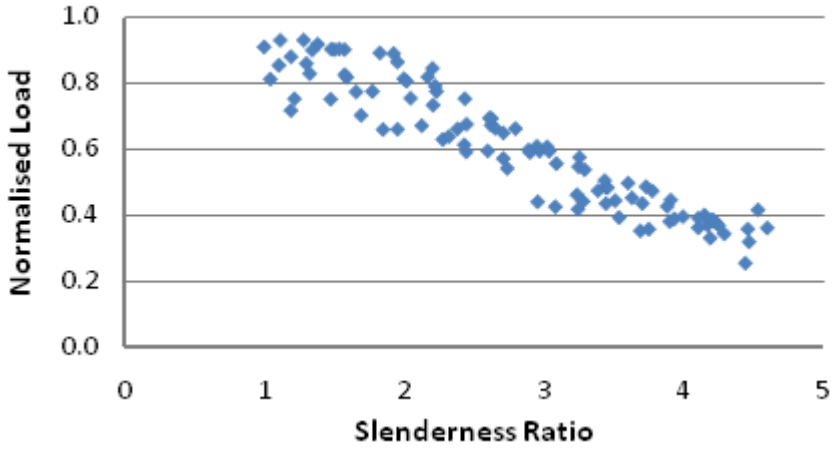

Figure 5.8 - Normalised Axial Failure Load against Slenderness Ratio for Panel with Plate Damage Only (Multiple Stiffened Panel)

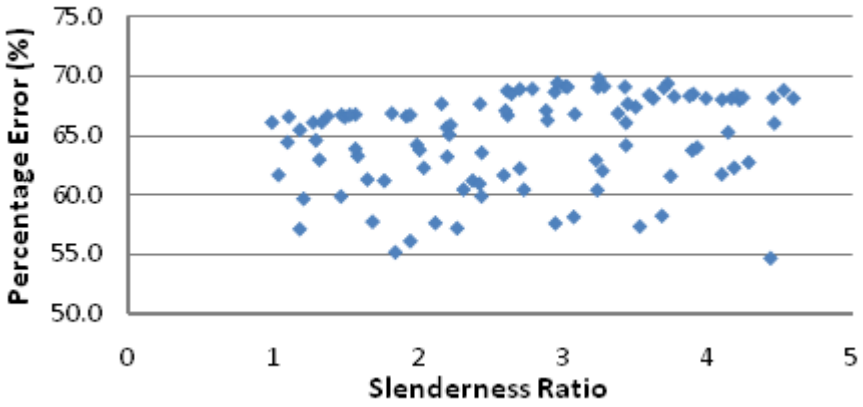

Figure 5.9 - Percentage Difference Between Multiple Stiffener Model and Original Single Stiffener Idealisation (Plate Damage Only)

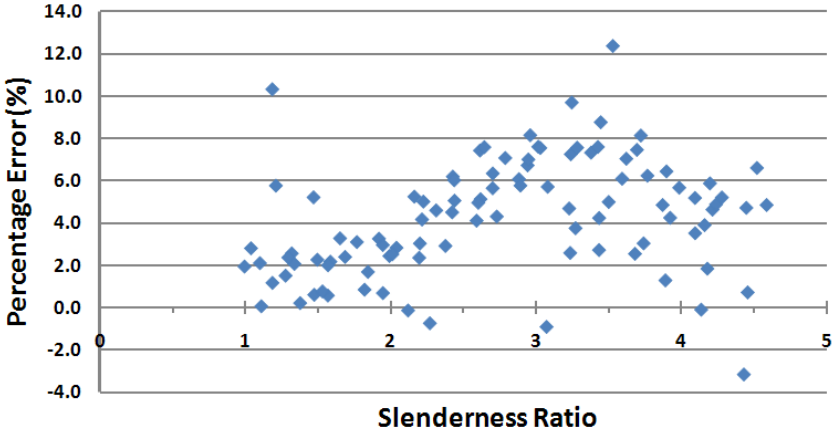

Figure 5.10 - Percentage Difference Between Multiple Stiffener Model and New Single Stiffener Idealisation (Plate Damage Only)

For the proposed new idealisation, it is possible to undertake a similar comparison to the multiple stiffened panel arrangement. The results can be seen in Figure 5.10, where the range for these results was between -3.1% and 12.4% with the mean error being 4.23%. From the one hundred panel arrangements, only five results had a negative value. This shows that for a local stress analysis, in situations where the stiffener was not damaged, the new idealisation method gave a reasonable level of accuracy when compared to the FEA. It also shows that the new idealisation in general gave a conservative estimate, though less conservative than the original idealisation. In the cases where there was a non-conservative estimate, the error was on average less than 1%.

5.6 Damaged Panel Analysis - Plate and Stiffener Damage

Having determined the results for the event where only the plate was damaged, a set of results were run for the event where the stiffeners themselves are damaged. The same set of 100 cases was generated, repositioning the centre of the damage in-line with the central stiffener of the three stiffener panel.

The results for the progressive collapse method idealisation, Equation 29, can be seen in Figure 5.11, where the panel is reduced to two intact panels as shown in Figure 5.1(c). The results for this analysis have a low variability at low slenderness ratio but at higher slenderness ratios show variability in Normalised Load of up to 0.04, caused by the included variation in material properties and plate thickness within the cases. The equivalent multi stiffener panel cases were also run, with results shown in Figure 5.13. For these results it is possible to see that the variability of these scenarios is higher than for the intact panel cases and also higher than the case where the damage was only in the plate itself. A comparison between the multiple stiffened panels and that of the progressive collapse idealisation showed that there was a difference between the results of between -5.8 and 36.2% with a mean value of 10.7%, as seen in Figure 5.14. This shows that the difference between this analysis and the progressive collapse idealisation is closer than for the damaged plate scenario in Section 5.5. This result is unsurprising as the idealisation works by removing damaged elements; hence 1/3rd of the panel is removed. However, it can be seen that even though the average difference between the methods is low, 10.2%, some of the errors can be much higher, 36.2%.

Implementing the new idealisation method, Equation 30, the results for which are shown in Figure 5.12, the panel is reduced to the approximation of two intact elements and the single damaged element. The correlation between the new idealisation results and the full panel results are shown in Figure 5.15, where it can be seen that the new idealisation results are much closer to the full panel FEA results, with mean of 3.7%, though having a range of -10% to 14.4%.

It should also be noted that a small number of the percentage differences were negative, showing that the original and new idealisation methods are not always conservative. This has been shown to be due to different deflection mode shapes appearing in the undamaged sections of the full three stiffened panel arrangement, which by idealising the structure as individual stiffened-plate elements is not accounted for due to the physical separation of its constituent parts.

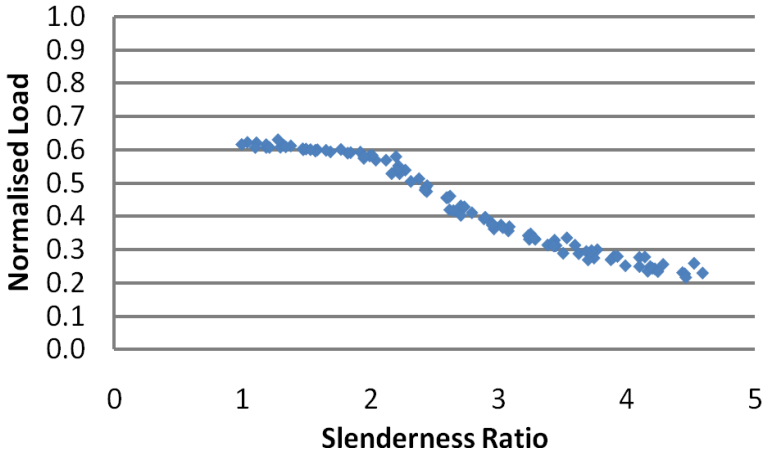

Figure 5.11 - Normalised Axial Failure Load of Stiffener Damaged Model against Slenderness Ratio (Single Stiffener Idealisation)

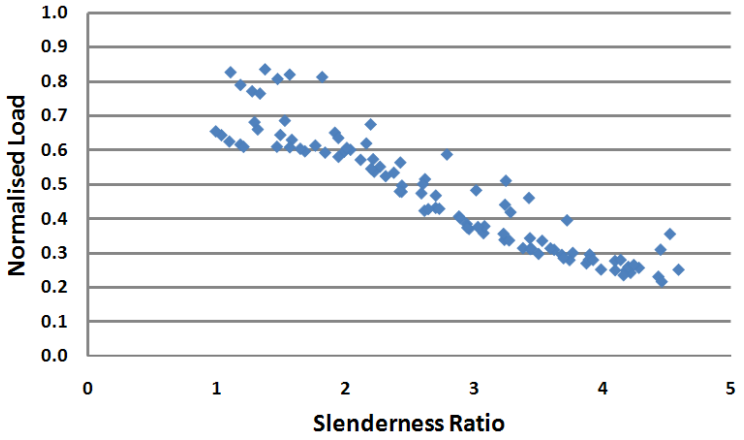

Figure 5.12 - Normalised Axial Failure Load of Stiffener Damaged Model against Slenderness Ratio (New Single Stiffener Idealisation)

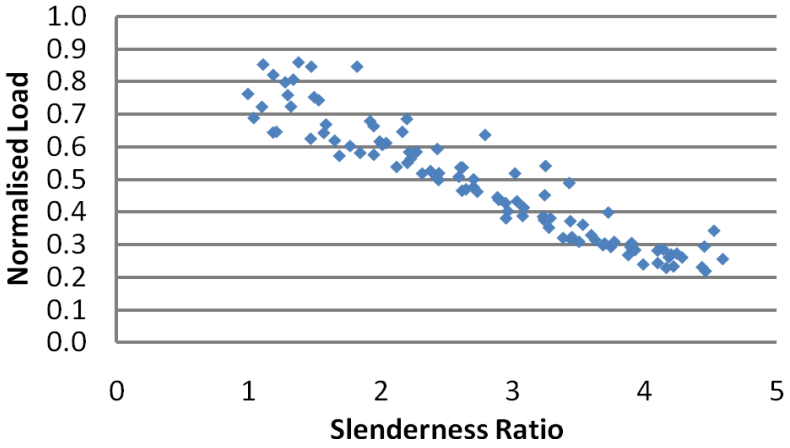

Figure 5.13 - Normalised Axial Failure Load of Stiffener Damaged Model against Slenderness Ratio (Multiple Stiffened Panel)

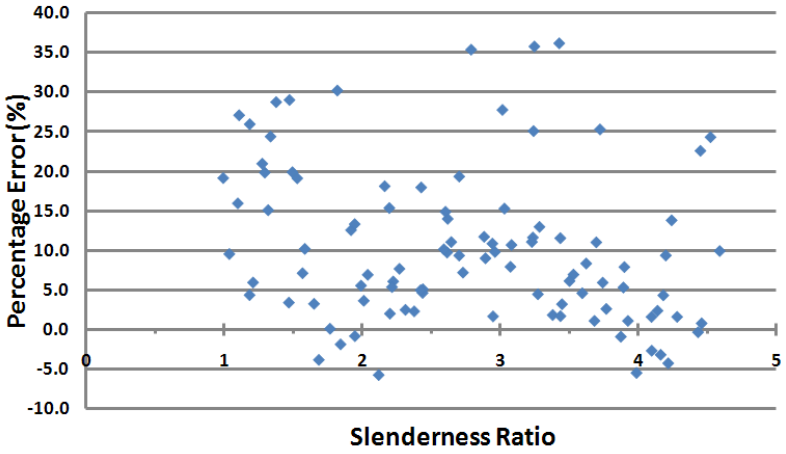

Figure 5.14 - Percentage Difference Between Multiple Stiffener Model and Original Idealisation (Stiffener Damage)

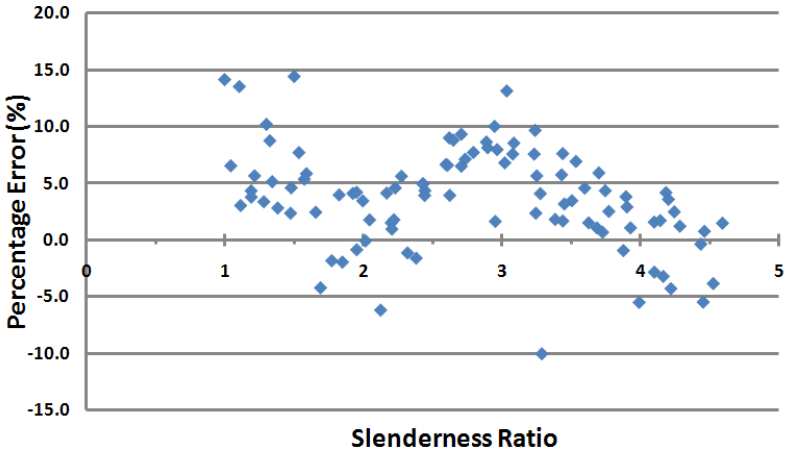

Figure 5.15 - Percentage Difference Between Multiple Stiffener Model and New Idealisation (Stiffener Damage)

5.7 Discussion

The investigation has shown that progressive collapse method, at its current level of structural idealisation, is able to provide reliable results for predicting the collapse strength of intact stiffened steel panels, idealising large panel arrangements as the sum of singularly stiffened plate-stiffener combinations, Equation 29. Results show that the current idealisation method provides conservative results by a mean of 5.1% when compared to FEA for the complete panel in the intact condition for the cases assessed.

In a damage scenario, where damage has occurred to the plate between stiffeners, comparisons of the current idealisation with FEA show the current method to be conservative by a mean of 65%, caused by the assumptions that are required to model damage by this method. A proposed new idealisation for the assessment of damaged steel-plated structure, whereby the strength of the damaged elements is included in the assessment as shown in Equation 30, has shown that the mean error can be reduced to 4.3% with a maximum error of 12.4%. It should be noted that application of the new idealisation has shown to provide non-conservative results in some cases. This is due to alternating deflection modes appearing in the surrounding undamaged structure seen in the full panel FEA, influenced by the damage aperture. This is not captured by the progressive collapse idealisation in its original or new form which, due to the physical separation of the elements, is unable to model the influence of the damage on surrounding structure. To capture these effects it will be necessary to increase the element size used in the progressive collapse method to at least that of a stiffened panel.

In the case where damage occurs to the central stiffener of a panel, progressive collapse idealisation is shown to be conservative by a mean of 10.7% and have maximum error of 36.2%. Implementing the new idealisation, the mean difference is reduced to 3.7% with maximum value of 14.4%. In both scenarios, the idealisation has been shown to provide some non-conservative results, again due to the influence of the damage aperture on the mode shapes developed in the surrounding structure being captured by the full panel FEA but not by the idealised structural methods.

5.8 Conclusions

This study has demonstrated the limitations to the progressive collapse idealisation for the assessment of damaged structures as it is currently applied. The study has demonstrated that a new idealisation incorporating damaged elements can be created; however, to implement the method in its current form would require stress-strain curves to be produced for all possible damage situations for each stiffened-plate element. The proposed method detailed in Chapter 3 and verified in Chapter 4, utilising RSM to capture the structural data, has indicated that the use of response surfaces may provide a solution to this problem by being able to capture a large amount of information incorporating multiple variables. Utilising FEA to benefit from the high level of accuracy possible, the source information required for the response surfaces could be created through careful selection of appropriate intact and damaged stiffened panel arrangements. This would allow assessment of both intact and damage events by one calculation method and could be developed to assess larger stiffened panel arrangements as well as stiffened-plate configurations.

The study has also shown the inability of progressive collapse method using structural idealisation at stiffened-plate level to capture the influence of the damage on surrounding undamaged structure. Increasing the size of the elements will allow this phenomenon to be captured, which can be incorporated into the new progressive collapse by RSM method, further demonstrating the method's potential for damaged strength assessment.

[Blank Page]

6 ASSESSMENT OF THE EFFECTS OF DAMAGE AREA AND SHAPE ON ULTIMATE COLLAPSE STRENGTH OF STIFFENED PANELS

6.1 Overview

From the results of the collapse strength analysis of intact stiffened panels detailed in Chapter 5, it can be seen that the variation due to changes in material properties and plate thicknesses is low. Therefore, it has been assumed that the variation seen in the damage events, as detailed later in Chapter 5, arises from the damage itself.

To investigate the effect of damage size in relation to the overall panel plate area, sets of 70 damage events were run for four panel arrangements of different slenderness ratio. The set size was determined to allow suitable incrementation of the damage aperture between models to produce sufficient results for the analysis. The stiffener profile is retained as ISA7045 6, plate thickness 6mm and material properties fixed with a yield stress of 250MPa, Young's Modulus of $2x10^5$ MPa and Poisson's Ratio of 0.3. A lateral pressure load of 30kPa is applied to the plate on the opposite side to the stiffeners (as shown in Figure 2.15), prior to application of the in-plane axial compressive load, providing a single half sine wave initial deflection shape. The events were configured to either damage the plate only or to damage both plate and central stiffener of a three stiffened panel arrangement. These are the same damage scenarios as per the analysis detailed in Chapter 5 and depicted in Figure 5.1. Stiffened panel models were run for diamond, elliptical and rectangular damage aperture. The length of the aperture was increased from small, approximately $1/16^{th}$ of the panel length, to equal the panel length, and breadth increased from approximately $1/10^{th}$ of the longitudinal stiffener spacing to equal the spacing dimension for that case, with a model created and assessed for each aperture size. Longitudinal stiffener spacing was determined to provide plate slenderness ratio values of 1, 2, 3 & 4, which have been shown by Zhang et al. [102] and Paik et al. [15] to cover the range of slenderness and aspect ratios that would be expected to be seen in the midship region of commercial vessels. The study uses the same FE model as used in Chapter 5 whose verification is presented in Section 4.2.

6.2 Results

The damage results for the case where only the plate of the three stiffener panel is damaged can be seen in Figure 6.1, Figure 6.2 and Figure 6.3, plotting normalised failure load against damage area ratio. The damage area ratio has been calculated as the ratio of area of plate removed to the area of plate between adjacent longitudinal and transverse stiffeners for the intact panel.

$$Damage\ Area\ Ratio = \frac{Damage\ Length * Damage\ Breadth}{Transverse\ Stiffener\ Spacing * Longitudinal\ Stiffener\ Spacing} \quad (31)$$

The results in Figure 6.1 to Figure 6.3 show that as the ratio of damage area ratio increases, the failure load of the panel reduces from the intact panel strength at an almost linear rate. This compares to the results for the case where the plate and central stiffener of the three stiffener panel is damaged, Figure 6.4 to Figure 6.6, where there is an initial rapid decline in panel strength as a section of the central stiffener is removed by the damage, before the strength reduces, again, to an almost linear rate of decline as the damage area ratio increases.

As can be seen from Figure 6.1 to Figure 6.6 and in Table 6.1, the effect of different damage aperture shapes on the normalised failure load for the panels for a given area ratio is minimal, with the mean difference shown to be less than 2% for all slenderness ratios assessed.

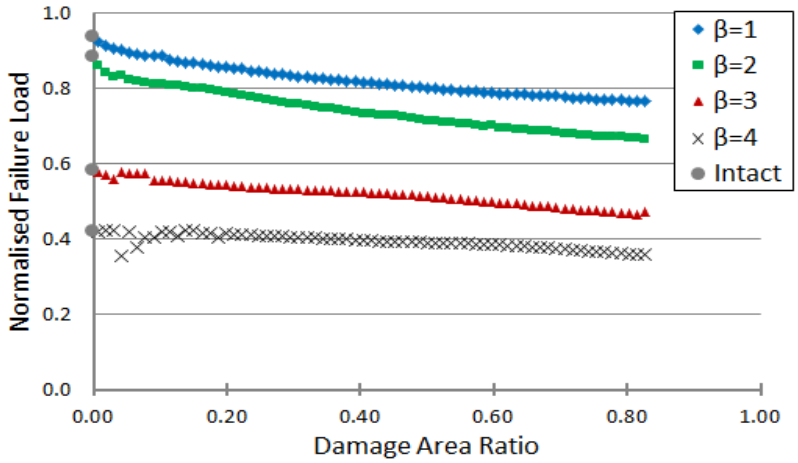

Figure 6.1 - Normalised Axial Failure Load Against Area Ratio for Plate Damage Only - Diamond Aperture

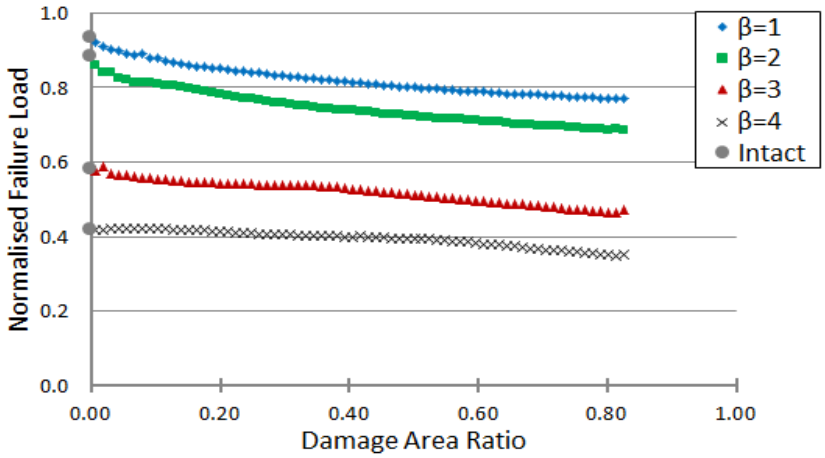

Figure 6.2 - Normalised Axial Failure Load Against Area Ratio for Plate Damage Only - Ellipse

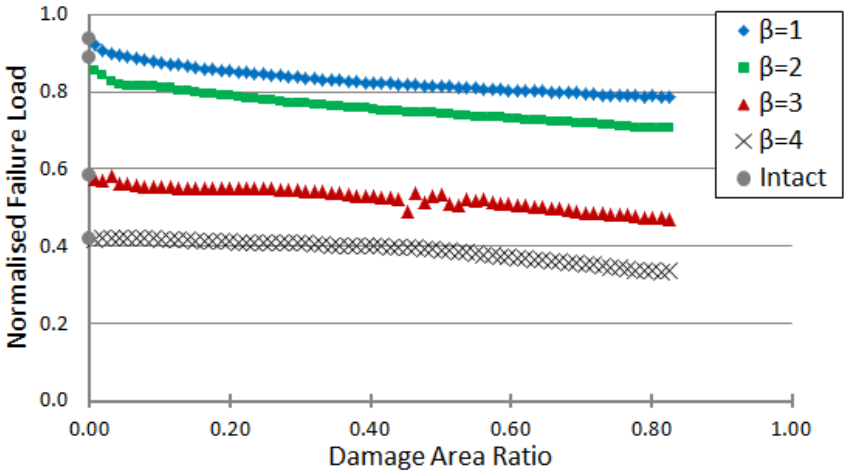

Figure 6.3 - Normalised Axial Failure Load Against Area Ratio for Plate Damage Only - Square Aperture

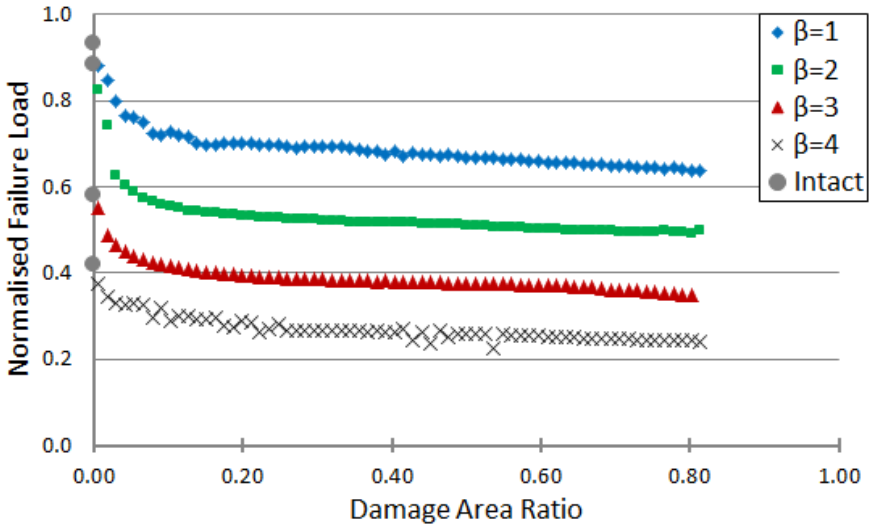

Figure 6.4 - Normalised Axial Failure Load Against Area Ratio for Plate and Stiffener Damage - Diamond Aperture

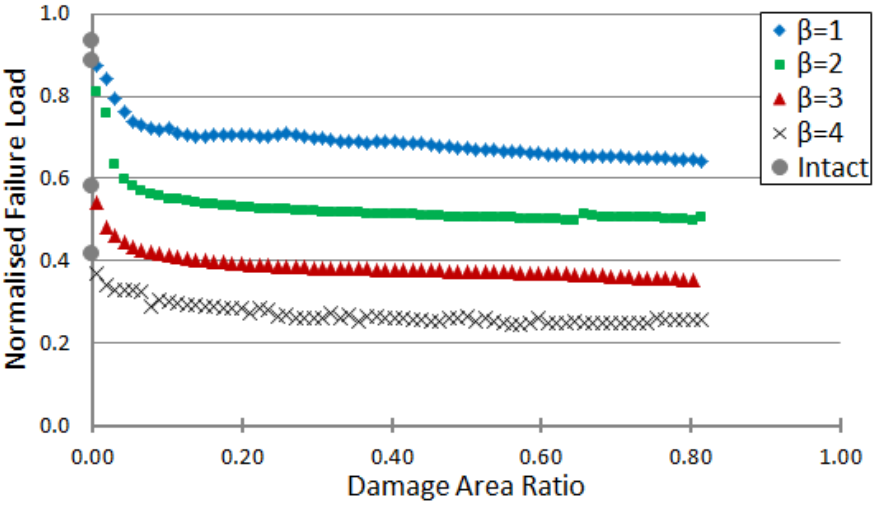

Figure 6.5 - Normalised Axial Failure Load Against Area Ratio for Plate and Stiffener Damage - Ellipse Aperture

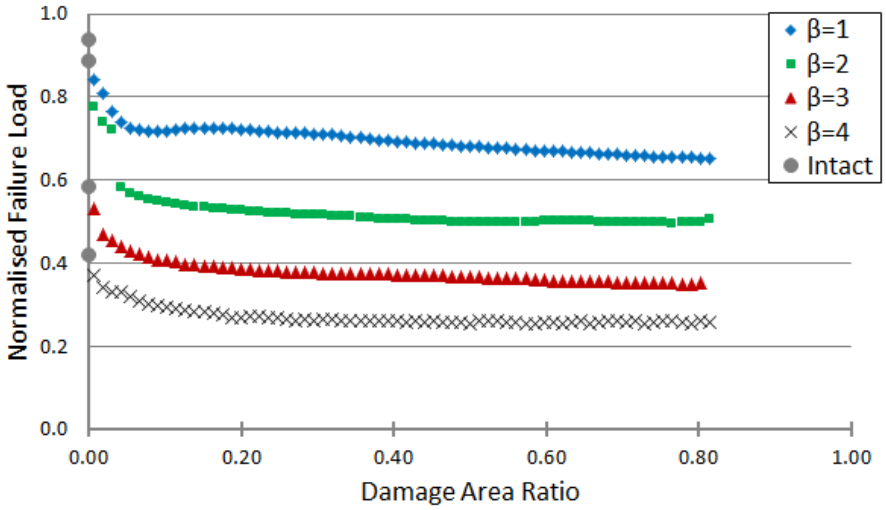

Figure 6.6 - Normalised Axial Failure Load Against Area Ratio for Plate and Stiffener Damage - Square Aperture

Plate Slenderness Ratio (β)	Plate Damage Only		Plate and Stiffener Damage	
	Mean % Difference in Failure Load	Maximum % Difference between aperture shapes	Mean % Difference in Failure Load	Maximum % Difference from Mean
1	0.63	2.96	0.92	4.90
2	1.66	6.09	0.59	14.99
3	0.70	6.13	1.43	3.89
4	0.73	18.1	0.54	16.11

Table 6.1 – Absolute Variation in Normalised Failure Load for Different Damage Aperture Shapes

Damage Shape	Failure Load	
	Mean Variation	Maximum Variation
Diamond	-0.17%	-11.94%
Square	+0.01%	-6.73%
Ellipse	+0.11%	+8.42%

Table 6.2 - Variation of Failure Load from the Mean Failure Load for a Given Damage Area Ratio for Different Damage Aperture Shapes

Analysis was performed to determine how the different aperture shapes affected the failure load of the multi stiffened plates; Table 6.1 shows there is low variation between the different damage aperture shapes for each plate slenderness ratio when calculated for each damage scenario assessed. Grouping the damage scenarios together, Table 6.2 shows that there is a low variation for the three different shapes that have been chosen. The results in Table 6.2 have been calculated as the mean or maximum variation for each damage aperture shape from the mean ultimate strength for panels of the same damage area ratio. The low mean variations shown in the tables are slightly offset by the maximum differences that could occur. The results show that the diamond and elliptical shapes had a larger variation from the mean than the square shape. The largest variation from the mean failure load was 11.94% for the diamond shaped damage. These maximum variations can be seen to occur in the results above, for example in Figure 6.3 for a slenderness ratio of 3, variations occur in the normalised failure load between area ratios of 0.43 and 0.53. In this region, fluctuations in the normalised failure load trend can clearly be seen as area ratio increases. This anomaly was noted in Section 5.7 and again has been shown to be due to the formation of different deflection mode shapes, with influence shown in the undamaged plate for these specific damage configurations. An example is shown in Figure 6.7 and Figure 6.8 where the failure load for damage area 0.50, 0.51, 0.52 and 0.54 are 1.545MN, 1.483MN, 1.470MN and 1.513MN respectively. In examples such as this, a scenario arises where increasing the damage size leads to an increase in the ultimate collapse strength of the panel.

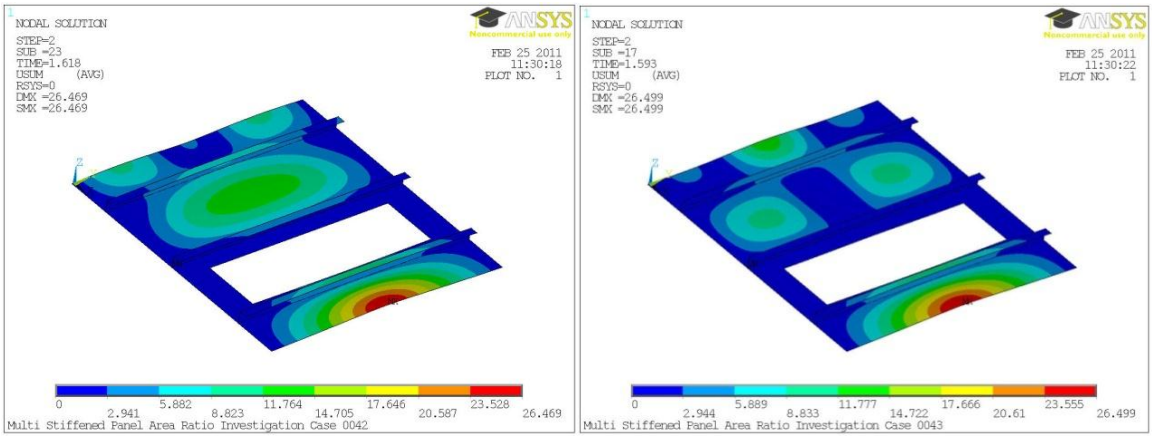

Figure 6.7 - Displacement plots of multi-stiffened panel with square damage of area ratio (a) 0.50 and (b) 0.51

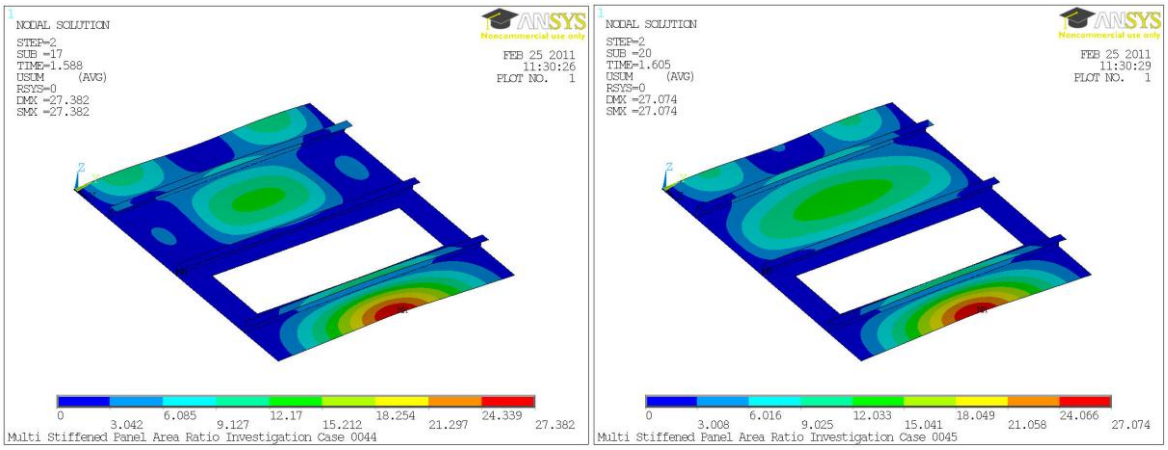

Figure 6.8 - Displacement plots of multi-stiffened panel with square damage of area ratio (a) 0.52 and (b) 0.54

The above results have been presented for a single stiffener profile, ISA70456, which for β 1, 2, 3 and 4, provides λ of 0.60, 0.64, 0.66 and 0.67 respectively. In the collapse assessment of stiffened steel structures, it is noted that column slenderness ratio, λ, is a significant factor. Therefore, the structural arrangements presented above have been run utilising three alternative stiffener profiles, ISA50306, ISA100656 and ISA125956, whose dimensions can be seen in Table 4.1, providing column slenderness ratio values as shown in Table 6.3. Tables of results for the additional case runs can be seen below in Table 6.4 to Table 6.9, with graphical plots of the results shown in Appendix B. No results are presented for stiffener profile ISA125956, β=1, because the arrangement is not believed to be desirable for practical application, having a flange breadth greater than half of the stiffener spacing.

Stiffener Profile	Plate Slenderness Ratio (β)	Column Slenderness Ratio (λ)
ISA50306	1	0.92
ISA50306	2	1.00
ISA50306	3	1.03
ISA50306	4	1.05
ISA100656	1	0.40
ISA100656	2	0.42
ISA100656	3	0.43
ISA100656	4	0.43
ISA125956	2	0.32
ISA125956	3	0.32
ISA125956	4	0.32

Table 6.3 – Column slenderness ratios for additional stiffener profiles

Plate Slenderness Ratio (β)	Plate Damage Only		Plate and Stiffener Damage	
	Mean % Difference in Failure Load	Maximum % Difference between aperture shapes	Mean % Difference in Failure Load	Maximum % Difference from Mean
1	1.14	4.55	1.27	10.51
2	0.71	4.96	0.22	9.74
3	2.85	12.53	2.00	38.82
4	3.57	20.47	7.78	34.02

Table 6.4 – Stiffener ISA 50306: Absolute Variation in Normalised Failure Load for Different Damage Aperture Shapes

Damage Shape	Failure Load	
	Mean Variation	Maximum Variation
Diamond	-1.46%	+27.46%
Square	+0.36%	-6.91%
Ellipse	+0.92%	+16.35%

Table 6.5 – Stiffener ISA50306: Variation of Failure Load from the Mean Failure Load for a Given Damage Area Ratio for Different Damage Aperture Shapes

Plate Slenderness Ratio (β)	Plate Damage Only		Plate and Stiffener Damage	
	Mean % Difference in Failure Load	Maximum % Difference between aperture shapes	Mean % Difference in Failure Load	Maximum % Difference from Mean
1	0.43	1.92	1.52	8.75
2	1.83	6.37	0.20	12.99
3	1.26	13.72	1.58	12.37
4	1.63	24.68	0.53	14.06

Table 6.6 - Stiffener ISA 100656: Absolute Variation in Normalised Failure Load for Different Damage Aperture Shapes

Damage Shape	Failure Load	
	Mean Variation	Maximum Variation
Diamond	-0.18%	-16.47%
Square	+0.13%	-9.89%
Ellipse	-0.03%	-10.22%

Table 6.7 - Stiffener ISA100656: Variation of Failure Load from the Mean Failure Load for a Given Damage Area Ratio for Different Damage Aperture Shapes

Plate Slenderness Ratio (β)	Plate Damage Only		Plate and Stiffener Damage	
	Mean % Difference in Failure Load	Maximum % Difference between aperture shapes	Mean % Difference in Failure Load	Maximum % Difference from Mean
2	1.64	4.94	0.16	16.61
3	0.60	17.86	1.90	9.90
4	2.47	10.54	1.54	16.89

Table 6.8 - Stiffener ISA 125956: Absolute Variation in Normalised Failure Load for Different Damage Aperture Shapes

Damage Shape	Failure Load	
	Mean Variation	Maximum Variation
Diamond	-0.48%	-8.35%
Square	+0.20%	+3.71%
Ellipse	-1.53%	-14.28%

Table 6.9 - Stiffener ISA125956: Variation of Failure Load from the Mean Failure Load for a Given Damage Area Ratio for Different Damage Aperture Shapes

The results presented in Table 6.4 to Table 6.9 show good correlation with the results presented earlier for ISA70456 stiffener profile. In all cases the mean variation between damage aperture shapes can be seen to be low, except for stiffener profile ISA50306, β=4, where the mean variation is shown to be 7.8%. In all cases except for the ISA125956 stiffener profile, the diamond shape aperture can be seen to provide the largest variation from the mean for a given damage aperture ratio. However, for the ISA125956 case, the elliptical aperture provides the greatest variation.

The graphical trends presented in Appendix B also correlate well with the results presented within this chapter. However, as the column slenderness ratio is increased for the larger plate slenderness ratios, a trend develops whereby increasing the damage area ratio from 0 to 0.4 leads to an increase in normalised failure load, before a trend of reducing failure load develops as damage area is increased further. The results show that the damage aperture may influence the failure mode of the structure for all plate and column slenderness ratios assessed.

6.3 Discussion

Assessment of the effect of damage aperture shape on the collapse strength of a damaged stiffened panel has shown that the shape has relatively small effect, with the mean difference between the cases shown to be less than 2% for stiffener profile ISA70456 and 4% for all cases. Conversely, the damage size plays a large factor in determining the strength of a damaged stiffened panel, though the rate of decline in strength is far more controlled than may have been expected. Similar observations are made for the assessment of different stiffener profiles, providing different column slenderness ratios.

In the damage scenario where the plate between stiffeners is damaged but stiffeners remain intact, an almost linear relationship exists between normalised failure load and area ratio for all slenderness ratios and all stiffener profiles assessed. In the scenario where the damage was located on the central stiffener of the panel, it can be seen that there is a rapid decline in the panel strength in the initial phase as the stiffener is breached, before the rate of decline of normalised failure load with increase in damage area ratio assumes an almost linear relationship. This shows the importance of accurate determination of the site of damage but not shape. This indicates that future damage modelling of different incidents should concentrate on accurate determination of size of damage and be categorised as such when designing for damage survivability or assessing a damaged steel-plated structure. Similar trends are again shown for the assessment of different stiffener profiles, providing different column slenderness ratios.

It should be noted that in some configurations, fluctuations in normalised failure load occurred, disrupting the orderly trends shown. Investigation into these fluctuations have shown that they are caused by alternating deflection shapes occurring in the undamaged plate, caused by the particular damage and panel geometry configuration. The fluctuations do not lead to the produced trends becoming obsolete, but continue to demonstrate a weakness in current interframe progressive collapse formation for damage assessment (detailed in Chapter 5). Due to the physical separation of component parts in the idealisation used by the interframe progressive collapse method, it is not possible to calculate the effect the damage event has on adjoining panels. In order to assess damaged structures and account for these influences, idealisation of the structure into larger structural units is necessary.

6.4 Conclusions

This study has shown that the reduction in collapse strength of a damaged stiffened panel is predominantly regular as damage aperture increases. The effect of damage aperture shape appears to have little impact on the collapse strength of the panel. This has been shown to be consistent for arrangements of different plate and column slenderness ratios which cover the configurations that would be expected to be found within existing ship structures. However, the influence of the damage aperture on the failure modes in the surrounding undamaged structure has been shown to affect the collapse load of the damaged panels for a number of damaged stiffened panel arrangements, an effect that is not captured by interframe progressive collapse method when modelling using stiffened-plate elements.

7 ASSESSMENT OF THE EFFECTS OF DAMAGE AREA ON THE ULTIMATE COLLAPSE STRENGTH OF GRILLAGES

7.1 Overview

The research studies presented in Chapters 5 and 6 have investigated the influence of damage on the collapse strength of stiffened steel plates and panels. It has also assessed the application of structural idealisation of stiffened steel structures at stiffened-plate level, as used in the current interframe progressive collapse method, Section 2.2.4. These studies have demonstrated that the presence of damage can influence the mode of failure of the structure; indicating that larger structural idealisation should be utilised within the progressive collapse method to capture these effects.

It has been noted from literature, and in Section 2.2.4, that in damage events it is likely that transverse frames may become damaged, which may further influence the mode of failure of the structure from interframe collapse to an overall collapse mode. In order to investigate this, the grillage model and boundary conditions verified in Section 4.3 has been used introducing a damage aperture into the model. The aperture has been steadily increased from a small area in comparison to the stiffener spacing, until its length is equal to two transverse stiffener spaces; hence damaging a transverse stiffener. A separate model has been generated and assessed for each damage aperture size. In all cases, the analysis is of grillage arrangements featuring four regularly spaced identical ISA70456 longitudinal stiffeners and five deeper orthogonally connected equally spaced transverse Admiralty T stiffeners. The definition of the used stiffener profiles can be seen in Table 4.2. Four different longitudinal stiffener spacing of 170mm, 340mm, 509mm and 678mm have been used to provide plate slenderness ratio values, β, of 1, 2, 3 and 4. The grillage is assumed to be bounded at its transverse ends by deep frames or bulkheads which remain plane and bound along its longitudinal edges to reflect the connection to further grillage structures on either side. As per the previous studies presented in Chapters 5 and 6, the damage aperture was located either between two longitudinal stiffeners so as to initially damage only the plate of the structure, case 1, Figure 5.1(b), or in line with one of the longitudinal stiffeners so as to always damage one longitudinal stiffener, case 2, Figure 5.1(c).

For the first damage case, the damage aperture was initially located centrally between two adjacent longitudinal and transverse stiffeners and increased in length and breadth between models until the damage length equalled the transverse stiffener spacing and damage breadth equalled the longitudinal stiffener spacing, where the damage area ratio, Equation 31, equals 1.0. For damage aperture ratios greater than 1.0, the damage breadth is maintained equal to the longitudinal stiffener spacing and damage length increased in one direction until the damage area ratio equals 2.0, damaging a single transverse stiffener. The damage definition at damage area ratio 1.0 and 2.0 can be seen in Figure 7.1 and Figure 7.2. For the second damage case, the same configuration has been utilised, but with a change of position of the centreline of the damage aperture to be in line with one of the central longitudinal stiffeners.

The damage aperture shape study detailed in Chapter 6 showed that whilst the presence of the damage could affect the failure mode of the structure, the shape of the aperture had minimal influence. For this reason a single diamond aperture shape has been used in this study. As detailed in Section 4.3, average initial imperfections quantities have been applied to the model prior to application of the axial compressive load.

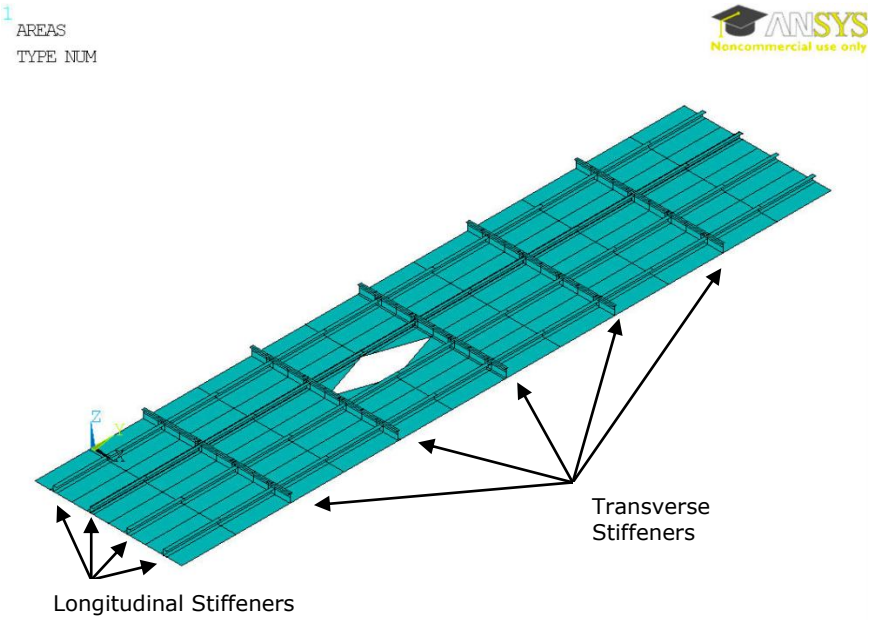

Figure 7.1 – Grillage Damage Definition for Damage Area Ratio 1.0

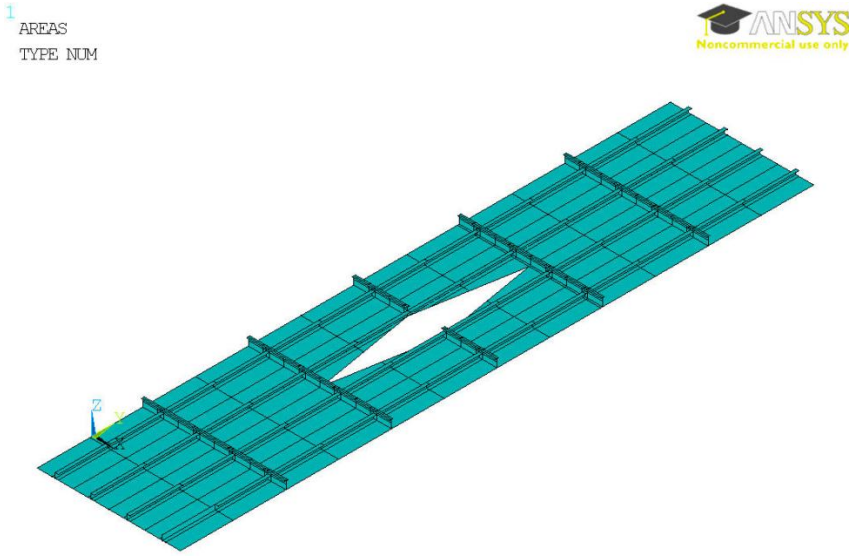

Figure 7.2 - Grillage Damage Definition for Damage Area Ratio 2.0

7.2 Results

Figure 7.3 to Figure 7.6 show the ultimate strength results for the grillage with damage located within the plate, though including damage to a single transverse stiffener for damage area ratios above 1.0. Figure 7.7 to Figure 7.10 show the results for the second damage scenario, damaging a single longitudinal stiffener in all cases and a single transverse stiffener for damage area ratios greater than 1.0. All graphs include an additional line to show the ultimate strength as calculated by interframe progressive collapse.

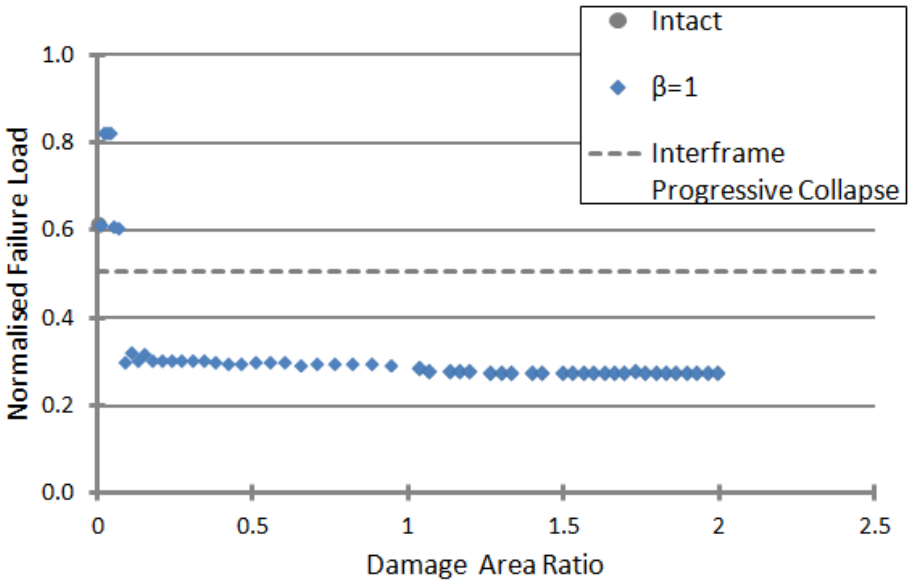

Figure 7.3 - Normalised Axial Failure Load Against Area Ratio for Plate Damage Only - Diamond Aperture, β=1

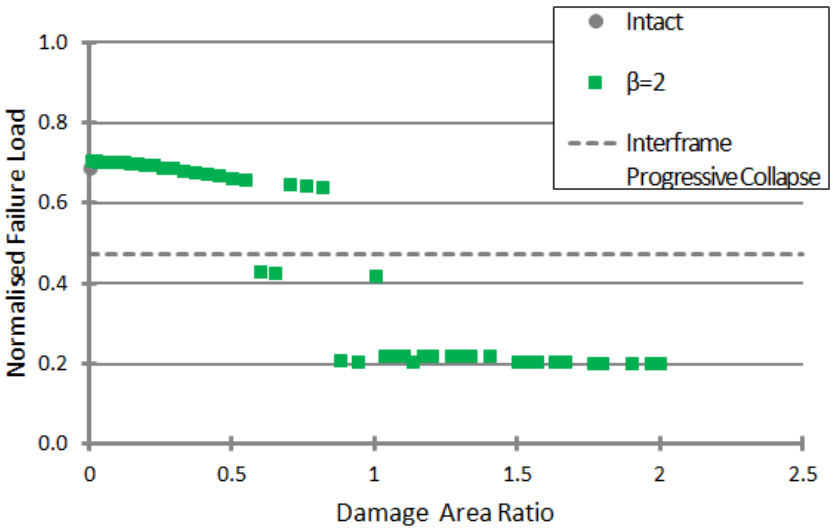

Figure 7.4 - Normalised Axial Failure Load Against Area Ratio for Plate Damage Only - Diamond Aperture, β=2

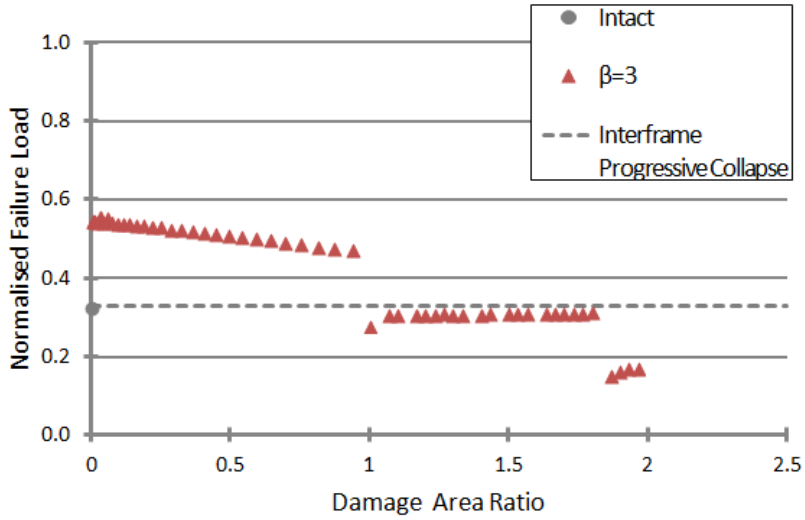

Figure 7.5 - Normalised Axial Failure Load Against Area Ratio for Plate Damage Only - Diamond Aperture, β=3

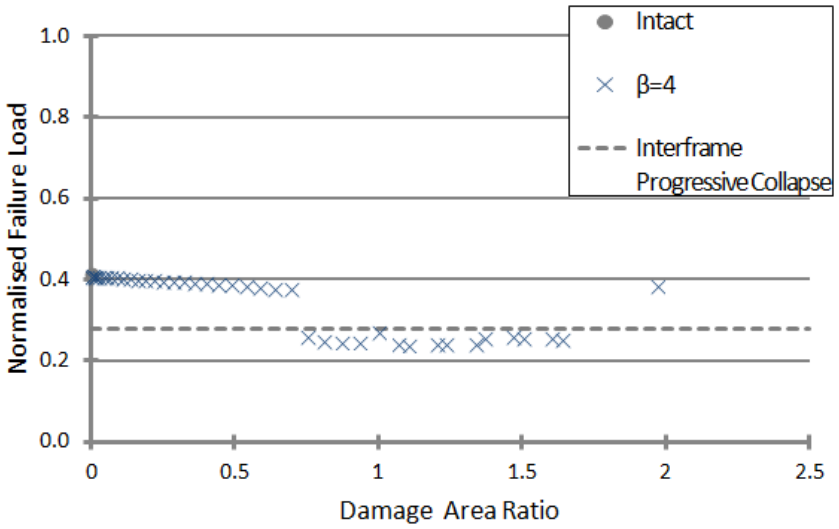

Figure 7.6 - Normalised Axial Failure Load Against Area Ratio for Plate Damage Only - Diamond Aperture, β=4

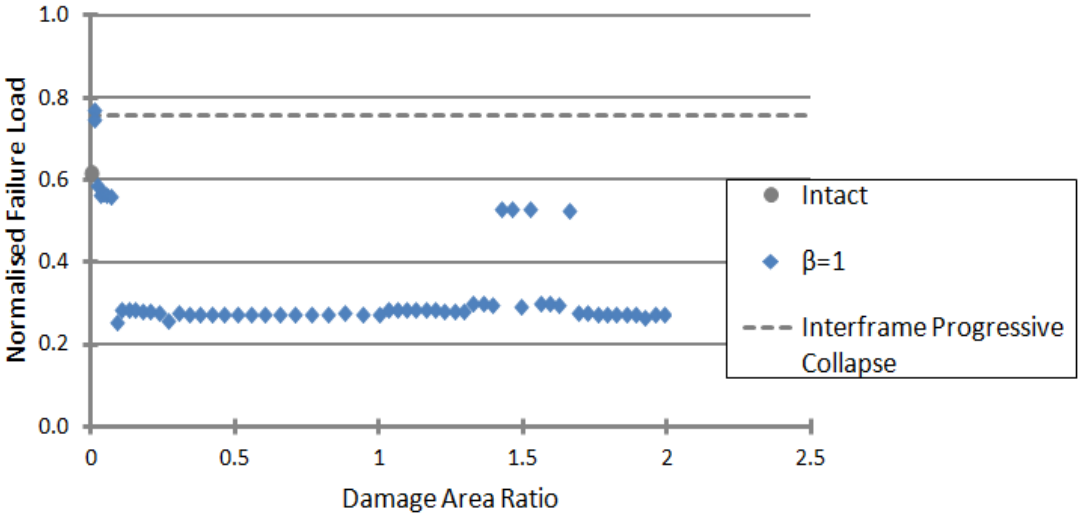

Figure 7.7 - Normalised Axial Failure Load Against Area Ratio for Plate and Stiffener Damage - Diamond Aperture, β=1

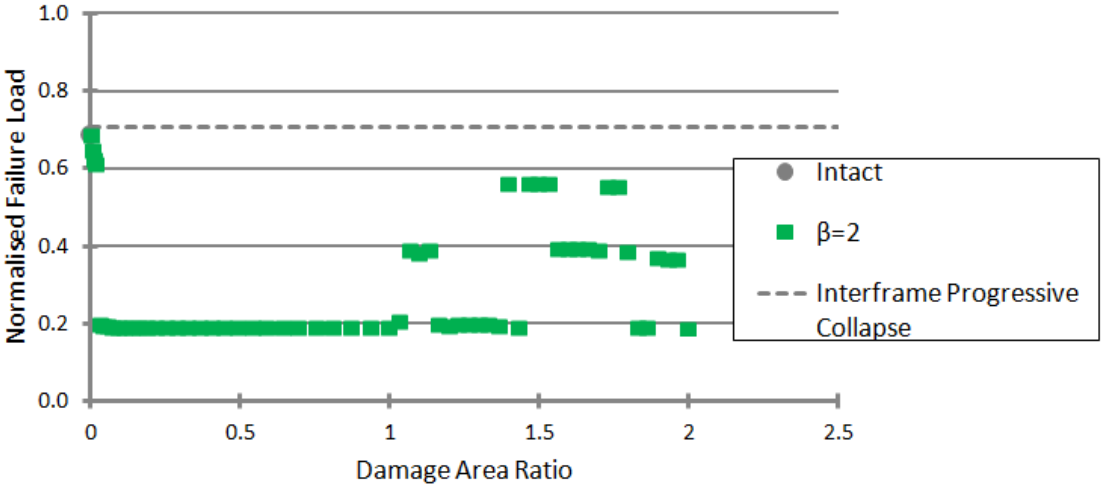

Figure 7.8 - Normalised Axial Failure Load Against Area Ratio for Plate and Stiffener Damage - Diamond Aperture, β=2

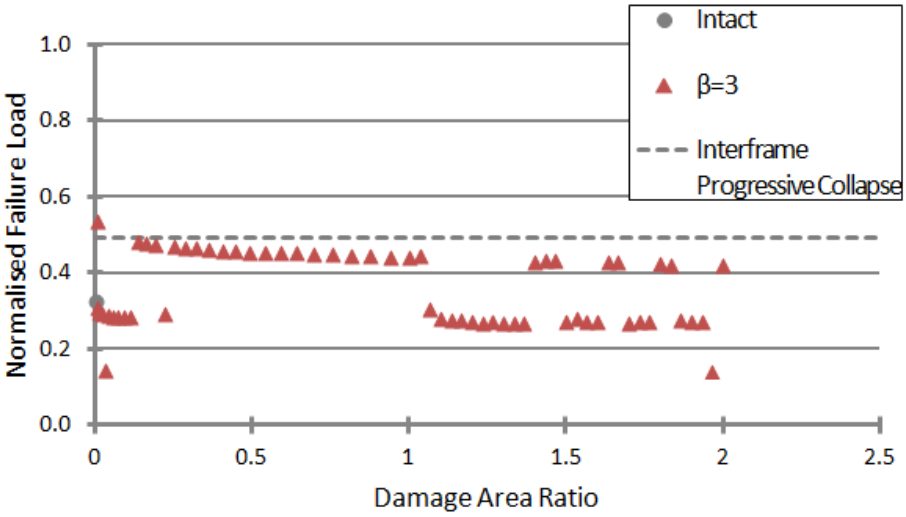

Figure 7.9 - Normalised Axial Failure Load Against Area Ratio for Plate and Stiffener Damage - Diamond Aperture, β=3

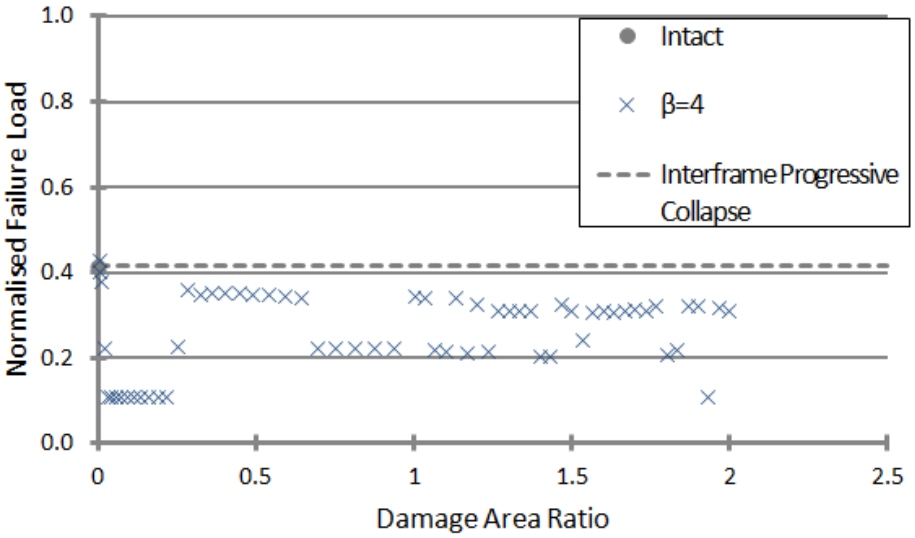

Figure 7.10 - Normalised Axial Failure Load Against Area Ratio for Plate and Stiffener Damage - Diamond Aperture, β=4

Across all of the damage cases and plate slenderness plots in Figure 7.3 to Figure 7.10, it can be seen that as the damage area increases the ultimate collapse strength of the grillage arrangements change. However, whilst intuitively it could be expected that as damage aperture size increases ultimate collapse strength would decrease, this is not always the case. Scenarios arise for all damage cases and slenderness ratios whereby increasing the damage size leads to an increase in the ultimate collapse strength of the grillage arrangements at some point.

For the first damage case β=1, Figure 7.3, the results show an initial increase in the strength of the grillage as the damage aperture is introduced before the strength significantly reduces as damage aperture is increased. It is unclear exactly why this occurs, but could be due to the damage aperture stabilising the developing failure mode of the panel, leading to an increase in ultimate collapse strength. However, the ultimate strength of the grillage then becomes relatively stable, reducing gradually with an approximately linear trend as damage aperture size is increased.

A similar trend can be seen for β=2, Figure 7.4, though here an initially linear reduction in ultimate collapse strength can be seen until the damage area ratio reaches 0.59; at this point a reduction in the ultimate collapse strength can be seen. As damage aperture is increased further to 0.7, the ultimate collapse strength increases and the results conform to an extrapolation of the original linear trend. Above damage area ratios of 0.87, the ultimate collapse strength reduces further, assuming a new stable linear trend, reducing ultimate collapse strength as damage area ratio is increased up to 2.0.

Figure 7.11 shows the collapse strength curves for the first damage scenario when β=2. The plotted results are for damage area ratio 0.54, 0.64 and 0.93, which fall in to the three areas discussed above. In all plots it can be seen how the initial stiffness in the elastic regions follow the same gradient as would be expected. However, as the compressive load is increased, the development of the collapse modes and resultant ultimate strength is different.

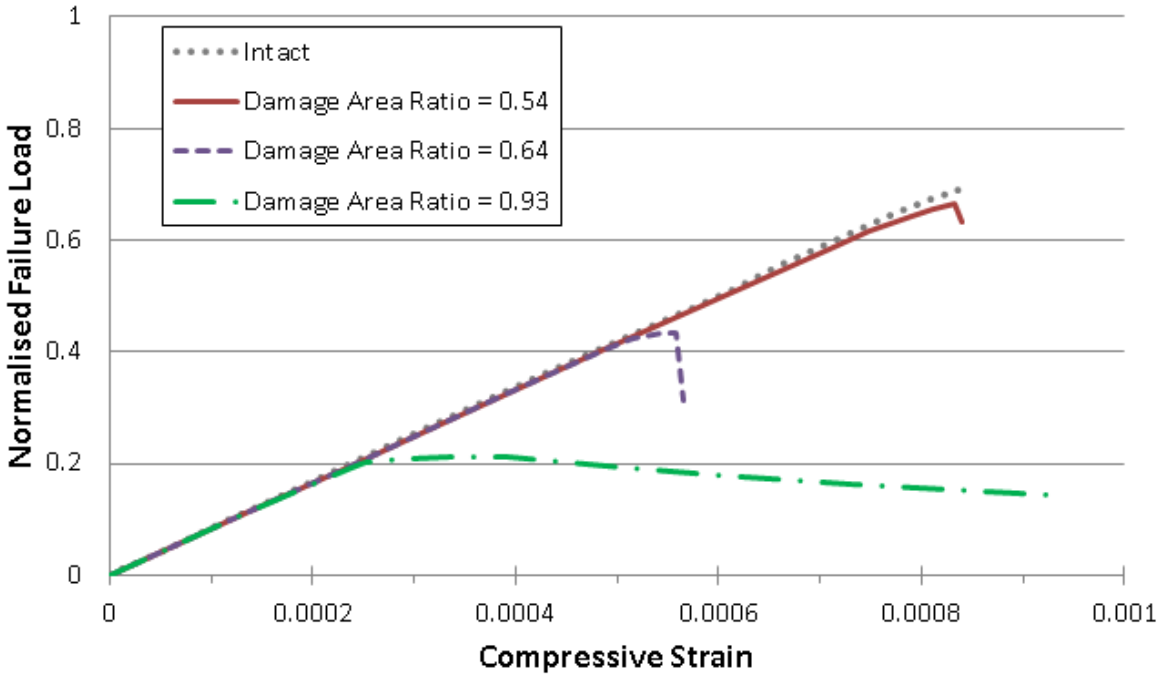

Figure 7.11 - Normalised Load Against Compressive Strain Plot for Plate Damage Only - Diamond Aperture, β=2

Figure 7.12 and Figure 7.13 show the stress and displacement plots for the first damage scenario, β=2 with damage area ratio 0.54. Here the developed failure mode is that of the interframe collapse mode seen in the intact condition with ultimate failure caused by yielding in the plate around the damage and in the longitudinal stiffeners. As damage area ratio is increased to 0.64 (Figure 7.14 and Figure 7.15) the mode shape can be seen to have changed to a longer overall collapse mode, leading to a reduction in the ultimate strength of the grillage, but with ultimate collapse due to yielding of the longitudinal stiffeners under this new displacement form. Further increasing the damage area ratio to 0.93 (Figure 7.16 and Figure 7.17), a third collapse mode can be seen to develop. This mode shape appears to be more elastic in nature, showing no yielding of the structure as the ultimate collapse strength is reached and demonstrating an overall collapse mode bound by the clamped constraints on the transverse ends of the structure. This failure mode is then maintained as the damage area ratio is increased above this point until a damage area ratio of 2.0 is reached.

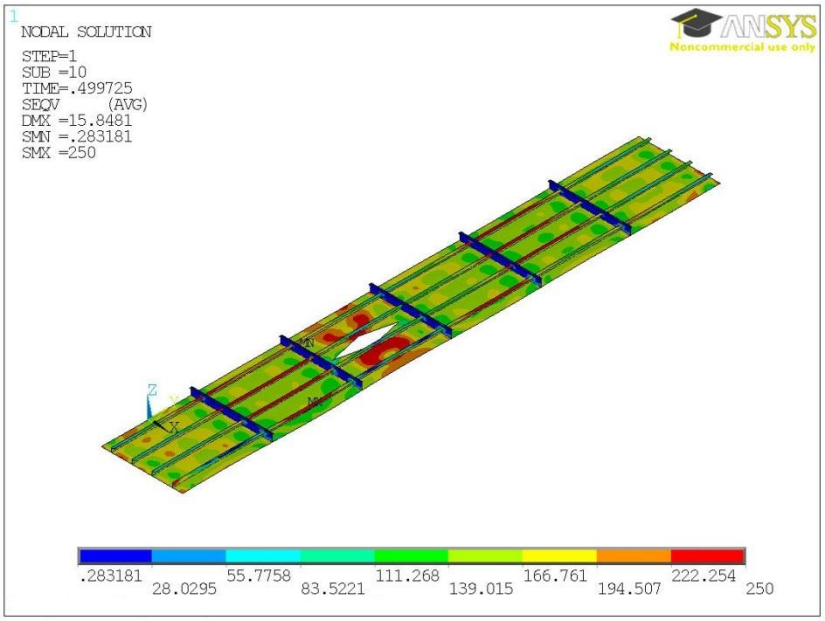

Figure 7.12 – Von Mises Stress Contour Plot: β=2 Damage Area Ratio 0.54

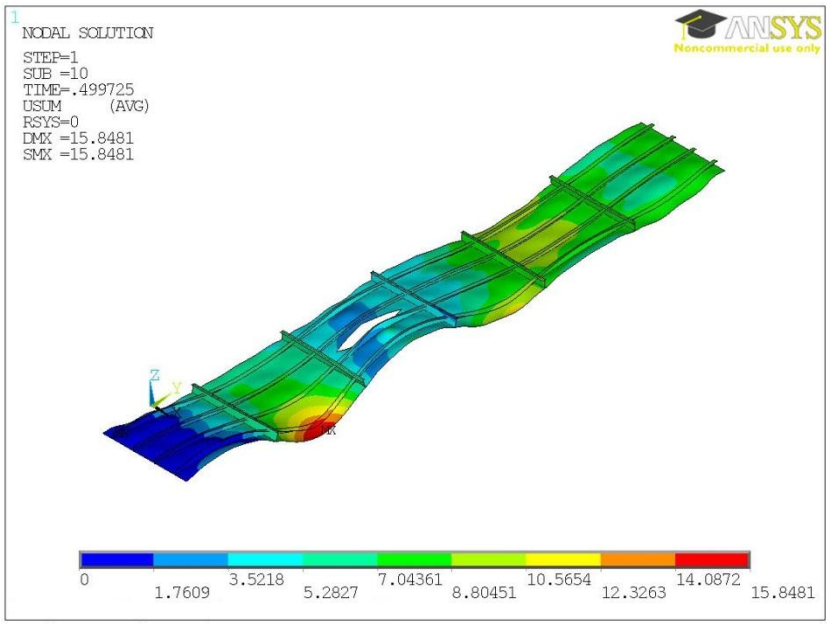

Figure 7.13 – Magnified Displacement Contour Plot: : β=2 Damage Area Ratio 0.54

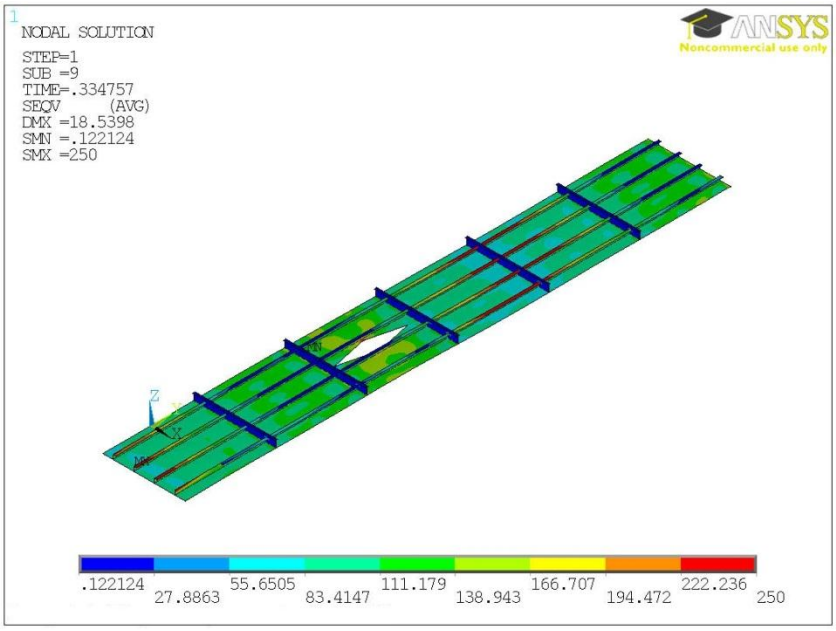

Figure 7.14 - Von Mises Stress Contour Plot: β=2 Damage Area Ratio 0.64

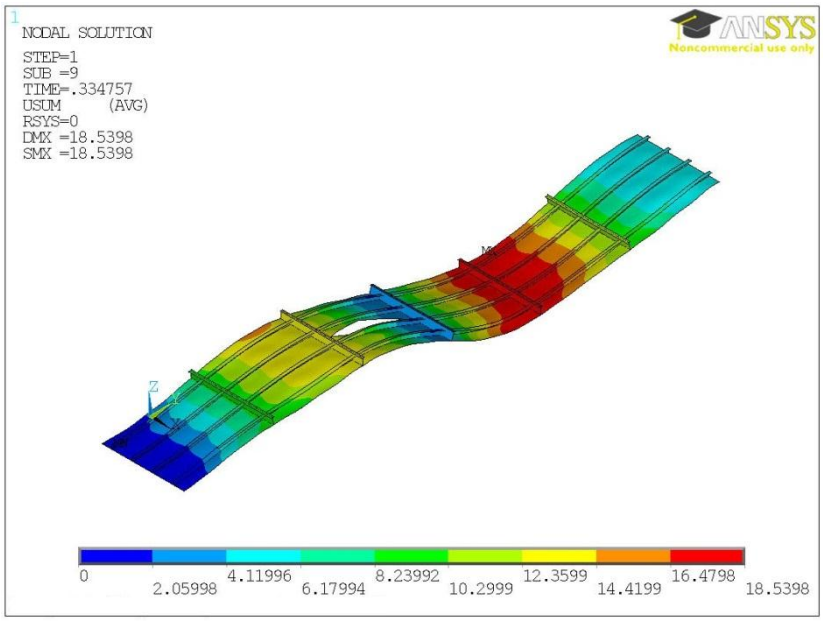

Figure 7.15 - Magnified Displacement Contour Plot: : β=2 Damage Area Ratio 0.64

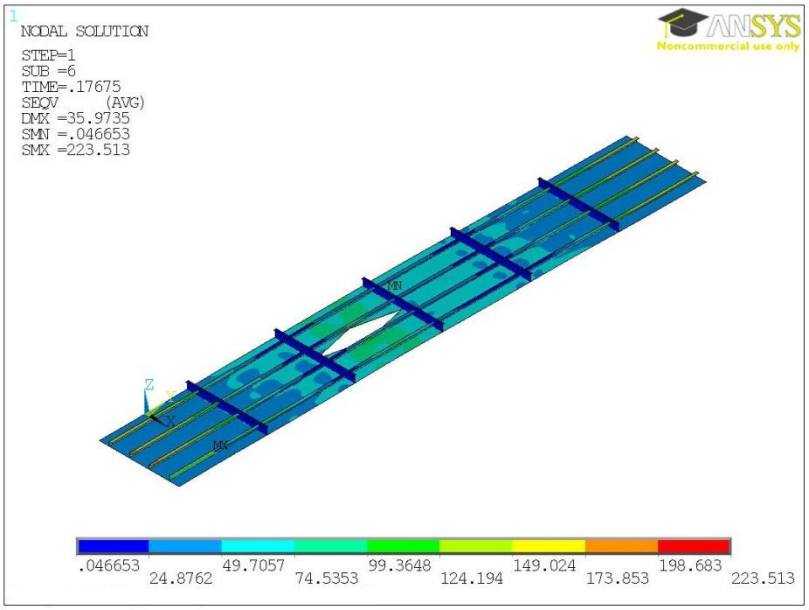

Figure 7.16 - Von Mises Stress Contour Plot: β=2 Damage Area Ratio 0.93

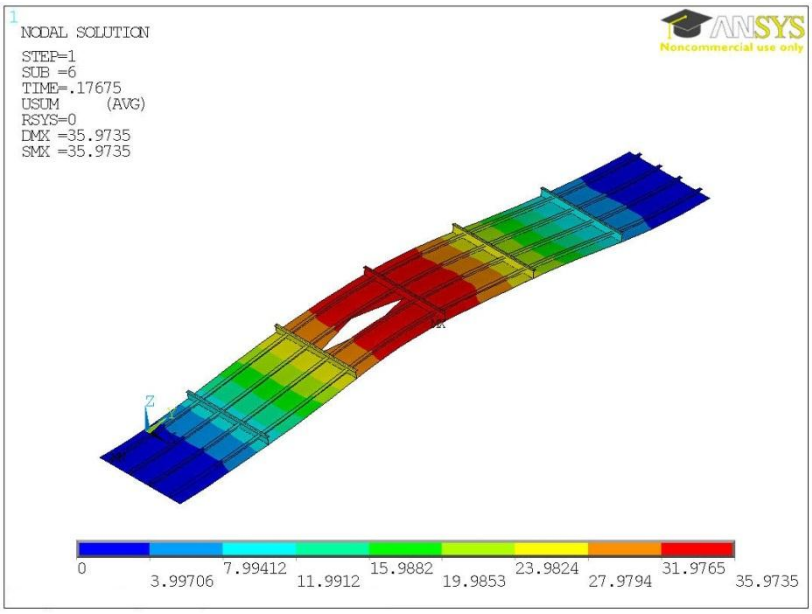

Figure 7.17 - Magnified Displacement Contour Plot: : β=2 Damage Area Ratio 0.93

Increasing β to 3 for the first damage, case Figure 7.5, it can be seen that the introduction of the smallest damage aperture investigated leads to an increase in the ultimate collapse strength of the grillage compared to the intact condition. The ultimate collapse strength then decreases linearly until damage area ratio reaches 1.0. Beyond this point a transverse stiffener becomes damaged and the ultimate strength reduces significantly before becoming stable as damage area ratio increases to 1.8 following which a further reduction in ultimate collapse strength can be seen. These step changes can again be shown to be due to changes occurring in the mode of failure of the grillage.

Analysis of the intact condition for β=4 shows the failure mode of the structure to be overall in nature. Introduction of the damage aperture in the first scenario initially doesn't affect this mode of failure, Figure 7.18, and a gradual linear reduction in ultimate collapse strength can be seen as damage area is increased to 0.69 in Figure 7.6. Beyond this point the ultimate collapse strength can be seen to reduce as the mode of failure changes, Figure 7.19, and a new linear trend in ultimate collapse strength is assumed that is almost stable throughout the remaining results. A small increase in ultimate collapse strength can be seen above a damage area ratio of 1.3 due to a third mode of failure developing, Figure 7.20. In this third mode shape, a single half sine wave mode is developed along the length of the grillage which leads to the failure of the grillage at a much lower peak deflection than can be seen for the other failure modes. These changes in mode shape have similar parallels to those presented above for β=2. The final damage case within this set at damage area ratio 2.0 shows an increase in ultimate collapse strength back in line with the results calculated at damage aperture ratio 0.69.

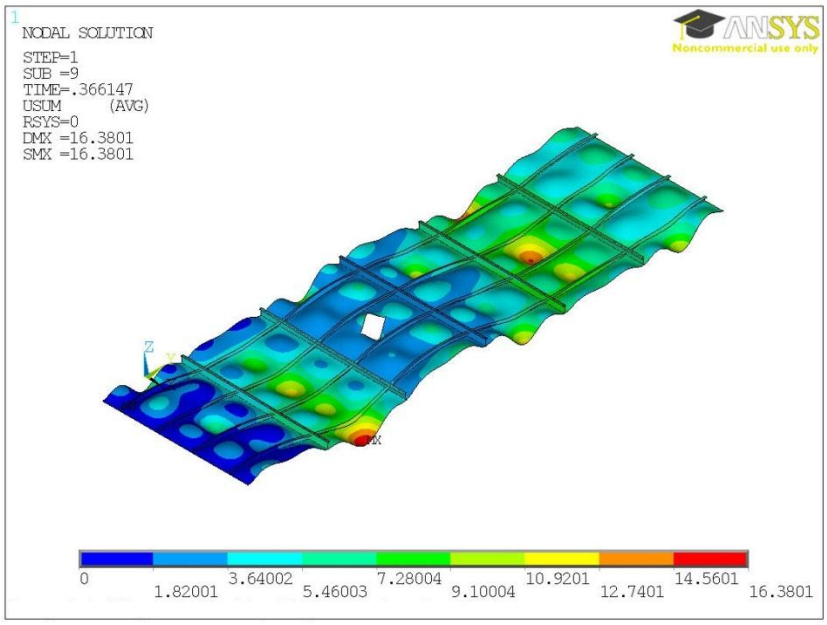

Figure 7.18 - Magnified Displacement Contour Plot: : β=4 Damage Area Ratio 0.10

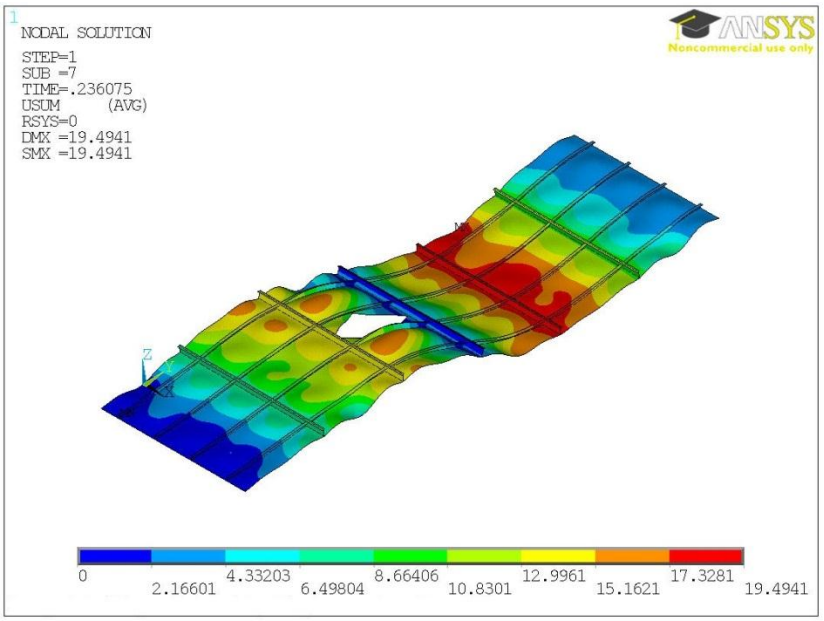

Figure 7.19 - Magnified Displacement Contour Plot: : β=4 Damage Area Ratio 0.93

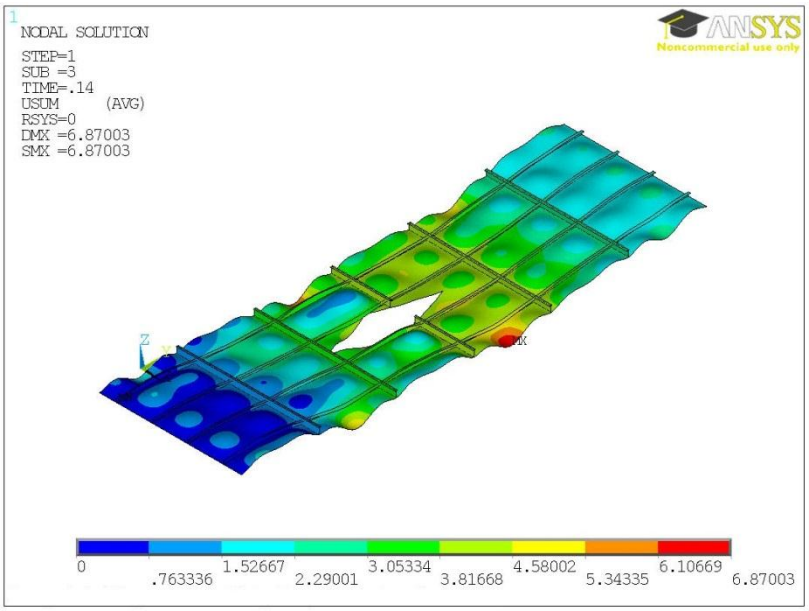

Figure 7.20 - Magnified Displacement Contour Plot: : β=4 Damage Area Ratio 1.5

In the presented results for damage case 2, Figure 7.7 to Figure 7.10, whilst some of the figures show a small increase in ultimate strength for the smallest damage apertures, there follows an initial reduction in ultimate collapse strength from the intact condition as the longitudinal stiffener the damage is aligned with is damaged. However, beyond this point different trends can be seen for the different plate slenderness ratios assessed. The initial trend of decreasing strength as the stiffener is breached is consistent with the results presented in Chapter 6 investigating the influence of damage aperture size and shape on the ultimate collapse strength of stiffened steel panels.

For the second damage scenario when β=1, Figure 7.7, there is an initial increase in ultimate collapse strength, consistent with the results for the first damage scenario at this plate slenderness ratio, before the sudden reduction in ultimate collapse strength as the longitudinal stiffener is breached. Beyond this point the ultimate collapse strength remains linear and stable as damage area ratio is increased to 2.0. In the region of damage area ratio 1.4 – 1.65 some fluctuation in the trend can be seen as the failure mode shape changes in this region, though this effect appears to be localised as the linear trend returns beyond this point as the damage aperture size is increased.

At β=2 for the second damage case, Figure 7.8, the results show an initial reduction in ultimate collapse strength as the longitudinal stiffener is breached and a stable linear trend forms as the failure mode assumes and overall collapse mode, Figure 7.21. This collapse mode remains constant as the damage area ratio increases to 1.0. Beyond this point a single transverse stiffener is also breached after which fluctuations in the ultimate collapse strength can be seen. From the results it can be seen that in the region of damage area ratio 1.0 - 2.0, increasing the damage size can increase the collapse strength of the panel. This can again be shown to be due to the different failure modes developing in the panel as it reaches its ultimate collapse strength, as shown in Figure 7.22 and Figure 7.23.

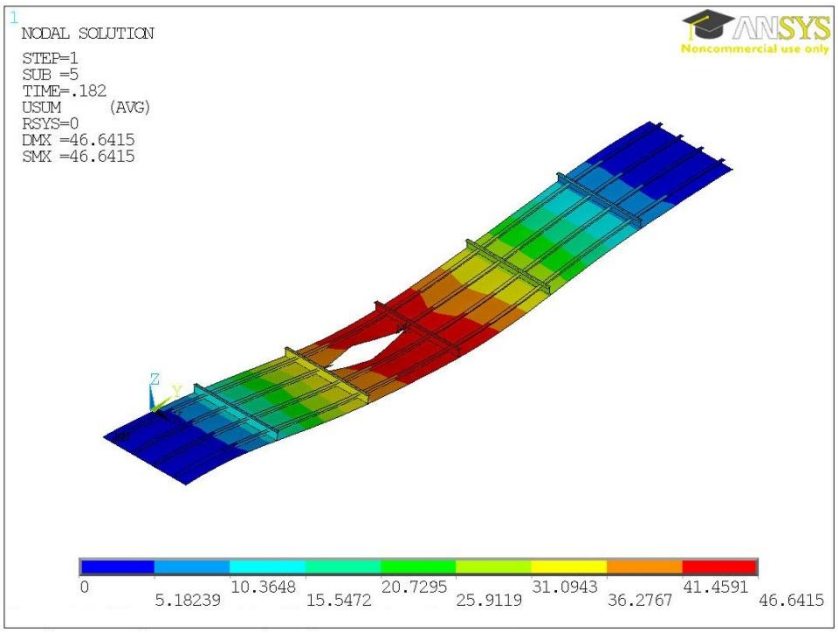

Figure 7.21 - Magnified Displacement Contour Plot: : β=2 Damage Area Ratio 0.93

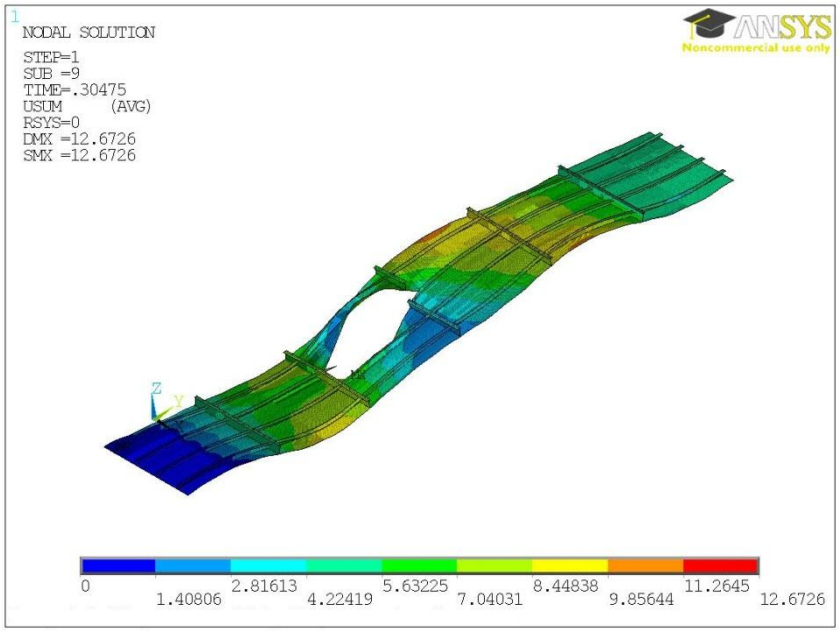

Figure 7.22 - Magnified Displacement Contour Plot: : β=2 Damage Area Ratio 1.13

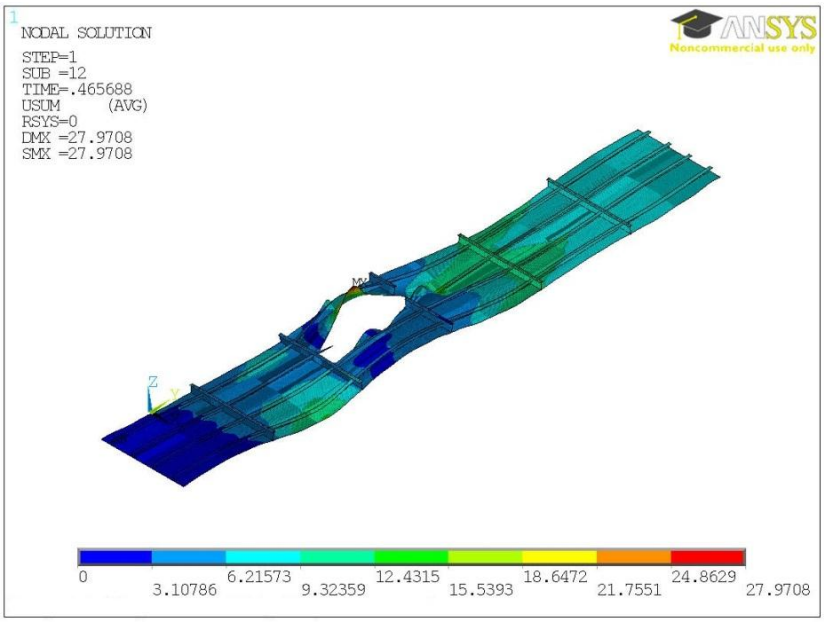

Figure 7.23 - Magnified Displacement Contour Plot: : β=2 Damage Area Ratio 1.46

The results in Figure 7.9 for the second damage case when β=3 show an initial increase in ultimate strength for the smallest damage size compared to the intact grillage, before a decrease in ultimate collapse strength can be seen as the longitudinal stiffener is damaged. This is followed by an increase in the ultimate collapse strength of the grillage. As the damage area ratio is increased from 0.13 – 1.0, the ultimate collapse strength can be seen to reduce gradually in an almost linear manner at a strength that is greater than for the intact condition. This is consistent with the results for the first damage case at this plate slenderness ratio, Figure 7.5. As the transverse stiffener is breached above damage area ratio 1.0, there is a reduction in the ultimate collapse strength which then shows fluctuations due to failure mode shape changes for damage area ratios above 1.33.

Figure 7.10 for the second damage case at β=4 shows a large number of fluctuations in the ultimate collapse strength. After an initial decrease in strength as the longitudinal stiffener is breached the collapse strength can be seen to increase above damage area ratio 0.24, reduce again above 0.69 and fluctuate further above 1.0. These changes are due to the change in developing failure mode shape in the structure.

Figure 7.3 to Figure 7.10 include an additional line to show the ultimate collapse strength of the damaged grillages as calculated by interframe progressive collapse. This assessment was undertaken using the stiffened-plate FEA model detailed in Section 4.2, using the same structural idealisation as used in the study presented in Chapter 5. In all cases it can be seen that the ultimate collapse strength of the damaged grillages by this method is a flat line. This is because the assumption is applied that all damaged or partially damaged structure is removed from the analysis; therefore, there is no change to the damaged structural idealisation as the damage aperture is increased.

For damage case 1, Figure 7.3 to Figure 7.6, it can be seen that for small damage apertures where the mode of failure predominantly remains in the interframe collapse form, the interframe progressive collapse method provides a conservative assessment of the ultimate collapse strength. However, as the damage is increased and the failure mode changes, it can be seen that the interframe progressive collapse method provides an over prediction compared to the full grillage FEA results. In contrast to the results for damage case 1, the results for damage case 2, Figure 7.7 to Figure 7.10, show that the interframe progressive collapse method over predicts the ultimate collapse strength when compared to the full grillage FEA for all damage sizes. This may have serious implications for the strength prediction and resulting safety of a damaged vessel should these effects not be accounted for.

7.3 Discussion

The results presented in this chapter for the strength of damaged grillages show trends consistent with the results presented in Chapter 6 investigating the strength of damaged stiffened panels. In both cases the presence of damage has been shown to influence the developing failure modes within the structure which will affect the ultimate collapse strength. However, for the analysis of damaged stiffened panels, the final failure mode remains interframe in nature due to the model being of an interframe section. The results presented in this chapter for the ultimate collapse strength of damaged grillages has shown how the influence of a damage aperture can affect the interframe collapse modes but also change them to overall collapse modes that can significantly reduce the ultimate collapse strength. Therefore, in the assessment of damaged stiffened steel structures it is critical to assess the structure using a method that can account for these potential changes in failure modes and calculate the ultimate strength correctly.

It has been noted earlier in this section that intuitively it might be expected that increasing the damage aperture size the ultimate collapse strength of the structure would decrease. However, due to the influence of the damage aperture on the developing failure modes, the presented results regularly show scenarios where increasing the damage aperture size leads to an increase in the ultimate collapse strength. Some of the results presented in Chapter 6 regarding the strength of damaged stiffened panels showed similar scenarios. However, as the overall failure mode was constrained to be interframe due to the model size, the resulting change in ultimate collapse strength is less significant than has been shown for the assessment of damaged grillages. It is believed that some of the reasoning behind the changes in mode shape can be laid to the stabilising influence of the damage aperture. Section 2.4 discusses the initial imperfection shapes that can be expected to be present in a fabricated stiffened steel panel or grillage as well as the expected collapse modes that would be likely to develop under compressive loading. It is believed that the presence of the damage aperture in many instances actually leads to stabilisation of the developing failure mode or can change them to higher or lower modes, as was shown for a damaged stiffened panel in Figure 6.7 and Figure 6.8. This influence leads to variations in the ultimate collapse strength that go against the natural intuition of the scenario. This type of stabilisation of failure modes appears consistent with the results presented by Nikolov et al. [72] in their research on the strength of steel plating with initial imperfections, where they state that the initial dishing imperfection can lead to a stabilisation of the collapse mode leading to an increase in strength.

7.4 Conclusions

Research into the ultimate collapse strength of damaged steel grillages has shown how the presence of a damage aperture can lead to a change in the developing failure mode of the structure. This is often counterintuitive, whereby an increase in damage aperture size can lead to an increase in the ultimate collapse strength of the structure. The results are consistent with those presented in Chapter 6 researching the strength of damage stiffened panels. However, where the stiffened panel model is only able to fail by interframe collapse, the influence of the damage within a grillage arrangement can change the failure mode to be overall in nature; this can significantly change the ultimate collapse strength of the grillage which may increase or decrease as the damage aperture is increased.

The presented results have also been compared against ultimate collapse strength calculations made by implementing the interframe progressive collapse method. These results have shown the method to be conservative in cases where only the plating between stiffeners is damaged and the grillage continues to fail by interframe collapse, though over predicts the ultimate collapse strength if this mode changes. However, it has been shown that the interframe progressive collapse method over predicts the ultimate collapse strength in cases where a longitudinal stiffener is damaged regardless of the failure mode that subsequently develops.

This study has shown how, for the ultimate strength assessment of damage stiffened steel structures, all potential failure modes of the structure must be able to be accounted for as the failure mode of the structure in the damaged condition cannot be assumed to be the same as for the intact condition. Failure to account for such mode changes could lead to incorrect assessment of the residual strength of a damaged structure and the safety of personnel on-board.

[Blank Page]

8 GLOBAL DAMAGED STRENGTH ASSESSMENT

8.1 Overview

The research studies presented in the preceding chapters have investigated the influence of damage on the collapse strength of steel-plated structures. These studies have confirmed weaknesses 1-5, identified in Section 2.2.4, relating the application of interframe progressive collapse to the assessment of damaged steel structures to be correct. Chapter 3 presents the formulation of a new method of performing progressive collapse analysis using the RSM kriging. RSM is used to capture the strength characteristics of the damaged steel structure and is then used within the method. A flow diagram of the implementation of the method can be seen in Figure 3.1. Chapter 4, Section 4.4, demonstrates the ability of the RSM to capture the required structural data of damaged stiffened-plates and grillages. This allows progressive collapse assessment using RSM to be implemented at a multiple frame or compartment level by idealising the structure into grillage elements. The investigation into the ultimate collapse strength of damaged grillages in Chapter 7 has demonstrated the need to be able to assess damaged structure at this level of idealisation due to the influence of the damage on the developing failure mode of stiffened steel structures.

This chapter presents a demonstration of the new compartment level progressive collapse method incorporating grillage elements for the ultimate strength assessment of damaged steel box girders, a common idealisation of ship cross-sections, Section 4.5. The assessments utilise the box girder FEA model presented in Section 4.5, introducing a damage aperture into the upper section of the structure. A bending moment is then applied to the box girder that puts the damaged section under compressive loading.

The interframe progressive collapse tool presented in Section 4.5 has been developed to perform the required compartment level progressive collapse analysis of box girder sections, using grillage elements within the model definition. This has allowed the results from the interframe, using stiffened-plate elements, and compartment level progressive collapse methods to be compared. To distinguish between the two methods, they are subsequently referred to as interframe progressive collapse and compartment progressive collapse.

For assessment of the new compartment level progressive collapse method, the Gordo et al. [98] H300 and H400 box girders were selected due to their geometrical configuration which are more closely related to those found in ship structures than the H200 model. Verification of the H300 and H400 FEA box girder models are detailed in Section 4.5. An FE area plot of the H400 model in the intact condition can be seen in Figure 8.1.

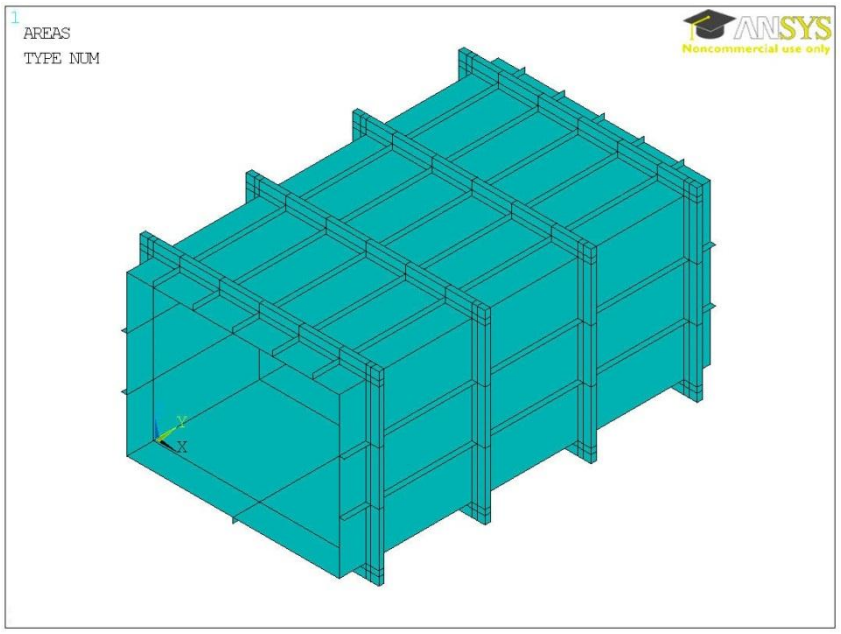

Figure 8.1 – H400 Box Girder Intact FE Model

To fully assess the ability of the new compartment level progressive collapse method, assessments of the box girders were undertaken in both the intact and damaged conditions, and are presented below.

Implementation of the compartment progressive collapse model in both the intact and damaged conditions uses a grillage element spanning the full length and width of the box girder model, Figure 8.2. The same grillage FE modelling process verified in Section 4.3 has been used to provide the required strength data of these elements. This includes the use of full stiffener spacing at each end of the grillage to maintain applicability to the verification presented in Section 4.3. However, the boundary condition along the longitudinal edges has been changed to simply supported, to represent the connection of the grillage to the box girder sides. This is because the previously applied symmetric condition is no longer appropriate in relation to the side shell connection, which would be expected to be able to rotate about the corner. Therefore, a simply supported condition is most appropriate.

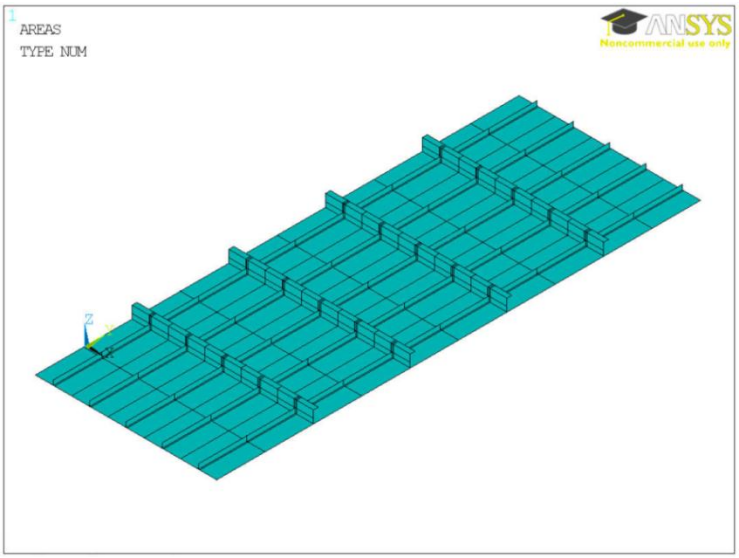

Figure 8.2 – H400 Upper Section Grillage Element

8.2 Intact Box Girder Assessment Results

Figure 8.3 and Figure 8.5 show a magnified displacement plot of the developed failure mode in the grillage element for the H300 and H400 box girders respectively. These demonstrate the interframe collapse nature of the arrangements in the intact condition, which matches with the same failure mode type as seen in the box girder analysis, Figure 8.4 and Figure 8.6. However, whilst the vertical direction of the displacements for the H400 grillage and box girder models match, the displacements of the H300 models do not. Figure 8.3 shows how the failure mode displacements are all in the same direction across the grillage, unlike the alternating mode seen in the box girder in Figure 8.4.

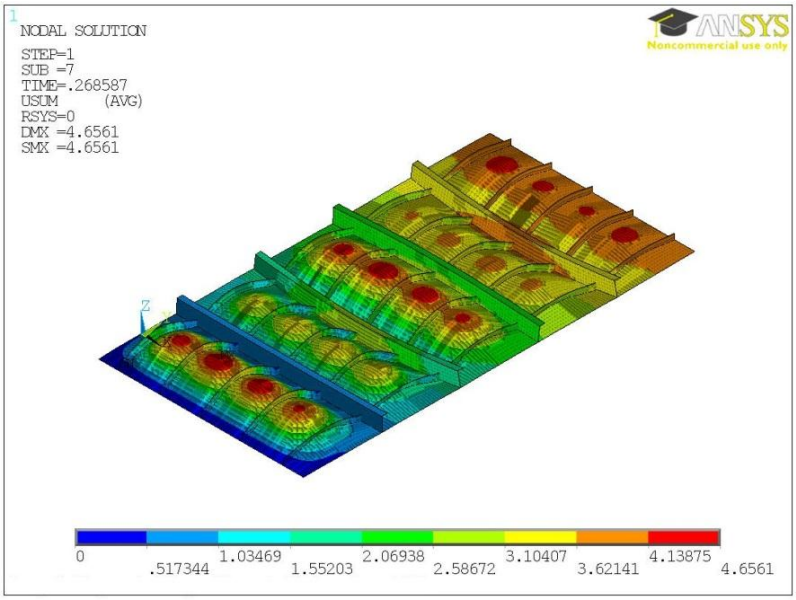

Figure 8.3 – H300 Upper Section Grillage Element Failure Mode – Magnified Displacement Plot

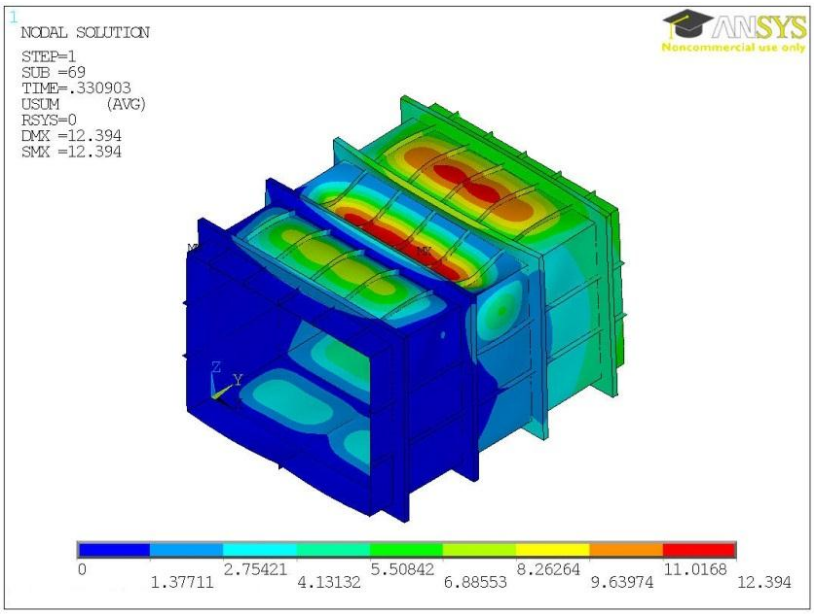

Figure 8.4 – H300 Failure Mode - Magnified Displacement Plot

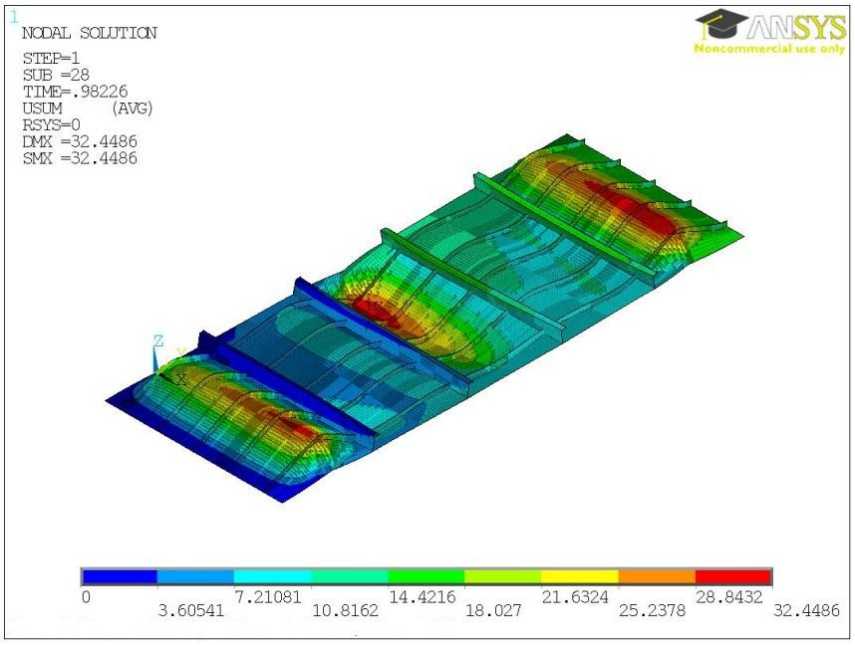

Figure 8.5 – H400 Upper Section Grillage Element Failure Mode – Magnified Displacement Plot

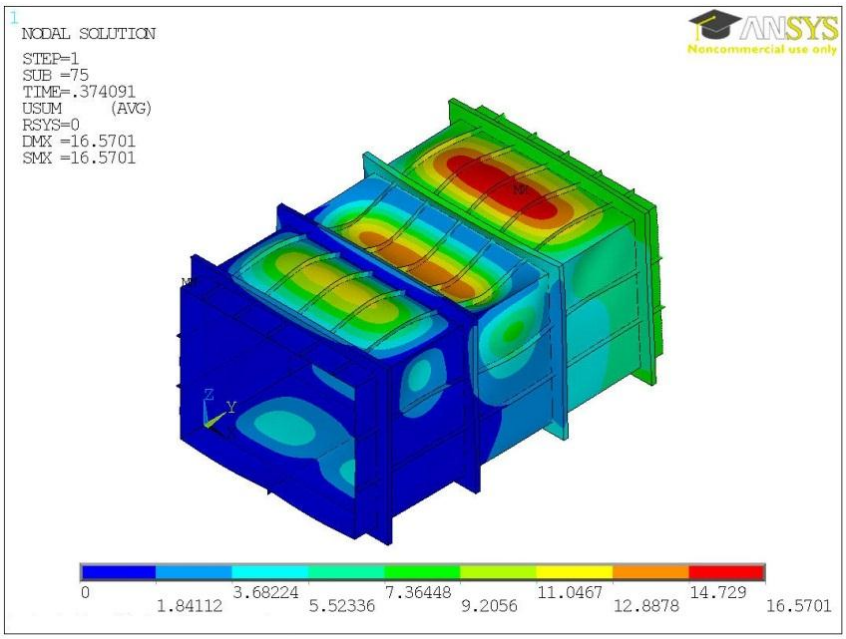

Figure 8.6 – H400 Failure Mode - Magnified Displacement Plot

The results of the intact H300 and H400 box girder assessments can be seen below in Figure 8.7, Figure 8.8, Table 8.1 and Table 8.2.

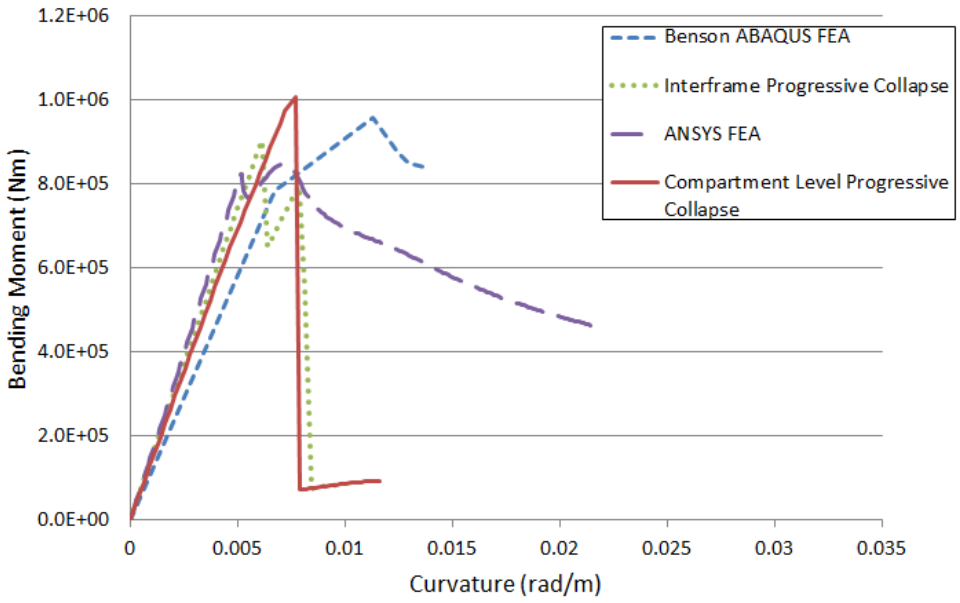

Figure 8.7 - Intact H300 Box Girder Ultimate Bending Strength Results

Method of Assessment	Maximum Bending Moment (Nm)
ANSYS Compartment FEA	842264.26
Benson ABAQUS Compartment FEA	956250.00
Interframe Progressive Collapse Analysis	904628.23
Compartment Level Progressive Collapse Analysis	1005186.89
Difference Interframe Progressive Collapse Analysis – ANSYS Compartment FEA	-6.89%
Difference Compartment Level Progressive Collapse - ANSYS Compartment FEA	-16.21%
Difference Interframe Progressive Collapse Analysis - Compartment Level Progressive Collapse Analysis	19.34%
Difference Interframe Progressive Collapse Analysis – ABAQUS Compartment FEA	5.71%
Difference Compartment Level Progressive Collapse – ABAQUS Compartment FEA	-4.87%

Table 8.1 - Intact H300 Box Girder Ultimate Bending Strength Results

As can be seen from the results for the H300 box girder assessment in Figure 8.7, whilst the initial stiffness in the elastic region matches well between the compartment level progressive collapse assessment, the ANSYS FEA and interframe progressive collapse analysis, the ultimate strength prediction is much greater than both methods, at 16.9% and 19.3% respectively. Whilst the initial stiffness is different to the ABAQUS FEA undertaken by Benson [34], the ultimate strength is much closer, though still greater by 4.9%.

It is believed that the increased ultimate bending strength predicted by the compartment level progressive collapse method may arise due to the strength data provided by the grillage FEA model. It is noted above how the failure mode displacement direction seen in the grillage element in Figure 8.3 is different to that seen in the box girder; where, for the grillage the displacement is in a single direction across the structure, whilst the box girder shows an alternating displacement form.

As detailed in Section 2.4, the most common initial imperfection shape seen in ship structures is the "hungry horse" form, whereby the vertical initial imperfection direction in the plates and stiffeners is the same across the structure. This is the form of initial imperfection shape that has been applied to the grillage FEA model. In the study presented in Chapter 7, the resulting failure modes in the grillages were seen to be of an alternating direction, for example Figure 7.13, as has been seen for the H400 grillage in Figure 8.5. Investigating the development of the H300 grillage failure mode shows how the initial imperfection shape is stable as the axial load is applied, leading to the failure developing with deflections in the same direction between stiffeners. It is believed that this has led to a stabilisation of the developing failure mode, and a higher ultimate strength than would be achieved by an alternating deflection shape. This correlates with the findings of Nikolov [72], where it was shown that the stabilising effect of imperfections in stiffened steel plates could lead to an increased ultimate strength under axial compressive load.

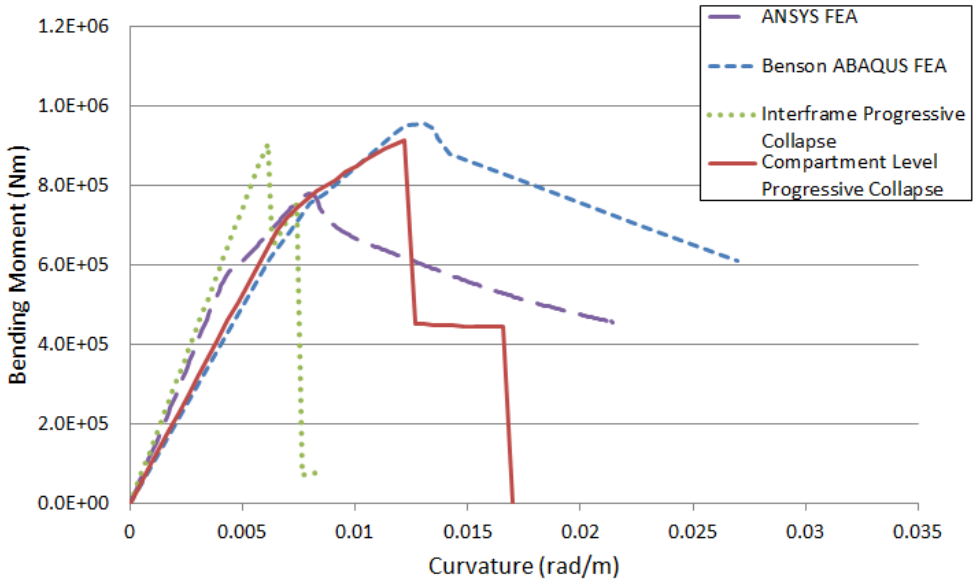

Figure 8.8 – Intact H400 Box Girder Ultimate Bending Strength Results

Method of Assessment	Maximum Bending Moment (Nm)
ANSYS Compartment FEA	779240.7
Benson ABAQUS Compartment FEA	956896.55
Interframe Progressive Collapse Analysis	906547.53
Compartment Level Progressive Collapse Analysis	913351.05
Difference Interframe Progressive Collapse Analysis – ANSYS Compartment FEA	-14.04%
Difference Compartment Level Progressive Collapse Analysis – ANSYS Compartment FEA	-14.68%
Difference Interframe Progressive Collapse Analysis – Compartment Level Progressive Collapse Analysis	0.75%
Difference Interframe Progressive Collapse Analysis – ABAQUS Compartment FEA	-0.06%
Difference Compartment Level Progressive Collapse – ABAQUS Compartment FEA	-0.05%

Table 8.2 – Intact H400 Box Girder Ultimate Bending Strength Results

The results in Figure 8.8 and Table 8.2 for the H400 box girder assessment show good correlation between the ultimate strength calculation by the compartment level progressive collapse method with the interframe progressive collapse method and ABAQUS FEA undertaken by Benson [34]. Comparison with ANSYS FEA shows a difference of 14%. It can also be seen that the initial stiffness of the compartment level progressive collapse method matches closely to the ABAQUS FEA results.

In this case, where the failure mode deflection in the grillage can be seen to match that of the box girder FEA, Figure 8.5 and Figure 8.6, the results compare more closely to the interframe progressive collapse method. It is noted that the compartment level progressive collapse method over predicts the failure compared to the ANSYS FEA box girder model by 14.7%. This is similar to the difference of 16.2% seen between the methods seen for the H300 box girder.

Whilst the variation between the results provided by the different analysis methods for the H300 and H400 box girders may appear large, they all fall within the potential variation trends demonstrated by the ISSC 2006 and 2012 ultimate strength committee bench mark studies [39, 40] discussed in Section 2.2.6.

8.3 Damaged Box Girder Assessment Results

To demonstrate the ability of the new compartment level progressive collapse method for use in a damage scenario, damage has been introduced into the H400 box girder. Assessment has been undertaken through the analysis of two damage events; the first is a small damage event positioned with its centre in line with the middle of the central stiffener of the upper section of the box girder, with damage breadth equal to the longitudinal stiffener spacing and damage area ratio of 0.3, as shown in Figure 8.9. The second damage case maintains the same damage location and breadth, but increases the length to provide a damage area ratio of 1.9. This damages two transverse stiffeners in addition to the single longitudinal stiffener, as shown in Figure 8.10. Figure 8.11 and Figure 8.12 show the equivalent damaged grillage elements for use within the compartment level progressive collapse analysis.

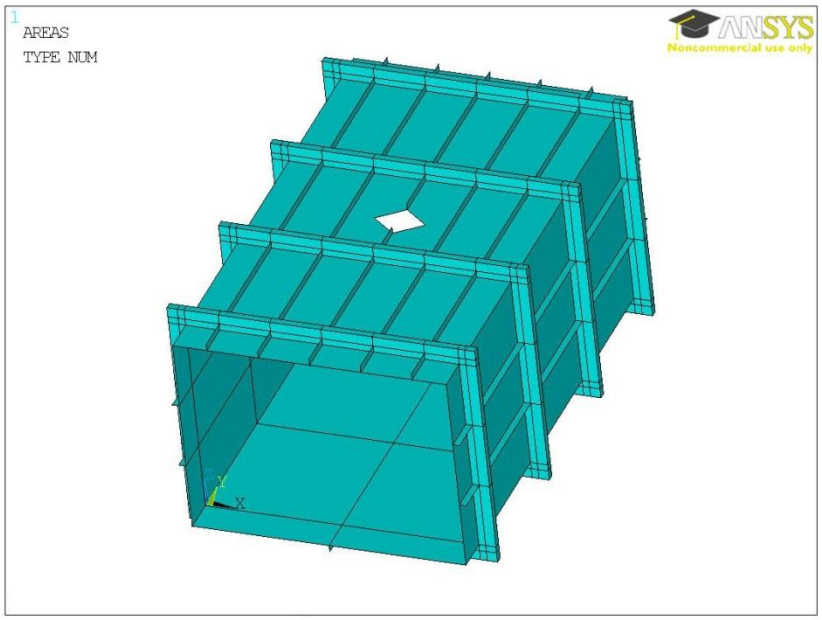

Figure 8.9 – H400 Box Girder - Damage Case 1

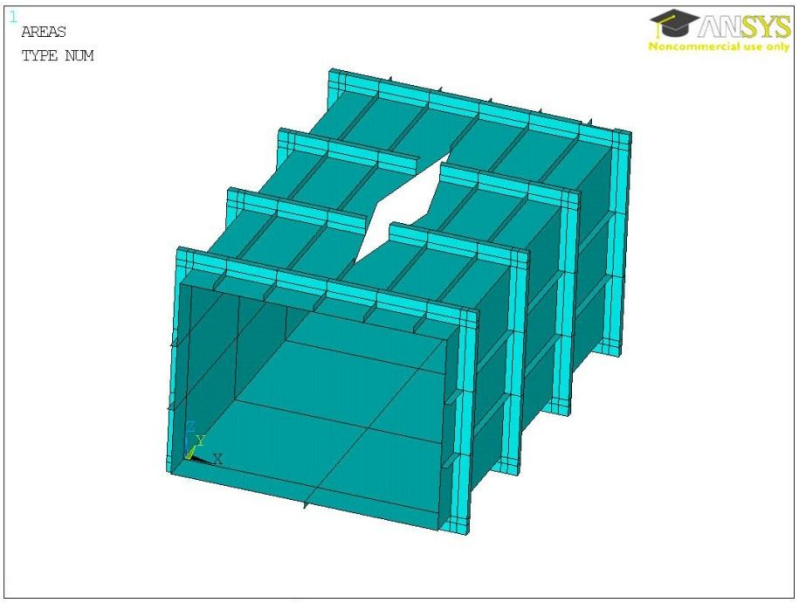

Figure 8.10 - H400 Box Girder - Damage Case 2

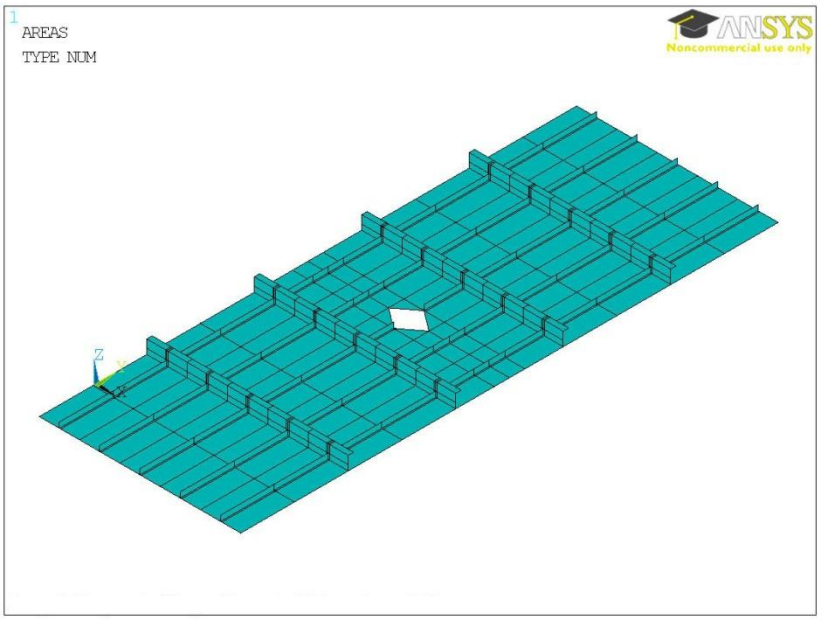

Figure 8.11 – H400 Grillage Element: Damage Case 1

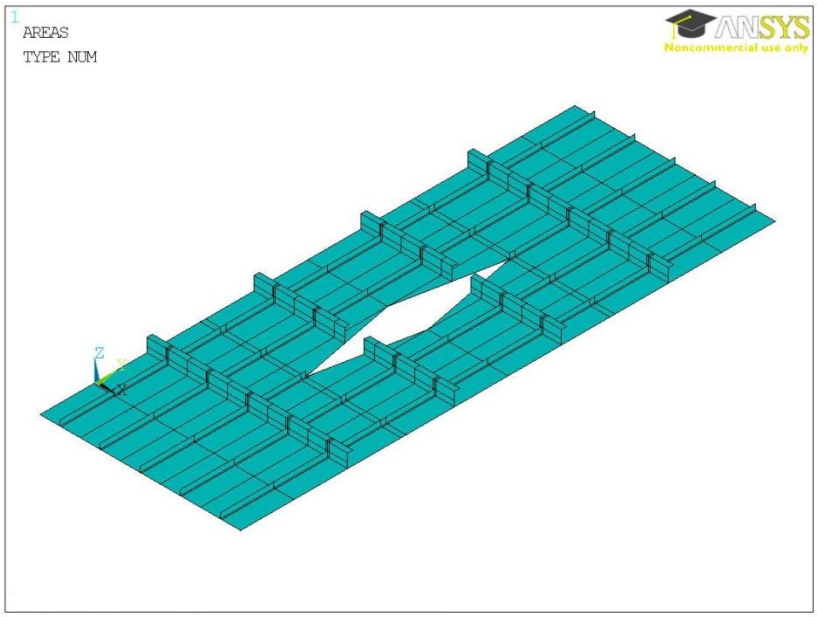

Figure 8.12 - H400 Grillage Element: Damage Case 2

Figure 8.13 and Figure 8.14 show the failure modes seen in the grillage and box girder FEA models respectively for the small damage. It can be seen that whilst the mode of failure in the two structures can be considered to be interframe in their form, the failure mode developed in the grillage model is more complex. It is believed that the connection of the upper grillage section to the side section, in particular the connection between the transverse frames, may be sufficient to prevent this mode of failure developing in the box girder. Therefore, further development of the grillage boundary conditions may be required to improve correlation and stiffen the current simply supported boundary condition on the longitudinal edges. However, due to the lack of availability of data against which to verify the suitability of any additional boundary conditions, which may lead to over-constraining of the model if not applied appropriately, additional boundary conditions have not been trialled within this assessment.

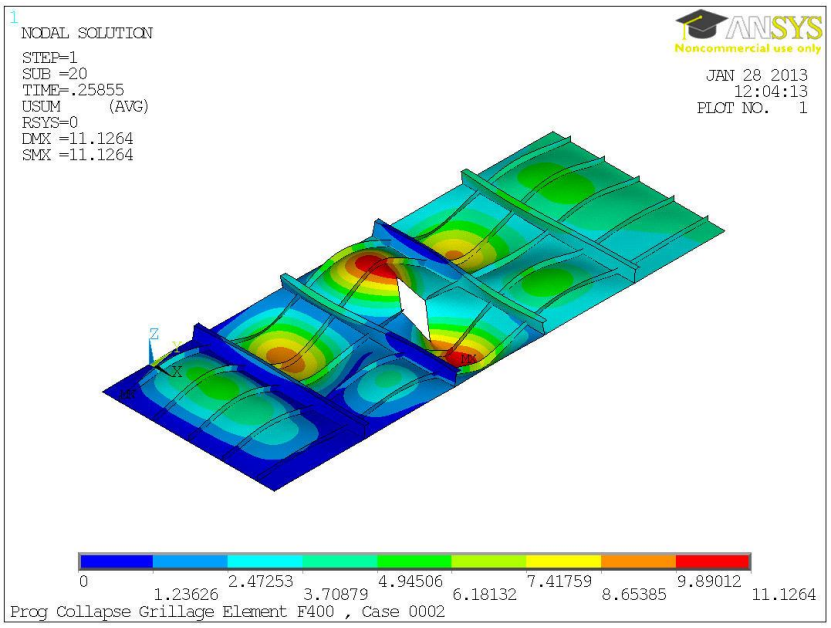

Figure 8.13 – H400 Grillage Element: Damage Case 1 Failure Mode - Magnified Displacement Plot

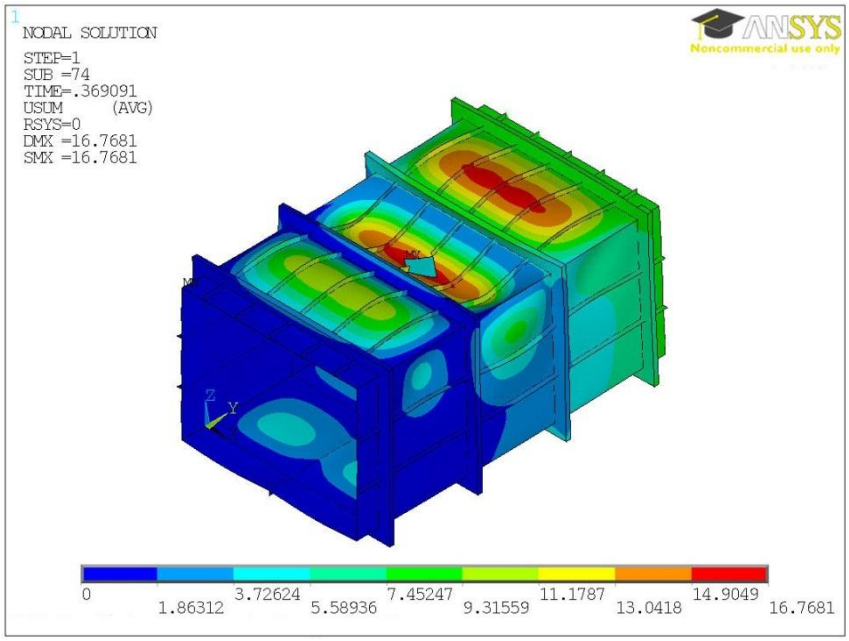

Figure 8.14 - H400 Box Girder: Damage Case 1 Failure Mode - Magnified Displacement Plot

Figure 8.15 and Figure 8.16 show the failure modes of the second damage case within the grillage and box girder structures. The displacement plots show good correlation between the cases, both developing the same form which is no longer interframe. However, the extent of the deformation seen in the grillage model is greater than in the box girder FEA model. This again suggests that the simply supported boundary conditions on the longitudinal sides may be too soft and the connection between the side structure may need to be carefully considered in future analysis.

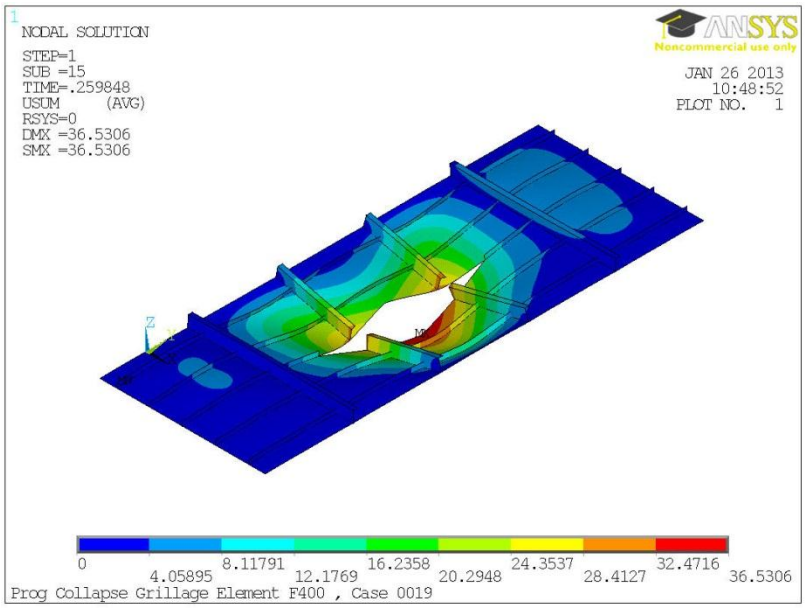

Figure 8.15 - H400 Grillage Element: Damage Case 2 Failure Mode Magnified Displacement Plot

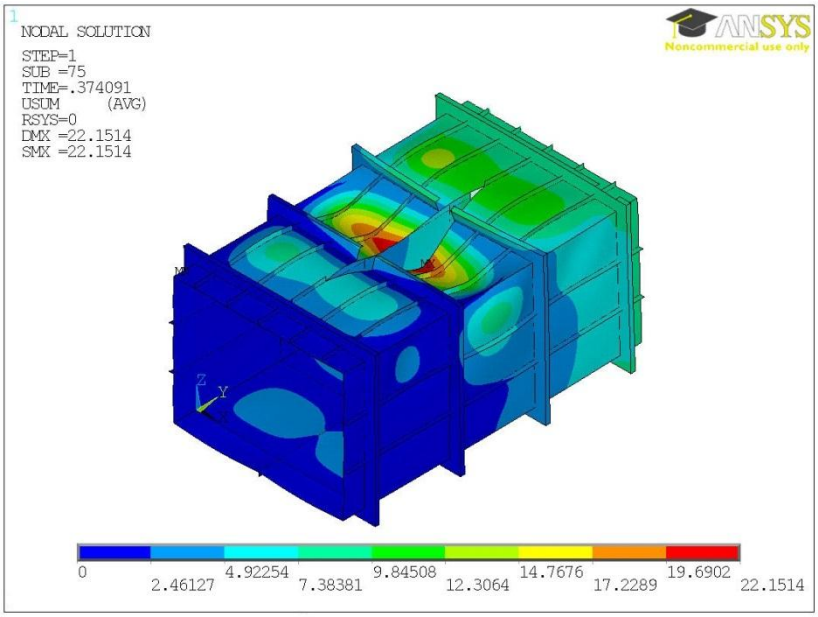

Figure 8.16 - H400 Box Girder: Damage Case 2 Failure Mode Magnified Displacement Plot

The results of the discussed damage cases are shown in Figure 8.17 and Figure 8.18 for damage case 1 and case 2 respectively. Comparison of the results can be seen in Table 8.3. It should be noted that as the two damage cases have been defined with the same breadth, the damage strength assessment by the interframe progressive collapse method is the same, as the interframe method is unable to account for the increased length of the damage seen in case 2.

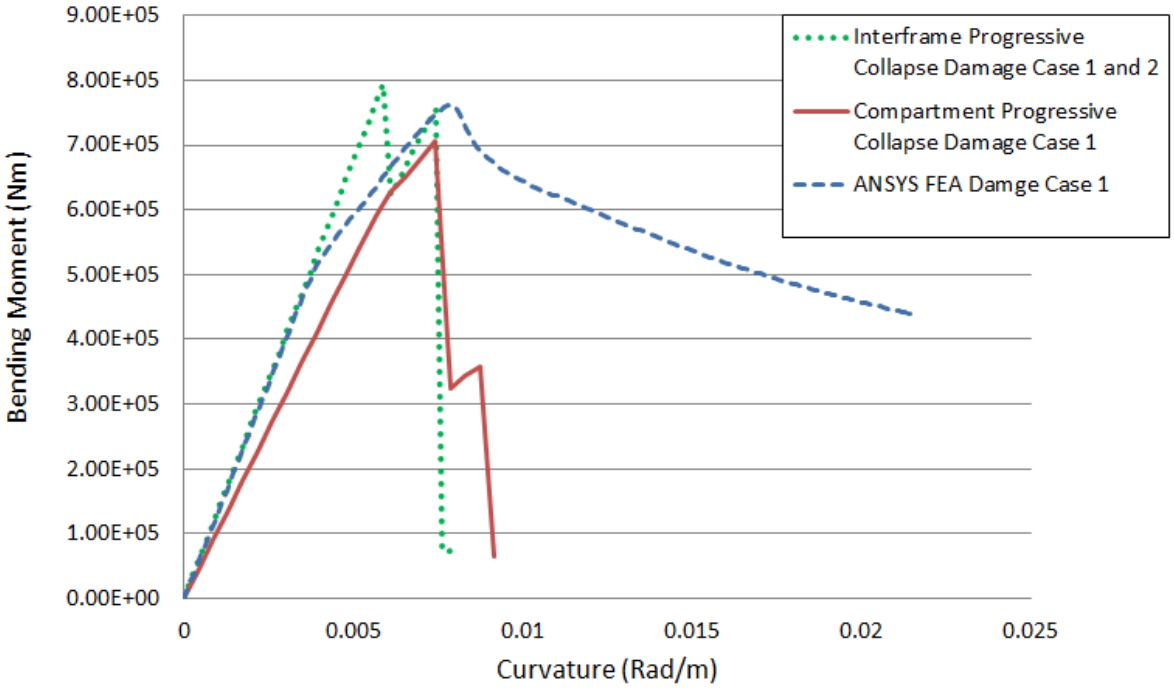

Figure 8.17 –H400 Box Girder Bending Strength Results – Damage Case 1

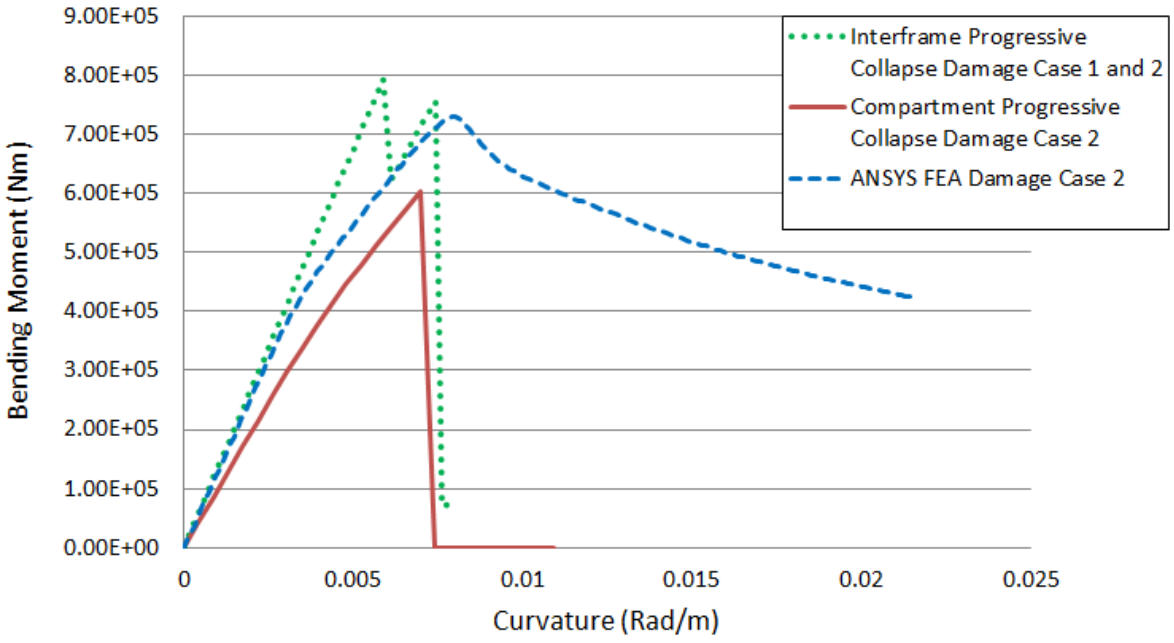

Figure 8.18 - H400 Box Girder Bending Strength Results – Damage Case 2

Method of Assessment and Damage Scenario	Ultimate Bending Moment (Nm)
Interframe Progressive Collapse - Damage Cases 1 & 2	7.94E+05
Compartment Progressive Collapse - Damage Case 1	7.06E+05
Compartment Progressive Collapse - Damage Case 2	6.04E+05
ANSYS Compartment FEA - Damage Case 1	7.62E+05
ANSYS Compartment FEA - Damage Case 2	7.30E+05
Difference ANSYS FEA to Compartment Level Progressive Collapse - Damage Case 1	-7.42%
Difference ANSYS FEA to Compartment Level Progressive Collapse - Damage Case 2	-17.21%
Difference ANSYS FEA to Interframe Progressive Collapse - Damage Case 1	4.21%
Difference ANSYS FEA to Interframe Progressive Collapse - Damage Case 2	8.77%
Difference Interframe Progressive Collapse to Compartment Level Progressive Collapse - Damage Case 1	-11.16%
Difference Interframe Progressive Collapse to Compartment Level Progressive Collapse - Damage Case 2	-23.89%

Table 8.3 – Damaged H400 Box Girder Ultimate Bending Strength Results

The difference in results between the ANSYS compartment FEA and compartment level progressive collapse method is much closer for damage case 1 than was shown for the intact condition. However, the difference is 17.2% for case 2, which may be due to the modelling assumptions used in the grillage element not accurately matching the true structure. It should be noted that despite these discrepancies, the compartment level progressive collapse results proved to be conservative when compared to the ANSYS FEA in both cases. This contrasts to the interframe progressive collapse method which appeared to over predict the ultimate bending strength in both cases.

The results show an over prediction of the damage strength of the structure by interframe progressive collapse in both damage scenarios when compared to the new compartment level progressive collapse method and ANSYS FEA, by 11.2% and 4.2% respectively for damage case 1, and 23.9% and 8.8% respectively for damage case 2.

8.4 Discussion

The implementation of the new compartment level progressive collapse method for use within intact and damage scenarios has been demonstrated within this chapter. Whilst the results have shown good correlation with full section FEA in many cases, differences between the results of the method and those obtained by interframe progressive collapse and full section FEA have also occurred.

Reviewing the failure modes seen in the grillage element FEA, whose strength data is used by the compartment level progressive collapse method, and the full section FEA models, differences can be seen in the developing failure modes. In many cases the grillage model can be seen to be softer than the equivalent section within the box girder model, which may account for the conservative ultimate bending strength prediction in these cases. Conversely, where the developed failure mode in the grillage model may lead to an increased strength of the section, an over prediction of the ultimate bending strength can be seen.

In the assessment of a damaged box girder, the method has demonstrated its ability to account for the change in failure mode shape that may occur, providing a conservative prediction of the ultimate bending strength when compared to full section FEA. This contrasts with the interframe progressive collapse assessment which over predicted the ultimate bending strength for the assessed damage cases.

Whilst account for some potential discrepancies between the new compartment level progressive collapse method and full section FEA ultimate bending strength results has been made above, consideration must also be made regarding the idealisation of the new method. When undertaking interframe progressive collapse analysis, the longitudinal extent of the assessed section is short in comparison to the total length of the section or vessel. Therefore, it is appropriate to assess the strength of the individual stiffened-plate elements under pure compression. This same approach has been applied to the analysis of the grillage elements applied to the new compartment level method. However, this assumption may require further research to determine its appropriateness for damage calculations. When considering the loading of the compressed grillage section within the full FEA model, the loading can't be considered to be pure axial compression in its nature. Therefore, more appropriate or representative loading may need to be applied to the grillage elements to ensure the most suitable strength data is generated for use by the method.

Application of the grillage element load may need to be approached in a similar method to that applied to the full section; by applying a rotational displacement to a reference node connected by rigid beam elements to the loaded end of the grillage. The positioning of the reference node will then be more critical than for the full section model, and should be located at the equivalent neutral axis position for the full section. It is recognised that as the full section progressively fails, the neutral axis position will move away from the failed sections. However, as the grillage elements are located furthest from the neutral axis within the modelled scenario, they would be expected to fail first before the neutral axis moves. When modelling a full ship section including deck structures, the influence of the shift of neutral axis on the grillage element loading may need to be considered.

Within the new method example cases presented within this chapter, a grillage element has been utilised within the upper compressed section, whilst the side shell has been considered to continue to fail by interframe collapse. This can be seen to be an appropriate assumption by viewing the failure modes of the side structure within the displacement plots in Figure 8.4, Figure 8.6, Figure 8.14 and Figure 8.16. It is possible that the use of larger elements within the side structure may also be possible, and the influence of side shell damage from a collision event may lead to this interframe collapse failure mode changing. Idealising the side shell into larger element sizes adds additional complexity in relation to the application of the appropriate bending load across the structure. It is not believed that any work has been presented on this type of grillage loading in either an intact or damaged condition.

Whilst the potential of the new method has been demonstrated, it is clear the further development and understanding of the modelling of the grillage elements is required to ensure successful implementation. For application within an emergency response scenario, care must also be taken to ensure that the failure mode developed in the grillage does not lead to a best case scenario, from which the resulting decisions may endanger lives.

Due to the similarities between the implementation of the new compartment level progressive collapse method and the existing interframe progressive collapse method, the time to run the solution of the methods is equivalent. Therefore, with further development of the approach to implementation of the new method, it is believed that compartment level progressive collapse analysis can be incorporated within an emergency response or salvage service.

8.5 Conclusions

The implementation of the new compartment level progressive collapse method has been demonstrated. When applied to the assessment of damaged box girder structures, the method has shown to provide good, though conservative prediction of the ultimate bending strength when compared to full section FEA and assessment by interframe collapse method. The method also demonstrated its ability to account for the reduced strength caused by the change in failure mode seen within the section of the box girder under compressive loading. This contrasts to the interframe progressive collapse method which was shown to over predict the damage strength when compared to full section FEA.

In the application of the new method to the assessment of intact box girder structure, discrepancies were shown between full section FEA and assessment by interframe collapse method. In comparison to ANSYS FEA, the method over predicted the ultimate bending strength results in both the H300 and H400 cases by 16.2% and 14.68% respectively. However, in comparison to Benson ABAQUS FEA [34] the method over predicted the ultimate bending strength for the H300 intact condition by 4.9%, but was shown to closely match the H400 case, under predicting the strength by 0.05%. It is believed that better correlation may be achieved through more careful consideration of the boundary conditions being applied to the grillage elements, though the accuracy of the method lies within the levels of variation seen between whole FEA shown in the ISSC 2012 benchmark study [40].

Assuming that the strength data for the damaged grillage elements is available from prior analysis, the time taken to build and analyse a structural model using the new compartment level progressive collapse method is equivalent to the existing interframe progressive collapse method. Therefore, in relation to the time to obtain a solution, the method is suitable for application within an emergency response or salvage service.

9 CONCLUSIONS

Annually across the globe, damage incidents involving ships continue to occur within all sectors of the shipping industry. Many of these vessels are not lost as a result of the damage sustained and require assistance to preserve life, prevent environmental impact and limit financial losses. Shore based emergency services and salvage companies require the use of numerical modelling tools to be able to provide guidance to ship's crew and owners on how best to stabilise the situation and ultimately salvage the vessel.

In Chapter 1 a number of aims and objectives were set out for the research undertaken and presented in this thesis, which have been achieved. In relation to the objectives set, a literature review was undertaken and presented in Chapter 2. This showed that no previous work had been presented to investigate the influence of damage in the form of a hole on the strength of damaged stiffened steel structures. The study also showed the interframe progressive collapse method (or Smith method), to be the current state of the art method for assessment of the residual strength of a vessel in an emergency situation. However, a number of potential weaknesses were identified in relation to its application to damaged ship assessment, presented in Section 2.2.4. The validity of these weaknesses and resolutions are investigated throughout the research studies presented.

It is known that the ultimate strength of an intact vessel under vertical bending is predominantly determined by the collapse strength of the local structure which is stiffened in the longitudinal direction and supported by deeper transverse framing. Therefore, understanding the damaged strength under compressive loading is critical to determining the residual ultimate bending strength. The research studies undertaken to investigate this and to make a novel and original contribution to this area of research, were undertaken at three distinct levels of structural idealisation: stiffened-plate, stiffened panel and grillage. The studies have demonstrated how the presence of damage can influence the failure modes developing in the structure, which can significantly affect the ultimate collapse strength.

The stiffened-plate and stiffened panel arrangements have been modelled by FEA. Simply supported boundary conditions are applied to the loaded and reactive end, and discrete plate approach along the longitudinal sides were applied in accordance with supporting literature referenced in Chapter 4. Use of these smaller structural units assumes that in the damaged condition the structure will continue to fail in an interframe manner. In these studies, it has been shown that as damage aperture size is increased, the predominant trend for all stiffener spacing, stiffener profiles and damage aperture shapes assessed, is a gradual reduction in ultimate collapse strength from the intact condition. If a longitudinal stiffener, along which the compressive loading is applied, is damaged, there is an initial drop in ultimate collapse strength from the intact condition before a trend towards a gradual reduction in ultimate collapse strength. However, these trends are affected locally by the influence of the damage aperture on the developing failure mode deflection shapes within the structure, which may increase or decrease the strength as aperture size increases. These effects have not been previously presented in available literature.

Whilst the influence of the damage aperture on the failure mode of the stiffened-plates and panels has been demonstrated, due to the model extent being limited to that of an interframe section, the true influence of the damage may not be correctly captured. Greater influence of the damage on the structure is demonstrated by increasing the structural arrangement to that of a grillage. Whilst the failure mode of the intact arrangements under axial compressive loading is expected to be interframe collapse between the transverse stiffeners, the introduction of a damage hole into the arrangement has been shown to change this in many cases. More complex failure mode shapes have been shown to develop within the structures, whose shape span across multiple frame spacings, generating an overall collapse mode. This change in mode shape can lead to a significant reduction in the ultimate collapse strength. The changes in the failure modes have been shown to fluctuate in some cases, leading to the counterintuitive scenario whereby increasing the damage aperture size can lead to an increase in the ultimate collapse strength. It is believed that the reasons for the changes in mode shape in this manner may be due to the damage aperture stabilising or preventing the development of the interframe collapse mode of failure, leading to the development of alternative failure modes.

Demonstration of the influence of damage on the ultimate collapse strength of stiffened steel structure shows the need for an analysis method that can capture these influences. One of the limitations of simply using larger structural definitions within a progressive collapse method is how to capture the required strength data so it is quickly available for emergency response use. It has been proposed and demonstrated that the use of the RSM kriging may be the solution. The method uses FEA data to define the surface including a number of variables, for example stiffener spacing, plating thickness, damage length, breadth and location. The captured data is then available for use by the new compartment level progressive collapse method using RSM. The method has been demonstrated and presented in Chapter 3, with illustration of the method concept and parts in Section 4.4 and Chapter 8. Demonstration of the method shows its ability to account for the influences of the damage and changing mode shapes within the damaged structure, how limiting the assessment of a damaged vessel to that of interframe collapse can lead to an overestimation of the residual bending strength, and has shown to correlate with full section FEA.

Due to the similarities of the new method to the existing interframe progressive collapse method, it is believed that incorporation in to existing software algorithms should be possible. The new compartment level method is capable of providing ultimate bending strength results in the same timescales as the current interframe method, and is therefore suitable for application within an emergency response or salvage service.

Modelling of the ultimate collapse strength of damaged stiffened steel plated structures is a complex issue. Within the studies presented in this thesis the damage event has been idealised in the form of a hole, modelled through the removal of structure, without modelling the damage event. This has removed additional uncertainties and complexities of performing such analysis, and has removed potential pre-stressing of the structure that the event may cause. However, the analysis undertaken has demonstrated the influence of a damage aperture at this level of idealisation.

The structural modelling presented in this thesis has considered the structure to be under pure axial compression. It has been noted in Chapter 8 that by increasing the level of structural idealisation to include grillage elements within a compartment level progressive collapse analysis, the loading condition may need to be reconsidered. The modelling type undertaken and demonstration of the new method has allowed damage to be introduced to the box girder model in the form found in a grounding scenario. However, the loading scenario experienced by the side shell of the box girder cannot be considered to be pure compression when the level of idealisation is increased beyond the stiffened-plate extents. No work on this area has been investigated within this thesis, nor is believed available in published literature in the intact or damaged condition, though the influence of damage to the side shell on the failure mode of the vessel could be significant.

Further to this, the damage events modelled have been symmetric about the vertical centreline in their arrangement. Therefore, the neutral axis of the section remains horizontal under the application of the vertical bending moment. However, in a real life collision or grounding event, where the damage is not symmetric, the neutral axis will likely shift and rotate. The resulting loading condition of the larger elements used within the new compartment progressive collapse method will become more complex, and again no longer of a purely compressive nature.

Within a damage event, whilst the number of potential variables present within the structural definition may be quite large, it must be acknowledged that the level of information regarding the damage extent may be limited. To account for potential variation in the damage definition as well as variations in other variables that may be included in the assessment, stochastic methods may be required. Some work has been undertaken by the author regarding the use of reliability analysis within an emergency response service, and are presented in the published papers in Appendix A, specifically Sobey et al. (2010), Underwood et al. (2010) and Underwood et al. (2012, ASRANet). It is possible that such methods may compliment the more defined structural modelling methods presented in this thesis.

Whilst there remains scope for considerable research into the modelling and analysis of damaged stiffened steel structures, it is believed that the research presented within this thesis meets the aim and objectives defined in Chapter 1. New evidence is provided on the influence of damage on the ultimate collapse strength of stiffened steel structures, and a new method of assessing the ultimate bending strength of a vessel by an emergency response or salvage service is presented.

10 RECOMMENDATIONS FOR FUTURE WORK

The recommendations for future work have been split in to two sections. The first relates to the development of further understanding of the influence of damage within stiffened steel plated structure, and the second relates to the development of the new compartment level progressive collapse method.

10.1 Damage Influence of Stiffened Steel Plated Structure

The literature study presented in Chapter 2 identified that no previous work had been presented to investigate the influence of damage on the ultimate strength of steel plated structures. Whilst significant work has been presented within this thesis and other publications of parts this work in this area, it is recommended that further work be undertaken to develop this understanding.

The approach to the studies presented in this thesis have idealised the damage hole through the removal of areas of structure, though without modelling the damage event itself. It is appreciated that the damage event will cause additional deformation and pre-stressing of the structure, which may affect the ultimate collapse strength. With increases in dynamic FEA capability, simulations of damage events and subsequent ultimate collapse strength assessment is a possibility. However, it is noted in Section 2.2.6 that verification of dynamic ship collision and grounding cases is difficult. It is likely that suitable model scale experimentation may be required to aid the verification and build confidence in the results provided by such simulations before this type of analysis is undertaken. However, simpler implicit analysis of pre-stressed damaged structures would provide useful guidance on the influence on the ultimate collapse strength and is recommended to be undertaken.

The applied loading within the studies presented in this thesis are predominantly of a pure axial compression. It is discussed in Section 8.4 that, for the analysis of grillage structures that may be located a significant distance from the neutral axis of the section, considering the loading condition as purely compressive may not be suitable. Investigation into the effects of different loading applications to intact and damaged grillages, for example application of a bending moment with rotation applied about the section's assumed neutral axis position, should be undertaken to quantify the effects on the ultimate strength and developing failure modes of the structures.

Modelling of grillage structures within the side shell of a ship section or box girder has not been undertaken within this research, and it is believed no work has been presented elsewhere on the strength of grillage structures under bending loads representative of those experienced in these areas of structure. However, the assessment of complete box girder structures in the intact and damaged conditions assessed, have shown the side shell to fail within an interframe section. It is likely that this failure mode will change should damage be located within the side shell structure. It is recommended that work be undertaken to investigate these effects.

Structural modelling within this research has concentrated on the ultimate collapse strength of flat steel structures. Whilst this type of structure forms significant areas of large tanker and containership structures, smaller vessels or higher speed vessels, including frigates, have more shape to their structure. No work has currently been presented on the strength of damaged curved grillage structures, where it is possible that the curved shape may lead to different damage failure modes developing in the damaged condition to those seen in the intact condition and to those seen in flat grillages presented within this thesis, and should be investigated.

Weakness 6 identified in relation to the application of the interframe progressive collapse method to the assessment of damaged ships stated that "only bending induced failure is assessed, neglecting any torsional or shear effects". No investigation on the strength of damaged structure under these loading types has been undertaken, though it has been noted that torsion can be significant in vessels with large hatch openings [38]; therefore, these loading types should be considered in relation to damaged vessels.

10.2 Compartment Level Progressive Collapse Method

Whilst the new compartment level progressive collapse method detailed in Section 3.2 has been shown to be capable of resolving five of the identified as weaknesses in the current interframe progressive collapse method for damaged ship assessment, demonstration of the idealisation in Chapter 8 has shown a number of areas for investigation and development before it may be implemented commercially.

Some of these areas for development have been discussed in the above recommendations, in relation to the application of appropriate loading on the grillage elements and investigation of the use of grillage elements within the side shell structure. However, investigation of the method within a true ship structure has not been undertaken. This analysis would allow identification of the true complexities of full implementation, including assessment of the extent of FEA that would be required to have appropriate strength data captured within the response surface in anticipation of an event.

It is recommended that further development of the response surface methodology is undertaken. Firstly to improve the accuracy of the surfaces to limit potential errors when applied within the compartment level progressive collapse method. Secondly, whilst some potential damage variables have been excluded from the response surface, which have been shown to have limited influence on the collapse strength of damaged steel plates and panels, further work may allow further reduction in variables. For example, if the attributes of the damage can be combined, for example in to a damage area ratio or similar, this would allow the combination of variables, subsequently reducing the amount of FEA data for the surface generation. It may also be desirable to include additional variables or develop the surfaces with a different focus for different emergency scenarios, for example for dented structure which has not been holed, particularly for denting in transverse frames which may lead to similar failure mode changes that have been witnessed in the holed structure assed within this thesis.

It is believed that for some ship types, for example tankers built to common structural rules, that generic response surfaces capturing damaged strength data could be developed for use by most tankers, providing a library of data for use by an emergency response service. Further work would be required to understand the extent to which generic data surfaces could be developed to cover vessels of different type. This would also require investigation in to the appropriate transverse extent of the structure being captured by the surface, to make the library of surfaces as useable as possible.

Assessment of the ultimate bending strength of damaged box girders presented in Chapter 8 is symmetric in its nature. Introducing asymmetric or irregular damage apertures in to the structure, coupled with potential listing of the vessel due to water ingress, will most likely lead to a rotation of the neutral axis. Therefore, the bending of the vessel will no longer be in the vertical plane, but a combination of vertical and horizontal bending moments and potential torsional moments. As discussed in relation to the loading of the side shell above, the loading on the sections of the vessel will no longer be pure compression, and more complex loading scenarios will be required to be assessed. Whilst it is believed the response surface would be capable of capturing the strength data of damaged structure under alternative loading conditions, no work has been undertaken to assess the influence of damage under alternative loading, and should be considered for future research work.

11 REFERENCES

[1] Shipping Times, 9th January 2013.

[2] Shipping Times, 22nd November 2010.

[3] Lloyd's List; October 2009.

[4] Safety and Shipping Review 2013. *Allianz Global Corporate & Speciality; January 2013.*

[5] Lloyd's List Intelligence Casualty Statistics. *Lloyd's List; December 2012.*

[6] Wheater P (2002). Emergency: Collision Forward. *Marine Engineers Review November 2002, IMarEST.*

[7] Smith T W P (2009). Wave Loading on Damaged Ships. PhD Thesis; December 2009.

[8] Wood C D (2013). Compartment flooding and motions of damaged ships. *Engineering Doctorate (EngD) Thesis, University of Southampton.*

[9] Fone D, Smith T W P, Drake K R, Borg J (2011). Global wave loads on damaged ship structures: An experimental procedure and some preliminary results. *Proceedings of The Damaged Ship International Conference, RINA 2011.*

[10] Gaillard A C, Wu G X, Wrobel P (2011). Simulations of motions of a damaged ship in regular waves. *Proceedings of The Damaged Ship International Conference, RINA 2011.*

[11] Davies J E, Sobey A J, Blake J I R, Shenoi R A (2013). Residual capability of damaged composite ship structures. *Damaged Ship II, RINA; pp92-100.*

[12] IMO MARPOL 73/78 - International Convention for the Prevention of Pollution from Ships, 2008.

[13] Dow R S, Hugill R C, Clark J D, Smith C S (1981). Evaluation of ultimate ship hull strength. *Extreme Loads Response Symposium, 1981; pp133-148.*

[14] Smith C S, Dow R S (1981). Residual Strength of Damaged Steel Ships and Offshore Structures. *Journal of Constructional Steel Research, Vol 1 No.4; pp2-15.*

[15] Paik J K, Thayamballi A K (1998). The strength and reliability of bulk carrier structure subject to age and accidental flooding. *Trans. SNAME Vol 106; pp1-40.*

[16] Hughes O F (1988). Ship structural design: A rationally-based, computer-aided, optimization approach; *SNAME.*

[17] Faulkner D, Adamchak J C, Snyder G J, Vetter M F (1973). Synthesis of welded grillages to withstand compression and normal loads. *Computers and Structures Vol 3; pp221-246.*

[18] Caldwell J B (1965). Ultimate longitudinal strength. *Trans. RINA 1965; pp411-430*.

[19] Ren H, Li C, Feng G, Li H (2008). Calculation method of the residual capability of damaged warships. *OMAE 2008; digital proceedings.*

[20] Qi E R, Cui W C (2006). Analytical method for ultimate strength calculations of intact and damaged ship hulls. *Ships and Offshore Structures 2006*; pp153-164.

[21] Paik J K, Mansour A E (1995). A simple formulation for predicting the ultimate strength of ships. *Journal of Marine Science and Technology; ppP52-62.*

[22] Ueda Y, Rashed S M H (1974). An ultimate transverse strength analysis of ship structures. *Journal of the society of Naval Architects of Japan, 136; pp309 - 324.*

[23] Ueda Y, Rashed S M H (1991). Advances in the application of ISUM to marine structures. *Proceedings of the 2nd International Conference on Advances in Marine Structures, Dunfermline, Scotland; pp628-649.*

[24] Ueda Y, Rashed S M H (1984). The idealized unit method and its application to deep girder structures. *Computers and Structures; Vol.18;* pp277-293.

[25] Paik J K, Thayamballi A K (2006). Ultimate limit state design of steel-plated structures. John Wiley & Sons, Ltd.

[26] Paik J, Thayamballi A (2003). A concise introduction to the idealised structural unit method for nonlinear analysis of large plated structures and its application. *Thin-Walled Structures 41; pp329-355.*

[27] Paik J K, Thayamballi A K (2003). A consise introduction to the idealised structural unit method for nonlinear analysis of large plated structures and its application. *Thin-Walled Structures 41; pp329-355.*

[28] Pei Z, Iijima K, Fujikubo M, Tanaka Y, Tanaka S, Okazawa S, Yao T (2012). Collapse behaviour of ship hull girder of bulk carrier under alternative heavy loading condition. *International Offshore and Polar Engineering Conference (ISOPE 2012); Digital proceedings.*

[29] Starossek U (2009). Progressive collapse of structures. *Thomas Telford Limited.*

[30] Hughes O F, Paik J K (2010). Ship structural design and analysis. The Society of Naval Architects and Marine Engineers.

[31] Guedes Soares C, Luis R M, Nikolov P, Downes J, Taczala M, Modiga M, Quesnel T, Toderan C, Samuelides M (2008). Benchmark study on the use of simplified structural codes to predict the ultimate strength of a damaged ship hull. *International Shipbuilding Progress 55; pp87-107.*

[32] Das P K, Chuang F (2007). Residual strength and survivability of bulk carriers after grounding and collision. *Journal of Ship Research, Vol 51; pp137-149.*

[33] Gordo J M, Guedes Soares C (2000). Residual strength of damaged ship hulls. *Proceedings of 9th International Maritime Association of Mediterranean Congress (IMAM 2000); pp79-86.*

[34] Benson S (2011). Progressive collapse assessment of lightweight ship structures. *PhD Thesis, Newcastle University School of Marine Science & Technology, UK.*

[35] Benson S, Downes J, Dow RS (2012). Compartment level progressive collapse analsysi of a lightweight girder. *6th International ASRANet Conference for Integrating Structural Analysis, Risk and Reliability (ASRANet 2012); Digital proceedings.*

[36] Paik J K, Thayamballi A, Che J S (1996). Ultimate strength of ship hulls under combined vertical bending, horizontal bending and shearing forces. *Society of Naval Architects and Marine Engineers - Transactions; Vol.104, pp31-59.*

[37] Paik J K, Thayamballi A, Terndrup Pedersen P, Park Y I (1999). Ultimate strength of ship hulls under torsion. *Ocean Engineering 28, pp1097-1133.*

[38] Hu Y, Chen B (2001). Limit state of torsion of ship hulls with large hatch openings. *Journal of Ship Research; Vol 45, pp95-102.*

[39] ISSC 2006 Committee III.1. Ultimate Strength. *16th International Ship and Offshore Structures Congress (ISSC 2006).*

[40] ISSC 2012 Committee III.1. Ultimate Strength. *18th International Ship and Offshore Structures Congress (ISSC 2012).*

[41] Servis D, Samuelides M, Louka T, Voudouris G (2002). Implementation of finite-element codes for the simulation of ship-ship collisions. *Journal of Ship Research Vol46, No.4; pp239-247.*

[42] Wisniewski K, Kolakowski P (2003). The effect of selected parameters on ship collision results by dynamic simulations. *Finite Elements in Analysis and Design 39; pp958-1006.*

[43] Ringsberg, J W (2010). Characteristics of material, ship side structure response and ship survivability in ship collisions. *Ships and Offshore Structures Vol 5, No.1; pp51-66.*

[44] Lee S-G, Nam J-H, Kim J-K, Zhao T, Nguyen H-A (2012). Structural safety assessment of ship collisions using FSI analysis technique. *22nd International Offshore and Polar Engineering conference (ISOPE 2012); Digital proceedings.*

[45] Abu Bakar A (2011). Simulation of and actual collision incident between a tanker and a bulk carrier. *UK Marine Technology Postgraduate Conference, University of Southampton (UK MTPC 2011); Abstracts pp41.*

[46] Toal D J J, Bressloff N W., Keane A J (2008). Kriging hyperparameter tuning strategies. *AIAA Journal, Vol.46; pp1240-1252*.

[47] Simpson T W, Mistree F (2001). Kriging models for global approximation in simulation-based multidisciplinary design optimization. AIAA Journal, Vol. 39; pp2233-2241.

[48] D. G. Krige (1951). A statistical approach to some basic mine valuation problems on the Witwatersrand. *Journal of the Chemical, Metallurgical and Mining Engineering Society of South Africa, Vol 52,6; pp119-139.*

[49] Jones D.R. (2001). A taxonomy of global optimization methods based on response surfaces. *Journal of Global Optimization, Vol. 21; pp345-383.*

[50] Forrester A., Sobester A., Keane A. (2008). Engineering design via surrogate modelling: a practical guide. *Chichester, UK, Wiley 2008.*

[51] Elbatouti A M T, Jan H Y, Stiansen S G (1976). Structural analysis of a containership steel model and comparison with the test results. *Society of Naval Architects and Marine Engineers - Transactions; Vol.84, pp146-168.*

[52] Mansour A, Yang J M, Thayamballi A (1990). An experimental investigation of ship hull ultimate strength. *Society of Naval Architects and Marine Engineers - Transactions; Vol. 98, pp411-439.*

[53] Dow R S (1991). Testing and analysis of a 1/3 scale frigate model. *Advanced Marine Structures 1991; pp749-773.*

[54] Storhaug G (2009). The 4400TEU Container Vessel MSC NAPOLI Broke Its Back, But Did Whipping Contribute? *Hydroelasticity 2009 Proceedings, Hydroelasticity in Marine Technology; pp233-243.*

[55] Bryan G H (1890). On the stability of a plane plate under thrusts in its own plane with application on the buckling of sides of a ship. *Proceedings of the London Mathematical Society*; pp54-67.

[56] Paik J K, Terndrup Pedersen (1995). Ultimate and crushing strength of plated structures. *Journal of Ship Research, Volume 39; pp250-261.*

[57] Smith C S, Davidson P C, Chapman J C, Dowling P J (1987). Strength and stiffness of ships' plating under in-plane compression and tension. *Trans RINA 1987; pp277-296.*

[58] Ueda Y, Yasukawa W, Yao T, Ikegami H, Ominami R (1975). Ultimate strength of square plates subjected to compression (1st Report) - Effects of initial deflection and welding residual stress. *Journal of the Society of Naval Architects of Japan, 137; pp210-221.*

[59] Paik J K (2007) Ultimate strength of steel plates with a single circular hole under axial compressive loading along short edges. *Ships and Offshore Structures Vol 2, No.4; pp355-360.*

[60] El-Sawy K M, Martini M I (2010). Stability of biaxially loaded square plates with single central holes. *Ships and Offshore Structures Vol 5, No.4; pp283-293.*

[61] Hong L, Amdahl J (2008). A comparative study on the plastic formulations of ship shell plating under patch loading. *OMAE 2008; digital proceedings.*

[62] Paik J K, Kim B J, Seo J K (2008). Methods for ultimate limit state assessment of ships and ship-shaped offshore structures: Part I - Unstiffened Plates. *Ocean Engineering 35; pp261-270.*

[63] Zhang S, Kumar P, Rutherford S E (2008). Ultimate shear strength of plates and stiffened panels. *Ships and Offshore Structure, Vol 3; pp102-112.*

[64] Paik J K (2005). Ultimate strength of dented steel plates under edge shear loads. *Thin-Walled Structures 43; pp1475-1492.*

[65] Paik J K (2008). Ultimate strength of perforated plates under combined biaxial compression and edge shear loads. *Journal of Thin Walled Structures; Vol.46, pp207-213.*

[66] Chalmers, D W (1993). MoD Design of Ships' Structures. *London HMSO*.

[67] Smith C S (1975). Compressive strength of welded steel ship grillages. Trans. RINA 1975; pp325-359.

[68] Daley C, Hermanski G, Pavic M, Hussein A (2007). Ultimate strength of frames and grillages subject to lateral loads - an experimental study. Proceedings of 10th International Symposium on Practical Design of Ships and Other Floating Structures, *PRADS 2007 Proceedings.*

[69] Cho S-R, Choi B-W, Frieze P A (1998). Ultimate strength formulation for ship's grillages under combined loadings. *Practical Design of Ships and Mobile Units; pp125-132.*

[70] Duggal S K (2000). Design of Steel Structures. Tata McGraw-Hill Publishing Company Ltd; Second Edition.

[71] Hu S Z, Chen Q, Pegg N, Zimmerman T J E (1997). Ultimate Collapse tests of stiffened-plate ship structural units. Marine Structures 10; pp587-610.

[72] Nikolov P I (2008). Collapse strength of damaged plating. *Proceedings of the ASME 27th International Conference on Offshore Mechanics and Arctic Engineering, OMAE2008; digital proceedings.*

[73] Paik J K, Bong J K, Seo J K (2008). Methods for ultimate limit state assessment of ships and ship-shaped offshore structures: Part II stiffened panels. *Ocean Engineering 35 (2008); pp271-280.*

[74] Witkowska M, Guedes Soares C (2008). Collapse strength of stiffened panels with local dent damage. *OMAE 2008; digital proceedings.*

[75] Gendy A S, Saleeb A F (1994). Consistent mixed model for stability of stiffened panels with cut-outs. *Computers and Structures Vol 54; pp119-130.*

[76] Alagusundaramoorthy P, Sundaravadivelu R, Ganapathy G (1999). Experimental Study on collapse load of stiffened panels with cutouts. *Journal of Constructional Steel Research 52; pp235-251.*

[77] Suneel Kumar M, Alagusundaramoorthy P, Sundaravadivelu R (2009). Interaction curves for stiffened panel with circular opening under axial and lateral loads. *Ships and offshore Structures Vol 4, pp133-143*.

[78] ISSC 2009 Committee III.1. Ultimate Strength. *17th International Ship and Offshore Structures Congress (ISSC 2009).*

[79] Dow R S, Smith C S (1984). Effects of localized imperfections on compressive strength of long rectangular plates. *Journal of Constructional Steel Research 4; pp51-76.*

[80] Ueda Y, Yao T (1985). The influence of complex initial deflection modes on the behaviour and ultimate strength of rectangular plates in compression. *Journal of Constructional Steel Research 5; pp265-302.*

[81] EN1993-1-1 Eurocode 3: Design of steel structures, general rules and rules for buildings (2005).

[82] Smith C S, Anderson N, Chapman J C, Davidson P C, Dowling P J, (1991). Strength of stiffened plating under combined compression and lateral pressure. *Transactions of the Royal Institution of Naval Architects, 1991: pp131-147.*

[83] Faulkner D, (1975). A Review of Effective Plating for use in the Analysis of Stiffened Plating in Bending and Compression. *Journal of Ship Research, 1975. 19(1): p. 1-17.*

[84] Paik J K, Thayamballi A K, Lee J M (2004). Effect of initial deflection shape on the ultimate strength behaviour of welded steel plates under biaxial compressive loads. *Journal of Ship Research, Vol 48 No.1; pp45-60.*

[85] Wells Jr. A H (1981). Some extreme effects of residual stresses in shipbuilding. *The Society of Naval Architects and Marine Engineers Extreme Loads Response Symposium 1981; pp189-202.*

[86] Design of Surface Ship Structures (1989). *Sea Systems Controllerate Publication No.23 (SSCP23). Crown Copyright 1989. EXTANT.*

[87] Rules and Regulations for the Classification of Naval Ships (2008). *Lloyd's Register.*

[88] Design of Submarine Structures (2001). *Sea Systems Publication No. 74 (SSP74). Crown Copyright 2001.*

[89] Eurocode1990:2002+A1:2005 Basis of structural design (2008). *British Standard BS EN 1990:2002+A1:2005.*

[90] EN1993-2 Eurocode 3: Design of steel structures Part 2: Steel bridges (2006).

[91] Paik J K, Thayamballi A, Hong Yang S (1998). Residual strength assessment of ships after collision and grounding. Journal of *Marine Technology; Vol. 35, pp38-54.*

[92] Russo M, Renaud F, Steen E, Kippenes J (2009). Residual strength of a FPSO vessel after collision damages. *Proceedings of the ASME 2009 28th International Conference on Ocean, Offshore and Arctic Engineering; Digital proceedings.*

[93] Paik J K, Thayamballi A (2002). Ultimate strength of ageing ships. *Proceedings of the Institution of Mechanical Engineers, Part M: Journal of Engineering for the Maritime Environment Vol.216 no.1; pp57-77.*

[94] Smith C S (1968). Elastic buckling and beam-column behaviour of ship grillages. *Transactions of the Royal Institution of Naval Architects, 1968; pp127-144.*

[95] Assakkaf, A.I., Ayyub, B.M., and Mattei, N.J. (2000) Reliability-based load and resistance factor design (lrfd) of hull structural components of surface ships. *In Association of Scientists and Engineers 37th Annual Technical Symposium,2000.*

[96] Hart, D.K., Rutherford, S.E., and Wickham, A.H.S., (1985) Structural reliability analysis of stiffened panels. *Transactions of the Royal Institution of Naval Architects, vol. 128; pp293–310.*

[97] Gordo J M, Guedes Soares C (2004). Experimental evaluation of the ultimate bending moment of a box girder. *Marine Systems and Ocean Technology, Vol1; pp33-46.*

[98] Gordo J M, Guedes Soares C (2009). Tests on ultimate strength of hull box girders made of high tensile steel. *Marine Structures 22; pp770-790.*

[99] Saad-Eldeen S, Garbatov Y, Guedes Soares C (2011). Corrosion-dependent ultimate strength assessment of aged box girders based on experimental results. *Journal of Ship Research, Vol55 No.4; pp289-300.*

[100] Saad-Eldeen S, Garbatov Y, Guedes Soares C (2012). Ultimate strength assessment of corroded box girders. *Ocean Engineering 58; pp35-47.*

[101] ANSYS v14. Structural Analysis Guide (2011). *ANSYS Inc.*

[102] Zhang S, Khan I (2009). Buckling and ultimate capability of plates and stiffened panels in axial compression. *Marine Structures 22; pp791-808.*

[Blank Page]

A1 PUBLISHED PAPERS

A1.1 Published Journal Paper

Underwood J M, Sobey A J, Blake J I R, Shenoi R A (2012). Ultimate collapse strength assessment of damaged steel-plated structures. *Engineering Structures 38; pp1-10.*

A1.2 Published Conference Papers

Sobey A J, Underwood J M, A J, Blake J I R, Shenoi R A (2010). Reliability Analysis of Damaged Steel Structures Using Finite Element Analysis. *5th International ASRANet Conference (ASRANet 2010). Digital Proceedings.*

Underwood J M, Sobey, A J, Blake J I R, Shenoi R A (2010). Local Stress Sensitivity Analysis of Damaged Steel Ship Hulls. *Practical Design of Ships and Other Floating Structures (PRADS 2010) Proceedings (P1006-1014).*

Underwood J M, Sobey A J, Blake J I R, Shenoi R A, Cuckson B R (2011). Determination of critical factors for the strength assessment of damaged steel ship structures. *30th International Conference on Ocean, Offshore and Arctic Engineering (OMAE 2011). Digital Proceedings.*

Underwood J M, Sobey A J, Blake J I R, Shenoi R A (2012). Determination of Critical Factors for the Damaged Strength Assessment of Steel Grillages. *22nd International Ocean and Polar Engineering Conference (ISOPE 2012). Digital Proceedings.*

Underwood J M, Sobey A J, Blake J I R, Shenoi R A (2012). Reliability Analysis of the Damage Strength of Steel Grillages for use in Ship Emergency Response. *6th International ASRANet Conference (ASRANet 2012). Digital Proceedings.*

Underwood J M, Sobey A J, Blake J I R, Shenoi R A (2013). Strength Assessment Of Damaged Steel Ships During Emergency Response. *RINA Damaged Ship II.*

[Blank Page]

B1 STIFFENED PANEL DAMAGE APERTURE INVESTIGATION GRAPHICAL RESULTS

This appendix presents additional graphical results of the research into the effects of damage aperture shape on the collapse strength of stiffened steel panels presented in Chapter 6, where β is the plate slenderness ratio. The graphical results presented here are for stiffener profiles ISA50306, ISA100656 and ISA125956, which are discussed within Chapter 6.

B1.1 Stiffener Profile: ISA50306

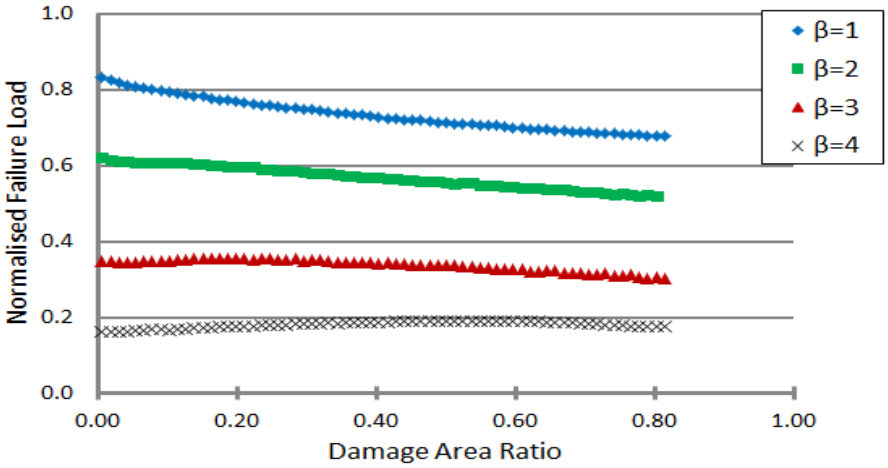

Figure B.1 - Normalised Axial Failure Load Against Area Ratio for Plate Damage Only - Diamond Aperture

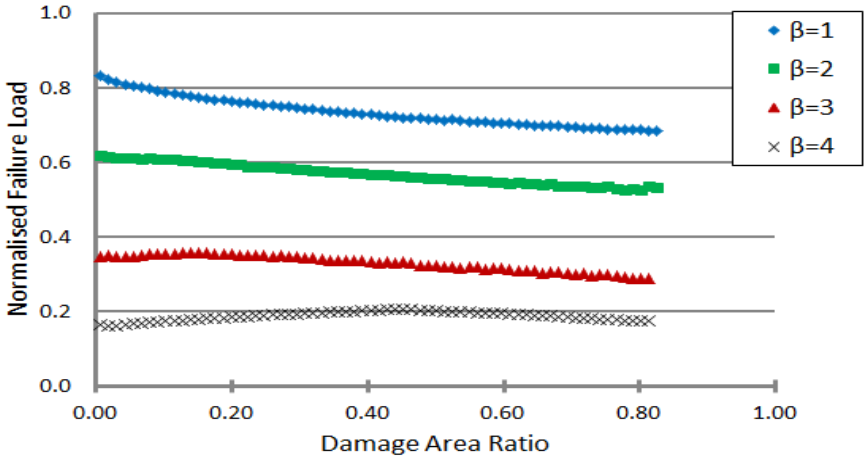

Figure B.2 - Normalised Axial Failure Load Against Area Ratio for Plate Damage Only – Elliptical Aperture

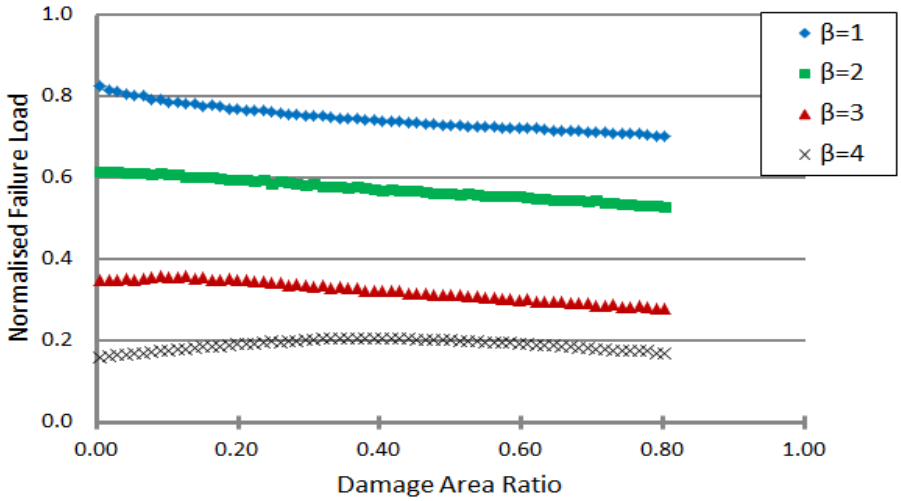

Figure B.3 - Normalised Axial Failure Load Against Area Ratio for Plate Damage Only - Square Aperture

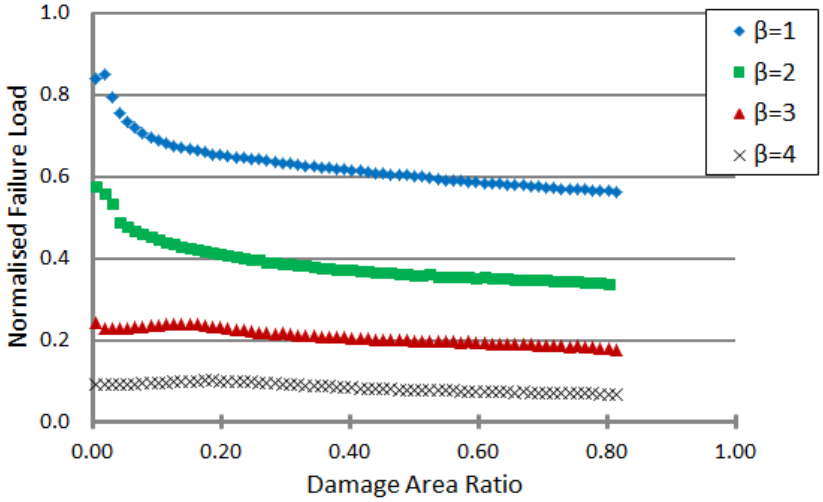

Figure B.4 - Normalised Axial Failure Load Against Area Ratio for Plate and Stiffener Damage - Diamond Aperture

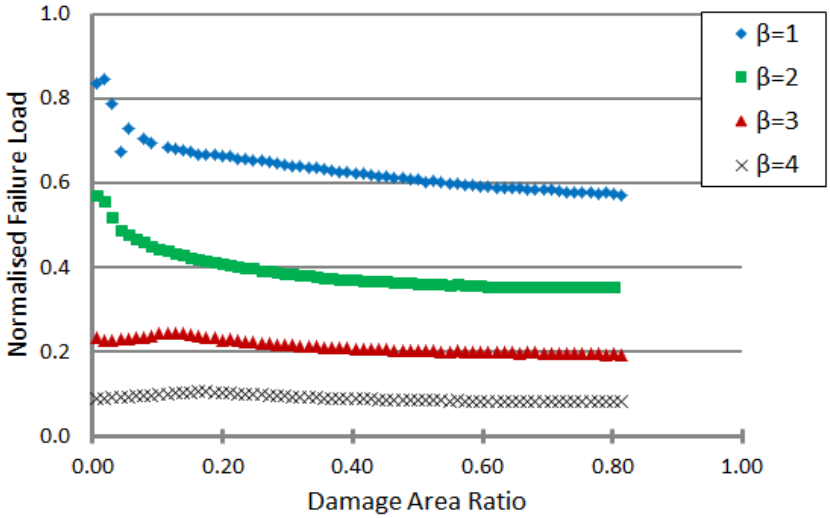

Figure B.5 - Normalised Axial Failure Load Against Area Ratio for Plate and Stiffener Damage - Elliptical Aperture

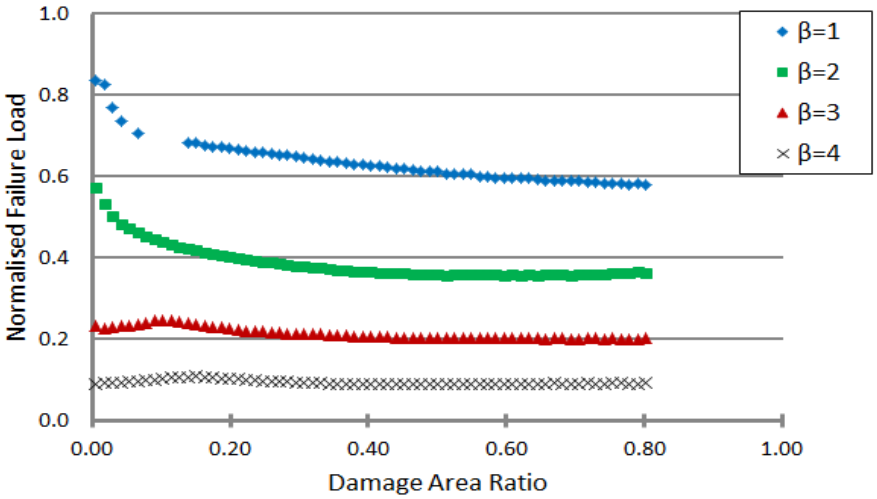

Figure B.6 - Normalised Axial Failure Load Against Area Ratio for Plate and Stiffener Damage - Square Aperture

B1.2 Stiffener Profile: ISA100656

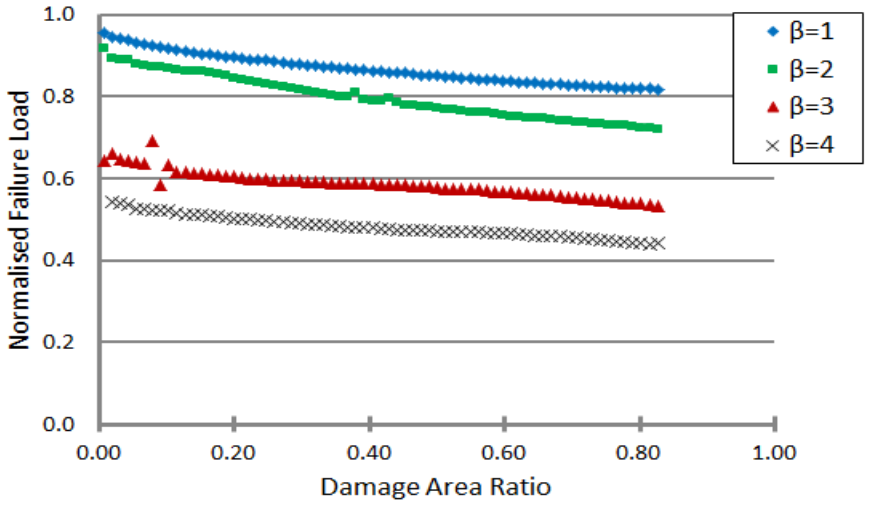

Figure B.7 - Normalised Axial Failure Load Against Area Ratio for Plate Damage Only - Diamond Aperture

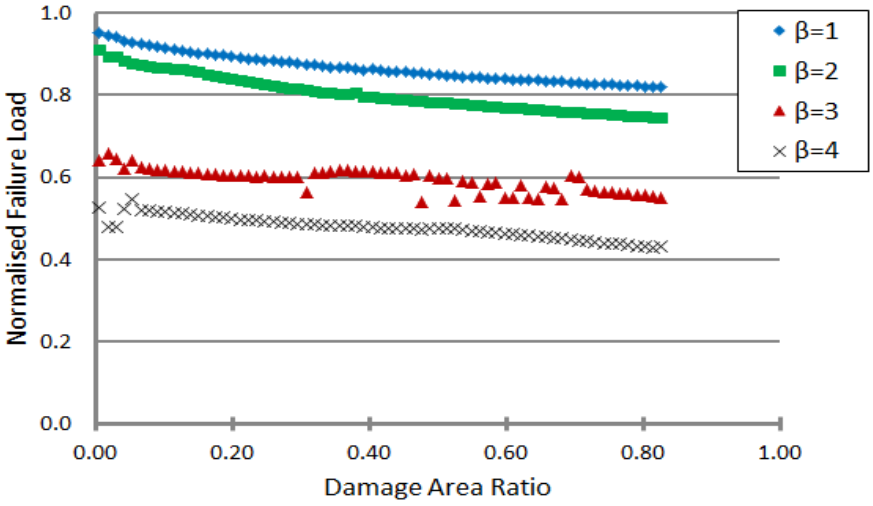

Figure B.8 - Normalised Axial Failure Load Against Area Ratio for Plate Damage Only - Elliptical Aperture

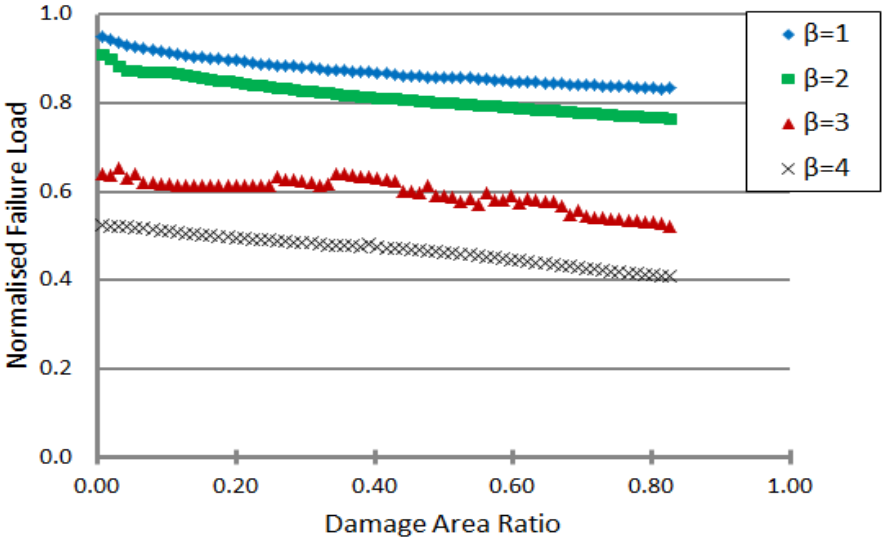

Figure B.9 - Normalised Axial Failure Load Against Area Ratio for Plate Damage Only - Square Aperture

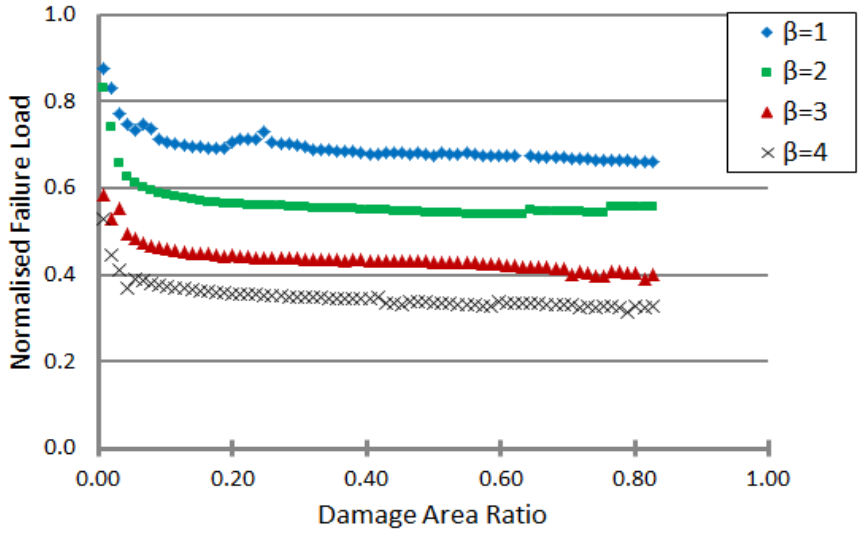

Figure B.10 - Normalised Axial Failure Load Against Area Ratio for Plate and Stiffener Damage - Diamond Aperture

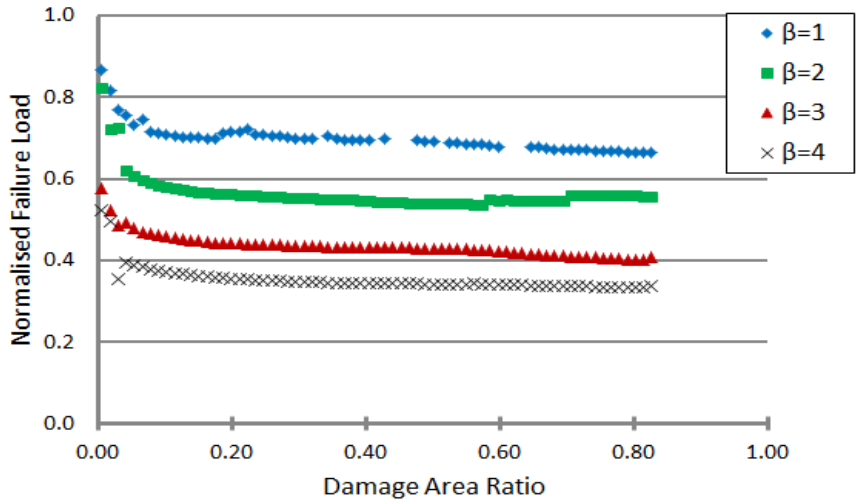

Figure B.11 - Normalised Axial Failure Load Against Area Ratio for Plate and Stiffener Damage - Elliptical Aperture

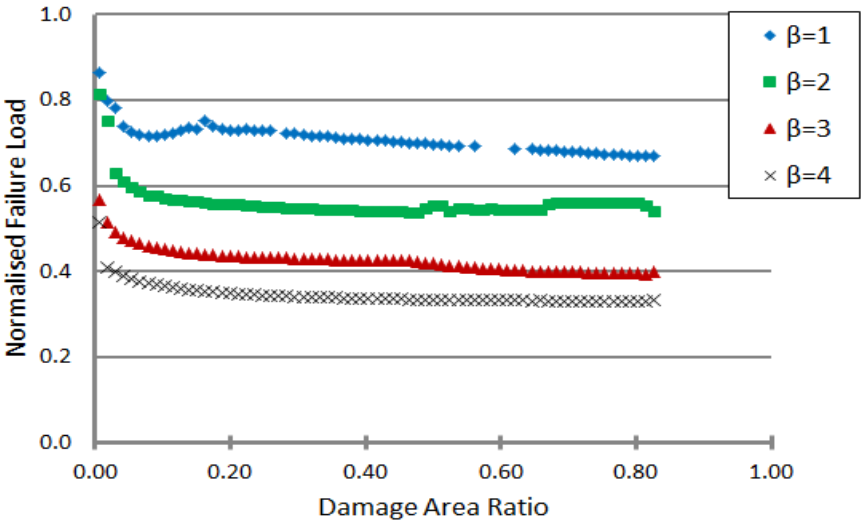

Figure B.12 - Normalised Axial Failure Load Against Area Ratio for Plate and Stiffener Damage - Square Aperture

B1.3 Stiffener Profile: ISA125956

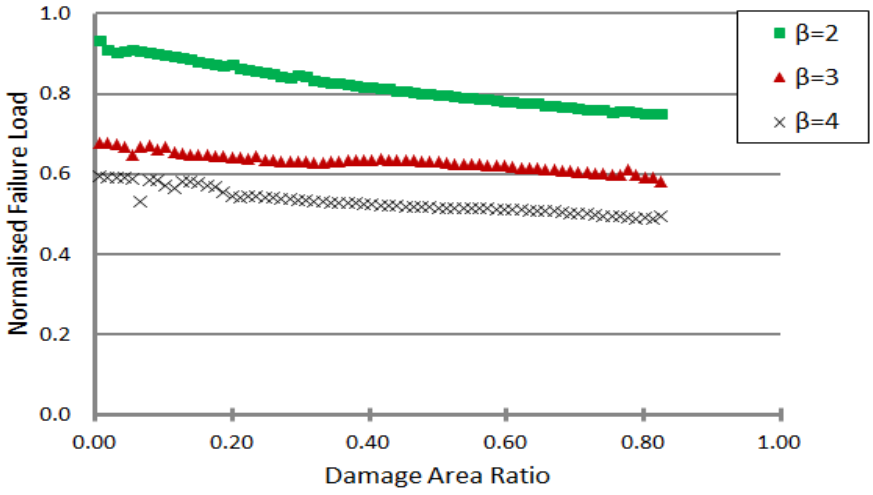

Figure B.13 - Normalised Axial Failure Load Against Area Ratio for Plate Damage Only - Diamond Aperture

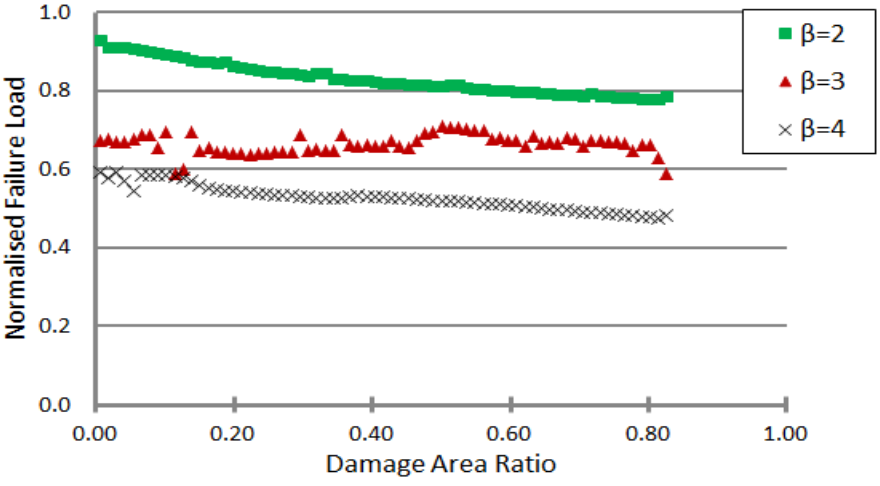

Figure B.14 - Normalised Axial Failure Load Against Area Ratio for Plate Damage Only - Elliptical Aperture

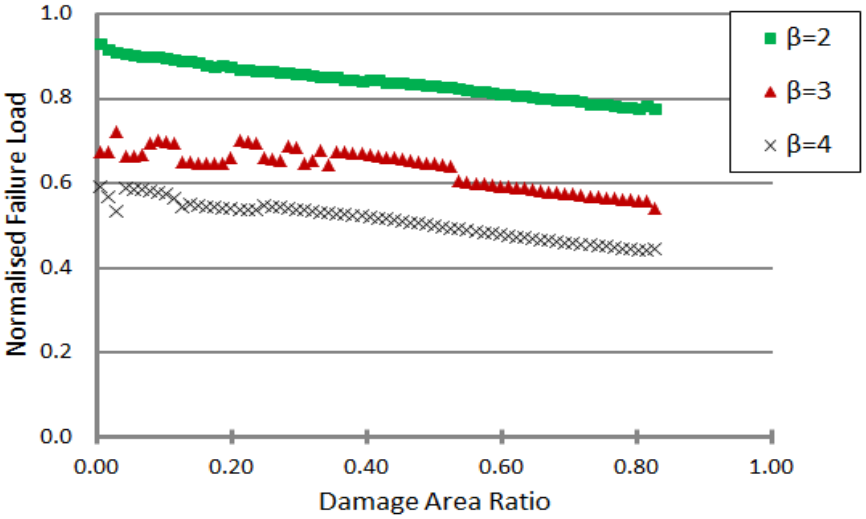

Figure B.15 - Normalised Axial Failure Load Against Area Ratio for Plate Damage Only - Square Aperture

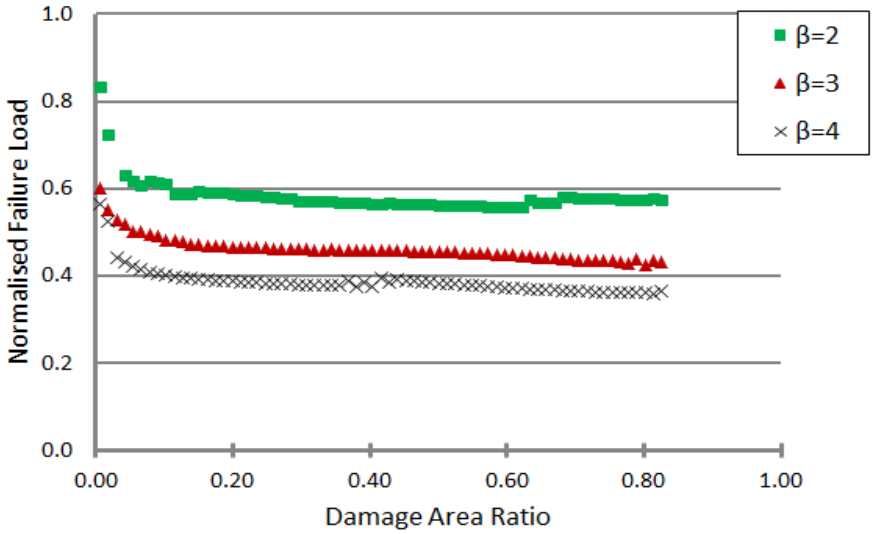

Figure B.16 - Normalised Axial Failure Load Against Area Ratio for Plate and Stiffener Damage - Diamond Aperture

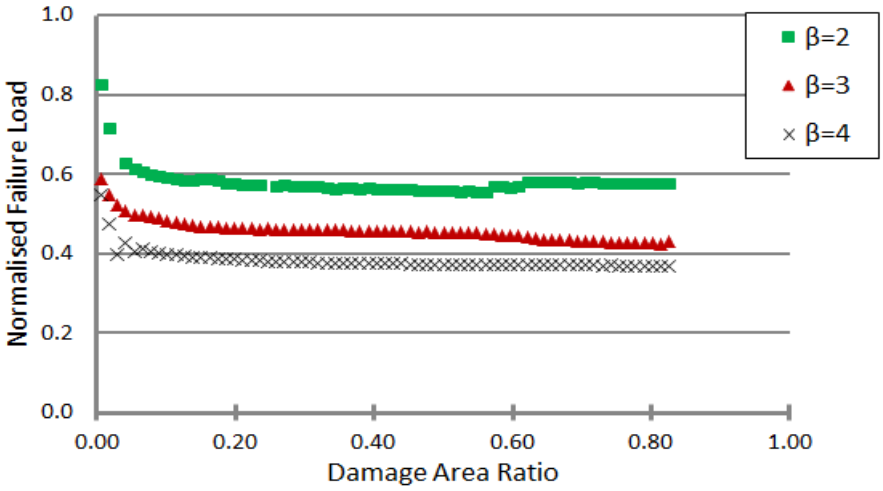

Figure B.17 - Normalised Axial Failure Load Against Area Ratio for Plate and Stiffener Damage - Elliptical Aperture

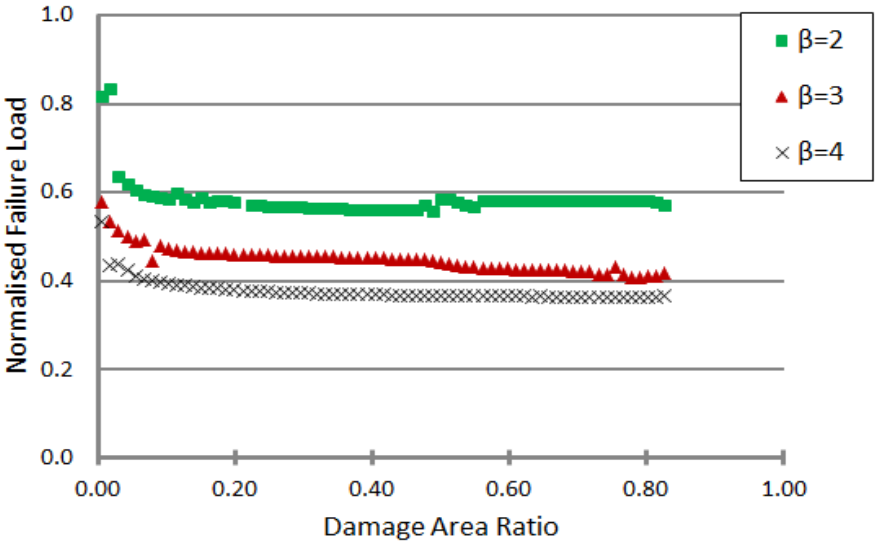

Figure B.18 - Normalised Axial Failure Load Against Area Ratio for Plate and Stiffener Damage - Square Aperture